Making sense of nonsense in the context of cystic fibrosis

Sacha Spelier

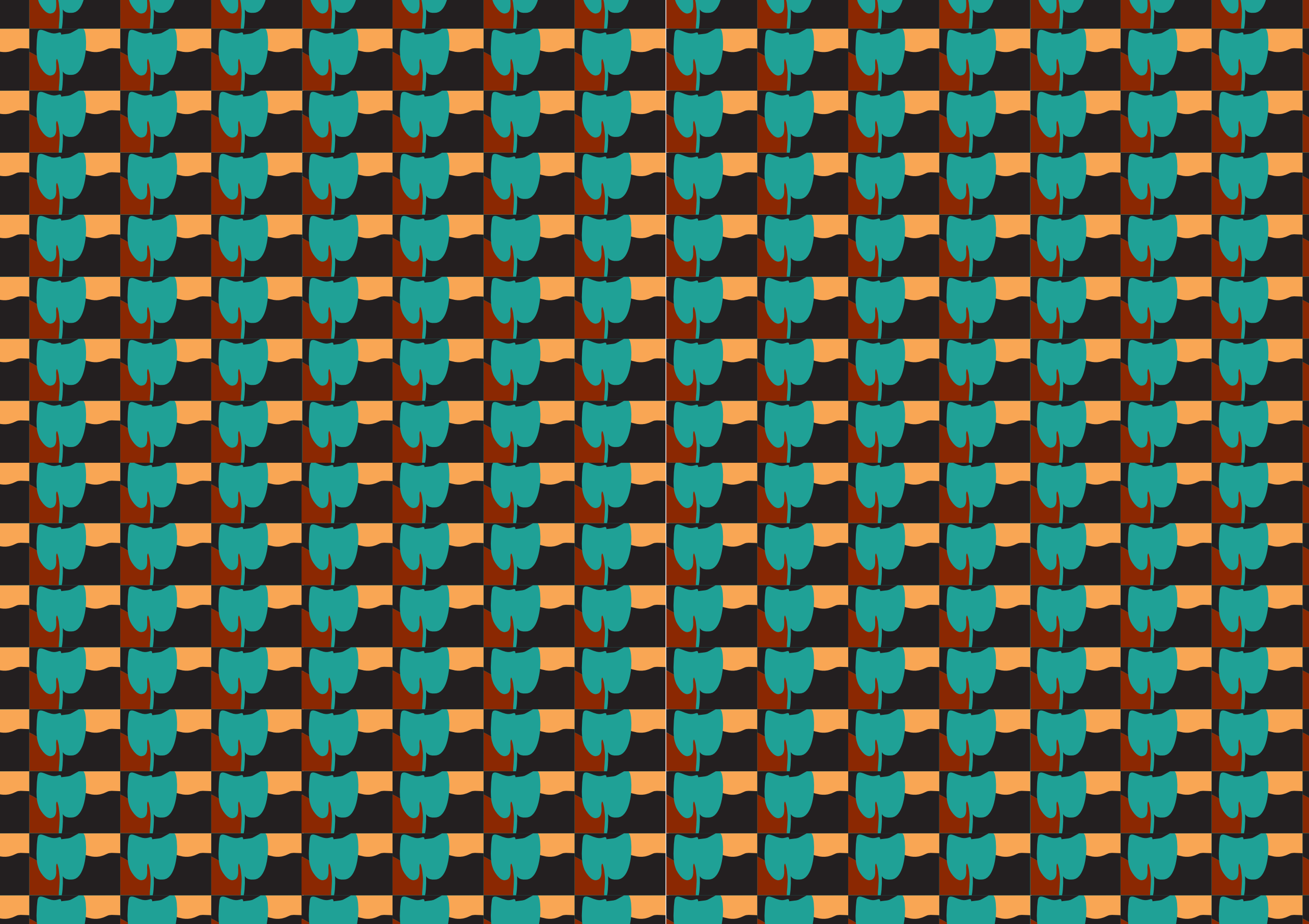

Making sense of nonsense in the context of cystic fibrosis

Sacha Spelier

Making sense of nonsense in the context of cystic fibrosis

Nieuwe behandelmethodes testen voor taaislijmziekte in intestinale organoïden

(met een samenvatting in het Nederlands)

Proefschrift

ter verkrijging van de graad van doctor
aan de Universiteit Utrecht
op gezag van de
rector magnificus, prof. dr. H.R.B.M. Kummeling,
ingevolge het besluit van het college voor promoties
in het openbaar te verdedigen op
donderdag 20 juni 2024 des middags te 12.15 uur

door
Alexandra Spelier
geboren op 2 juli 1995
te Utrecht.

Making sense of nonsense in the context of cystic fibrosis
PhD thesis, Utrecht University, The Netherlands
Author: Sacha Spelier
Cover illustration and design: Jan Olijhoek, het Omslag Grafische Vormgeving
Printing: Repro VU Printservices
ISBN: 978-90-393-7693-5

Promotors:

Prof. dr. J.M. Beekman
Prof. dr. C.K. van der Ent

Beoordelingscommissie:

Prof. dr. M. Amaral
Prof. dr. L.J. Bont
Dr. J. Lueck
Prof. dr. R. Masereeuw (voorzitter)
Prof. dr. M. Tanenbaum

CONTENTS

Chapter | 1

General introduction

Sacha Spelier, Cornelis K. van der Ent and Jeffrey M. Beekman

Obtaining a thorough and complete understanding of rare genetic diseases is a major challenge in biomedical research, let alone developing treatment regimens to effectively treat the disease. Conventionally, most treatments for genetic diseases centered around relieving symptoms, rather than treating the underlying molecular defect. A major paradigm shift in terms of treatment development however took place in the last decades for a wide range of diseases resulting in an increasing number of precision medicine strategies. Precision medicine, also known as personalized medicine, is the approach where the underlying molecular defect of a disease is targeted, taking into account the genetic background or even environmental and lifestyle factors of a specific person [1]. As such, precision medicine allows for precise tailoring of medical care and treatment to the specific characteristics of each person. This is a major benefit for a wide range of medical conditions, ranging from monogenetic and multifactorial genetic diseases to non-genetic diseases.

The success rate of precision medicine development differs however to a large extent between diseases, which is influenced by several factors. First, a thorough understanding of the genetic and molecular defect underlying the disease is pivotal for precise therapeutic targeting. In this context, recent progress in the development of state-of-the-art sequencing techniques contributes significantly to obtaining a thorough understanding of the exact genetic base of a disease and consequential associated molecular defects. Accordingly, monogenetic diseases are generally easier to understand and consequently to target than diseases with complex genetic backgrounds such as cancers. Secondly, the existence of disease-specific, biologically relevant, patient-based preclinical models can significantly increase the success rate of precision medicine development by optimizing the chances of translating preclinical results into a clinical setting. Such disease-recapitulating, patient-derived models have been developed for a broad range of diseases in the last decade, yet biological accuracy and model robustness differs between disease models. Additionally, the presence of robust clinical endpoints that allow for precise characterization of disease severity *in vivo* with precision and accuracy is pivotal for precision medicine development, as this aids in obtaining a full understanding of clinical efficacy of novel treatment strategies. Lastly, some mutation types such as large deletions are unlikely to be corrected by small compounds. Consequently, a low prevalence of such challenging mutations in the patient population can increase the chances of successful development of precision medicine strategies.

Cystic fibrosis (CF) is an example of a genetic disease for which recently highly effective precision medicine strategies have been developed for a significant proportion of all people with CF (pwCF). This success can be partially contributed to characteristics of CF that match with the above suggested hallmarks for potential successful development of precision medicine strategies. In brief, its well-understood monogenetic character, the existence of biologically relevant, patient-derived preclinical models of which the outcomes correlate with clinical endpoints and the 85-90% prevalence throughout the CF population of a single mutation: the 3 base-pair deletion of phenylalanine 508 (F508del), which is highly responsive to the developed precision medicine strategies [2].

However, 10-15% of all pwCF do not benefit from these recent advances in precision medicine development and still suffer from a large unmet clinical need. In this thesis, we study novel treatment strategies for those pwCF that do not benefit from precision therapies at present-day, as well as identify those pwCF who may benefit from these treatment strategies using state-of-the-art preclinical assays in CF patient-derived cells.

Cystic fibrosis: the most common, rare genetic disease

CF is a monogenetic, autosomal, recessive disease caused by malfunctioning of the CF transmembrane conductance regulator (CFTR) protein. CF is often described as the most common rare disease, with approximately 1 case per 3000 births in Europe and the United States, affecting around 32000 individuals in Europe and 105 000 individuals worldwide [3]. More than 2000 distinct *CFTR* mutations have been described, of which 700 are estimated to be disease-causing (Cystic Fibrosis Mutation Database, [4]). CFTR is a transport channel expressed on the apical cell membrane of epithelial cells across various tissues, including lung and intestine. CFTR passively transports chloride and bicarbonate ions from the intracellular to the extracellular environment, which is followed by water transport across tissue epithelium [5]. If both *CFTR* alleles harbor mutations resulting in malfunctioning CFTR protein, chloride secretion is deficient resulting in aberrant fluid transport and consequently the secretion of aberrant thick and sticky mucus in various organ systems. Mucociliary clearance of this viscous mucus is impaired, resulting in mucus obstruction promoting chronic bacterial infections and associated changes in the microbiome. Consequently, the epithelia adapt into a vicious cycle inducing a pro-inflammatory state and ultimately leading to a progressive loss-of-function in affected organs **(Figure 1A).** Ultimately, pulmonary abnormalities and progressive lung damage represent the primary cause of morbidity in most pwCF. Furthermore, pwCF may suffer from severe gastrointestinal problems, malnutrition, inflammation and an increased risk of gastrointestinal cancer [6]. The impact of CFTR loss-of-function (CFTR-LoF) further extends to various other organ such as the pancreas, sweat glands, liver's biliary duct and the male reproductive tract.

CFTR: regulation, localization and structural characteristics

Transcriptional regulation of *CFTR* is complex and differs per tissue and cell type. Transcription factors such as cAMP-responsive element-binding protein (CREBs), which are activated by cAMP signaling and CFTR-associated factors (CAFs) [8], play an important role in transcription initiation. Co-activators such as WNT3A and proinflammatory signaling molecules such as TNF-alpha, further influence *CFTR* transcription in response to infection or inflammation [9]. As membrane protein, CFTR is primarily expressed in the apical membrane of epithelial cells. In the context of airway cells, it remains controversial which cells precisely express CFTR. First single-cell RNA (scRNA) sequencing studies identified the ionocyte as rare airway cell type that expresses high levels of CFTR [10]. Latest scRNA sequencing data however indicates that whilst ionocytes indeed express the highest CFTR levels per cell, their absolute contribution to the total amount of CFTR is low whilst secretory cells contributed most to total CFTR protein levels and function [11]. In the context of intestinal cells, CFTR is expressed as a gradient in the intestinal

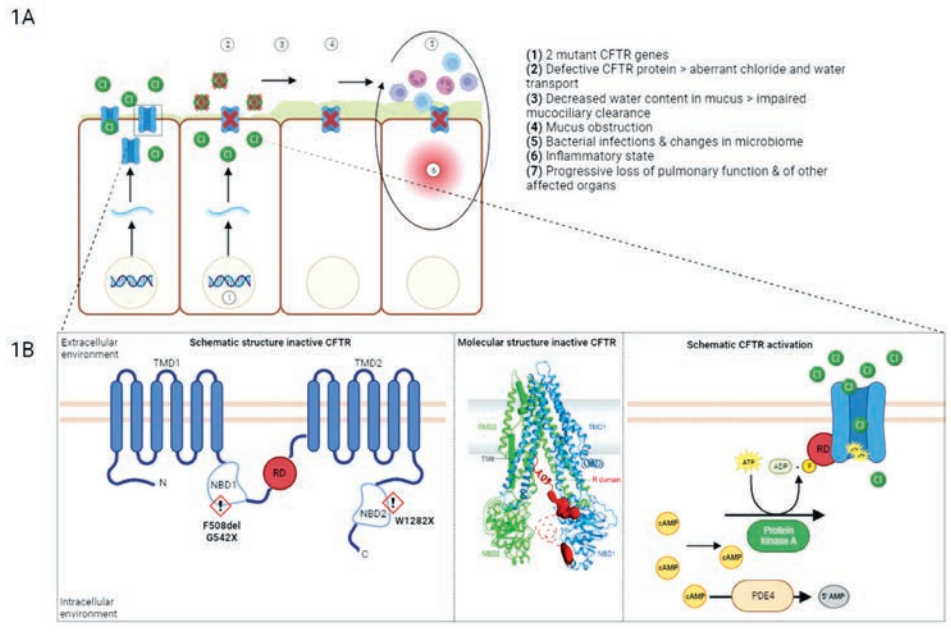

Figure 1. Consequences of CFTR loss-of-function (CFTR-LoF) and structural characteristics of CFTR.

(A) Schematic of the consequences of CFTR-LoF. The CFTR gene encodes the CFTR protein, an apical chloride ion channel in epithelial cells which secretes chloride and bicarbonate out of the cell after which water follows passively (1). Consequently, *CFTR* mutations on both *CFTR* alleles result in aberrant fluid homeostasis (2), decreased water content in the mucus and consequently a thick mucus layer that is more difficult to remove by mucociliary clearance (3). Resulting mucus obstructions are prone for bacterial infections (4) and can result in changes in the microbiome (5). A continuous pro-inflammatory state results in a vicious cycle of inflammation and cellular damage (6), ultimately resulting in organ failure (7). **(B)** Schematic of structural characteristics of inactive human CFTR (left) as well as the molecular structure of inactive human CFTR in its dephosphorylated ATP-free form based on electron cryomicroscopy (middle, adapted from Liu *et al* [7]). Both depictions highlight the main domains of CFTR: TMD1 and TMD2, NBD1 and NBD2 and the R-domain. On the right, the underlying pathway of CFTR activation is schematically depicted. The main activator of CFTR is cyclic AMP (cAMP), which is produced in response to external signals like hormones and neurotransmitters. Increased cAMP levels results in activation of protein kinase A (PKA), which phosphorylates the R-domain of CFTR and results in a confirmational change, allowing chloride ions and water to flow out of the cell. cAMP pools can be diminished by PDE4 enzymes, which convert cAMP into 5' AMP.

crypts with the highest expression at the base of the crypts in the adult stem cell (ASCs) population [12].

Upon successful transcription and translation, the CFTR protein is composed of multiple domains, including two transmembrane domains (TMD1 and TMD2), two nucleotide-binding domains (NBD1 and NBD2), and a regulatory domain (R domain) [13]. Upon translocation to the cell membrane, the TMDs span the cell membrane, while the NBDs are located inside the cell. In its inactivated state, the channel is closed, preventing the passage of chloride ions and maintaining a balance of ions and water on both sides of the cell membrane. The main activator of CFTR is cyclic AMP (cAMP), which is produced in response to external signals like hormones and neurotransmitters. Increased cAMP levels results in activation of protein kinase A (PKA), which phosphorylates the R-domain of CFTR and results in a confirmational change of CFTR, allowing chloride ions and water to flow out of the cell **(Figure 1B).**

Categorizing CFTR mutations

The roughly 2000 *CFTR* genetic alterations that have so far been described, can be subdivided in different categories, either based on the genetic identity of the mutation or based on the molecular and functional defect of CFTR. When categorizing based on genetic identity, 39.6% of all *CFTR* mutations are missense mutations, 15.6% are frameshift mutations, 11.4% are splice mutations, 8.3% are nonsense mutations and 4.6% are deletions or insertions [14].

Grouping all mutations based on their molecular and functional defect allows for a second type of classification, which connects to potential types of treatment regimens. Multiple variants for this classification system have been proposed with varying complexity, but the most used classification system differentiates 6 classes of functional defects **(Table 1)** [14], [15]. The main focus in this thesis is on class I mutations, encompassing mutations that result in a highly reduced synthesis and stability of CFTR, e.g. large deletions, severe splicing mutations and nonsense or premature termination codon (PTC) mutations. Class II mutations, such as F508del (c.1521_1523delCTT; p.Phe508del; 69.7% allele frequency in CFTR2), impact CFTR protein by causing misfolding and subsequent retention and degradation in the endoplasmic reticulum (ER). Class III mutations impair the regulation of the opening and closing state, so-called gating, of the CFTR channel at the cell membrane. Class IV mutations result in aberrant conductance by resulting in conformational changes of the ion conduction pore hampering ion transport. Class V mutation result in reduced synthesis of aberrant CFTR protein variants due to splice mutations further from splice sites. Lastly, class VI mutations cause a decrease in CFTR plasma membrane stability. Importantly, this classification system remains a simplification as many mutations result in CFTR protein with characteristics corresponding to more than one mutation class, e.g. F508del is characterized by both a trafficking defect (class II) as well as a gating defect (class III).

Table 1: CFTR mutational classes.

	Class I	Class II	Class III	Class IV	Class V	Class VI
Mutation type	Nonsense mutations, splice mutations, large deletions	Missense mutations/ small in-frame deletions	Missense mutations/small in-frame deletions	Missense mutations	Splice mutations further from splice site	Varying
Defect on a protein level	Low levels of non-functional protein	No traffic to cell membrane	Impaired gating at cell membrane	Impaired ion flow due to pore alteration	Reduced synthesis	Decreased plasma membrane stability
Example	G542X/W1282X 711+1G>T	F508del N1303K	F508del G551D	R117H R334W	2789+5G>A	4279insA
Treatment regimen	*Nonsense:* Readthrough compounds *Splice:* ASOs	CFTR correctors	CFTR potentiators	CFTR potentiators	ASOs, amplifiers	CFTR stabilizers
Clinically approved treatments	NA	VX-809 VX-445 VX-661	VX-770	VX-770	NA	NA

Preclinical characterization of CFTR function

Golden standard

To preclinically study CFTR biology, different strategies can be discriminated. A golden standard for characterizing CFTR function has long been the measurement of CFTR-dependent chloride conductance via electrophysiology in Fischer Rat Thyroid (FRT) cells expressing ectopic *CFTR* variants [16]. Other exploited cells that hold increased biological complexity, are human bronchial epithelial (HBE) cells [17]. HBE cells can be obtained through bronchial biopsies or brushings and can be cultured under air-liquid-interface (ALI) conditions, allowing for differentiation of basal progenitor cells into the cell types present in the airway epithelium [18]. Differentiated monolayers subsequentially allow characterization of CFTR function by transepithelial current measurements in Ussing chambers. Importantly, outcomes of such Ussing measurements on patient-derived HBEs correlate with various clinical parameters [19]. In comparison to HBEs, human nasal epithelial cells (HNECs) are even more readily accessible by means of nasal brushing. Similarly as for HBEs, previous studies underline a correlation between preclinical transepithelial ion transport measurements in HNECs and clinical outcomes [20].

Whilst FRT cells, HBECs and HNECs have proven very useful for the development of precision medicine strategies for CF as well as subsequent identification of responsive *CFTR* alleles, they have limitations. FRT cells lack biological complexity and endogenous CFTR biology and don't allow for individual patient stratification. Patient-derived HBECs and HNECs do allow for this personalized character of preclinical experiments, yet their longevity is low due to limited proliferation capacity which hampers continuous experiments and establishment of living biobanks. Furthermore, ALI-differentiation significantly limits

throughput and robustness, and consequently the suitability of HBECs/HNECs for a broad range of experiment types.

In vitro recapitulation of in vivo biological complexity: a paradigm shift

Recent discoveries on establishing patient-derived cell cultures resulted in a major paradigm shift within the field of CF research and beyond. The discovery that patient-derived cells from biopsies of a wide range of tissues or tumors can be cultured as so-called organoids, or mini-organs, in a lab-setting for an indefinite time, had a major impact on many biology-related research-fields. These self-organizing, 3D organoids recapitulate the tissue they are derived from in terms of self-renewal kinetics, cell-type composition and cell polarity [21]. Of major importance for these properties, is the presence of adult stem cells (ASCs) in the original biopsy and lab-cultured cells. ASCs hold regenerative capacity and consequently contribute to tissue homeostasis by regulating cell turnover and differentiation. The first characterized preclinical ASC-based organoid model was based on mouse intestinal crypt-based stem cells, which self-organize into 3D crypt-like structures containing all differentiated cell types [22]. This exploratory work was shortly thereafter followed up by studies on human stem cell cultures of a wide range of epithelial tissues, ranging from the intestine to the lung [23], [24].

Exploiting CF patient-derived cell models to study CFTR function

In the context of CF, patient-derived intestinal organoids (PDIOs) have proven particularly useful for preclinical research. Intestinal organoids contain a central lumen lined by the apical membrane and express under standard culturing conditions CFTR as only ion channel at the apical side of the organoids [25]. If CFTR is functional, it can be activated with cAMP-inducing stimuli such as forskolin, resulting in ion and fluid secretion into the organoid lumen and swelling of the organoid structure. This forskolin-induced swelling (FIS) allows for quantification of CFTR function in a patient-specific manner and has been optimized in our lab in previous studies [25]–[27]. As such, the FIS assay in PDIOs has proven highly useful for fundamental biology studies on CFTR biology in a highly biologically relevant preclinical setting, identification of novel therapeutic regimens for CF and ultimately a precision medicine approach where preclinical stratification of PDIOs can point into the direction of potential clinical responders **(Figure 2).** Importantly, FIS measurements in PDIOs associate with disease severity indicators of CF, long-term disease progression and therapeutic response of the person the PDIOs are derived of [25], [28]–[30]. These preclinical-to-clinical correlations consequently allow screening the effectiveness of available CFTR-restoring drugs at a personal level. Furthermore, PDIOs can be generated within a month after bringing the rectal biopsies into culture, and robust protocols allow freeze-thaw cycles. Altogether, these characteristics enable the establishment of a so-called living biobank [26]. Previous efforts made in our lab on collecting biopsies and establishing PDIO cultures resulted in a biobank with > 1000 PDIOs representing a wide range of *CFTR* genotypes, enabling preclinical studies in an individual and genotype-specific manner.

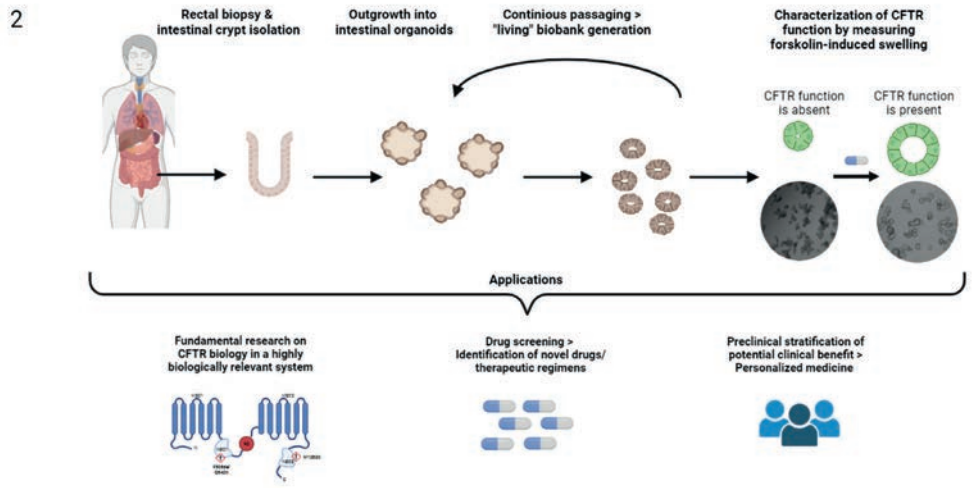

Figure 2. Characterization of CFTR function in patient-derived intestinal organoids (PDIOs). Intestinal crypts can be isolated from rectal biopsies and expanded into 3D patient-derived intestinal organoids (PDIOs), which can be cultured under the right culture conditions in the lab. These PDIOs can be passaged continuously and stored under specific conditions, allowing the generation of a living biobank. PDIOs serve as excellent model for characterization of CFTR function, by means of quantification of forskolin-induced swelling (FIS) of the structures. Here, forskolin induces fluid secretion into the lumen of the PDIOs resulting in subsequent swelling of the structures. The FIS assay is highly suitable for various applications ranging from fundamental research, to the identification of efficient therapeutic regiments and stratification of which pwCF might benefit from these therapeutic regimens.

In addition to the PDIO model, other culture models can be valuable for characterization of organ-specific responses to drugs. As CF particularly affects the airways, ASC-derived airway organoids (AOs) are particularly exploited in the context of CF research. Airway-derived cells can be obtained from different airway locations, ranging from the epithelium of the lower and upper bronchi's to the nasal epithelium [24]. Recent efforts resulted in optimization of quantification of CFTR function in HNEC-derived organoids by FIS assays in a similar manner as in PDIOs [31]. However, longevity and throughput-associated challenges remain for these airway cell systems. Furthermore, whilst many studies have described robust correlations between the FIS assay in CF PDIOs and clinical parameters, no studies yet described a robust correlation between FIS outcomes of HNEC-derived organoids and clinical parameters. Additional studies are needed to affirm its significance as reliable predictor of clinical drug effectiveness. Another important difference between PDIOs and AOs, is the expression of additional ion channels other than CFTR in AOs such as ion channel TMEM16a in bronchial-derived organoids and Na+ channels in nasal spheroids [32]. Clearly, this expression is essential in studies investigating such alternative ion channels, yet it hampers drawing firm conclusions on whether observed fluid secretion is purely CFTR-mediated.

Altogether, both CF PDIOs and AOs hold potential for relevant preclinical studies as well as a personalized medicine approach. The comparison of CFTR restoring potential of specific treatment regimens between PDIOs and AOs can be beneficial and the choice for a specific model should be based on the research question. In this thesis, we aim at characterizing therapeutic regimens that enhance CFTR-mediated fluid secretion as well as performing preclinical experiments with a high preclinical-to-clinical translational value. Based on these goals and the characteristics of PDIOs and AOs, we mainly exploited the PDIO model system throughout this thesis.

Mutation-specific treatment: a paradigm shift *(yet not for everyone)*

Until recently, treatment of pwCF was mostly aimed at treating CF symptoms, e.g. by means of mucolytics to dissolve thick mucus, anti-inflammatory agents to decrease chronic inflammation and antibiotics to treat or prevent infections. Whilst these symptomatic treatments significantly improved medical care and survival for pwCF, the molecular defect underlying CF is not targeted by such treatments. In the last decades, massive progress has been made in the context of precision therapy development for CF resulting in highly effective CFTR protein targeting modulator therapies (HEMTs) which facilitate strong clinical improvements in a significant proportion of pwCF [33].

The development of CFTR modulators

HEMT is the overarching term for combinatorial treatment regimens developed by Vertex, which consist of CFTR correctors that correct CFTR folding and CFTR potentiators that increase CFTR open probility at the cell membrane [34]. The discovery of lumacaftor (VX-809) marked a first significant step toward correcting CFTR misfolding, shortly after which the United States Food and Drug Administration (FDA) approved ivacaftor (VX-770) for clinical use as the first CFTR potentiator. In 2015, the FDA approved the combination of lumacaftor and ivacaftor (marketed as Orkambi), which act together synergistically and proved useful especially in the context of homogeneous F508del-*CFTR* mutations. Follow-up studies resulted in the development of the more potent triple combination therapy of correctors elexacaftor and tezacaftor, combined with ivacaftor (ETI, marketed as Trikafta). The effect of ETI in a clinical setting was outstanding, improving clinical parameters of particularly pwCF with homozygous and heterozygous F508del *CFTR*, outperforming any other currently available CF therapy [35]. Furthermore, > 100 CFTR variant have been indicated as responsive to CFTR modulator treatment by Vertex, accounting for an estimated ~80%. In line with this, the FDA and European Medicines Agency (EMA) at present-day have approved ETI for all non-homozygous F508del genotypes and the FDA specifically approved ETI for several rare genotypes [36], [37]. At present-day, the compounds produced by Vertex are the only regulatory approved CFTR modulators, but CFTR modulators from different companies such as Galapagos (GLPG) are progressing through preclinical studies and clinical trial pipelines as well [38].

It is estimated that 10-15% of all pwCF carry *CFTR* mutations that are unresponsive to HEMTs as monotherapy. Consequently, the focus in the CF research-field has shifted to-

wards filling the unmet clinical need for those genotypes that result in CFTR protein that is not rescued by HEMTs. Various CFTR rescuing strategies can be discriminated, from studying novel mutation-type specific compounds, to characterization of drug repurposing potential of FDA/EMA approved drugs.

Making sense of nonsense

Therapy development has proved particularly challenging for nonsense, or premature termination codon (PTC) mutations, which change the original amino acid (AA) encoding codon into a stop codon upstream of the normal termination codon (NTC). Globally, there are roughly 6000 known genetic disorders of which approximately 10% of the underlying pathological mutations are PTC mutations, accounting for a significant number of affected people [39], [40]. PTC mutations have furthermore been reported in the context of cancer in tumor-suppressor genes such as PTEN and TP53 [41], [42]. As such, compounds targeting PTC mutations have broad, disease-encompassing potential. In the context of CF, pwCF with nonsense mutations represent approximately 8.3% of the worldwide CF population, where G542X (c.1624G>T; p.Gly542X; 2.5% allele frequency in CFTR2) and W1282X are the most prevalent PTC mutations (c.3846G>A; p.Trp128X; 1,2% allele frequency in CFTR2). The presence of a PTC mutation results in aberrant translation termination and consequently the production of truncated protein. Moreover, PTC-bearing mRNAs are degraded by the nonsense-mediated decay (NMD) machinery to prevent the accumulation of potentially hazardous truncated proteins. Consequently, PTC mutations cannot be molecularly restored by HEMTs that solely correct protein folding and increase gating function [43].

Preclinically, the most investigated strategy for treating PTC mutations is aimed at enhancing ribosomal readthrough and incorporating an AA at the PTC site, allowing continuation of translation until the NTC and result in the production of a full-length protein. Since the discovery that aminoglycosides can stimulate ribosomal readthrough by slowing down the ribosome, thereby increasing the chance of incorporation of an AA at the PTC site, many preclinical studies aimed at finding novel readthrough inducing compounds [44]. However, whilst preclinical data on readthrough compounds often indicated promising results, only one readthrough compound has so far reached clinical trials in pwCF, the chemically-engineered aminoglycoside derivative ELX-02 (NB124; Eloxx Pharmaceuticals [45]) **(Figure 3A).** Recent results from ELX-02 clinical trials however show disappointing results and it is unclear now whether Eloxx Pharmaceuticals will continue with further clinical characterization of ELX-02 [45], [46]. The challenging nature of treatments for PTC mutations is further underlined by results of readthrough compounds in other diseases. At present-day, only readthrough compound ataluren has been approved for clinical use in a subset of people with Duchenne Muscular Dystrophy (DMD).

Whilst preclinical studies on readthrough compound monotherapy generally report promising results, its challenging nature has been described by some studies [43], [47], [48]. Main contributors for the challenging nature of readthrough compound monotherapy are **a)** the degradation of PTC harboring mRNAs by NMD, which significantly reduces the pool of

mRNAs for readthrough compounds to act on and **b)** the incorporation of non-cognate AAs at the PTC site upon successful readthrough, which can result in CFTR protein variants with missense mutations that are less functional than the wildtype protein version. As such, PTC functional restoration could be improved by combining readthrough compounds with compounds with different, complementary mode-of-actions. Alternatively, readthrough compounds with different modes-of-action might result in incorporation of specific AAs instead of random AAs at the PTC site [49].

Alternative strategies to rescue PTC mutations such as anticodon-engineered tRNA (ACE-tRNA) technology, are heavily studied as well. ACE-tRNAs are engineered tRNAs that bind to a PTC and carry an AA of choice, resulting in incorporation of the original cognate AA at the PTC site and subsequentially a full-length, wildtype protein [50]. Whilst ACE-tRNAs offer advantages over current pharmacological RT approaches in terms of selectivity and toxicity, challenges such as efficient delivery to the right cell types across various organs need to be tackled.

Drug repurposing in the context of CF

A different strategy for finding novel treatment regimens, is based on characterization of clinically approved drugs for a different disease or treatment group than originally indicated [51]. When repurposing a drug, the risk of failure is diminished due to its established safety profile from preclinical models and early-stage human trials, lowering the chances of safety-related setbacks in subsequent clinical trials. This is advantageous, as drug development is a costly, lengthy and a challenging process, in particular in the context of rare diseases where the numbers of patients are low. It is estimated that the costs for bringing a repurposed drug into a new clinical setting is approximately $300 million, in comparison to $2-3 billion for new compounds [52]. Lastly, studies on drug repurposing potential can increase the understanding of pathways and targets connected to both the originally indicated disease as well as the newly studied disease. In these regards, drug repurposing is an attractive approach in the context of CF.

Altogether, there is a great urgency for finding novel therapeutic approaches for treating nonsense mutations in pwCF and to match such treatment regimens to responders. In this thesis, we employ various strategies **(Figure 3B).**

Clinical parameters for characterizing CFTR function

In this thesis, we often refer to preclinical-to-clinical translation. In this regard, there are different clinical endpoints to characterize CF severity and potential efficacy of CFTR-targeting therapies in pwCF. Two categories of endpoints can be distinguished, clinical endpoints and surrogate endpoints. The FDA characterizes clinical endpoints as direct assessments of a patient's well-being, e.g. functional capacity and survival. Consequently, these are valuable indicators of therapy effectiveness. Surrogate endpoints are laboratory measurements or physical indicators that can stand in for clinical endpoints, which are typically employed when clinical benefits are challenging to observe in trials due to factors such as cost, du-

ration, or sample size constraints. An important surrogate biomarker indicative of disease severity is lung function, which is often seen as the most critical measure of CF progression [54]. Lung function is generally assessed by spirometry, which allows for quantification of the forced expiratory volume in one second (FEV1). Consequently, an over-time increase of FEV1 indicates improvement of lung function. Furthermore, previous studies revealed a robust link between FEV1 and survival, both for absolute FEV1 levels and a relative decrease [55]. Clearly, FEV1 provides valuable information about lung function, yet several challenges accompany FEV1 measurements making it less reliable as a standalone clinical

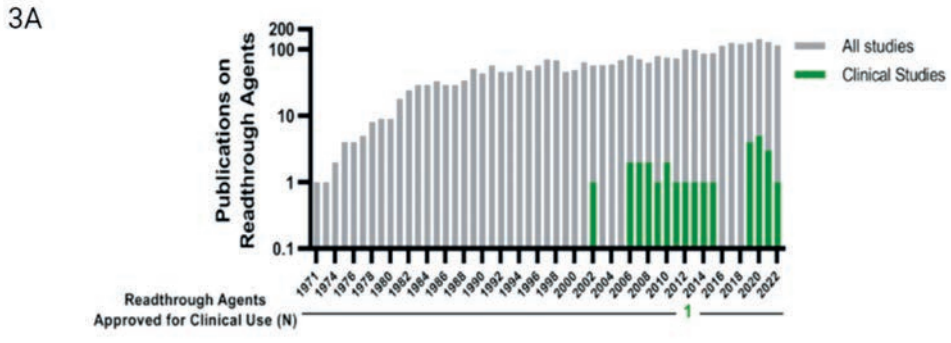

Figure 3. Therapy development for CFTR nonsense mutations: a remaining challenge.
(A) Overview of the number of publications on readthrough (RT) compounds based on a search conducted in PubMed (18/10/2022). Publications specifically on clinical trials are indicated in green, and clinical approval of RT compounds is indicated below the graph. Figure originally from [53]. **(B)** The main three strategies particularly focused on in this thesis for finding novel treatment strategies for nonsense mutations: the characterization of combinatorial treatment regiments, the characterization of highly efficient new-generation readthrough compounds and the study of anticodon-engineered tRNAs.

endpoint for CF. Particularly challenging characteristics of FEV1 measurements are **a)** its variability, FEV1 measurements can vary from test to test and even within the same day, and **b)** the lack of specificity, whilst FEV1 reflects overall lung function it does not provide specific information about the underlying causes of lung dysfunction and CFTR function directly. As such, various non-pulmonary measurements are additionally often exploited as surrogate clinical biomarkers, such as the characterization of weight and body mass index (BMI) of pwCF. An additional clinical parameter that is widely used as diagnostic tool and that allows for direct characterization of CFTR function, is the measurement of chloride ion concentration in sweat. The high salt content in the sweat of pwCF was first observed in the 1950s, and resulted in the development of a sweat chloride test that rapidly became a reliable diagnostic tool for CF [56]. Furthermore, the assessment of the self-reported quality of life (QoL) can aid in characterization of the impact of CF on the overall well-being and daily lives of pwCF. In this context, the CF Questionnaire-Revised (CFQ-R) is widely exploited [57]. The CFQ-R is divided into several domains, each of which focuses on specific aspects of a person's life, such as the vitality domain and respiratory domain.

Additional to these in-patient *(in vivo)* measurements, the previously mentioned PDIOs allow for *ex-vivo* characterization of CF state and/or CFTR function by means of the FIS assay. As these outcomes correlate to clinical parameters of the corresponding person, FIS on PDIOs can also be regarded as surrogate biomarker.

Thesis outline

In this thesis, we aim to characterize novel treatment regimens for those pwCF that do not benefit from HEMTs at present-day. We exploited PDIOs to measure FIS, facilitating discrimination of CF individuals who would benefit from specific drugs. We expect to create impact on **a)** characterization of strategies for rescuing function of genes that carry PTC mutations, b) the development of better CFTR targeting treatments in a nonsense-mutation overarching manner and **c)**, identifying those pwCF who may benefit from these drugs.

The most studied strategy for treating nonsense mutations is by enhancing ribosomal readthrough of PTC mutations, to restore the production of the full-length protein. In the past decade several compounds with readthrough potential have been identified. However, although preclinical results on these compounds are promising, clinical studies in pwCF have not yielded positive outcomes. In **chapter 2,** we review preclinical and clinical research related to readthrough compounds, characterize factors that likely contributed to this observed translational gap and offer recommendations on how to narrow this disparity.

PTC functional restoration might not be feasible by readthrough compound monotherapy. Potentially, combining readthrough compounds with compounds with different, complementary mode-of-actions could have an additive effect. In **chapter 3,** we characterized restoration of PTC-CFTR function in PDIOs with different PTC genotypes, using a combination of readthrough compounds, NMD inhibitors and CFTR modulators.

In **chapter 4,** we continued with investigation of the new-generation readthrough compound DAP, with our collaborator dr. Fabrice Lejeune at the Inserme Institute (France). DAP holds a unique mode-of-action and therefore we hypothesized that it potentially has sufficient potency to function as standalone therapy. We characterized DAP in a newly developed CF mouse model as well as in PDIOs.

Whilst the small-molecule based readthrough compounds investigated in chapter 3 and 4 hold various advantages, different readthrough strategies also hold potential and deserve further investigation. As such, we set up a collaboration with the lab of dr. John Lueck at the University of Rochester (USA) to study ACE-tRNA technology. We describe the efficacy of ACE-tRNAs in different cell systems including PDIOs in **chapter 5.**

We acknowledge that rapid preclinical-to-clinical translation of the results described in chapters 3-5 is challenging, particularly as clinical trials on NMD inhibitors, DAP and ACE-tRNAs have yet to start and clinical trial results of ELX-02 are discouraging. A different strategy that could prove useful and that allows a more rapid translation of preclinical results into a clinical setting, is drug repurposing of FDA-approved compounds. To enable screening a large number of approved drugs, we first upscaled our FIS assay from a 96-WP format to a 384-WP format **(chapter 6).** Subsequently, we exploited this assay for screening CFTR increasing potential of 1400 compounds in PDIOs harboring PTC mutations.

Using the high-throughput FIS screen optimized in chapter 6, we aimed to further investigate drug repurposing potential of the 1400 FDA-approved compounds in a *CFTR* genotype overarching manner. As such, in **chapter 7** we describe the screening of the 1400 FDA-approved compounds in 76 PDIOs which harbor a broad range of (rare) *CFTR* mutations. This resulted in the discovery of several promising candidates, including PDE4 inhibitors and CFTR modulators, which were further investigated.

Due to the diverse molecular working mechanisms of the candidates found and characterized in chapter 6 and 7, we hypothesized that a combination of CFTR modulators, roflumilast and statins could combinatorically restore CFTR function. In **chapter 8,** we describe preclinical data of the drug combination of ETI, roflumilast and simvastatin in PDIOs and present a case study where an individual with CF received this drug combination.

In all studies described above, we exploited CFTR modulators from the company Vertex. Whilst these modulators are generally extremely efficacious, several societal challenges accompany a fair distribution of Vertex HEMTs to all pwCF who would theoretically benefit from them. As such, it remains important to investigate and improve other CFTR modulators. We investigated a different triple therapy consisting of 2 other CFTR modulators and one other CFTR potentiator in PDIOs with a wide range of CFTR mutations in **chapter 9.**

In **chapter 10,** we discuss the strengths and limitations of readthrough therapies and CF precision medicine in an overarching manner.

References

[1] E. A. Ashley, "Towards precision medicine," *Nat. Rev. Genet.,* vol. 17, no. 9, pp. 507–522, 2016.

[2] M. A. Mall, N. Mayer-Hamblett, and S. M. Rowe, "Cystic fibrosis: emergence of highly effective targeted therapeutics and potential clinical implications," *Am. J. Respir. Crit. Care Med.,* vol. 201, no. 10, pp. 1193–1208, 2020.

[3] J. Guo, A. Garratt, and A. Hill, "Worldwide rates of diagnosis and effective treatment for cystic fibrosis," *J. Cyst. Fibros.,* vol. 21, no. 3, pp. 456–462, 2022.

[4] U. C. F. CFTR2 database, "The Clinical and Functional TRanslation of CFTR (CFTR2); available at http://cftr2.org.," *24-09-2022.*

[5] J. R. Riordan *et al.,* "Identification of the cystic fibrosis gene: cloning and characterization of complementary DNA," *Science (80-.).,* vol. 245, no. 4922, pp. 1066–1073, 1989.

[6] Y. Çolak, B. G. Nordestgaard, and S. Afzal, "Morbidity and mortality in carriers of the cystic fibrosis mutation CFTR Phe508del in the general population," *Eur. Respir. J.,* vol. 56, no. 3, 2020.

[7] F. Liu, Z. Zhang, L. Csanády, D. C. Gadsby, and J. Chen, "Molecular structure of the human CFTR ion channel," *Cell,* vol. 169, no. 1, pp. 85–95, 2017.

[8] V. A. McCarthy and A. Harris, "The CFTR gene and regulation of its expression," *Pediatr. Pulmonol.,* vol. 40, no. 1, pp. 1–8, 2005.

[9] E. Maillé *et al.,* "Regulation of normal and cystic fibrosis airway epithelial repair processes by TNF-α after injury," *Am. J. Physiol. Cell. Mol. Physiol.,* vol. 301, no. 6, pp. L945–L955, 2011.

[10] D. T. Montoro *et al.,* "A revised airway epithelial hierarchy includes CFTR-expressing ionocytes," *Nature,* vol. 560, no. 7718, pp. 319–324, 2018.

[11] K. Okuda *et al.,* "Secretory cells dominate airway CFTR expression and function in human airway superficial epithelia," *Am. J. Respir. Crit. Care Med.,* vol. 203, no. 10, pp. 1275–1289, 2021.

[12] R. Bhattacharya, Z. Blankenheim, P. M. Scott, and R. T. Cormier, "CFTR and gastrointestinal cancers: an update," *J. Pers. Med.*, vol. 12, no. 6, p. 868, 2022.

[13] D. N. Sheppard and M. J. Welsh, "Structure and function of the CFTR chloride channel," *Physiol. Rev.,* vol. 79, no. 1, pp. S23–S45, 1999.

[14] K. De Boeck and M. D. Amaral, "Progress in therapies for cystic fibrosis," *Lancet Respir. Med.,* vol. 4, no. 8, pp. 662–674, 2016.

[15] G. Veit *et al.,* "From CFTR biology toward combinatorial pharmacotherapy: expanded classification of cystic fibrosis mutations," *Mol. Biol. Cell,* vol. 27, no. 3, pp. 424–433, 2016.

[16] F. Van Goor, H. Yu, B. Burton, and B. J. Hoffman, "Effect of ivacaftor on CFTR forms with missense mutations associated with defects in protein processing or function," *J. Cyst. Fibros.,* vol. 13, no. 1, pp. 29–36, 2014, doi: 10.1016/j.jcf.2013.06.008.

[17] P. H. Karp *et al.,* "An in vitro model of differentiated human airway epithelia: methods for establishing primary cultures," *Epithel. cell Cult. Protoc.,* pp. 115–137, 2002.

[18] M. L. Fulcher *et al.,* "Novel human bronchial epithelial cell lines for cystic fibrosis research," *Am. J. Physiol. Cell. Mol. Physiol.,* vol. 296, no. 1, pp. L82–L91, 2009.
[19] N. T. Awatade *et al.,* "Measurements of functional responses in human primary lung cells as a basis for personalized therapy for cystic fibrosis," *EBioMedicine,* vol. 2, no. 2, pp. 147–153, 2015.
[20] I. Pranke *et al.,* "Might brushed nasal cells be a surrogate for CFTR modulator clinical response?," *Am. J. Respir. Crit. Care Med.,* vol. 199, no. 1, pp. 123–126, 2019.
[21] H. Clevers, "Modeling development and disease with organoids," *Cell,* vol. 165, no. 7, pp. 1586–1597, 2016.
[22] T. Sato *et al.,* "Single Lgr5 stem cells build crypt-villus structures in vitro without a mesenchymal niche," *Nature,* vol. 459, no. 7244, pp. 262–265, 2009.
[23] T. Sato *et al.,* "Long-term expansion of epithelial organoids from human colon, adenoma, adenocarcinoma, and Barrett's epithelium," *Gastroenterology,* vol. 141, no. 5, pp. 1762–1772, 2011.
[24] N. Sachs *et al.,* "Long–term expanding human airway organoids for disease modeling," *EMBO J.,* vol. 38, no. 4, p. e100300, 2019.
[25] J. F. Dekkers *et al.,* "A functional CFTR assay using primary cystic fibrosis intestinal organoids," *Nat. Med.,* vol. 19, no. 7, pp. 939–945, 2013.
[26] A. M. Vonk *et al.,* "Protocol for Application, Standardization and Validation of the Forskolin-Induced Swelling Assay in Cystic Fibrosis Human Colon Organoids," *STAR Protoc.,* vol. 1, no. 1, p. 100019, 2020, doi: 10.1016/j.xpro.2020.100019.
[27] J. F. Dekkers *et al.,* "Characterizing responses to CFTR-modulating drugs using rectal organoids derived from subjects with cystic fibrosis," *Sci. Transl. Med.,* vol. 8, no. 344, pp. 344ra84-344ra84, 2016.
[28] D. Muilwijk *et al.,* "Forskolin-induced Organoid Swelling is Associated with Long-term CF Disease Progression," *Eur. Respir. J.,* 2022.
[29] K. M. de Winter-de Groot *et al.,* "Stratifying infants with cystic fibrosis for disease severity using intestinal organoid swelling as a biomarker of CFTR function," *Eur. Respir. J.,* vol. 52, no. 3, 2018.
[30] G. Berkers *et al.,* "Lumacaftor/ivacaftor in people with cystic fibrosis with an A455E–CFTR mutation," *J. Cyst. Fibros.,* vol. 20, no. 5, pp. 761–767, 2021.
[31] J. M. B. Gimano D. Amatngalim, Lisa W. Rodenburg, Bente L. Aalbers, Henriette H. M. Raeven, Ellen M. Aarts, Iris A.L. Silva, Wilco Nijenhuis, Sacha Vrendenbarg, Evelien Kruisselbrink, Jesse E. Brunsveld, Cornelis M. van Drunen, Sabine Michel, Karin M. de Winter-de, "Measuring cystic fibrosis drug responses in organoids derived from 2D differentiated nasal epithelia," *bioRxiv,* 2022.
[32] G. D. Amatngalim *et al.,* "Measuring cystic fibrosis drug responses in organoids derived from 2D differentiated nasal epithelia," *Life Sci. Alliance,* vol. 5, no. 12, 2022.
[33] K. A. McBennett, P. B. Davis, and M. W. Konstan, "Increasing life expectancy in cystic fibrosis: Advances and challenges," *Pediatr. Pulmonol.,* vol. 57, pp. S5–S12, 2022.
[34] K. A. Despotes and S. H. Donaldson, "Current state of CFTR modulators for treatment of Cystic Fibrosis," *Curr. Opin. Pharmacol.,* vol. 65, p. 102239, 2022.

[35] P. G. Middleton *et al.,* "Elexacaftor–tezacaftor–ivacaftor for cystic fibrosis with a single Phe508del allele," *N. Engl. J. Med.,* vol. 381, no. 19, pp. 1809–1819, 2019.
[36] "KaftrioFDA approval," 2023. https://www.accessdata.fda.gov/scripts/cder/daf/index.cfm?event=overview.process&ApplNo=212273
[37] "Kaftrio EMA approval", [Online]. Available: https://www.ema.europa.eu/en/medicines/human/EPAR/kaftrio
[38] E. Bardin *et al.,* "Modulators of CFTR. Updates on clinical development and future directions," *Eur. J. Med. Chem.,* vol. 213, p. 113195, 2021.
[39] M. Mort, D. Ivanov, D. N. Cooper, and N. A. Chuzhanova, "A meta-analysis of nonsense mutations causing human genetic disease," *Hum. Mutat.,* vol. 29, no. 8, pp. 1037–1047, 2008.
[40] S. Nguengang Wakap *et al.,* "Estimating cumulative point prevalence of rare diseases: analysis of the Orphanet database," *Eur. J. Hum. Genet.,* vol. 28, no. 2, pp. 165–173, 2020.
[41] M. W. Ferguson *et al.,* "The antimalarial drug mefloquine enhances TP53 premature termination codon readthrough by aminoglycoside G418," *PLoS One,* vol. 14, no. 5, p. e0216423, 2019.
[42] S. Luna *et al.,* "A global analysis of the reconstitution of PTEN function by translational readthrough of PTEN pathogenic premature termination codons," *Hum. Mutat.,* vol. 42, no. 5, pp. 551–566, 2021.
[43] M. A. Aksit *et al.,* "Decreased mRNA and protein stability of W1282X limits response to modulator therapy," *J. Cyst. Fibros.,* vol. 18, no. 5, pp. 606–613, 2019.
[44] J. F. Burke and A. E. Mogg, "Suppression of a nonsense mutation in mammalian cells in vivo by the aminoglycoside anthiotics G–418 and paromomycin," *Nucleic Acids Res.,* vol. 13, no. 17, pp. 6265–6272, 1985.
[45] J. Woolford, "Eloxx Pharmaceuticals Reports Positive Topline Results from Monotherapy Arms of Phase 2 Clinical Trial of ELX-02 in Class 1 Cystic Fibrosis Patients," 2021. [Online]. Available: https://investors.eloxxpharma.com/node/11986/pdf
[46] J. Woolford, "Eloxx Pharmaceuticals Reports Topline Results from Phase 2 Combination Clinical Trial of ELX-02 in Class 1 Cystic Fibrosis (CF) Patients," 2022. [Online]. Available: https://investors.eloxxpharma.com/news-releases/news-release-details/eloxx-pharmaceuticals-reports-topline-results-phase-2?fbclid=IwAR31GRojriXkl1n-jErqm3qQCY6-Cw4bgmqP-hzogmDAz58cY9C_2xnjZeXw
[47] O. Laselva *et al.,* "Functional rescue of c. 3846G> A (W1282X) in patient-derived nasal cultures achieved by inhibition of nonsense mediated decay and protein modulators with complementary mechanisms of action," *J. Cyst. Fibros.,* vol. 19, no. 5, pp. 717–727, 2020.
[48] W. Wang, J. S. Hong, A. Rab, E. J. Sorscher, and K. L. Kirk, "Robust stimulation of W1282X-CFTR channel activity by a combination of allosteric modulators," *PLoS One,* vol. 11, no. 3, p. e0152232, 2016.
[49] C. Trzaska *et al.,* "2, 6-Diaminopurine as a highly potent corrector of UGA nonsense mutations," *Nat. Commun.,* vol. 11, no. 1, pp. 1–12, 2020.

[50] J. D. Lueck *et al.,* "Engineered transfer RNAs for suppression of premature termination codons," *Nat. Commun.,* vol. 10, no. 1, pp. 1–11, 2019.
[51] S. Pushpakom *et al.,* "Drug repurposing: progress, challenges and recommendations," *Nat. Rev. Drug Discov.,* vol. 18, no. 1, pp. 41–58, 2019.
[52] M. Rudrapal, S. J. Khairnar, and A. G. Jadhav, "Drug repurposing (DR): an emerging approach in drug discovery," *Drug repurposing-hypothesis, Mol. Asp. Ther. Appl.,* vol. 10, 2020.
[53] S. Spelier, E. P. M. van Doorn, C. K. van der Ent, J. M. Beekman, and M. A. J. Koppens, "Readthrough compounds for nonsense mutations: bridging the translational gap," *Trends Mol. Med.,* 2023.
[54] M. S. Muhlebach *et al.,* "Biomarkers for cystic fibrosis drug development," *J. Cyst. Fibros.,* vol. 15, no. 6, pp. 714–723, 2016.
[55] R. Szczesniak, S. L. Heltshe, S. Stanojevic, and N. Mayer-Hamblett, "Use of FEV1 in cystic fibrosis epidemiologic studies and clinical trials: a statistical perspective for the clinical researcher," *J. Cyst. Fibros.,* vol. 16, no. 3, pp. 318–326, 2017.
[56] A. C. Gonçalves *et al.,* "Chloride and sodium ion concentrations in saliva and sweat as a method to diagnose cystic fibrosis," *J. Pediatr. (Rio. J).,* vol. 95, pp. 443–450, 2019.
[57] A. L. Quittner *et al.,* "Psychometric evaluation of the Cystic Fibrosis Questionnaire-Revised in a national sample," *Qual. Life Res.,* vol. 21, pp. 1267–1278, 2012.

Chapter | 2

Readthrough compounds for nonsense mutations: bridging the translational gap

Trends in Molecular Medicine, April 2023, Volume 29, Issue 4

Sacha Spelier[1,2], Eveline P.M. van Doorn[1], Cornelis K. van der Ent[1,2], Jeffrey M. Beekman[1,2,3] and Martijn A.J. Koppens[1,2,4]

1. Department of Pediatric Respiratory Medicine, Wilhelmina Children's Hospital, University Medical Center, Utrecht University, 3584, EA, Utrecht, The Netherlands **2.** Regenerative Medicine Utrecht, University Medical Center, Utrecht University, 3584 CT, Utrecht, The Netherlands **3.** Center for Living Technologies, Eindhoven-Wageningen-Utrecht Alliance, Utrecht, The Netherlands **4.** Department of Metabolic Diseases, Wilhelmina Children's Hospital, University Medical Center, Utrecht University, 3584 EA, Utrecht, The Netherlands

Highlights

- Approximately 10% of all pathological mutations are nonsense mutations which are responsible for the most severe cases of genetic diseases but for which no treatment regimens are available.
- The main strategy for treating nonsense mutations is by enhancing ribosomal readthrough of premature stop codons through the action of readthrough compounds, thus restoring production of full-length protein.
- Most preclinical studies on readthrough compounds have yielded positive results, but have been performed in reporter-based assays despite recent scientific developments that have significantly improved disease models, such as patient-derived cells in functional assays.
- Clinical trials have yielded disappointing results, and further interpretation of readthrough compound efficacy across clinical trials is challenging because of differences in research design, treatment length, and clinical endpoints.
- Characterization of factors that contribute to the translational gap between readthrough compounds in preclinical studies versus clinical trial results is necessary to make sense of nonsense mutation therapy.

Abstract

Approximately 10% of all pathological mutations are nonsense mutations that are responsible for several severe genetic diseases for which no treatment regimens are currently available. The most widespread strategy for treating nonsense mutations is by enhancing ribosomal readthrough of premature termination codons (PTCs) to restore the production of the full-length protein. In the past decade several compounds with readthrough potential have been identified. However, although preclinical results on these compounds are promising, clinical studies have not yielded positive outcomes. We review preclinical and clinical research related to readthrough compounds and characterize factors that contribute to the observed translational gap.

Keywords

Nonsense mutations - rare diseases – readthrough - nonsense-mediated decay - translational gap

The striking gap between preclinical and clinical studies

In the past decade several new therapeutics have been developed for rare hereditary diseases. However, the therapeutic perspective differs to a large extent between patients and is greatly influenced by the type of mutation. Therapy development has proved particularly challenging for nonsense or PTC mutations which change the original amino acid (AA) codon into a stop codon. Nonsense mutations result in aberrant translation and low levels of truncated proteins with loss-of-function characteristics [1,2]. For patients carrying PTC mutations, treatment is based on treating symptoms because no curative treatments are available. Globally, there are roughly 6000 known genetic disorders, of which the best known PTC disease examples are cystic fibrosis (CF, see Glossary) and Duchenne muscular dystrophy (DMD) [3]. Approximately 10% of all pathological mutations are PTC mutations, accounting for a significant number of affected patients [1]. In addition, PTC mutations have been reported in the context of cancer in tumor-suppressor genes such as PTEN and TP53 [4,5]. As such, compounds targeting PTC mutations have broad, disease-encompassing potential.

The most widespread strategy for treating PTC mutations is aimed at enhancing ribosomal readthrough of premature stop codons by incorporating an AA at the PTC site, thus restoring the production of a full-length, functional protein. Since the discovery of aminoglycosides as the first class of compounds that stimulate ribosomal readthrough by slowing down the ribosome, thereby increasing the chance of inducing incorporation of AAs at the PTC site [6], >30 therapeutic readthrough compounds have been identified and characterized in preclinical studies. However, only ataluren has been approved for a subset of patients with a single disease: DMD. This difference between the vast number of preclinical studies and disappointing outcomes from clinical studies is striking **(Figure 1A)**. To investigate factors contributing to this translational gap, we review preclinical and clinical research related to readthrough compounds. We first summarize the characteristics of the most recently discovered and validated readthrough compounds, focusing on the types of assays in which those compounds were discovered and validated. We then review the outcomes of clinical trials of readthrough compounds. This double-sided overview will give insight into which preclinical and clinical aspects contribute to the observed translational gap. Finally, we summarize which steps could contribute to advancing the field of readthrough biology **(Figure 2, Key figure).**

Translation termination and readthrough in health and disease

During translation, tRNAs charged with AAs bind to the ribosomal acceptor-site (A-site) via its anticodon sequence. Consequently, the tRNA-associated AA is coupled to the growing polypeptide chain. Translation termination occurs when the ribosomal A-site reaches one of the three natural termination codons (NTCs): UAA, UAG, or UGA. Translation termination is heavily regulated by an intricate termination complex, of which eukaryotic release factor 1 (eRF1) and eRF3 are key components [7,8]. The presence of a PTC mutation upstream of the NTC results in aberrant translation termination and consequently the production of truncated protein **(Figure 1B).** Moreover, PTC-bearing mRNAs are degraded by the nonsense-mediated decay (NMD) machinery to prevent the accumulation of potentially hazardous truncated proteins [9]. NMD is a heavily regulated quality control mechanism and has recently been reviewed in great detail by Lejeune, Supek, and colleagues [10,11]. Based on the characteristics of PTC harboring mRNAs, two main routes for NMD induction have been proposed **(Figure 1C).**

Under native conditions, a small fraction (<0.1%) of PTCs undergo translational readthrough [12]. This is even less frequent at NTCs owing to PTC–NTC differences such as the increased distance of PTCs from the 3'-end and thus reduced interaction with translation termination agonists such as poly(A) tail-binding proteins (PABPs). In addition, multiple

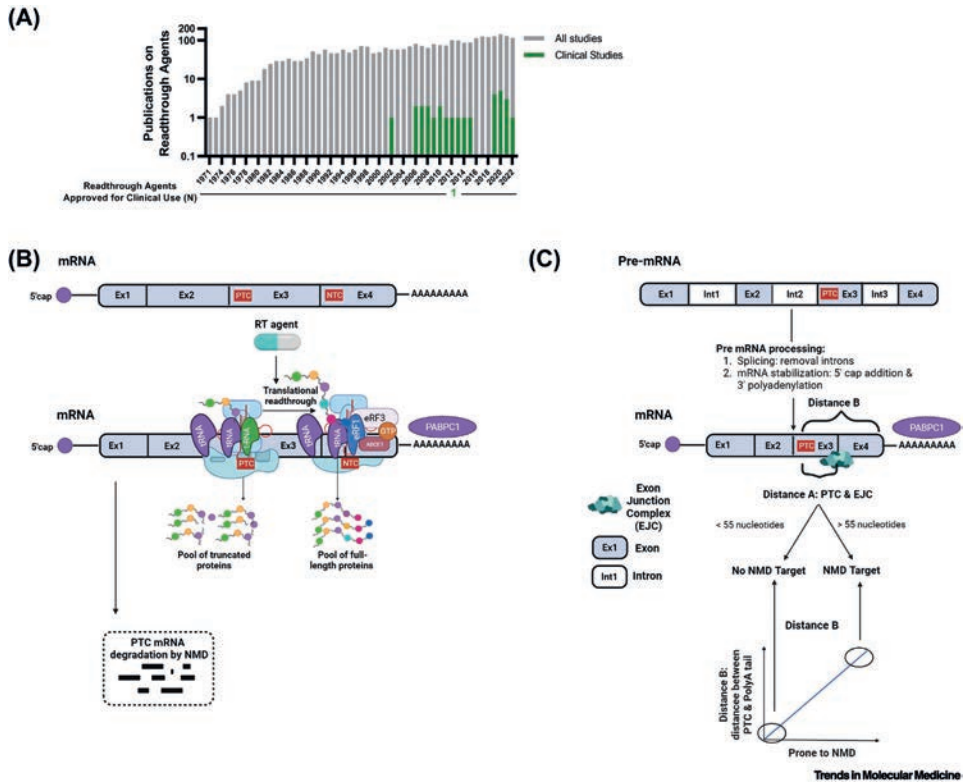

Figure 1. Translation termination in health and disease.
(A) Overview of the number of publications on readthrough (RT) compounds found in PubMed (search conducted on 18 October 2022). Publications specifically on clinical trials are indicated in green, and clinical approval of RT compounds is indicated below the graph. **(B)** In the top panel, translation termination at a premature termination codon (PTC) site is schematically summarized. In brief, eukaryotic release factor 1 (eRF1), that structurally resembles a tRNA, binds directly to the PTC site located in the ribosomal acceptor (A)-site [7.]. The GTPase eRF3 then hydrolyses GTP to GDP resulting in a conformational change of eRF1, promoting peptide release and replacement of eRF3 by ATPase ABCE1. ABCE1 promotes ATP to ADP hydrolysis, resulting in recycling of the ribosomal subunits [101.]. Poly(A) tail-binding protein C1 (PABPC1) resides on the poly(A) tail and interacts with eRF3 to promote translation termination [102.]. Subsequently, PTC mRNAs are rapidly degraded by nonsense-mediated decay (NMD). The bottom panel shows that compounds with RT activity can induce ribosomal RT at the PTC site, resulting in full-length protein. **(C)** Schematic of NMD and the two main routes resulting in NMD [103.]. Because exon junctions always precede the natural termination codon (NTC), an exon junction complex (EJC) downstream of a stop codon indicates the presence of a PTC (distance A). In addition, the increased distance between PTC sites and proteins binding to the poly(A) tail such as PABPC1 is a second trigger for the NMD process to start (distance B). Although eRF3 plays a role in translation termination regulation, it is also involved in NMD, as do up-frameshift (UPF) proteins [9.] and suppressor of morphogenesis in genitalia (SMG) proteins [104.]. Abbreviations: Ex, exon; Int, intron.

alternative stop codons are often found downstream of the NTC, further decreasing the chance of extensive readthrough of the 3'-untranslated region (UTR) [8,13,14]. Importantly, this absence of NTC quality control mechanisms at PTC sites provides a rationale for the development of therapies that can selectively increase readthrough at PTCs over NTCs.

Readthrough compounds: classes and efficacy determinants

Readthrough compounds act through various modes of action (MoAs) to promote the incorporation of near-cognate tRNAs that outcompete the translation termination complex and consequently drive translation beyond the PTC site **(Figure 3A)** [6,15,16]. The first class of identified readthrough compounds were aminoglycosides, originally used as antibiotics, that inhibit ribosome proofreading fidelity – thereby increasing the chance of non-cognate tRNAs binding to the PTC [17]. Although initial results on the readthrough activity of aminoglycosides were promising, their use was associated with persistent and serious ototoxicity and nephrotoxicity [18]. Other categories encompass compounds such as CC90009 and SRI-41315 that inhibit factors of the translation termination complex [19,20], compounds such as 2,6-diaminopurine (DAP) that reduce the fidelity of specific tRNAs [21], and nucleoside analogs such as clitocine [22]. For several readthrough compounds, the exact MoA has not been clarified.

Multiple factors influence the efficacy of most readthrough compounds irrespective of their MoA [23]. In brief, the main determinants are (i) mRNA transcript levels, depending on the gene in question and overall NMD activity, (ii) PTC identity, location, and sequence context, and (iii) the characteristics of the affected protein **(Table 1).**

The search for novel and optimized readthrough compounds can be divided into three main categories: (i) high-throughput compound screening, (ii) computational approaches, and (iii) empirical, hypothesis-driven approaches **(Figure 3B).** In the next section we review preclinical studies on the most recently discovered and validated readthrough compounds, focusing on the types of assays in which those compounds were discovered and validated.

Readthrough compound discovery

The first widely used assays to measure readthrough were based on expression of PTC-bearing luciferase transgenes in cell lines, enabling sensitive readthrough measurements through detection of chemiluminescence. Owing to the straightforward read-out, luciferase reporter systems have been used in many high-throughput screens for readthrough compound discovery. For instance, they were used to demonstrate the readthrough activity of gentamicin, G418, paromomycin, clitocine, and amlexanox [6,24,25]. Ataluren was discovered in a similar manner in an ultra-high-throughput screen of ~800 000 compounds [26]. In follow-up experiments, however, ataluren was found to directly bind to and stabilize firefly luciferase, indicating an indirect, false-positive effect in previous studies [27]. Subsequent validation studies yielded conflicting results [28] because no readthrough activity was demonstrated in cell models for obesity [29], peroxisome biogenesis disorders [30], long-QT syndrome [31], or CF [32].

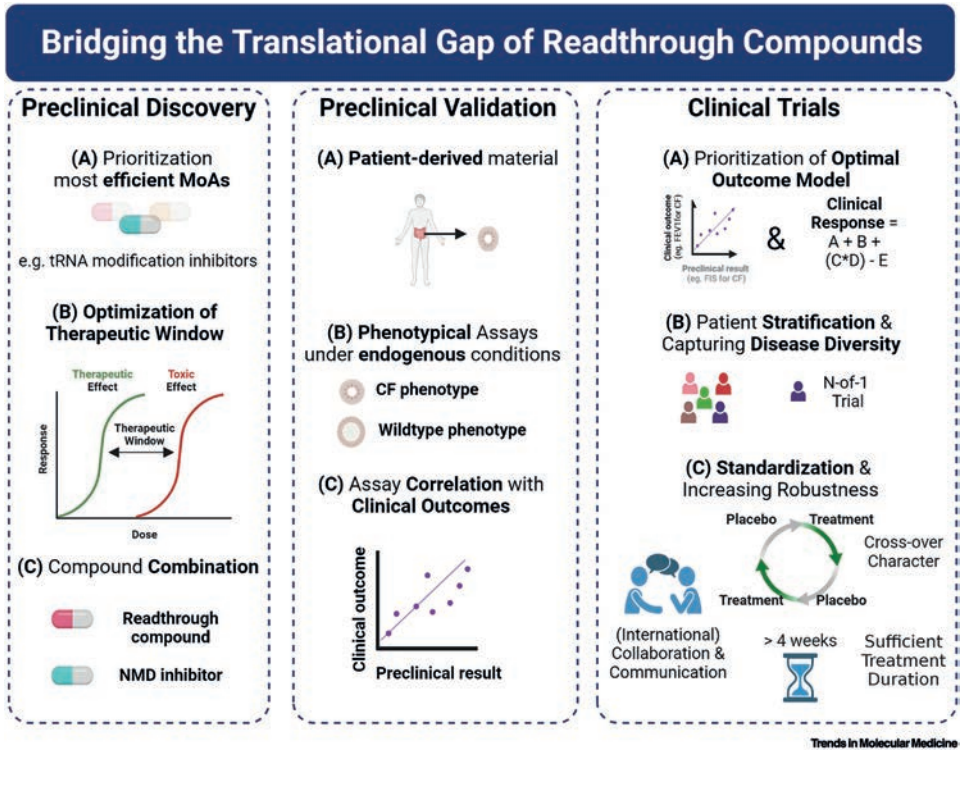

Figure 2 (Key figure). Readthrough compounds for nonsense mutations: bridging the translational gap.

There is a large translational gap between the success of readthrough compounds in preclinical studies and the absence of effect in clinical trials. To bridge this gap, the field should give attention to several aspects: (i) the preclinical discovery phase (left panel) could prioritize the development of readthrough compounds with more potent MoAs, (ii) the preclinical validation phase (middle panel) could employ preclinical assays that correlate with clinical outcomes, and (iii) clinical trials (right panel) could, for example, prioritize the development of more complex and complete clinical outcome models. Abbreviations: CF, cystic fibrosis; MoA, mode of action; NMD, nonsense-mediated decay.

Table 1: Summary of determinants that influence the efficacy of readthrough compounds.

Determinant	Depends on	Potential to interfere	Reference
mRNA transcript levels	1. Nonsense-mediated decay (NMD) activity 2. Stability mRNA	1. Yes, inhibition of NMD. 2. Yes, mRNA stabilization by amplifiers.	1. [24], [25] 2. [26]
PTC identity, location and surrounding sequence	1. PTC proximity to NTC affecting size and function of the truncated peptide 2. Readthrough susceptibility: UGA < UAG < UAA & PTC surrounding sequence 3. Identity of incorporated AA	1. No 2. No 3. Yes, depending on the mode-of-action of the readthrough compound.	1. No 2. [14] 3. [21]
Protein identity	1. Half-life protein 2. Minimal amount of protein for proper function	a) No b) Partially, protein modulators can aid in proper folding and protein function. Overall minimal amount of protein for sufficient function is disease-dependent.	1. – 2. [24], [25]

Legends:
Determinants are divided into three main categories, affecting (i) mRNA transcript levels, depending on the gene in question and overall NMD activity, (ii) PTC identity, location, and its sequence context; and (iii) the characteristics of the affected protein. NA, not available.

However, readthrough activity of ataluren was demonstrated in other experiments for the same and other disease models, including Usher syndrome [33], Miyoshi myopathy [34], DMD [26], and CF [35].

Although luciferase reporter assays are sensitive detectors of readthrough, they can result in compounds with readthrough activity that is negligible in a physiological setting. Updated versions of luciferase reporters include dual reporters that enable internal expression normalization and thereby increase the robustness of readthrough quantification [36, 37, 38, 39], as well as intronic reporters that allow screening in the context of NMD [21,40]. Dual reporter assays were instrumental in the discovery of NB30 and NB54 [41] and were used to reassess the readthrough activity of gentamicin, amikacin, negamycin, and escin [42, 43, 44]. Intronic reporter assays resulted in the discovery of the readthrough capacity of DAP in a 164 compound medium-throughput screen [40]. SRI-37240 and SRI-41315 were similarly discovered in an ultra-high-throughput screen of ~771 345 compounds [19].

Alternative approaches have been designed to complement luciferase-based assays. Du *et al*. developed a protein-based transcription-translation (PTT) ELISA to screen 34 000 compounds and identified 12 non-aminoglycosides with readthrough activity, including RTC13 and RTC14 [45]. Screening of a second library of ~36 000 compounds resulted in discovery of GJ071 and GJ072 [46]. Alternatively, Liang *et al*. measured readthrough by fusing a PTC-bearing cystic fibrosis transmembrane conductance regulator (CFTR) transgene to the horseradish peroxidase (HRP) gene whose protein product is detectable through its chemiluminescence activity [47]. Although both PTT-ELISA and CFTR-transgene-HRP assays may complement luciferase-based reporter systems, they could similarly produce false-positive hits that augment HRP activity. A different dual fluorescent reporter system

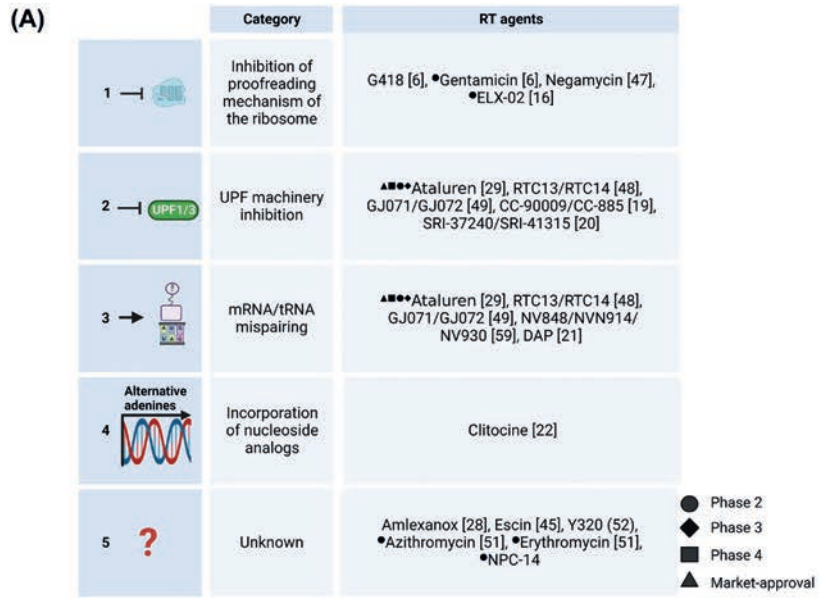

Figure 3. Ribosomal readthrough as therapeutic strategy.
(A) The modes of action (MoAs) of readthrough compounds can be divided into five main categories. Category 1 compounds, which include aminoglycosides, interact with 16S rRNA at the ribosomal acceptor (A)-site to inhibit stop codon recognition by release factors. Consequently, near-cognate tRNAs can outcompete the translation termination complex [6.,16.,44.]. Category 2 compounds directly inhibit components of the translation termination complex. For example, CC-90009 and CC-885 have been shown to inhibit eRF1 and eRF3 levels [19.,20.,26.,45.,46.]. Category 3 compounds reduce the fidelity of

near-cognate tRNAs, thus increasing their chance of binding to stop codons [21.,26.,45.,46.,56.]. Category 4 compounds are nucleoside analogs that are incorporated into the mRNA during transcription and become part of the premature termination codon (PTC) [22.]. Such PTCs are not recognized by eRF1 as a stop codon, increasing the probability of near-cognate tRNA insertion. Category 5 compounds include compounds for which the exact MoA has not been clarified [25.,42.,48.,49.]. **(B)** A schematic of the experimental approaches towards readthrough compound discovery and validation. In the discovery phase (left panel), three different approaches can be employed: high-throughput screening, computational biology, and target-driven research. In the compound validation phase, experimental approaches can be discriminated based on (i) the gene studied and PTC identity, and (ii) the model system employed, ranging from conventional 2D cell lines and more complex patient-derived organoids and animal studies (middle panel). The main assay types used for either compound discovery or validation are illustrated in the right panel and can be divided into (i) ectopic assays in which PTC-harboring DNA constructs are used that allow high-throughput reporter system assays, (ii) endogenous conventional protein detection assays such as western blotting, and (iii) complex phenotypic assays such as the forskolin-induced swelling (FIS) assay for cystic fibrosis (CF). Abbreviation: WT, wild type.

with a readout based on flow cytometry was developed by Caspi and colleagues, resulting in discovery of azithromycin and erythromycin as readthrough compounds [48]. Their vector system – which is not based on luciferase expression – has advantages over luciferase-based constructs which have shown to interact directly with, for example, ataluren. Detecting protein levels from the endogenous gene of interest rather than transgenic assays is generally less sensitive and less scalable, but its hit detection is likely more robust. Y320 was discovered in this manner, and increased readthrough of endogenous TP53637C>T (encoding TP53-R213X) as measured with immunofluorescence microscopy [49].

Unbiased high-throughput screening methods contrast with hypothesis-driven approaches. Baradaran-Heravi *et al.* sought to inhibit release factors, hypothesizing that their depletion increases the chance of ribosomal readthrough by stalling translation termination at stop codons [20]. Compounds CC-885 and CC-90009, that are known to degrade eRF3a, indeed enhanced readthrough in a panel of disease models.

Overall, the discovery phase in general requires high-throughput assay capacity which is often best achieved with exogenous reporter systems, as exemplified in studies on DAP, ataluren, SRI-41315, RTC13/RTC14, and GJ071/GJ072. However, it is essential that the outcomes of such experiments are validated in more complex, phenotypic experiments in patient-derived model systems that capture the complex biology of the disease in question.

Readthrough compound validation

A first challenge after compound discovery is the subsequent hit-to-lead drug development process in which hits are optimized in terms of safety, efficacy, and pharmacokinetic properties. Computational chemistry has played an important role in this hit-to-lead stage, for example, by decreasing the toxicity and increasing the efficacy of aminoglycoside derivatives ataluren [50, 51, 52, 53, 54] and ELX-02, which were shown to be less toxic than gentamicin or G418 [16,37,55,56]. Ataluren derivatives NV848/NV914 and NV930 are in particular worth mentioning because their preclinical work in the context of CF is promising and recent pharmacokinetic data highlight a favorable pharmacokinetic profile in animal

Table 2: Summary of outcomes of Phase 2/3/4 clinical trials for readthrough compounds[a,b]

NCT number	Phase and number of participants (participant age)	Timeframe (weeks)[c]	Study design	ΔFEV1pp	Remarks	Refs
Ataluren for cystic fibrosis						
NCT00237380	Phase 2; *N* = 23 (≥18 years)	**2**–2–**2**–2	INT, SG, OLA	Cycle 1: ↑ Cycle 2: NA		[76]
NCT00351078	Phase 2; *N* = 19 (≥18 years)	**12**–4	INT, SG, OLA	NS		[105]
NCT00234663	Phase 2; *N* = 24 (≥18 years)	**8**–408	INT, SG, OLA, NR	NA	Trial outcomes are not available online or in publication form	
NCT00458341	Phase 2; *N* = 30 (6–18 years)	**2**–2–**2**–2	INT, CO, OLA, R	NS		[106]
NCT00803205	Phase 3; *N* = 209 (≥6 years)	**48**–4	INT, P, R	NS ↑ + 5% (*P* = 0.0082)	*Post hoc* analysis on patients not treated with tobramycin	[62]
NCT02139306	Phase 3; *N* = 279 (≥6 years)	**48**–4	INT, P, R	NS		[77]
NCT01140451	Phase 3; *N* = 191 (≥6 years)	**96**–4	INT, P, R	NA	Extension of NCT00803205	
NCT02107859	Phase 3; *N* = 61 (≥6 years)	**192**–4	INT, SG, OLA		Terminated due to lack of success of NCT02139306	
NCT02456103	Phase 3; *N* = 246 (≥6 years)	**96**–4	INT, SG, OLA			
NCT03256968	Phase 5; *N* = 1 (31 years)	**48**–368	INT, SG, OLA	NS	Combined with ivacaftor	[78]
NCT03256799	Phase 5; *N* = 1 (32 years)	**48**–368	INT, SG, OLA	NS	Combined with ivacaftor	[78]
Ataluren for Duchenne muscular dystrophy						
NCT00264888	Phase 2; *N* = 38 (≥5 years)	**4**–244	INT, NR, SG, OLA	NA	Trial outcomes are not available online or in publication form	[81]
NCT00592553	Phase 2; *N* = 174 (≥5 years)	**48**–6	INT, R, P, QM	NS (*P* = 0.056)	Longer before 10% decline in 6MWD	[82]
NCT00759876	Phase 2; *N* = 36 (all ages)	**96**–0	INT, SG, OLA		Terminated due to lack of efficacy of ataluren in NCT00592553	
NCT00847379	Phase 2; *N* = 173 (≥5 years)	**96**–6	INT, SG, OLA			
NCT01009294	Phase 3; *N* = 6 males (≥7 years)	**50**–366	INT, SG, OLA			
NCT02090959	Phase 3; *N* = 219 (7–15 years)	**144**–6	INT, R, P, QM		Terminated, due to withdrawal of sponsor and commercial availability of ataluren for DMD	
NCT01826487	Phase 3; *N* = 230 (7–16 years)	**48**–6	INT, R, P, QM	NS	All outcomes positive in a prespecified group, 6MWD >300 and <400 m	[80]
NCT01557400	Phase 3; *N* = 94 (all ages)	**240**–6	INT, SG, OLA	NS		[79]
NCT02819557	Phase 2; *N* = 14 (2–5 years)	**52**–4	INT, SG, OLA	NA	Trial outcomes are not available online or in publication form	
NCT03796637	Phase 2; *N* = 6 (all ages)	NA	INT, SG, OLA	NA		
NCT03648827	Phase 2; *N* = 20 (2–7 years)	NA	INT, SG, OLA	NA		
NCT04336826	Phase 2; *N* = 10 (6 months–2 years)	**24**–52	IN Schermarbeelding		Recruiting	
NCT01247207	Phase 3; *N* = 270 (all ages)	**384**–4	INT, SG, OLA		Enrolling by invitation	
NCT03179631	Phase 3; *N* = 360 (≥5 years)	NA	INT, R, P, QM		Active, not recruiting	[107]
Ataluren for methylmalonic acidemia			INT, SG, OLA			
NCT01141075	Phase 2; *N* = 11 (≥2 years)	**96**–48	INT, SG, OLA	NA	Terminated due to low patient enrollment	
Ataluren for hemophilia						
NCT00947193	Phase 2; *N* = 13 (≥18 years)	**2**–2–**2**–2	INT, SG, OLA	NA	Terminated, sponsor withdrawal	
Ataluren for Dravet syndrome (DS) and CDKL5 deficiency syndrome (CDD)						
NCT02758626	Phase 2; *N* = 16 (2–12 years)	**12**–4–**12**–4–16	INT, R, CO, QM	NS		[108]
Ataluren for aniridia						
NCT02647359	Phase 2; *N* = 39 (≥2 years)	**240**–4	INT, R, P, QM	NS		
NCT04117880	Phase 2; *N* = 0 (≥2 years)	NA	INT, SG, OLA		Withdrawn	
ELX-02 for cystic fibrosis						
NCT04135495	Phase 2; *N* = 16 (≥18 years)	**9**–0	INT, R, P, QM		Recruiting	[77]
NCT04126473	Phase 2; *N* = 16 (≥16 years)	**9**–0	INT, SG, OLA		Recruiting, extension of NCT04135495, ivacaftor addition	[78]
ELX-02 for nephropathic cystinosis						
NCT04135495	Phase 2; *N* = 16 (≥18 years)	**9**–0	INT, R, P, QM		Recruiting	[77]
NCT04126473	Phase 2; *N* = 16 (≥16 years)	**9**–0	INT, SG, OLA		Recruiting, extension of NCT04135495, ivacaftor addition	[78]
ELX-02 for nephropathic cystinosis						
NCT04069260	Phase 2; *N* = 3 (≥12 years)	6–**4**–4	INT, SG, OLA	NA	Terminated prematurely due to study design limitations	
Gentamicin for junctional epidermolysis bullosa (JEB)						
NCT04140786	Phase 2; *N* = 6 (all ages)	**12**–12.8 **3.4**–12.8	INT, NR, OLA	NA	Primary outcome is safety, not an efficacy-associated parameter	[109]
NCT03526159	Phase 2; *N* = 5 (all ages)	**2**–10	INT, SG, OLA		Recruiting	
Gentamicin for recessive dystrophic epidermolysis bullosa (RDEB)						
NCT03012191	Phase 2; *N* = 6 (all ages)	**24**[d]	INT, SG, OLA	NA	Primary outcome is safety, not an efficacy-associated parameter	
NCT03392909	Phase 2; *N* = 9 (≥7 years)	**2**–22 **12**–12	INT, SG, OLA	NA	Trial outcomes are not available online or in publication form	
NCT02698735	Phase 2; *N* = 5 (all ages)	**12**[d]	INT, NR, P, TM	NA	Increase in anchoring fibrils (AFs) and wound closure, significance NA	[85]
Gentamicin for hypotrichosis simplex						
NCT03492866	Phase 2; *N* = 8 (18–12 years)	**2**–10	INT, NR, CO, OLA	NA	Trial outcomes are not available online or in publication form	
Erythromycin for adenomatous polyposis						
NCT02175914	Phase 5; *N* = 20 (≥18 years)	**12**–36	INT, SG, OLA	NA	Trial outcomes are not available online or in publication form	
NCT02354560	Phase 5; *N* = 30 (6–18 years)	**16**–32	INT, SG, OLA	NA	Trial outcomes are not available online or in publication form	
Azithromycin for adenomatous polyposis						
NCT04454151	Phase 5; *N* = 15 (10–17 years)	**16**–48	INT, SG, OLA	NA	Trial outcomes are not available online or in publication form	
NPC-14 for Duchenne muscular dystrophy						
NCT01918384	Phase 2; *N* = 21 males (≥4 years)	**36**–2	INT, R, P, TM	NA	Trial outcomes are not available online or in publication form	

Legends:

a) Abbreviations: ↑, improved outcome; CO, crossover; ΔFEV1pp, forced expiratory volume in one second; INT, interventional; 6MWD, 6 minute walk distance; NA, not available; NR, not randomized; NS, not significant; OBS, observational; OLA, open label assignment; P, parallel; PROS, prospective; QM, quadruple masking; R, randomized; SG, single group; TM, triple masking.

b) Overview of primary and secondary outcomes in clinical trials on readthrough compounds. Results were pooled in case of separation into groups (e.g., for different doses). If statistical testing of outcome measurements is not described in a publication or on ClinicalTrials.Gov, outcome results are summarized as 'NA'.

c) Timeframe: treatment time (in weeks) is given in bold font, follow-up time in regular font.

d) The timeframe (e.g., follow-up vs. treatment time) in these cases is not clearly described.

models [57]. In addition, a recent finding indicates that NV848/NV914 and NV930 exert an MoA similar to that of DAP, a potent readthrough compound that specifically results in incorporation of tryptophan at a UGA site [58].

Proper validation of final compounds of interest is pivotal and can be divided into two steps: (i) demonstration of target protein elevation, and (ii) demonstration of recovery of protein function. Although protein level characterization is relatively straightforward by conventional techniques such as western blotting, and has been performed in validation studies for most readthrough compounds, the confirmation of protein rescue at a functional level has proved to be more challenging.

A prime example of phenotypic, functional characterization is the measurement of CFTR function in CF patient-derived intestinal organoids (PDIOs) with the forskolin-induced swelling (FIS) assay [59]. Importantly, results on PDIOs obtained by FIS assays correlate with clinical results for the patient the PDIOs are derived from [60,61]. As such, observing no effect of a compound suggests that the compound will not be effective in the clinic, which was indeed the case for ataluren [32,62]. Validation of ELX-02 in FIS assays yielded conflicting results. Although one study observed CFTR rescue with ELX-02 as monotherapy for G542X homozygous and heterozygous patient-derived cells [63], our own study showed little effect of a commercial ELX-02 variant as a single compound across a panel of CFTR PTC genotypes [64]. One readthrough compound that did induce functional recovery as monotherapy in FIS assays is DAP (our unpublished data), warranting prioritization of this readthrough compound in further (pre)clinical studies. An important remark concerning comparison of DAP to NV848/NV914/NV930 is that NV848/NV930 and NV914 fall into category 4/5 of the Globally Harmonized System (GHS) of Classification and Labeling of Chemicals, underlining their low health risk identity. DAP, however, although it was not toxic in preclinical work including mouse studies, could hold additional challenges in this respect owing to (i) its original characterization as an anticancer reagent, and (ii) the simplicity of its structure, as an adenosine analog, there is ample space for biochemical and structural optimization to further optimize the therapeutic window.

In addition to the FIS assay, electrical current measurements on patient-derived airway cells correlate with clinical outcome measurements in CF patients [65,66]. The development of predictive preclinical assays has proved to be more challenging for other genetic diseases, including DMD. However, recently developed muscle cell contractility assays on iPSC-derived muscle cells show promise as functional assays for DMD patient-derived material [67, 68, 69]. Prioritization of those assays whose outcomes correlate with clinical disease manifestation is pivotal.

Finally, animal models can provide additional systemic and metabolic complexity in terms of validating compounds and associated metabolites for efficacy and toxicity. The differences between various *in vivo* models have been extensively reviewed (e.g., CF [70] and DMD [71]). In the context of nonsense mutations, rodent models are the most widely used.

However, some animal models are known to incompletely or inaccurately model human diseases, as evidenced by intestinal obstruction being the most common morbidity in CF mouse models whereas airway obstruction is less prominent. An often used readout in the context of CF is the FIS assay on mouse-derived intestinal organoids. In such settings it has been shown, for example, that G418 restores CFTR function in homozygous G542X mouse organoids whereas ataluren did not [72]. In a previous study, however, ataluren did result in reappearance of CFTR protein in intestinal glands as well as partial restoration of function based on current-based measurements in *CFTR*-/- G542X mice [73]. It can therefore be debated whether animal models have sufficient translational value in all elements of hit validation. For DMD, muscle function can be functionally assessed in mouse models, thus providing additional advantages over cellular models that simplify the complexity of the muscle system. As such, ataluren promoted dystrophin expression in primary muscle cells in mice expressing dystrophin nonsense alleles, and also rescued muscle function [26]. These differences between (i) the efficacy of readthrough compounds in different disease contexts, and (ii) positive results obtained in mouse studies with ataluren versus absence of clinical efficacy of ataluren, are striking and underline the complexity of animal studies. Prioritization of non-rodent animal models for CF and DMD could be beneficial in the context of nonsense mutations. For CF, the pig model could hold additional value because (i) porcine *CFTR* is genetically very similar to human *CFTR*, and (ii) the porcine respiratory system has many similarities to the human respiratory system in terms of anatomy, size, and physiology [74]. However, to date porcine models with CF nonsense genotypes have not been developed. With regard to DMD animal models, dystrophin-deficient dogs recapitulate the DMD clinical course in many aspects [71]. Canine models with dystrophin PTC mutations are not yet available, but may provide a great asset for validation of readthrough compounds in the context of DMD.

Readthrough compounds in clinical trials

A systematic search for clinical studies on readthrough compounds resulted in a total of 48 clinical trials **(Supplemental Figure S1).** Because this review focuses on the clinical efficacy of readthrough compounds, we do not elaborate on Phase 1 trials and safety endpoints. Overall, no severe side effects in any of the trials were reported. Ataluren, ELX-02, and gentamicin have been the most extensively studied for various disease indications **(Figure 4).** Outcome measures of finalized trials for those readthrough compounds are described in **Supplemental Tables S1–S4** in the supplemental information online. We summarize these finalized trials as well as ongoing trials in **Table 2,** and highlight the outcome for the most relevant clinical parameter in each disease.

Interpretation of readthrough compound efficacy across clinical trials is challenging owing to differences in research design, treatment length, and clinical endpoints. In the context of rare diseases and small population sizes, crossover (CO) designs, in which participants receive treatment and placebo sequentially in a randomly selected order, can be useful [75]. An important requirement for CO studies is that responses are rapidly detectable, which can be challenging depending on the disease and disease stage. In the context of

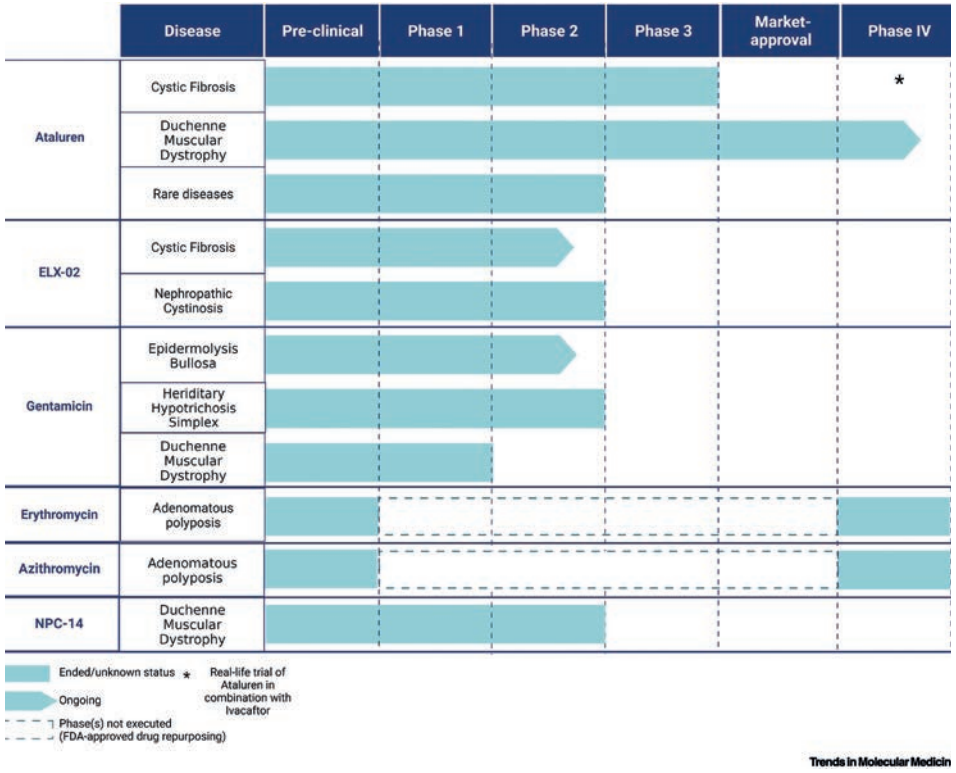

Figure 4. Readthrough compounds in clinical trials stall in Phase 2.
Outline of the stage of readthrough compounds in clinical trials conducted between February 2000 and June 2022. Although the clinical development of ataluren for nonsense mutation-induced cystic fibrosis (CF) stopped after a negative outcome Phase 3 trial, two real-life setting N = 1 Phase 4 trials have been performed to assess ataluren efficacy in combination with ivacaftor (NCT03256968 and NCT03256799). In some cases, compounds were already FDA-approved for other disease indications, and drug repurposing can allow a faster clinical study pipeline (see Figure S1 in the supplemental information online).

readthrough compound trials, only three clinical studies had a CO design (NCT00458341, NCT02758626, and NCT03492866). Depending on disease and disease stage, it is pivotal that treatment length is sufficient to result in changes in clinical parameters. It can be questioned whether trials with treatment periods for 1 month or shorter (e.g. NCT00458341) allowed the detection of such changes. In the context of CF, the first ataluren trial indicated a significant improvement in forced expiratory volume (FEV1) (NCT00237380), but this was not confirmed in a large Phase 3 trial (NCT00803205) [62,76]. Post hoc analyses showed that use of antibiotic tobramycin was associated with lack of efficacy, which was confirmed in preclinical analyses (NCT00803205) [62.]. Unfortunately, a Phase 3 follow-up study in patients not receiving aminoglycosides (NCT02139306) did not show clinical improvement [77]. A combination of compounds that target different cellular mechanisms could enhance

treatment efficacy; however, both Phase 4 trials in which ataluren and the CFTR modulator ivacaftor were combined in a single patient (N = 1 trial) did not report clinical improvement (NCT03256968 and NCT03256799) [78], ending clinical trial investigations of ataluren in the context of CF [78].

In the context of DMD, ataluren has been found to stabilize DMD patients in the mid-range phase of the disease [79,80]. However, multiple clinical trials with ataluren in patients with DMD yielded conflicting outcomes, likely owing to overall lack of efficacy but possibly also reflecting differences in trial set-up, disease stage and outcome measures [81,82]. Nevertheless, ataluren received conditional approval in July 2018 from the European Medicines Agency (EMA) for treating pediatric, ambulatory DMD patients (≥2 years). Post-marketing studies are currently recruiting patients to further evaluate ataluren in DMD (NCT03179631, NCT01247207).

ELX-02 is currently being evaluated in two Phase 2 trials (NCT04126473 and NCT04135495) in CF patients with at least one PTC allele. Preliminary results showed a minor decrease in sweat chloride concentration, indicating only limited treatment efficacy [83]. ELX-02 is additionally being investigated in combination with the CFTR modulator ivacaftor (NCT04135495); however, a first press release reported no significant improvement upon this dual therapy [84]. Another Phase 2 trial of ELX-02 in nephropathic cystinosis patients (NCT04069260) was initiated but has been halted prematurely owing to design limitations. A Phase 2 trial with ELX-02 and patients with Alport syndrome is expected to start in 2023. Gentamicin has been investigated in Phase 1/2 trials in several rare diseases including the skin disorder recessive dystrophic epidermolysis bullosa (RDEB). RDEB patients who received gentamicin exhibited a persistent increase in collagen VII expression and enhanced wound healing (NCT02698735) [85]. Erythromycin, azithromycin, and NPC-14 have been investigated for various disease indications, but no results have been published, suggesting absence of effect in a clinical setting (NCT02175914, NCT02354560, NCT04454151, NCT01918384).

Overall, although various clinical studies of readthrough compounds have been initiated, this has not resulted in encouraging outcomes except for the conditional approval of ataluren for a subset of DMD patients.

Concluding remarks

Readthrough biology remains an area of intense investigation because of its potentially large impact for the ~10% of genetic disorders that are caused by nonsense mutations. Despite the development and preclinical validation of >30 different readthrough compounds, only ataluren is clinically approved for a subset of DMD patients. To increase the chances of readthrough compounds reaching the clinic, it is essential to characterize which elements in preclinical discovery, preclinical validation, and clinical study stages could be improved **(Figure 2).** Preclinically, prioritization of the development of functional preclinical models that correlate with clinical outcomes is likely to result in better prediction of drug efficacy

in the clinic. Clinically, a main challenge lies in patient stratification for the first clinical trials and in clinical trial standardization to allow comparison of different studies.

Overall, preclinical studies yield promising results when simplified experimental approaches are undertaken. However, when more complex validation experiments are performed (such as FIS assays in the context of CF [32,64]), results for readthrough compounds as monotherapy have been disappointing overall. Although the scalability of readthrough reporter assays hold value in the discovery phase, they lack the genetic and physiological context of the targeted genetic disorder. In particular, single or dual reporter assays are sensitive readthrough detectors and have resulted in a vast amount of positive preclinical results. Although both types are valuable for finding new leads on compounds with readthrough activity, the use of intronic reporter assays could be beneficial by selecting molecules with higher readthrough capacity in the context of NMD.

Irrespective of the type of discovery assay, it is pivotal that hits are validated with disease-specific functional assays. Currently, functional assays on patient-derived cells where outcomes correlate with clinical outcome are available for CF in particular. Prioritizing further development of such assays for other genetic diseases is warranted as well as achievable; for example, in DMD promising results have been achieved with muscle cell contractility assays on patient iPSC-derived muscle cells. A pivotal element in making the most of these patient-derived, functional preclinical assays is that the outcomes of such preclinical assays should be compared with clinical outcome measures to guide prioritization. For additional validation experiments that complement patient-derived models, the development of porcine and canine models with nonsense mutations could be beneficial in providing additional systemic complexity in comparison to conventional rodent models.

Limited clinical efficacy and small population sizes in trials can hamper the establishment of such correlations. For this reason it can be beneficial to develop a composite endpoint model in which several outcomes measurements are combined into a single statistical model. In particular, Bayesian methods allow probability calculations to test whether a treatment is likely to lie in the effective range based on all available trial and external data including patient long-term history, preclinical experiments, and the literature [86]. Importantly, a correlation at the group level does not necessarily interpolate to the individual patient. Therefore, N = 1 trials with a priori preclinical stratification could further increase our knowledge on readthrough compound efficacy.

Overall, unfortunately, the clinical trial results discussed herein have been disappointing. Although the main reason for this absence of effect is presumably lack of efficacy, the vast differences in set-ups and outcome measurements between clinical trials hamper the drawing of overarching, firm conclusions. Clinical trial standardization is therefore essential. In addition, implementation of specific elements in clinical trial design may improve the detection of clinical benefit, such as (i) repeated measurements of clinical outcomes, (ii) trials with a CO design, (iii) treatment duration of >4 weeks (depending on disease and

disease stage), and (iv) an international collaborative effort to ensure that disease and PTC diversity is captured.

Finally, it could be beneficial to perform Phase 2 trials in a subselection of patients who may be most amenable to efficient readthrough compound therapy. The exact requirements of such a preselection will be disease- and compound-dependent, but such strategies could include (i) selection of homozygous PTC patients who have two alleles for readthrough compounds to act on, preferably UGA mutations because these have been shown to be most prone to readthrough therapy, or patients selected based on the MoA of the investigated readthrough compounds (e.g., selection for PTCs where originally a tryptophan was encoded, because DAP specifically results in restoration of a tryptophan at the PTC site) [14.], (ii) selection of patients who are in a stage of the disease in which clinical benefit is still expected from therapy, and (iii) preselection based on informative preclinical assays on patient-derived material. Hereafter, in case of positive outcomes, additional Phase 2/3 trials with different stratification strategies can further allow stratification of patients or patient groups who could benefit from the therapy.

Although improvements in preclinical and clinical study design may lead to a better assessment of readthrough compounds, the overall issue of limited drug efficacy requires further attention. The prime reason for this is the small amount of PTC-harboring mRNA are a result of NMD. A potential strategy to enlarge the small pool of PTC-harboring mRNAs will be to combine readthrough compounds with NMD inhibitors. Preclinically, it has been shown that such combinations can result in sufficiently high mRNA levels to increase protein activity [64,87]. A challenge is that NMD, like ribosomal translation control, is a pivotal cellular quality control process, and inhibition is associated with toxicity [88]. Inhibition of SMG1 via SMG1i has been studied most, and has shown large potential in preclinical studies, but high concentrations are associated with in vitro cellular toxicity, and this is probably the reason why SMG1i has not yet entered clinical trials. Optimization of the therapeutic window of NMD inhibitors will be of great value for their use in enhancing the efficacy of readthrough compounds. Inhibitors of other elements of the NMD machinery have also been proposed, such as vidaza (5-azacytidine, a cytidine analog), that is FDA-approved for the treatment of myelodysplastic syndrome and myeloid leukemia, and that was subsequently shown to additionally inhibit NMD in an indirect, MYC-dependent fashion [89,90]. However, vidaza therapy is associated with severe side effects and was shown to be ineffective in a previous study by our group and others [64,87]. Investigation of the potential inhibition of other proteins involved in the NMD pathway is ongoing, underlined by a recent study in which SMG6 was found to be specifically involved in CFTR degradation [91]. In addition to NMD inhibitors, readthrough compounds can be combined with drugs that enhance protein activity. CF research has yielded several drugs that enhance cellular CFTR activity, most notably amplifiers, modulators, and potentiators [92,93]. However, clinical trials on the combination of ataluren and CFTR potentiator ivacaftor did not result in positive clinical outcomes, and preliminary results of the combination therapy consisting of ELX-02 and ivacaftor indicate a similar lack of synergy.

In addition, a favorable therapeutic window is a main requirement for success of readthrough compounds as monotherapy. ELX-02 and ataluren were previously shown to have poor pharmacokinetic characteristics, indicated by their peak plasma concentrations after 2 h and rapid excretion [94]. Preliminary results of the latest trial on ELX-02 indicate similar pharmacokinetic challenges [83]. Steady-state drug levels in patients from this trial were considerably lower than the concentrations at which ELX-02 had been tested preclinically (2 μM vs. 80–160 μM) [16,63]. A biochemistry-centered drug development pipeline could aid in improving this essential pharmacokinetics–safety balance.

Finally, the field of readthrough biology is continuing the exploration of readthrough compounds with novel and potent MoAs to improve the therapeutic window and increase clinical efficacy. DAP, an inhibitor of the tRNATrp modifier FTSJ1, is an example of a compound with a well-understood, potent MoA that we believe holds great potential. Interestingly, recent work on NV848/NV914 and NV930 indicates that these ataluren derivatives act in a similar manner to DAP [58]. Because both compounds have yielded promising preclinical results in relevant model systems, as well as showing a favorable safety profile in animal models [57,95], the assessment of NV848/NV914/NV930 and DAP in a clinical trial setting will be followed with great interest. Aside from this, their MoAs highlight the potential of discovering inhibitors of other tRNA-modifying proteins. Finally, multiple alternative strategies such as CRISPR technology [96,97], antisense oligonucleotide (ASO)-based strategies [98], and anticodon-engineered tRNA (ACE-tRNA) technology [99,100] **(Figure 5)** to rescue PTC mutations did not fall within the scope of this review but are worthy of further study.

In this review we have addressed several hurdles that require attention to bridge the translational gap in readthrough research **(Outstanding questions and Figure 2).** In brief, it can be beneficial to prioritize preclinical assays and models that accurately recapitulate the disease and correlate with clinical outcome measures. In a clinical setting, trial standardization is pivotal. These improvements, together with a better understanding of readthrough biology and the underlying exploitable mechanisms, will be essential to make sense of nonsense mutation therapy.

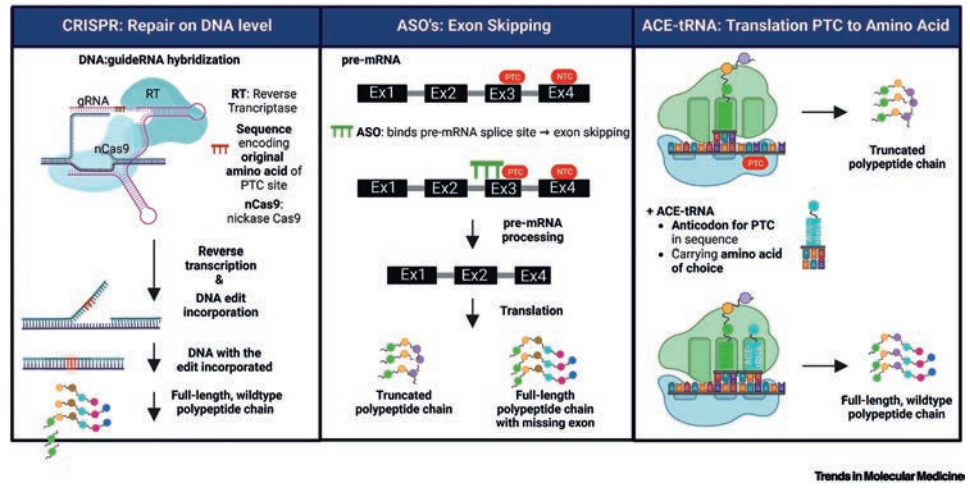

Figure 5. Non-small molecule readthrough strategies.
Abbreviations: ACE-tRNA, anticodon-engineered tRNA; ASO, antisense oligonucleotide; Ex, exon; gRNA, guide RNA; NTC, natural termination codon; PTC, premature termination codon.

Clinicians Corner

- Readthrough drugs comprise an area of intense preclinical investigation owing to the potential applicability to genetic disorders caused by nonsense mutations, and for which no treatment is available today.
- In contrast to results obtained in preclinical studies, readthrough drugs have not yielded success in clinical trials, with the exception of ataluren for a subset of patients with Duchenne muscular dystrophy. To increase the translatability of preclinical results, assays that correlate with clinical outcome measures should be prioritized. Such assays should (i) recapitulate disease biology, for example, using patient-derived cells, and (ii) have a functional/phenotypic character that characterizes the function of the targeted gene, instead of conventional experiments in which protein amounts are characterized.
- It is pivotal that such preclinical assays are compared to clinical data to establish correlations between preclinical results and clinical outcome. Deciding on the optimal clinical outcome for establishing those correlations is essential. In the case of a small effect size and/or small population size, it can be beneficial to develop a composite endpoint model in which several outcome measurements are combined into a single statistical model.
- Because numbers of affected patients are low and the effect size is small, clinical trials set-ups need to be optimized. We recommend (i) standardization of clinical trials, mainly focusing on outcome measures, treatment length, and dosage; (ii) increasing statistical power by performing repeated measures and on/off cycles, and performing N = 1 trials allowing a personalized approach.
- Although improvements in preclinical and clinical study design may lead to a better assessment of readthrough compounds, the overall issue of limited drug efficacy requires

further attention. In particular, degradation of premature termination codon (PTC)-harboring mRNAs by the nonsense-mediated decay (NMD) quality control system results in an additional challenge when it comes to effective readthrough therapy. To date, no NMD inhibitor has been characterized in a clinical setting, and further development of NMD inhibitors with an emphasis on reducing toxicity is warranted.

Outstanding Questions

- Robust preclinical assays on patient-derived material are available for CF, but not for other genetic diseases caused by PTCs. Can we prioritize the development of such assays to increase the translatability of preclinical studies?
- It can be challenging to choose which clinical parameter is optimal to develop correlations between preclinical studies and clinical outcome. How should we approach this challenge?
- Future studies should focus on readthrough compounds with novel and more potent MoAs, such as the readthrough compound DAP which affects tRNATrp fidelity. Can other readthrough compounds with similar MoAs be discovered or developed for other PTC genotypes?
- It is possible that currently existing readthrough compounds will not be sufficiently potent as monotherapy because of degradation of PTC-harboring mRNAs by the NMD machinery. Because no NMD inhibitors are currently under investigation in clinical trials, studies should focus on developing NMD inhibitors that have a favorable therapeutic window.
- Standardization of clinical trials to draw more firm, overarching conclusions is essential. Specifically, standardization of trial set-up, treatment duration, and clinical end-points per disease should be prioritized.
- New technologies such as CRISPR and ACE-tRNAs will enable the development of new readthrough compounds. What can be done to prevent these novel technologies from encountering the same translational gap as current readthrough compounds?

Acknowledgements

This study was supported by the Nederlandse Cystic Fibrosis Stichting (NCFS) HIT-CF3 program and Elisabeth von Freyburg Stichting. We thank Dr Saskia Houwen (rehabilitation physician, Radboud University Medical Center) and Dr Friso Langen (Fletiopharma consultant) for sharing their knowledge and experience in the context of DMD. All illustrations were created with BioRender.com.

Declaration of Interests

J.M.B. reports personal fees from Vertex Pharmaceuticals, Proteostasis Therapeutics, Eloxx Pharmaceuticals, Teva Pharmaceutical Industries, and Galapagos, outside the submitted work. In addition, J.M.B. has a patent related to the FIS assay with royalties paid. C.K.v.d.E. reports grants from GSK, Nutricia, TEVA, Gilead, Vertex, ProQR, Proteostasis, Galapagos NV, and Eloxx outside the submitted work. In addition, C.K.v.d.E. has a patent 10006904 with royalties paid. The other authors declare no conflicts of interest.

.

Supplemental Information

Readthrough Compounds for Nonsense Mutations: Bridging the Translational Gap

Sacha Spelier, Eveline P.M. van Doorn, Cornelis K. van der Ent, Jeffrey M. Beekman, Martijn A.J. Koppens Department of Pediatric Respiratory Medicine, Wilhelmina Children's Hospital, University Medical Center, Utrecht University, 3584 EA Utrecht, The Netherlands
Correspondence: m.a.j.koppens@umcutrecht.nl (M. Koppens)

Supplemental Figure 1. Clinical trials included in this review *(related to Figure 3).*

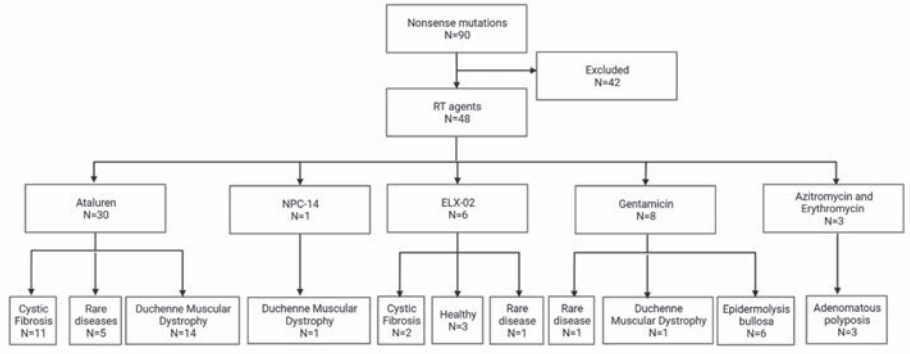

Overview of all clinical trials conducted between February 2000 and June 2022 with search term 'nonsense mutations', assigned to the readthrough compound and genetic disorder. N denotes the number of trials. A systematic search was performed to identify all interventional clinical trial studies on readthrough compounds that have been terminated, withdrawn, completed, or continuously recruited participants. The search term 'nonsense mutations' was used as a starting point, exploiting the website of clinicaltrials.gov on which all clinical trials are numerically described. Out of 90 findings, 42 did not meet the criterium of the interventional character of treatment with a small-molecule-based readthrough compound and were excluded. 48 clinical trials remained, describing six readthrough compounds: Ataluren, NPC-14, ELX-02, Gentamicin, azithromycin, and erythromycin.

timeline)			TEPD (mV)	transport response (N= or %)	TEPD (mV)	transport normalization (N= or %)	BMI (kg or kg/m²)	protein (%)	(mmol/L)	(N/mL)	FEV₁/FVC (%/change from baseline)				(% or N events)	markers (cells/mL or µg/mL, ng/mL)	(mg/L)	
NCT00237380 ● ● ○ ○ ○ N=23 (≥18 years) 2-2-2-2	INT, SG, OLA	G542X N=3; W1282X N=13; other N=7.	p	p	s	p	s *(Cycle 1)* s *(Cycle 2)*	s	s	s *(Cycle 1)* s *(Cycle 2)*	s *(Cycle 1)* s *(Cycle 2)*	-	-	-	-	-	-	-
NCT00351078 ● ● ○ ○ ○ N=19 (≥18 years) 12-4	INT, SG, OLA	W1282X N=10; W1282X/ W1282X N=3; other N=6	p	other	p	-	s	s	-	-	s	-	s	s	-	s	-	-
NCT00234663 ● ● ○ ○ ○ N=24 (≥18 years) 8-408	INT, SG, OLA, NR	Unknown	p	-	p	-	-	s	-	-	s	-	-	-	-	-	-	-
NCT00458341 ● ● ○ ○ ○ N=30 (6-18 years) 2-2-2-2	INT, CO, OLA, R	G542X N=14; W1282X N=4; other N=12	p	p	s	p	s	s	s	s	s	-	s	-	-	s	s	-
NCT00803205 ● ● ● ○ ○ N=209 (≥ 6 years) 48-4	INT, P, R	W1282X N=86; G542X N=83; others N=40	other	other	other	-	other	-	s	-	p+s	s	-	s	s	other	other	other
Post hoc analysis: NCT00803205			-	-	-	-	-	-	-	-	p	-	-	-	s	-	-	-
NCT02139306 ● ● ● ○ ○ N=279 (≥ 6 years) 48-4	INT, P, R	G542X N=85; W1282X N=67; other N=128	-	-	-	-	s	-	-	-	p	s	-	-	s	-	-	-
NCT01140451 ● ● ● ○ ○ N=191 (≥ 6 years) 96-4	INT, P, R	Unknown	s	-	s	-	s	-	s	-	s	s	-	-	s	-	-	s
NCT02107859 ● ● ● ○ ○ N=61 (≥ 6 years) 192-4	INT, SG, OLA	Unknown	Terminated due to a prior study NCT02139306 that did not meet its endpoints															
NCT02456103 ● ● ● ○ ○ N=246 (≥ 6 years) 96-4	INT, SG, OLA	Unknown	Terminated due to a prior study NCT02139306 that did not meet its endpoints															
NCT03256968 ● ● ● ○ ● N=1 (31 years) 48-368	INT, SG, OLA Extension arm: VX-770	W1282X/ G542X N=1	s/other	-	s/other	-	s/other	-	s/other	-	p	s/other	-	-	s/other	-	-	-
NCT03256799 ● ● ● ○ ● N=1 (32 years) 48-368	INT, SG, OLA Extension arm: VX-770	W1282X/ W1282X N=1	s/other	-	s/other	-	s/other	-	s/other	-	p	s/other	-	-	s/other	-	-	-

p Primary outcome
s Secondary outcome
- Not implemented as an outcome
No outcome available
Positive significant outcome
Negative outcome

Supplemental Table 1A. Outcomes of Ataluren trials for patients with CF with nonsense mutations.

Results are based on Clinicaltrials.gov & publications on the specific NCT number. Safety, compliance, and pharmacokinetic secondary measure outcomes are suspended from the analysis. TEPD= transepithelial potential difference; **Cl-**= chloride; BMI= body mass index; CFTR= cystic fibrosis transmembrane conductance regulator; FEV1= forced expiratory volume in 1 second; FVC= forced vital capacity; CFQ-R= cystic fibrosis questionnaire-revised application; **CRP**= C-reactive protein; CT= computerized tomography.

Study Summary (Phase, N, timeline)	**Study design**	**Nonsense mutations**	**6MWD (m)**	**Time to 10% decline in 6MWD (%)**	**Dystrophin expression mRNA and protein (%)**	**Weight/ height/ body mass (kg, m)**	**Palatability**	**NSAA (scale)**	**Myometry**	**TFTs (sec)**	**Lung function FEV₁/ FVC (%)**	**CK levels (IU/L)**	**Heart rate (BPM)**	**Digit span task (score)**	**Fall (N)**	**PedsQL, HRQL, TSQM (score)**	**SAM detections (N)**	**Daily living activity (score/ EK scale)**
NCT00264888 ● ● ○ ○ ○ N=38 (≥ 5 years) 4-244	INT, NR, SG, OLA	E2035X N=3; R3034X N=3; other N=32	-	-	p+s	-	-	-	other	other	-	other	-	-	-	-	-	-
NCT00592553 ● ● ○ ○ ○ N=174 (≥ 5 years) 48-6	INT, R, P, QM	UAA N=43; UAG N=48; and UGA N=83	p	s	s	-	-	-	s	s	-	s	s	s	s	s	s	-
NCT00759876 ● ● ○ ○ ○ N=36 (all ages) 96-0	INT, SG, OLA	Unknown	Terminated, due to lack of efficacy of Ataluren in NCT00592553															
NCT00847379 ● ● ○ ○ ○ N=173 (≥ 5 years) 96-6	INT, SG, OLA	Unknown	Terminated, due to lack of efficacy of Ataluren in NCT00592553 and withdrawal from sponsor															
NCT01009294 ● ● ○ ○ ○ N=6 (≥ 7 years) 50-366	INT, SG, OLA	Unknown	Terminated, due to lack of efficacy of Ataluren in NCT00592553															
NCT02090959 ● ● ● ○ ○ N=219 (7-15 years) 144-6	INT, SG, OLA	Unknown	Terminated, due to withdrawal of sponsor and commercial availability of Ataluren for DMD															
NCT01826487 ● ● ● ○ ○ N=230 (7-16 years) 48-6	INT, R, P, QM	Unknown	p	s	-	-	-	other	-	s	-	-	-	-	-	other	-	other
NCT01557400 ● ● ● ○ ○ N=94 (all ages) 240-6	INT, SG, OLA	Unknown	s	-	-	-	-	s	-	s	s	-	-	-	-	-	-	s
NCT02819557 ● ● ○ ○ ○ N=14 (2-5 years) 52-4	INT, SG, OLA	Unknown	-	-	-	s	s	s	-	s	-	-	-	-	-	-	-	-
NCT03796637 ● ● ○ ○ ○ N=6 (all ages) 36 – Exact Timeline unclear	INT, SG, OLA	Unknown	-	-	p+s	-	-	-	-	-	-	-	-	-	-	-	-	-
NCT03648827 ● ● ○ ○ ○ N=20 (2-7 years) 40 – Exact Timeline unclear	INT, SG, OLA	Unknown	-	-	p+s	-	-	-	-	-	-	-	-	-	-	-	-	-

p Primary outcome
s Secondary outcome
- Not implemented as an outcome
No outcome available
Positive significant outcome
Negative outcome

Supplemental Table 1B. Outcomes of Ataluren trials for patients with DMD with nonsense mutations.

6MWD= 6-minute walking distance; NSAA= north star ambulatory assessment; TFT= timed function test; CK= creatine kinase; **PedsQL**= pediatric quality of life inventory; **HRQL**= health-related quality of life; **TSQM**= treatment satisfaction questionnaire for medication; **SAM**= step activity monitoring; kg= kilogram; FEV1= forced expiratory volume in 1 second; FVC= forced vital capacity; **BPM**= beats per minute; **EK**= Egen Classification.

Aniridia Study Summary (Phase, N, timeline)	Study design	Nonsense mutation	Maximum reading speed of oculus unitas (% change)	Reading accessibility index both eyes (units on a scale)	BCVA (logMAR)	Maximum reading speed of oculus dexter (% change)	Reading accessibility of right and left eye (units on a scale)	CPS of both, right, and left eye (logMAR)	RA of both eyes (logMAR)	Iris area (mm^2)	Severity of corneal keratop athy (N)
NCT02647359 ● ● ○ ○ ○ N=39 (≥2 years) 240-4	INT, R, P, QM	Unknown	p	s	s	s	s	s	s	s	s
NCT04117880 ● ● ○ ○ ○ N=0 (≥2 years) 140 – Exact Timeline unclear	INT, SG, OLA	Unknown	Withdrawn before protocol was implemented								

Hemophilia Study Summary (Phase, N, timeline)	Study design	Nonsense mutation	Outcomes
NCT00947193 ● ● ○ ○ ○ N=13 (≥18 years) 2-2- 2-2	INT, SG, OLA	Unknown	Terminated, due to withdrawal by the sponsor

p Primary outcome
s Secondary outcome
- Not implemented as an outcome
No outcome available
Positive significant outcome
Negative outcome

Supplemental Table 1C. Outcomes of Ataluren trials for with nonsense mutations in other genes.
Results are based on Clinicaltrials.gov & publications on the specific NCT number. Safety, compliance, and pharmacokinetic secondary measure outcomes are suspended from the analysis. Safety, compliance and pharmacokinetic secondary measure outcomes are suspended from the analysis. N denotes the number of patients enrolled in the study. **BCVA**= best-corrected visual acuity; **CPS**= critical print size; **RA**= reading acuity; CDKL5= cyclin-dependent kinase-like 5; **MAR**= minimum angle of resolution; DS= Dravet syndrome; CDD= cyclin-dependent kinase-like 5 deficiency disorder.*Measurements were not done in the same time frame.

Methylmalonic acidemia Study Summary (Phase, N, timeline)	Study design	Nonsense mutation	Outcomes
NCT01141075 ● ● ○ ○ ○ N=11 (≥2 years) 96-48	INT, SG, OLA	Unknown	Terminated, due to low patient enrollment and lack of information

DS and CDD Study Summary (Phase, N, timeline)	Study design	Nonsense mutation	Safety	Seizure frequency (N)	Cognitive behavior/QOL (score)
NCT02758626 ● ● ○ ○ ○ N=16 (2-12 years) 12-4-12-4-16	INT, R, CO, QM	Unknown	p	s	other

p Primary outcome
s Secondary outcome
- Not implemented as an outcome
No outcome available
Positive significant outcome
Negative outcome

EB: RDEB Study Summary (Phase, N, timeline)	Study design	Nonsense mutation	Collagen VII expression (% or fluorescence intensity)	Number of patients with increased AFs (N=)	Wound closure/ reduced blistering (%)	Safety	EBDASI (score)/disease activity/QOL
NCT03012191 ● ● ○ ○ ○ N=6 (all ages) 24 – Exact Timeline unclear	INT, SG, OLA	R578X/V168GfsX12 N=1; R578X/R578X N=1; other N=4	p	p	-	p	s
NCT02698735 ● ● ○ ○ ○ N=5 (all ages) 12 – Exact Timeline unclear	INT, NR, P, TM	R578X/V168GfsX12; R578X/R578X; others N=3	p	p	other	-	-
NCT03392909 ● ● ○ ○ ○ N=9 (≥7 years) 2-22 12-22	INT, SG, OLA	Unknown	p	p	other	p	s

EB: JEB Study Summary (Phase, N, timeline)	Study design	Nonsense mutation	Laminin expression (% or fluorescence intensity)	Hemidesmosomes (%)	Reduced blistering (%)	Wound closure (N= or %)	Safety	EBDASI (score)
NCT04140786 ● ● ○ ○ ○ N=6 (all ages) 12-12.8	INT, NR, OLA	C325*, Q625* and 3 others	p	-	-	s	p	s

Hypotrichosis simplex Study Summary (Phase, N, timeline)	Study design	Nonsense mutation	Hair density of the scalp (score)	Presence of vellus hairs (N= or %)	Activity of hair loss (N or %)	Photographic documentation (observation)
NCT03492866 ● ● ○ ○ ○ N=8 (all ages) 2-10	INT, NR, CO, OLA	Unknown	p	s	s	s

p Primary outcome
s Secondary outcome
- Not implemented as an outcome
No outcome available
Positive significant outcome
Negative non-significant outcome

Supplemental Table 1D. Outcomes of Gentamicin trials for patients with nonsense mutations.
Results are based on Clinicaltrials.gov & publications on the specific NCT number. Safety, compliance, and pharmacokinetic secondary measure outcomes are suspended from the analysis. Safety, compliance and pharmacokinetic secondary measure outcomes are suspended from the analysis. . N denotes the number of patients enrolled in the study. RDEB= recessive dystrophic epidermolysis bullosa; JEB= junctional epidermolysis bullosa; EB= epidermolysis bullosa; EBDASI= epidermolysis bullosa disease activity and scarring index; QOL= quality of life; DMD= Duchenne muscular dystrophy; AF= anchoring fibril.

References

1. Mort, M. *et al*. (2008) A meta-analysis of nonsense mutations causing human genetic disease. Hum. Mutat. 29, 1037–1047
2. Karousis, E.D. *et al*. (2022) The broader sense of nonsense. Trends Biochem. Sci. 47, 921–935
3. Nguengang Wakap, S. *et al*. (2022) Estimating cumulative point prevalence of rare diseases: analysis of the Orphanet database. Eur. J. Hum. Genet. 28, 165–173
4. Ferguson, M.W. *et al*. (2019) The antimalarial drug mefloquine enhances TP53 premature termination codon readthrough by aminoglycoside G418. PLoS One 14, e0216423
5. Luna, S. *et al*. (2021) A global analysis of the reconstitution of PTEN function by translational readthrough of PTEN pathogenic premature termination codons. Hum. Mutat. 42, 551–566
6. Burke, J.F. *et al*. (1985) Suppression of a nonsense mutation in mammalian cells in vivo by the aminoglycoside antibiotics G-418 and paromomycin. Nucleic Acids Res. 13, 6265–6272
7. Song, H. *et al*. (2000) The crystal structure of human eukaryotic release factor eRF1 – mechanism of stop codon recognition and peptidyl-tRNA hydrolysis. Cell 100, 311–321
8. Behm-Ansmant, I. *et al*. (2007) A conserved role for cytoplasmic poly(A)-binding protein 1 (PABPC1) in nonsense-mediated mRNA decay. EMBO J. 26, 1591–1601
9. Chamier, H. *et al*. (2008) NMD factors UPF2 and UPF3 bridge UPF1 to the exon junction complex and stimulate its RNA helicase activity. Nat. Struct. Mol. Biol. 15, 85–93
10. Lejeune, F. (2022) Nonsense-mediated mRNA decay, a finely regulated mechanism. Biomedicines 10, 141
11. Supek, F. *et al*. (2021) To NMD or not to NMD: nonsense mediated mRNA decay in cancer and other genetic diseases. Trends Genet. 37, 657–668
12. Floquet, C. *et al*. (2012) Statistical analysis of readthrough levels for nonsense mutations in mammalian cells reveals a major determinant of response to gentamicin. PLoS Genet. 8, e1002608
13. Cassan, M. *et al*. (2001) UAG readthrough in mammalian cells: effect of upstream and downstream stop codon contexts reveal different signals. BMC Mol. Biol. 2, 3
14. Howard, M.T. *et al*. (2000) Sequence specificity of aminoglycoside-induced stop codon readthrough: potential implications for treatment of Duchenne muscular dystrophy. Ann. Neurol. 48, 164–169
15. Welsh, M.J. *et al*. (1993) Molecular mechanisms of CFTR chloride channel dysfunction in cystic fibrosis. Cell 73, 1251–1254
16. Crawford, D.K. *et al*. (2020) ELX-02 generates protein via premature stop codon readthrough without inducing native stop codon read-through proteins. J. Pharmacol. Exp. Ther. 374, 264–272
17. François, B. *et al*. (2005) Crystal structures of complexes between aminoglycosides and decoding A site oligonucleotides: role of the number of rings and positive charges in the specific binding leading to miscoding. Nucleic Acids Res. 33, 5677–5690

18. Qian, Y. *et al*. (2009) Interaction of aminoglycosides with human mitochondrial 12S rRNA carrying the deafness-associated mutation. Antimicrob. Agents Chemother. 53, 4612–4618
9. Sharma, J. *et al*. (2021) A small molecule that induces translational readthrough of CFTR nonsense mutations by eRF1 depletion. Nat. Commun. 12, 4358
20. Baradaran-Heravi, A. *et al*. (2021) Effect of small molecule eRF3 degraders on premature termination codon readthrough. Nucleic Acids Res. 49, 3692–3708
21. Trzaska, C. *et al*. (2020) 2,6-Diaminopurine as a highly potent corrector of UGA nonsense mutations. Nat. Commun. 11, 1509
22. Friesen, W.J. *et al*. (2017) The nucleoside analog clitocine is a potent and efficacious readthrough agent. RNA 23, 567–577
23. Palma, M. *et al*. (2021) Deciphering the molecular mechanism of stop codon readthrough. Biol. Rev. 96, 310–329
24. Singh, A. *et al*. (1979) Phenotypic suppression and misreading in Saccharomyces cerevisiae. Nature 277, 146–148
25. Gonzalez-Hilarion, S. *et al*. (2012) Rescue of nonsense mutations by amlexanox in human cells. Orphanet. J. Rare Dis. 7, 58
26. Welch, E.M. *et al*. (2007) PTC124 targets genetic disorders caused by nonsense mutations. Nature 447, 87–91
27. Auld, D.S. *et al*. (2010) Molecular basis for the high-affinity binding and stabilization of firefly luciferase by PTC124. Proc. Natl. Acad. Sci. U. S. A. 107, 4878–4883
28. McElroy, S.P. *et al*. (2013) A lack of premature termination codon read-through efficacy of PTC124 (ataluren) in a diverse array of reporter assays. PLoS Biol. 11, e1001593
29. Brumm, H. *et al*. (2012) Rescue of melanocortin 4 receptor (MC4R) nonsense mutations by aminoglycoside-mediated read-through. Obesity 20, 1074–1081
30. Dranchak, P.K. *et al*. (2011) Nonsense suppressor therapies rescue peroxisome lipid metabolism and assembly in cells from patients with specific PEX gene mutations. J. Cell. Biochem. 112, 1250–1258
31. Harmer, S.C. *et al*. (2012) Readthrough of long-QT syndrome type 1 nonsense mutations rescues function but alters the biophysical properties of the channel. Biochem. J. 443, 635–642
32. Zomer-van Ommen, D.D. *et al*. (2016) Limited premature termination codon suppression by read-through agents in cystic fibrosis intestinal organoids. J. Cyst. Fibros. 15, 158–162
33. Goldmann, T. *et al*. (2012) A comparative evaluation of NB30, NB54 and PTC124 in translational read-through efficacy for treatment of an USH1C nonsense mutation. EMBO Mol. Med. 4, 1186–1199
34. Peltz, S.W. *et al*. (2013) Ataluren as an agent for therapeutic nonsense suppression. Annu. Rev. Med. 64, 407
35. Roy, B. *et al*. (2016) Ataluren stimulates ribosomal selection of near-cognate tRNAs to promote nonsense suppression. Proc. Natl. Acad. Sci. U. S. A. 113, 12508–12513
36. Grentzmann, G. *et al*. (1998) A dual-luciferase reporter system for studying recoding signals. RNA 4, 479–486

37. Bidou, L. *et al*. (2004) Premature stop codons involved in muscular dystrophies show a broad spectrum of readthrough efficiencies in response to gentamicin treatment. Gene Ther. 11, 619–627
38. Xue, X. *et al*. (2014) Synthetic aminoglycosides efficiently suppress cystic fibrosis transmembrane conductance regulator nonsense mutations and are enhanced by ivacaftor. Am. J. Respir. Cell Mol. Biol. 50, 805–816
39. Cardno, T.S. *et al*. (2009) A homogeneous cell-based bicistronic fluorescence assay for high-throughput identification of drugs that perturb viral gene recoding and readthrough of nonsense stop codons. RNA 15, 1614–1621
40. Benhabiles, H. *et al*. (2017) Optimized approach for the identification of highly efficient correctors of nonsense mutations in human diseases. PLoS One 12, e0187930
41. Nudelman, I. *et al*. (2006) Redesign of aminoglycosides for treatment of human genetic diseases caused by premature stop mutations. Bioorg. Med. Chem. Lett. 16, 6310–6315
42. Mutyam, V. *et al*. (2016) Discovery of clinically approved agents that promote suppression of cystic fibrosis transmembrane conductance regulator nonsense mutations. Am. J. Respir. Crit. Care Med. 194, 1092–1103
43. Allamand, V. *et al*. (2008) Drug-induced readthrough of premature stop codons leads to the stabilization of laminin α2 chain mRNA in CMD myotubes. J. Gene Med. 10, 217–224
44. Hamada, M. *et al*. (1970) A new antibiotic, negamycin. J. Antibiot. (Tokyo) 23, 170–171
45. Du, M. *et al*. (2009) Poly-L-aspartic acid enhances and prolongs gentamicin-mediated suppression of the CFTR-G542X mutation in a cystic fibrosis mouse model. J. Biol. Chem. 284, 6885–6892
46. Du, L. *et al*. (2013) A new series of small molecular weight compounds induce read through of all three types of nonsense mutations in the ATM gene. Mol. Ther. 21, 1653–1660
47. Liang, F. *et al*. (2017) High-throughput screening for readthrough modulators of CFTR PTC mutations. SLAS Technol. 22, 315–324
48. Caspi, M. *et al*. (2016) A flow cytometry-based reporter assay identifies macrolide antibiotics as nonsense mutation readthrough agents. J. Mol. Med. 94, 469–482
49. Hosseini-Farahabadi, S. *et al*. (2021) Small molecule Y-320 stimulates ribosome biogenesis, protein synthesis, and aminoglycosideinduced premature termination codon readthrough. PLoS Biol. 19, e3001221
50. Hoffer, L. *et al*. (2018) Chemistry-driven hit-to-lead optimization guided by structure-based approaches. Mol. Inform. 37, 1800059
51. Popadynec, M. *et al*. (2021) Reducing the toxicity of designer aminoglycosides as nonsense mutation readthrough agents for therapeutic targets. ACS Med. Chem. Lett. 12, 1486–1492
52. Pibiri, I. *et al*. (2016) Exploring the readthrough of nonsense mutations by non-acidic ataluren analogues selected by ligand based virtual screening. Eur. J. Med. Chem. 122, 429–435
53. Tutone, M. *et al*. (2019) Deciphering the nonsense readthrough mechanism of action of ataluren: an in silico compared study. ACS Med. Chem. Lett. 10, 522–527

54. Pibiri, I. *et al*. (2020) Targeting nonsense: optimization of 1,2,4-oxadiazole trids to rescue CFTR expression and functionality in cystic fibrosis cell model systems. Int. J. Mol. Sci. 21, 6420
55. Nudelman, I. *et al*. (2009) Development of novel aminoglycoside (NB54) with reduced toxicity and enhanced suppression of disease-causing premature stop mutations. J. Med. Chem. 52, 2836–2845
56. Bidou, L. *et al*. (2017) Characterization of new-generation aminoglycoside promoting premature termination codon readthrough in cancer cells. RNA Biol. 14, 378–388
57. Corrao, F. *et al*. (2022) Nonsense codons suppression. An acute toxicity study of three optimized TRIDs in murine model, safety and tolerability evaluation. Biomed. Pharmacother. 156, 113886
58. Carollo, P.S. *et al*. (2022) Inhibition of FTSJ1, a tryptophan tRNA-specific 2'-O-methyltransferase as possible mechanism to readthrough premature termination codons (UGAs) of the CFTR mRNA. In XVI FISV Congress, 3R: Research, Resilience, Reprise, pp. 102-102, Federazione Italiana Scienze Della Vita
59. Dekkers, J.F. *et al*. (2013) A functional CFTR assay using primary cystic fibrosis intestinal organoids. Nat. Med. 19, 939–945
60. Dekkers, J.F. *et al*. (2016) Characterizing responses to CFTRmodulating drugs using rectal organoids derived from subjects with cystic fibrosis. Sci. Transl. Med. 8, 344ra84
61. Berkers, G. *et al*. (2019) Rectal organoids enable personalized treatment of cystic fibrosis. Cell Rep. 26, 1701–1708
62. Kerem, E. *et al*. (2014) Ataluren for the treatment of nonsense mutation cystic fibrosis: a randomised, double-blind, placeboc ontrolled phase 3 trial. Lancet Respir. Med. 2, 539–547
63. Crawford, D.K. *et al*. (2021) Targeting G542X CFTR nonsense alleles with ELX-02 restores CFTR function in human-derived intestinal organoids. J. Cyst. Fibros. 20, 436–442
64. de Poel, E. *et al*. (2021) Functional restoration of CFTR nonsense mutations in intestinal organoids. J. Cyst. Fibros. 21, 246–253
65. Awatade, N.T. *et al*. (2015) Measurements of functional responses in human primary lung cells as a basis for personalized therapy for cystic fibrosis. eBioMedicine 2, 147–153
66. Amatngalim, G.D. *et al*. (2022) Measuring cystic fibrosis drug responses in organoids derived from 2D differentiated nasal epithelia. Life Sci. Alliance 5, e202101320
67. Pioner, J.M. *et al*. (2020) Absence of full-length dystrophin impairs normal maturation and contraction of cardiomyocytes derived from human-induced pluripotent stem cells. Cardiovasc. Res. 116, 368–382
68. Piga, D. *et al*. (2019) Human induced pluripotent stem cell models for the study and treatment of Duchenne and Becker muscular dystrophies. Ther. Adv. Neurol. Disord. 12 1756286419833478
69. Uchimura, T. *et al*. (2021) A muscle fatigue-like contractile decline was recapitulated using skeletal myotubes from Duchenne muscular dystrophy patient-derived iPSCs. Cell Reports Med. 100298

70. McCarron, A. *et al*. (2021) Animal and cell culture models for cystic fibrosis: which model is right for your application? Am. J. Pathol. 191, 228–242
71. McGreevy, J.W. *et al*. (2015) Animal models of Duchenne muscular dystrophy: from basic mechanisms to gene therapy. Dis. Model. Mech. 8, 195–213
72. McHugh, D.R. *et al*. (2018) A G542X cystic fibrosis mouse model for examining nonsense mutation directed therapies. PLoS One 13, e0199573
73. Du, M. *et al*. (2008) PTC124 is an orally bioavailable compound that promotes suppression of the human CFTR-G542X nonsense allele in a CF mouse model. Proc. Natl. Acad. Sci. U. S. A. 105, 2064–2069
74. Rogers, C.S. *et al*. (2008) Disruption of the CFTR gene produces a model of cystic fibrosis in newborn pigs. Science 321, 1837–1841
75. Abrahamyan, L. *et al*. (2016) Alternative designs for clinical trials in rare diseases. Am. J. Med. Genet. C: Semin. Med. Genet. 172, 313–331 '
76. Kerem, E. *et al*. (2008) Effectiveness of PTC124 treatment of cystic fibrosis caused by nonsense mutations: a prospective phase II trial. Lancet 372, 719–727
77. Konstan, M.W. *et al*. (2020) Efficacy and safety of ataluren in patients with nonsense-mutation cystic fibrosis not receiving chronic inhaled aminoglycosides: the international, randomized, double-blind, placebo-controlled Ataluren Confirmatory Trial in Cystic Fibrosis (ACT CF). J. Cyst. Fibros. 19, 595–601
78. Peabody Lever, J.E. *et al*. (2020) Ataluren/ivacaftor combination therapy: two N-of-1 trials in cystic fibrosis patients with nonsense mutations. Pediatr. Pulmonol. 55, 1838–1842
79. McDonald, C.M. *et al*. (2021) Ataluren delays loss of ambulation and respiratory decline in nonsense mutation Duchenne muscular dystrophy patients. J. Comp. Eff. Res. 11, 139–155
80. McDonald, C.M. *et al*. (2017) Ataluren in patients with nonsense mutation Duchenne muscular dystrophy (ACT DMD): a multicentre, randomised, double-blind, placebo-controlled, phase 3 trial. Lancet 390, 1489–1498
81. Finkel, R.S. *et al*. (2013) Phase 2a study of ataluren-mediated dystrophin production in patients with nonsense mutation Duchenne muscular dystrophy. PLoS One 8, e81302
82. Bushby, K. *et al*. (2014) Ataluren treatment of patients with nonsense mutation dystrophinopathy. Muscle Nerve 50, 477–487
83. Woolford, J. *et al*. (2021) Eloxx pharmaceuticals reports positive topline results from monotherapy arms of Phase 2 clinical trial of ELX-02 in class 1 cystic fibrosis patients. Eloxx Published online November 17, 2021. https://investors.eloxxpharma.com/node/11986/pdf
84. Woolford, J. *et al*. (2022) Eloxx pharmaceuticals reports topline results from Phase 2 combination clinical trial of ELX-02 in class 1 cystic fibrosis (CF) patients. GlobeNewswire Published online September 14, 2022. https://www.globenewswire.com/newsrelease/2022/09/14/2516392/0/en/Eloxx-PharmaceuticalsReports-Topline-Results-from-Phase-2-Combination-ClinicalTrial-of-ELX-02-in-Class-1-Cystic-Fibrosis-CF-Patients.html

85. Woodley, D.T. *et al*. (2017) Gentamicin induces functional type VII collagen in recessive dystrophic epidermolysis bullosa patients. J. Clin. Invest. 127, 3028–3038
86. Kidwell, K.M. *et al*. (2022) Application of Bayesian methods to accelerate rare disease drug development: scopes and hurdles. Orphanet J. Rare Dis. 17, 186
87. Laselva, O. *et al*. (2020) Functional rescue of c. 3846GN A (W1282X) in patient-derived nasal cultures achieved by inhibition of nonsense mediated decay and protein modulators with complementary mechanisms of action. J. Cyst. Fibros. 19, 717–727
88. McHugh, D.R. *et al*. (2020) Synergy between readthrough and nonsense mediated decay inhibition in a murine model of cystic fibrosis nonsense mutations. Int. J. Mol. Sci. 22, 344
89. Bhuvanagiri, M. *et al*. (2014) 5-Azacytidine inhibits nonsensemediated decay in a MYC-dependent fashion. EMBO Mol. Med. 6, 1593–1609
90. Fenaux, P. *et al*. (2010) Azacitidine prolongs overall survival compared with conventional care regimens in elderly patients with low bone marrow blast count acute myeloid leukemia. J. Clin. Oncol. 28, 562–569
91. Sanderlin, E.J. *et al*. (2022) CFTR mRNAs with nonsense codons are degraded by the SMG6-mediated endonucleolytic decay pathway. Nat. Commun. 13, 2344
92. Dukovski, D. *et al*. (2020) Amplifiers co-translationally enhance CFTR biosynthesis via PCBP1-mediated regulation of CFTR mRNA. J. Cyst. Fibros. 19, 733–741
93. Keating, D. *et al*. (2018) VX-445–tezacaftor–ivacaftor in patients with cystic fibrosis and one or two Phe508del alleles. N. Engl. J. Med. 379, 1612–1620
94. Leubitz, A. *et al*. (2019) Safety, tolerability, and pharmacokinetics of single ascending doses of ELX-02, a potential treatment for genetic disorders caused by nonsense mutations, in healthy volunteers. Clin. Pharmacol. Drug Dev. 8, 984–994
95. Leroy, C. *et al*. (2023) Use of 2,6-diaminopurine as a potent suppressor of UGA premature stop codons in cystic fibrosis. Mol. Ther. (in press)
96. Geurts, M.H. *et al*. (2020) CRISPR-based adenine editors correct nonsense mutations in a cystic fibrosis organoid biobank. Cell Stem Cell 26, 503–51097. Geurts, M.H. *et al*. (2021) Evaluating CRISPR-based prime editing for cancer modeling and CFTR repair in intestinal organoids. Life Sci. Alliance 4, e202000940
98. Kim, Y.J. *et al*. (2022) Exon-skipping antisense oligonucleotides for cystic fibrosis therapy. Proc. Natl. Acad. Sci. U. S. A. 119, e2114858118
99. Ko, W. *et al*. (2022) Efficient suppression of endogenous CFTR nonsense mutations using anticodon-engineered transfer RNAs. Mol. Ther. Acids 28, 685–701
100. Lueck, J.D. *et al*. (2019) Engineered transfer RNAs for suppression of premature termination codons. Nat. Commun. 10, 822
101. Alkalaeva, E.Z. *et al*. (2006) In vitro reconstitution of eukaryotic translation reveals cooperativity between release factors eRF1 and eRF3. Cell 125, 1125–1136
102. Ivanov, A. *et al*. (2016) PABP enhances release factor recruitment and stop codon recognition during translation termination. Nucleic Acids Res. 44, 7766–7776
103. Kashima, I. *et al*. (2006) Binding of a novel SMG-1–Upf1–eRF1–eRF3 complex (SURF) to the exon junction complex triggers Upf1 phosphorylation and nonsense-mediated mRNA decay. Genes Dev. 20, 355–367

104. Yamashita, A. *et al*. (2001) Human SMG-1, a novel phosphatidylinositol 3-kinase-related protein kinase, associates with components of the mRNA surveillance complex and is involved in the regulation of nonsense-mediated mRNA decay. Genes Dev. 15, 2215–2228
105. Wilschanski, M. *et al*. (2011) Chronic ataluren (PTC124) treatment of nonsense mutation cystic fibrosis. Eur. Respir. J. 38, 59–69
106. Sermet-Gaudelus, I. *et al*. (2010) Ataluren (PTC124) induces cystic fibrosis transmembrane conductance regulator protein expression and activity in children with nonsense mutation cystic fibrosis. Am. J. Respir. Crit. Care Med. 182, 1262–1272
107. Mercuri, E. *et al*. (2020) Safety and effectiveness of ataluren: comparison of results from the STRIDE Registry and CINRG DMD Natural History Study. J. Comp. Eff. Res. 9, 341–360
108. Devinsky, O. *et al*. (2021) Ataluren for drug-resistant epilepsy in nonsense variant-mediated Dravet syndrome and CDKL5 deficiency disorder. Ann. Clin. Transl. Neurol. 8, 639–644
109. Mosallaei, D. *et al*. (2022) Molecular and clinical outcomes after intravenous gentamicin treatment for patients with junctional epidermolysis bullosa caused by nonsense variants. JAMA Dermatol. 158, 366–374

Chapter | 3

Functional restoration of CFTR nonsense mutations in intestinal organoids

Journal of Cystic Fibrosis, March 2022, Volume 21, Issue 2

E. de Poel[1,2,3,*], **S. Spelier [1,2,*],** S.W.F. Suen[1,2], E. Kruisselbrink[1,2], S.Y. Graeber[4,5,6], M.A. Mall[4,5,6], E.J.M. Weersink[7], M.M. van der Eerden[8], G.H. Koppelman[9,10], C.K. van der Ent[1] and J.M. Beekman[1,2,3]

**** These authors contributed equally to this work***

1. Department of Pediatric Respiratory Medicine, Wilhelmina Children's Hospital, University Medical Center, Utrecht University, 3584 EA Utrecht, The Netherlands **2.** Regenerative Medicine Utrecht, University Medical Center, Utrecht University, 3584 CT Utrecht, The Netherlands **3.** Center for Living Technologies, Eindhoven-Wageningen-Utrecht Alliance, The Netherlands **4.** Department of Pediatric Respiratory Medicine, Immunology and Critical Care Medicine, Charité-Universitätsmedizin Berlin, 13353 Berlin, Germany **5.** Berlin Institute of Health (BIH), 10178 Berlin, Germany **6.** German Center for Lung Research (DZL), associated partner, 13353 Berlin, Germany **7.** Amsterdam University Medical Center, location AMC, 1105 AZ Amsterdam, The Netherlands **8.** Department of Pulmonology, Erasmus MC, University Medical Center, 3015 GD Rotterdam, The Netherlands **9.** University of Groningen, University Medical Center Groningen, Beatrix Children's Hospital, Department of Pediatric Pulmonology and Pediatric Allergology, Groningen, The Netherlands **10.** University of Groningen, University Medical Center Groningen, Groningen Research Institute for Asthma and COPD (GRIAC), Groningen, The Netherlands

Highlights

- Pharmacological repair of CFTR function beyond F508del/F508del-VX809/VX770 in intestinal organoids with homozygous PTC mutations.
- The read-through agent ELXds-02, the NMD-inhibitor SMG1i and the CFTR modulators therapy VX-661/VX-445/VX-770 were required for maximal efficacy.
- W1282X-CFTR function is partially rescued with the NMD-inhibitor SMG1i combined with the CFTR-modulators VX-661/VX-445/VX770.

Abstract

Background

Pharmacotherapies for people with cystic fibrosis (pwCF) who have premature termination codons (PTCs) in the cystic fibrosis transmembrane conductance regulator (*CFTR*) gene are under development. Thus far, clinical studies focused on compounds that induce translational readthrough (RT) at the mRNA PTC location. Recent studies using primary airway cells showed that PTC functional restoration can be achieved through combining compounds with multiple mode-of-actions. Here, we assessed induction of CFTR function in PTC-containing intestinal organoids using compounds targeting RT, nonsense mRNA mediated decay (NMD) and CFTR protein modulation.

Methods

Rescue of PTC CFTR protein was assessed by forskolin-induced swelling of 12 intestinal organoid cultures carrying distinct PTC mutations. Effects of compounds on mRNA CFTR level was assessed by RT-qPCRs.

Results

Whilst response varied between donors, significant rescue of CFTR function was achieved for most donors with the quintuple combination of a commercially available pharmacological equivalent of the RT compound (ELX-02-disulfate or ELX-02ds), NMD inhibitor SMG1i, correctors VX-445 and VX-661 and potentiator VX-770. The quintuple combination of pharmacotherapies reached swelling quantities higher than the mean swelling of three VX-809/VX-770-rescued F508del/F508del organoid cultures, indicating level of rescue is of clinical relevance as VX-770/VX-809-mediated F508del/F508del rescue in organoids correlate with substantial improvement of clinical outcome.

Conclusions

Whilst variation in efficacy was observed between genotypes as well as within genotypes, the data suggests that strong pharmacological rescue of PTC requires a combination of drugs that target RT, NMD and protein function.

Keywords

intestinal organoids - CFTR nonsense mutation - premature termination codon - cystic fibrosis- read-through - CFTR modulation - nonsense mRNA mediated decay inhibition

Introduction

Cystic fibrosis (CF) is a monogenic, autosomal-recessive disease caused by mutations in the *CFTR* gene [1]. Highly efficacious pharmacotherapy of the most prevalent F508del mutation shifts the unmet clinical need towards approximately 15% of people with CF (pwCF) who carry non- or low-responder *CFTR* mutations. The spectrum of mutations that are poorly responsive to clinically approved pharmacotherapies include the class I mutations that do not lead to full length protein (e.g. by nonsense mutations, frameshifts, consensus splice mutations, or larger rearrangements).

Approximately 10% of the worldwide CF population carry mutations that result in premature termination codons (PTC) resulting in production of truncated CFTR protein. Early work demonstrates that aminoglycoside antibiotics including gentamicin and G418 enable rescue of CFTR PTC in cell lines [2]. These compounds reduce the fidelity of translation by affecting the pairing of cognate and near-cognate tRNAs with the mRNA, resulting in incorporation of non-cognate amino acids at the PTC site. This readthrough (RT) process facilitates continuation of translation, albeit at low efficacy [2]. Subsequent efforts identified PTC124 (Ataluren) as selective inducer of PTC-readthrough [3]. However, efficacy in many preclinical models was not reproduced [4,5] and clinical trials with Ataluren failed to reach their primary endpoints [6]. A recently chemically-engineered aminoglycosides derivative termed ELX-02 (NB124; Eloxx Pharmaceuticals) is currently in early clinical development [7] and showed to be effective as single treatment in intestinal organoids [8].

Whilst readthrough agents hold potential for increasing full length protein production, their efficacy is inhibited by a control system called nonsense-mediated mRNA decay (NMD) that leads to degradation of PTC-containing mRNA molecules [9,10]. By pharmacological inhibition of critical effectors of NMD such as SMG1 kinase (through SMG1i) or SMG7 (through NMDI-14), increased efficacy of readthrough agents has been observed in various preclinical models and laboratories [10, 11, 12, 13, 14]. A potential alternative to NMD-inhibition may be a recently identified CFTR amplifier (PTI-428 or nesolicaftor [15]) that increases CFTR mRNA quantity independent of PTC-mutations.

The reduced translational fidelity by readthrough agents induces a pool of proteins with different amino acids at the PTC site [16], underlining the potential of combining CFTR protein modulators with readthrough agents to further enhance CFTR restoration [8, 10, 17]. CFTR (co-)potentiators such as VX-770, ASP-11 [18] and to some extend VX-445 [19], may increase the channel open probability of the readthrough-induced CFTR protein pool, whereas CFTR correctors may enhance trafficking of readthrough-CFTR protein towards the apical surface. Their combination will likely be most effective in restoring CFTR function upon readthrough.

To study the impact and repair of PTCs, we use intestinal organoids and the forskolin-induced swelling (FIS) assay as CFTR-dependent phenotypic readout that allows to quantitate individual CFTR function in response to CFTR function modulators [20,21]. CFTR func-

tion measurements in this assay model correlate with clinical disease indicators [22,23] and CFTR modulator responses [21, 24]. Our previous work on readthrough demonstrated no efficacy of PTC124 in intestinal organoids [4], consistent with clinical trial data by others [6], supporting the use of this assay for preclinical drug development. The purpose of this study was to investigate the capacity of commercially-available compounds with different modes-of-action to increase ELX-02ds-induced CFTR function rescue in organoids with multiple PTCs.

Materials and methods

Collection of primary epithelial cells of CF patients (pwCF)

Informed consent for tissue collection, generation, storage, and use of the organoids was obtained from all participating patients. Biobanked intestinal organoids are stored and catalogued (https://huborganoids.nl/) at the foundation Hubrecht Organoid Technology (http://hub4organoids.eu). Collection of patient tissue and data was performed following the guidelines of the European Network of Research Ethics Committees (EUREC) following European, national, and local law, and the study was approved by the local the medical ethical committee at UMC Utrecht biobank (TcBio document 14-008), at Charite, Berlin and at The Hebrew University, Jerusalem.

Human intestinal organoid culture

Crypts were isolated from biopsies of subjects with cystic fibrosis as previously described [21]. Organoids were incubated in a humidified chamber with 5% CO2 at 37°C. Medium was refreshed every 2–3 days, and organoids were passaged 1:4 every 7–8 days. Prior to forskolin induced swelling assay measurements, organoids were grown at least 3 weeks after crypt isolation or thawing.

Functional assessment of CFTR function

Functional assessment of CFTR function was assessed with the forskolin-induced swelling assay, performed as described by Vonk *et al.* [25]. But instead of using recombinant Human R-Spondin 3 Protein, we used R-Spondin condition medium [21]. Details about the compound concentrations and incubation times can be found in Table 1. Organoid swelling was monitored during 60-180 minutes using a Zeiss LSM 710 confocal microscope. Total

Table 1: *Final assay conditions of pharmacotherapies included in this manuscript.*

Compound	Hours added prior to FIS assay or organoid collection for PCR	Final concentration (μM)	Manufacturer	Mode of action
ELX-02 disulfate	48	80	MedChemExpress	Readthrough-agent
SMG1i	24	0.3	Cystic fibrosis foundation	NMD-inhibitor
PTI-428	24	0-20	MedChemExpress	CFTR amplifier
VX-770	0, added together with forskolin	3	selleck biochemicals	CFTR potentiator
VX-661, VX-445	24	3	selleck biochemicals	CFTR corrector
ASP-11	0, added together with forskolin	0-20	Kindly provided by UCSF	CFTR co-potentiator
NMDI-14	24 and 48	0-20	MedChemExpress	NMD-inhibitor
Vidaza	24	0-20	SelleckChem	NMD-inhibitor

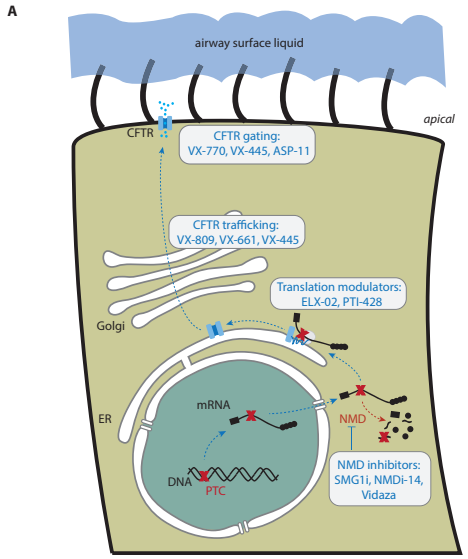

Figure 1: Schematic presentation of impact of pharmacotherapies and demographics of CFTR mutation types and PTC allele frequencies.
(A) Schematic presentation of intracellular tracking of CFTR and impact of pharmacotherapies. **(B)** Relative allele frequencies of specific PTC mutations in our biobank (right) compared to world wide incidence (left). **(C)** Location in the CFTR gene of the PTC mutations included in this study.

organoid surface area per well was quantified based on calcein green staining as described by Vonk *et al*. [25].

Quantitative real time PCR

Organoids were cultured in tissue culture plates, either in regular culture medium or culture medium supplemented with compounds described in Table 1. Organoids were collected from 24-well tissue culture plates, washed once with advanced DMEM/F12 and RNA was extracted using RNeasy Mini Kit (Qiagen, catalog no. 74104), following manufacturers protocol. cDNA was synthesized of 100 ng RNA with IscriptTM according to the supplied protocol (Biorad, catalog no. 1708891). qPCR reactions were executed in 96-well format with IQ SYBR green (Bio-Rad, catalog no. 1708880) and following primer sets: CFTR reverse: CCCAGGTAAGGGATGTATTGTG, CFTR forward: CAACATCTAGTGAGCAGTCAGG;YHWAZ reverse: AAGGGACTTCCTGTAACAATGCA, YHWAZ forward: CTGGAACGGTGAAGGTGACA. Using a Biorad CFX PCR device, samples were incubated for 3 minutes at 95°C and for 39 cycles at: 10 seconds at 95°C, 30 seconds at 62°C. Relative expression levels of the treated PTC organoids were analyzed by means of ΔΔCt calculations, for which YWHAZ served as housekeeping gene and mean expression level of two replicate experiments of 5 healthy control organoid samples was used as calibrator. YWHAZ expression was not affected by the different compound therapies. Melt peaks were analyzed to confirm specific primer binding.

Statistics

Data are represented as mean ± SD or SEM (specified in figure legends). One-way ANOVA's were performed to compare mean FIS or ΔΔCt values upon treatment with pharmacotherapies with DMSO at group level with Dunnett T-test as post-hoc analysis. No statistical testing was performed between the different pharmacotherapies on individual donor level. P values < 0.05 were considered statistically significant. Data analysis was performed in SPSS.

Results

Overview of compound mode-of-actions and patient samples used in this study

We selected a diverse set of compounds that are commercially available **(Figure 1A)** to study their capacity to enhance functional restoration upon RT of CFTR. The incorporation of an amino acid at the place of the PTC results in a pool of full-length transcripts of which function could be enhanced with CFTR modulation therapy (VX-770, VX-661, VX-445 and ASP-11). The amplifier PTI-428, or the NMD inhibitors SMG1i, NMDi-14 and Vidaza should increase the level of mRNA transcript and thereby expand the pool of PTC mRNA prone for RT. Combining these small molecules acting on different steps along the CFTR biosynthesis pathway, channel trafficking and channel gating might collectively result in CFTR function restoration of PTCs in general, to clinically relevant levels.

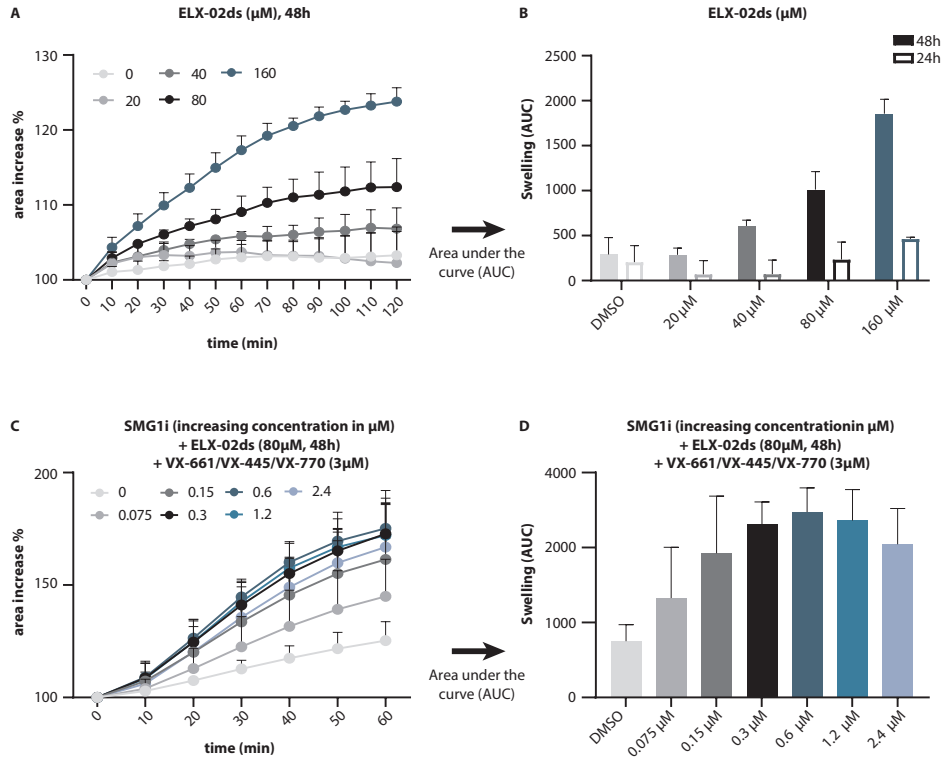

Figure 2: Dose-response assays on a W1282X/W1282X organoid culture to determine optimal pharmacotherapy conditions.
(A) Area increase in time (in total for 120 min) of W1282X/W1282X organoids upon addition of increasing concentration of ELX-02ds for 24h or 48h prior to the FIS-assay. Organoid area increase was measured with the addition of 5 µM forskolin. Datapoints represent mean+SD, n=3. **(B)** FIS, measured as area under the curve of each condition shown in **(A). (C)** Area increase in time (in total for 60 min) of W1282X/W1282X organoids upon addition of increasing concentration of SMG1i for 24h or 48h and ELX-02ds (80 µM) for 48h + VX-661/VX-445 (3 µM) for 24h prior to the FIS-assay. Organoid area increase was measured with the addition of 0.128 µM forskolin + 3 µM VX-770. Datapoints represent mean+SD, n=3. **(D)** FIS, measured as area under the curve of each condition shown in **(C).**

Currently 10% of our biobank consists of PTC mutations in which most prevalent PTC mutations are represented **(Figure 1B);** yet distribution is to some extent shifted towards rare PTC variants. Also, locations of PTC mutations described in this study are well distributed across the CFTR gene **(Figure 1C)** which allows us to investigate whether the location of the PTC in the CFTR gene influences drug response.

Rescue of W1282X/W1282X function by RT, NMD-inhibition and CFTR modulation

First, we assessed the dose-dependency and incubation times required for optimal rescue of CFTR function by RT agent ELX-02ds in 2-hours FIS measurements in a W1282X/

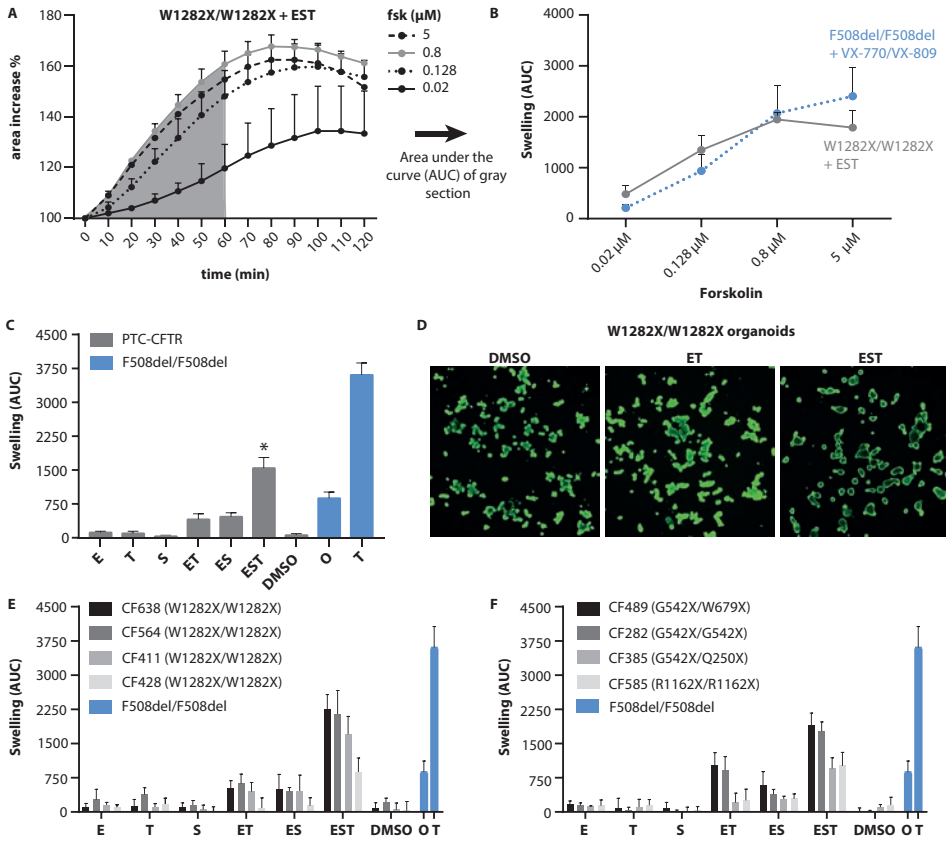

Figure 3: FIS of various homozygous PTC expressing organoid cultures upon treatment with pharmacotherapies that (collectively) stimulate read-through, inhibit NMD and/or modulate CFTR protein tra cking or gating.
(A) Area increase in time (min) of W1282X/W1282X organoids upon addition of increasing concentration of fsk. Organoids were pre-stimulated with EST (bars represent mean+SD, n=3). **(B)** Swelling (area under the curve of t=0 to t=60 minutes, gray area in **A**) of W1282XX/W1282X organoids pre-stimulated with EST (datapoints represent mean+SD, n=3) and mean swelling of three F508del/F508del organoid cultures pre-stimulated with VX-809 (3 µM, 24h) + VX-770 (3 µM, 0h)datapoints represent mean+SD, n=9) upon stimulation with increasing concentration of fsk. To determine the therapeutic value of EST with 0.128 µM fsk, the swelling levels were compared to the mean swelling levels of three organoid cultures expressing F508del/F508del-CFTR upon rescue with VX-770 (3 µM, added with fsk) + VX-809 (3 µM, 24h), datapoints represent mean+SD, n=9). Similar F508del/F508del data is shown in C-F and supplmental figure 2 . **(C)** Mean FIS of all homozygous PTC organoid cultures, measured for 1h in presence of 0.128 uM fsk Organoid cultures were pre-stimulated with E, S or T and all combinations thereof. Bars represent mean+SEM, n=8. *p-value<0.05, compared to DMSO. **(D)** Miscroscopic images of W1282X/W1282X organoids after 60 minutes stimulation with 0.128 µM fsk, untreated or pre-stimulated with ET or EST. **(E and F).** FIS (1h, 0.128 µM FSK) responses of four individual organoid cultures, carrying two copies of the W1282X mutation **(E)** or two PTC mutations other than W1282X **(F)** upon pharmacotherapy treatment. Abbreviations: fsk = forskolin; E = ELX-02ds (80 µM, 48h); S = SMG1i (0.3 µM, 24h); T = VX-661 (3 µM, 24h) + VX-445 (3 µM, 24h) + VX-770 (3 µM, added simultaneously with fsk); O = VX-809 (3 µM, 24h) + VX-770 (3 µM, added simultaneously with fsk).

W1282X organoid culture. ELX-02ds increased FIS dose-dependently and to a higher extend after 48h ELX-02ds pre-incubation when compared to 24h **(Figure 2A-B).** We selected 80 µM of ELX-02ds and 48h pre-incubation as condition for combination studies. Based on the dose-response of SMG1i on top of ELX-02ds and VX-661/VX-445/VX-770 **(Figure 2C-D)** and reported toxicity concerns of SMG1i [17], 0.3 µM and 24h incubation were chosen for further studies. Concentrations of VX-661, VX-445 and VX-770 were set to 3 µM based on previous work and dose-dependency was not studied in detail here. Pre-stimulation with 0.625 µM NMDI-14 for 24 or 48h slightly increased swelling when combined with ELX-02ds **(Supplemental Figure S1),** but significantly less than the combination of SMG1i and ELX-02ds. NMDI-14 concentrations >2.5 µM became toxic, shown by a decreased swelling response. We could not detect any impact of PTI-428, ASP-11 and Vidaza on rescuing W1282X/W1282X-CFTR, despite varying concentrations (0-20 µM, 1:2 diluted) and compound backgrounds (ELX-02ds + SMG1i w/w/o VX-661/VX-445/VX-770) **(Supplemental Figure S1).** For these reasons, NMDi-14, PTI-428, ASP-11 and Vidaza were excluded from further experiments.

PTC rescue with combinations of ELX-02ds, SMG1i and VX-661/VX-445/VX-770
We next set out to study rescue of CFTR function by combined use of ELX-02ds, SMG1 and VX-661/VX-445/VX-770, and compared efficacy to VX809/VX770 or VX661/VX445/VX770 treatment of F508del/F508del organoids. Organoids were stimulated with different fsk concentrations for 1h to define a fsk concentration that can quantitate PTC rescue in the dynamic range of the assay, and enable comparison with previous work. Fsk titrations demonstrated a dose-dependent relation with swelling **(Figure 3A-B).** Maximal swelling was observed from 0.128 µM fsk and higher, and fsk dose dependency and efficacy of EST in W1282X/W1282X organoids (n=3 donors) conditions was comparable to VX770/VX809 in F508del/F508del (n=3 donors). We selected fsk 0.128 µM for 1h for comparison of RT compound efficacies between the various organoid conditions.

We next assessed the CFTR restoring capacity of ELX-02ds, SMG1i and VX-661/VX-445/VX-770 as stand-alone compounds and combinations thereof in 8 organoid cultures homozygous for distinct PTC mutations **(Figure 3C-F)** and 3 organoid cultures compound heterozygous for PTC mutations **(Supplemental Figure S2A).** Two organoid cultures homozygous for consensus splice mutations showed no response to compound treatment indicating PTC-dependent rescue **(Supplemental Figure S2B).** No single compound restored CFTR function to such extend it could be detected with 1h 0.128 µM fsk stimulation. Swelling levels significantly increased when organoids were treated with ELX-02ds and either SMG1i (ES in **Figure 3)** or VX-661/VX-445/VX-770 (ET in **Figure 3),** nearly reaching AUC levels similar to VX-809/VX-770-rescued F508del/F508del organoids **(Figure 3C-D).** The magnitude of swelling increase was donor dependent and within-genotype (W1282X/W1282X) variation was observed **(Figure 3E-F).** As recent literature described that differences in mRNA sequence surrounding the PTC might influence RT, all four homozygous W1282X organoid cultures were sequenced. However, no SNPs were observed in the region 600 nucleotides before and 400 nucleotides after the PTC (data not shown). Whilst

the combination SMG1i and VX-661/VX-445/VX-770 (ST in **Supplemental Figure S2C)** moderately rescued W1282X-CFTR, although again with within-genotype variation, functional rescue of the PTCs R1162X, G542X or W679X require the addition of the RT-agent: ELX-02ds **(Supplemental Figure S2C).** The most effective pharmacotherapy showed to consist of the combination of ELX-02, SMG1i and VX-661/VX-445/VX-770 (EST in **Figure 3)** and resulted in tripling of the mean AUC value compared to the dual compound therapies **(Figure 3C-D).** Interestingly, in three of the W1282X/W1282X **(Figure 3E)** and two homozygous PTC donors **(Figure 3F)** rescue of CFTR function reached AUC levels that were in between reference AUC values of F508del/F508del organoids treated with VX-809/VX-770 (mean AUC 940 +/- 32, n=9) and VX-661/VX-445/VX-770 (mean AUC of 3327 +/-383, n=9). As can be observed in **Supplemental Figure S2A,** level of swelling was halved in organoid cultures expressing one PTC mutation, yet levels were still comparable to VX-809/VX-770-rescued F508del/F508del-CFTR. These data show that combining RT agents with NMD inhibitors and CFTR modulators represents a potential therapeutic option for treating PTC mutations.

CFTR mRNA rescue of panel of various PTC harboring organoid lines in response to combinations of ELX-02ds, SMG1i and VX-661/VX-445/VX-770

Additionally, the expression of CFTR mRNA in response to all compounds by qRT-PCR was characterized. In general, the expression level of CFTR mRNA is lower in organoid cultures having two PTC mutations compared to WT organoids, as the expression levels of the different donors in the DMSO condition shown in **Figure 4A-B** are below 50% of WT expression. Whilst not significant, ELX-02 shows a minor increase in CFTR mRNA. Yet, all conditions including SMG1i resulted in a significant increase in mRNA similar to or higher than 100% of WT expression in all organoid cultures. Moreover, the level of mRNA expression increase correlates with the level of CFTR function rescue by EST (R2 of 0.74, **Figure 4C).** This indicates that treatment with NMD-inhibitors is required for a high quantity of functional protein following RT, which can be further enhanced with CFTR modulation.

Discussion

In this paper, we hypothesized that CFTR function of CF patient-derived organoids harboring PTC mutations, can be rescued by a combination of pharmacotherapies and investigated the contributions of PTC rescue by molecules that **a)** amplify *CFTR* transcription (PTI-428), **b)** enhance PTC-RT (ELX-02ds), **c)** inhibit NMD (SMG1i, NMDi-14 and Vidaza), **d)** stimulate correct CFTR protein trafficking (VX-661 and VX-445) and **e)** enhance gating activity of CFTR at the cell membrane (VX-770 and ASP-11). We found that a combination of ELX-02ds, SMG1i and VX-661/VX-445/VX-770 resulted in robust CFTR rescue, higher than observed with VX-809/VX-770-treated F508del/F508del organoids. We characterized compound efficacy for a panel of 12 organoid lines harboring various PTC mutations, including the most common W1282X and G542X alleles as well as less prevalent PTC alleles. We observed differences in efficacy between genotypes as well as differences within one genotype.

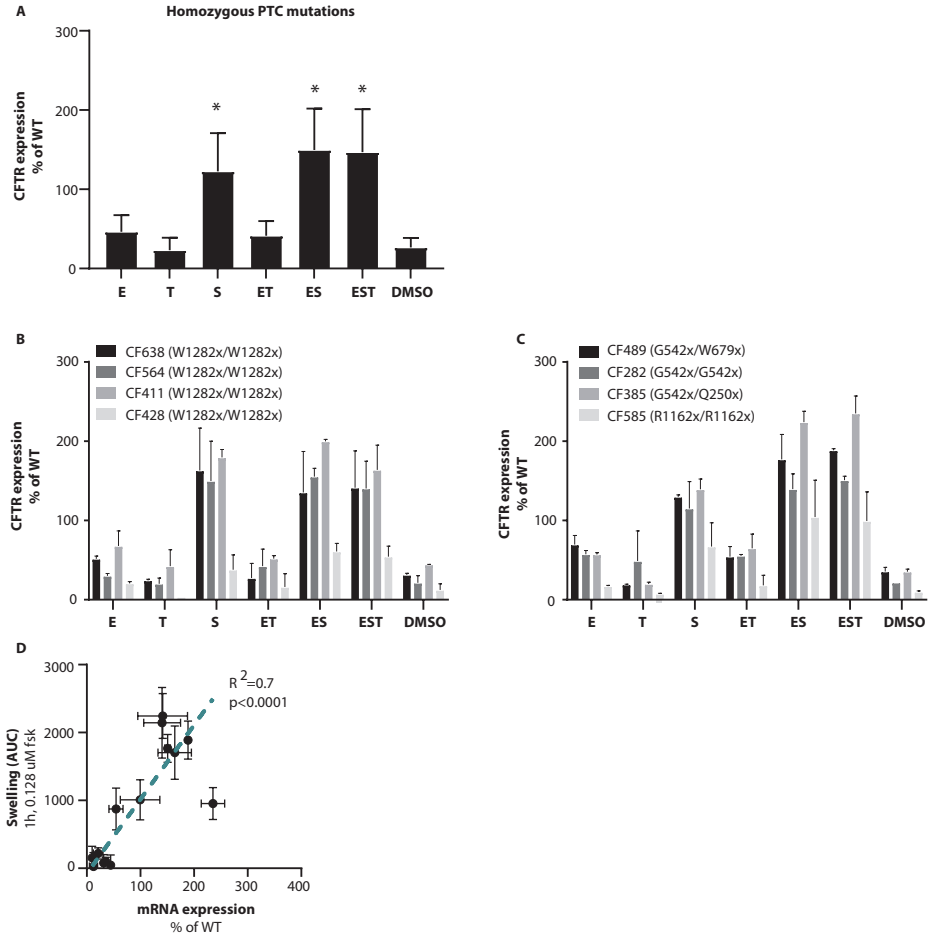

Figure 4: CFTR mRNA expression of organoid cultures homozygous for PTC mutations upon pharmacotherapy.

(A) mean mRNA expression level of CFTR, normalized to the reference genes YWHAZ and expressed in % of mean of 5 WT/WT organoid cultures (bars represent mean+SD, n=2). *p<0.05, compared to DMSO. **(B and C)** mRNA expression level of CFTR of individual organoid cultures. The organoid cultures and pre-treatments in A and B correspond to those in figure 3 E and F, respectively. **(D)** Correlation between level of swelling (1h, 0.128 µM) and mRNA expression level of untreated (DMSO) or organoid cultures or pre-stimulated withEST.

Abbreviations: WT = wildtype; E = ELX-02ds (80 µM, 48h); S = SMG1i (0.3 µM, 24h); T = VX-661 (3 µM, 24h) + VX-445 (3 µM, 24h) + VX-770 (3 µM, added simultaneously with forskolin);

As the presence of a PTC mutation results in a truncated variant of the protein, efficacy of the RT-agent ELX-02ds was first characterized. In contrast to a recent study [8], ELX-02ds as single agent did not result in AUC values that are comparable to VX-809/VX-770-treated F508del/F508del organoids. Moreover, CFTR mRNA was increased by ELX-02-mediated NMD-inhibition in the recent study, a mode of action we could not fully confirm with our qPCR data. This difference might be contributed to the commercially available ELX-02ds used in this study, versus the ELX-02 from Eloxx Pharmaceuticals itself. Despite this difference, the commercially available version has RT activity that can be strongly enhanced by NMD inhibition and clinically available CFTR protein modulators. Whilst RT is essential for restoring full-length CFTR, the pool of mRNA susceptible for RT is diminished by NMD. Multiple compounds that inhibit different components of the NMD machinery have been described, but especially SMG1 inhibition has yielded success in various preclinical models [10,14]. We indeed found that SMG1 inhibition resulted in a concentration-dependent elevation of functional CFTR levels. A challenge concerning NMD inhibition however remains that NMD influences multiple cellular pathways. As a result, a high concentration of SMG1i has been associated with in vitro cellular toxicity [17] and caution must be taken with using NMD-inhibitors as a therapeutic compound, which is likely to be the reason only a single NMD-inhibitor has reached the clinic at present-day. The NMD-inhibitor Vidaza (5-Azacytidine) has been approved for the treatment of myelodysplastic syndrome and myeloid leukemia [26, 27, 28], however Vidaza therapy is associated with severe side-effects, and showed to be ineffective in our study, which was confirmed by others [10]. Compared to Vidaza or NMDi-14, SMG1i was the least toxic and effectively increased CFTR mRNA expression at a relatively low concentration. SMG1i is therefore an interesting target for further drug development, aiming to develop a safer, yet still effective NMD inhibitor. A strategy to develop more specific NMD inhibitors is to target a different effector protein involved in the NMD machinery. According to our results, targeting SMG7 with NMDi14 or MYC, an endogenous NMD-inhibitor, with Vidaza had no effect on CFTR function rescue. Nevertheless, many other effector proteins remain to be investigated and could potentially be targeted for more selective NMD inhibition.

Theoretically, RT and NMD together could result in normal amounts of full-length CFTR, yet we did not observe high rescue of CFTR function in our FIS assay with this dual pharmacotherapy. This can be contributed to the fact that amino acid incorporation upon RT varies per type of PTC and even per single transcript [16] and may thus not fully recapitulate WT protein function or stability. A previous study has shown that function of such W1282X variants can indeed be enhanced by combining RT agents with conventional CFTR correctors or potentiators [16]. In line with this study, swelling of PTC organoids upon treatment with ELX-02ds/SMG1i and VX-770/VX-661/VX-445 indeed reached AUC levels higher than that of VX-770/VX-809 treated F508del/F508del organoids. The optimal conditions for PTC restoration did not reach efficacies associated with VX-445/VX-661/VX-770 on F508del/F508del organoids. Whilst the results obtained with the ELX-02ds/SMG1i/VX-770/VX-661/VX-445 combination are promising, pharmacokinetic and drug-drug interaction studies will have to further elucidate the feasibility of combining these 5 different pharmacotherapies in vivo. On this note, in this study the effect of VX-445/VX-661/VX-770 was only tested

in combination. Future research should investigate whether this is indeed necessary, or whether the combination with ELX-02ds/SMG1i and a single CFTR modulator could result in sufficient functional CFTR rescue.

This report focusses on the use of intestinal organoids as preclinical test model for restoration of PTCs. Organoid FIS is completely CFTR dependent and the relation between in vitro swelling response and in vivo drug response and disease severity has been well characterized. Earlier work also found that G418 can induce CFTR function in PTC-containing organoids, but CFTR restoration by PTC-124 was not detected consistent with lack of efficacy in clinical trials with this drug [4,6]. Biobanks of organoids have been established and such infrastructures enable not only large-scale preclinical testing in patient cells but also the recruitment of preclinical responders for clinical trials. Whereas the simple phenotypic swell readout represents one of the strengths of this model, it also represents a limitation as swelling is limited by organoid stretch that limits the dynamic range of the assay at high CFTR function. The data could be further strengthened by protein analysis to demonstrate that ELX-02ds and the various combinations induced full length mature CFTR protein, as recently showed by Crawford *et al*. [8] in PTC-containing organoids rescued by ELX-02. Contradictory to this study however, Laselva *et al* did not observe an effect of G418 on CFTR protein level in human nasal cells [10]. Potentially low CFTR levels, below the detection limit of certain assays such as western blot, are sufficient to detect effects on a functional level. This is likely dependent on the exploited phenotypic assay, its sensitivity and the studied cell model. Evidently, comparison of results in different models is valuable. In contrast to the results described in this study, inhibition of nonsense mediated decay by SMG1i with addition of effective protein modulators exerted a dominant functional rescue of W1282X in primary nasal cultures that was not enhanced with the addition of G418. Whether this discrepancy is a consequence of the use of a different in vitro model and cell type, the differences between G418 and ELX-02ds, G418 induced toxicity or even patient to patient variation warrants further investigation. Future research could be conducted to assess whether functional recue of PTC's in nasal or bronchial epithelial cells is achievable with the compounds discussed in this study and whether its efficacy is comparable to the results achieved in intestinal organoids.

Overall, we observed CFTR function rescue in all organoid cultures, yet in between-genotype and within-genotype variation in the level of CFTR function rescue was also observed. RT efficacy has been described to be dependent on the identity of the PTC, from least to most susceptible: UAA<UAG<UGA, yet a donor carrying a UGA mutation on both alleles (R1162X/R1162X-CFTR), showed to be one of the lowest responding donors, indicating the between-genotype variation cannot only be explained by PTC-dependency of RT. While RT-efficacy is also moderated by the local and distant sequence surrounding the PTC [29,30], we did not find additional SNPs in our four W1282X/W1282X organoid cultures which could not explain the observed within-genotype variation. Nevertheless, even the low responding organoid cultures almost reached swelling levels comparable to F508del/F508del-CFTR rescued with VX-770/VX-809, indicating that independent of the PTC mutation, the level of CFTR function rescue has clinical potential.

In conclusion, this proof of concept study shows that truncated, defective CFTR protein harboring PTC mutations can be effectively repaired with a combination of pharmacotherapies. Whilst further studies are necessary to translate these studies to the clinic, we provide a potential mechanism to resolve the unmet need for a therapeutic approach for people carrying PTC mutations.

Supplemental Information

Supplemental data can be found online, at https://doi.org/10.1016/j.jcf.2021.09.020

Author Contribution Statement

E.d.P. and S.S contributed to the design of the study, the acquisition, verification, analysis and interpretation of the data and have drafted the manuscript. S.W.F.S., E.K., K.B., S.Y.G., M.A.M., E.J.M.W., M.M.vd.E. and G.H.K. contributed to the acquisition of study data, provided resources and revised the manuscript. C.K.v.d.E and J.M.B. have made substantial contributions to the conception and design of the study, interpretation of data and revised the manuscript.

Declaration of Competing Interest

J.M.B. and C.K.v.d.E. are inventors on patent(s) related to the FIS-assay and received financial royalties from 2017 onward. J.M.B report receiving research grant(s) and consultancy fees from various industries, including Vertex Pharmaceuticals, Proteostasis Therapeutics, Eloxx Pharmaceuticals, Teva Pharmaceutical Industries and Galapagos outside the submitted work. C.K.v.d.E report receiving research grant(s) grant(s) from Vertex Pharmaceuticals (money to institution) outside the submitted work. G.H.K. reports research grants from Vertex Pharmaceuticals, GSK, TEVA, Ubbo Emmius Foundation, European Union, Lung Foundation Netherlands (Money to institution), outside the submitted work. M.A.M. reports research grants and patient recruitment fees for clinical trials from Vertex, for which his institution Charité-Universitätsmedizine Berlin received payment; fees for consulting and advisory board participation from Antabio, Arrowhead, Boehringer Ingelheim, Enterprise Therapeutics, Kither Biotech, Sathera, Sterna Biologicals, and Vertex outside the submitted work. S.Y.G. reports fees for advisory board participation from Chiesi outside the submitted work. All other authors have nothing to disclose.

Acknowledgements

This work was supported by grants of the Dutch Cystic Fibrosis Foundation (NCFS), the Dutch Muco & Friends Foundation, the American organization Emily's Entourage and the German Federal Ministry for Education and Research (82DZL0098B1 to M.A.M.). S.Y.G is participant of the BIH- Charité Clinician Scientist Program funded by the Charité – Universitätsmedizin Berlin and the BIH. S.Y.G. is supported by a financial grant from the Christiane Herzog Stiftung, Stuttgart, Germany and the Mukoviszidose Institut gGmbH, Bonn, the research and development arm of the German Cystic Fibrosis Association Mukoviszidose e.V. Furthermore, we would like to thank the UCSF Medical Center for kindly providing ASP-11 and Michael Wilschanski and Prof. Batsheva Kerem from The Hebrew University Jerusalem for kindly providing intestinal organoids.

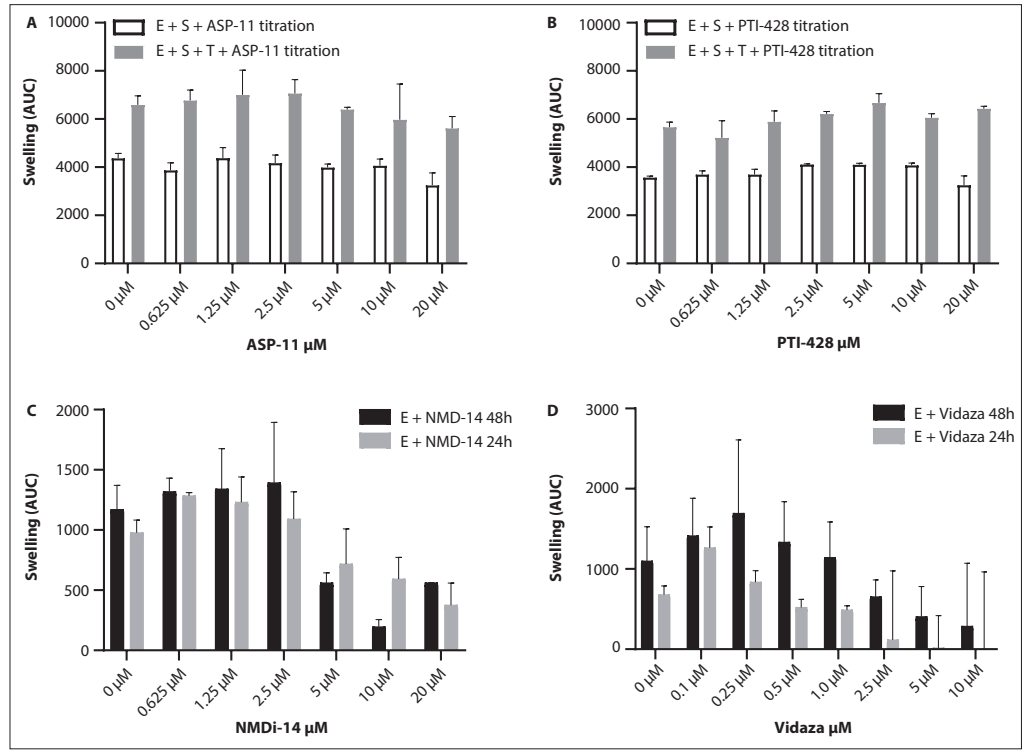

Supplemental Figure 1: Dose-response assays on a W1282X/W1282X organoid culture to define proper pharmacotherapy conditions.
(A) FIS, measured for 2h in presence of 5 µM forskolin in presence of increasing concentration of ASP-11. The organoids were pre-stimulated with either E+S (white bars) or E+S+T (gray bars). **(B)** FIS, measured for 2h in presence of 5 µM forskolin in presence of increasing concentration of PTI-428, added 24h prior to FIS-assay. The organoids were pre-stimulated with either E+S (white bars) or E+S+T (gray bars). **(C)** FIS, measured for 2h in presence of 5 µM forskolin of organoids pre-stimulated for 48h with ELX-02 and an increasing concentration of NMDi-14 for 24h (black bars) or 48h (gray bars). Bars represent mean+SD, n=3. **(D)** FIS, measured for 2h in presence of 5 µM forskolin of organoids pre-stimulated for 48h with ELX-02 and an increasing concentration of Vidaza for 24h (black bars) or 48h (gray bars). Bars represent mean+SD, n=3.

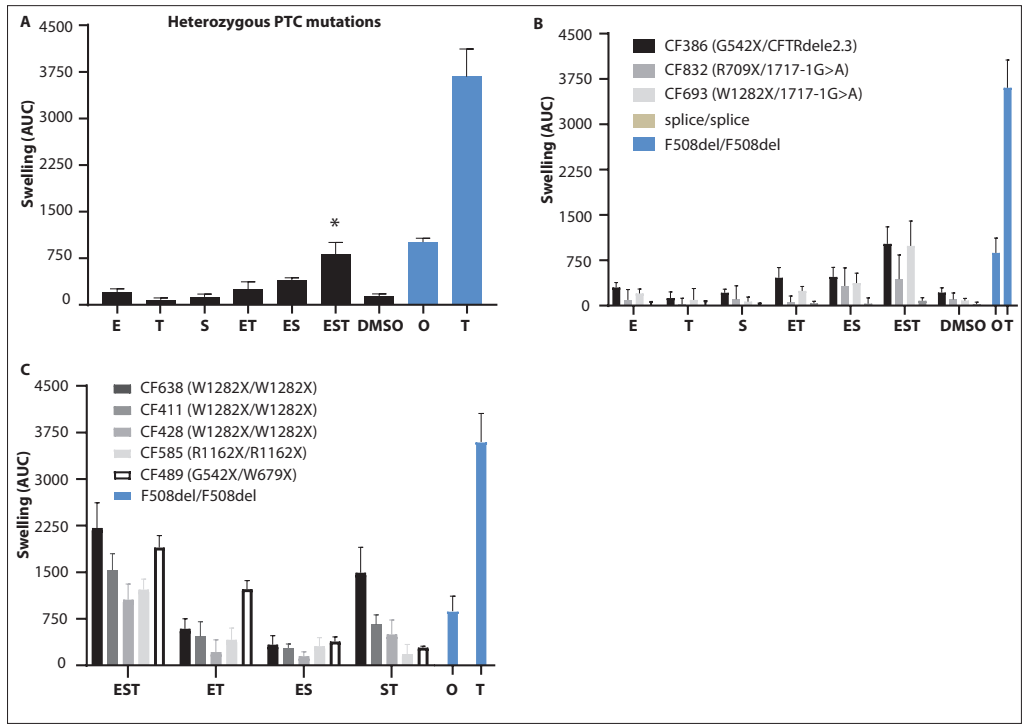

Supplemental Figure 2: Response of compound heterozygous organoid cultures to pharmacotherapies and SMG1i+VX-445/VX-661/VX-770 rescued FIS of homozygous PTC organoid cultures.

(A) FIS (mean+SEM) of 3 organoid cultures compound heterozygous for a PTC mutation, measured for 1h in presence of 0.128 μM forskolin upon pharmacotherapy treatment. Organoid cultures were pre-stimulated with E, S and/or T. To determine the therapeutic value of the investigational pharmacotherapies, the swelling levels were compared to the mean swelling levels of three organoid cultures expressing F508del/F508del-CFTR upon rescue with CFTR modulator cocktails (bue bars, mean+SD, n=9) of which clinical value is known. *p<0.05, compared to DMSO. **(B)** FIS of each individual compound heterozygous organoid culture upon pharmacotherapy. Three organoid cultures homozygous for consensus splice mutations (1811+1G>C or 1717-1G>A) were included to assess whether pharmacotherapy speci cally rescue PTC-CFTR. Bars represent mean+SD. **(C)** FIS of homozygous PTC organoid cultures pre-stimulated with S+ T (ST), measured for 1 hour with 0.128uM forskolin. The ST pharmacotherapy was compared to the other investigational pharmacotherapies discussed in the study. Bars represent mean+SD. Abbreviations: E = ELX-02ds (80 μM, 48h); S = SMG1i (0.3 μM, 24h); T = VX-661 (3 μM, 24h) + VX-445 (3 μM, 24h) + VX-770 (3 μM, added simultaneously with forskolin); O = VX-809 (3 μM, 24h) + VX-770 (3 μM, added simultaneously with forskolin).

References

1. Mall MA, Mayer-Hamblett N, Rowe SM. Cystic fibrosis: Emergence of highly effective targeted therapeutics and potential clinical implications. Am. J. Respir. Crit. Care Med. 2020;201:1193–208.
2. Howard M, Frizzell RA, Bedwell DM. Aminoglycoside antibiotics restore CFTR function by overcoming premature stop mutations. Nat. Med. 1996;2:467–9.
3. Welch EM, *et al*. PTC124 targets genetic disorders caused by nonsense mutations. Nature 2007;447:87–91.
4. Ommen Zomer-van, D D, *et al*. Limited premature termination codon suppression by read-through agents in cystic fibrosis intestinal organoids. J. Cyst. Fibros. 2016;15: 158–62.
5. McElroy SP, *et al*. A lack of premature termination codon read-through efficacy of PTC124 (Ataluren) in a diverse array of reporter assays. PLoS Biol. 2013;11.
6. Kerem E, *et al*. Ataluren for the treatment of nonsense-mutation cystic fibrosis: A randomised, double-blind, placebo-controlled phase 3 trial. Lancet Respir. Med. 2014;2:539–47.
7. Leubitz A, *et al*. A Randomized, Double-Blind, Placebo-Controlled, Multiple Dose Escalation Study to Evaluate the Safety and Pharmacokinetics of ELX-02 in Healthy Subjects. Clin. Pharmacol. Drug Dev. 2021;02451.
8. Crawford DK, *et al*. Targeting G542X CFTR nonsense alleles with ELX-02 restores CFTR function in human-derived intestinal organoids. J. Cyst. Fibros.2021:1–7.
9. Sharma N. Capitalizing on the heterogeneous effects of CFTR nonsense and frameshift variants to inform therapeutic strategy for cystic fibrosis. PLoS Genetics 2018;14.
10. Laselva O, *et al*. Functional rescue of c.3846G>A (W1282X) in patient-derived nasal cultures achieved by inhibition of nonsense mediated decay and protein modulators with complementary mechanisms of action. J. Cyst. Fibros. 2020;19:717–27.
11. Keenan MM, *et al*. Nonsense-mediated RNA decay pathway inhibition restores expression and function of W1282X CFTR. Am. J. Respir. Cell Mol. Biol. 2019;61:290–300.
12. Yeh JT, Hwang TC. Positional effects of premature termination codons on the biochemical and biophysical properties of CFTR. J. Physiol. 2020;598:517–41.
13. Aksit MA, *et al*. Decreased mRNA and protein stability of W1282X limits response to modulator therapy. J. Cyst. Fibros. 2019;18:606–13.
14. Valley HC, *et al*. Isogenic cell models of cystic fibrosis-causing variants in natively expressing pulmonary epithelial cells. J. Cyst. Fibros. 2019;18:476–83.
15. Giuliano KA, *et al*. Use of a high-throughput phenotypic screening strategy to identify amplifiers, a novel pharmacological class of small molecules that exhibit functional synergy with potentiators and correctors. SLAS Discov. 2018;23:111–21.
16. Xue X, *et al*. Identification of the amino acids inserted during suppression of CFTR nonsense mutations and determination of their functional consequences. Hum. Mol. Genet. 2017;26:3116–29.
17. McHugh DR, Cotton CU, Hodges CA. Synergy between readthrough and nonsense mediated decay inhibition in a murine model of cystic fibrosis nonsense mutations. Int. J. Mol. Sci. 2021;22:1–20.

18. Phuan PW, *et al*. Combination potentiator ('co-potentiator') therapy for CF caused by CFTR mutants, including N1303K, that are poorly responsive to single potentiators. J. Cyst. Fibros. 2018;17:595–606.
19. Laselva O, *et al*. Rescue of multiple class II CFTR mutations by elexacaftor+ tezacaftor+ivacaftor mediated in part by the dual activities of Elexacaftor as both corrector and potentiator. Eur. Respir. J. 2020;2002774. doi:10.1183/ 13993003.02774-2020.
20. Dekkers JF, *et al*. A functional CFTR assay using primary cystic fibrosis intestinal o rganoids. Nat. Med. 2013;19:939–45.
21. Berkers G, *et al*. Rectal organoids enable personalized treatment of cystic fibrosis. Cell Rep. 2019;26:1701–8 .e3.
22. de Winter-De Groot KM, *et al*. Stratifying infants with cystic fibrosis for disease severity using intestinal organoid swelling as a biomarker of CFTR function. Eur. Respir. J. 2018;52.
23. de Winter – de Groot KM, *et al*. Forskolin-induced swelling of intestinal organoids correlates with disease severity in adults with cystic fibrosis and homozygous F508del mutations. J. Cyst. Fibros. 2020;19:614–19.
24. Dekkers JF, *et al*. Supplementary materials for characterizing responses to CFTR-modulating drugs using rectal organoids derived from subjects with cystic fibrosis. Sci. Transl. Med. 2016;8:344–84.
25. Vonk AM, *et al*. Protocol for application, standardization and validation of the forskolin-induced swelling assay in cystic fibrosis human colon organoids. STAR Protoc. 2020;1:100019.
26. Silverman LR, *et al*. Further analysis of trials with azacitidine in patients with myelodysplastic syndrome: Studies 8421, 8921, and 9221 by the Cancer and Leukemia Group B. J. Clin. Oncol. 2006;24:3895–903.
27. Fenaux P, *et al*. Azacitidine prolongs overall survival compared with conventional care regimens in elderly patients with low bone marrow blast count acute myeloid leukemia. J. Clin. Oncol. 2010;28:562–9.
28. Bhuvanagiri M, *et al*. 5 -azacytidine inhibits nonsense-mediated decay in a MYC-dependent fashion 2014;6:1593–609.
29. Pranke I, *et al*. Factors influencing readthrough therapy for frequent cystic fibrosis premature termination codons. ERJ Open Res 2018;4:00080–2017.
30. Cridge AG, Crowe-Mcauliffe C, Mathew SF, Tate WP. Eukaryotic translational termination efficiency is influenced by the 3 nucleotides within the ribosomal mRNA channel. Nucleic Acids Res 2018;46:1927–44.

Chapter | 4

Use of 2,6-diaminopurine as a potent suppressor of UGA premature stop codons in cystic fibrosis

Molecular Therapy, April 2023, Volume 31, Issue 4

Catherine Leroy[1,2,*], **Sacha Spelier[3,4,5,*],** Nadège Charlene Essonghe[6,7], Virginie Poix[1,2], Rebekah Kong[1,2], Patrick Gizzi[8], Claire Bourban[8], Séverine Amand[9], Christine Bailly[9], Romain Guilbert[10], David Hannebique[10], Philippe Persoons[10], Gwenaëlle Arhant[1,2,] Anne Prévotat[11,] Philippe Reix[12,] Dominique Hubert[13], Michèle Gérardin[14], Mathias Chamaillard[6], Natalia Prevarskaya[6,7], Sylvie Rebuffat[9], George Shapovalov[6,7], Jeffrey Beekman[3,4,5] and Fabrice Lejeune[1,2]

**** These authors contributed equally to this work***

1. University Lille, CNRS, INSERM, UMR9020-U1277-CANTHER-Cancer Heterogeneity Plasticity and Resistance to Therapies, 59000 Lille, France **2.** Unité Tumorigenèse et Résistance aux Traitements, Institut Pasteur de Lille, 59000 Lille, France **3.** Pediatric Respiratory Medicine, Wilhelmina Children's Hospital, University Medical Center, Utrecht University, 3584 EA Utrecht, the Netherlands **4.** Regenerative Medicine Utrecht, University Medical Center, Utrecht University, 3584 CT Utrecht, the Netherlands **5.** Center for Living Technologies, University Medical Center, Utrecht University, 3584 CT Utrecht, the Netherlands **6.** University Lille, INSERM, U1003-PHYCEL-Physiologie Cellulaire, 59000 Lille, France; **7.** Laboratory of Excellence, Ion Channels Science and Therapeutics, 59655 Villeneuve d'Ascq, France **8.** Plateforme de Chimie Biologique Intégrative de Strasbourg, UAR 3286 CNRS-Université de Strasbourg, 67404 Illkirch, France **9.** Muséum National d'Histoire Naturelle, Centre National de la Recherche Scientifique, Laboratory of Molecules of Communication and Adaptation of Microorganisms (MCAM), UMR 7245 CNRS-MNHN, CP 54, 57 Rue Cuvier, 75005 Paris, France; **10.** Institut Pasteur de Lille-PLEHTA (Plateforme d'Expérimentation et de Haute Technologie Animale), 59019 Lille, France **11.** University Lille, Clinique des Maladies Respiratoires, CRCM Hôpital Calmette, CHRU Lille, 59000 Lille, France **12.** CRCM Pédiatrique Lyon, Hôpital Femme Mère Enfant, Hospices Civils de Lyon, UMR 5558 (EMET), CNRS, LBBE, Université de Lyon, 69622 Villeurbanne, France **13.** Pulmonary Department and Adult CF Centre, Cochin Hospital, AP-HP, Paris, France **14.** CF Pediatric Centre, Robert Debré Hospital, AP-HP, 75019 Paris, France

Abstract

Nonsense mutations are responsible for around 10% of cases of genetic diseases, including cystic fibrosis. 2,6-diaminopurine (DAP) has recently been shown to promote efficient readthrough of UGA premature stop codons. In this study, we show that DAP can correct a nonsense mutation in the *CFTR* gene in vivo in a new CF mouse model, in utero, and through breastfeeding, thanks, notably, to adequate pharmacokinetic properties. DAP turns out to be very stable in plasma and is distributed throughout the body. The ability of DAP to correct various endogenous UGA nonsense mutations in the *CFTR* gene and to restore its function in mice, in organoids derived from murine or patient cells, and in cells from patients with cystic fibrosis reveals the potential of such readthrough-stimulating molecules in developing a therapeutic approach. The fact that correction by DAP of certain nonsense mutations reaches a clinically relevant level, as judged from previous studies, makes the use of this compound all the more attractive.

Keywords

cystic fibrosis - nonsense mutation - readthrough molecule - 2,6-diaminopurine - mouse model

Introduction

Cystic fibrosis (CF) is the most frequent rare disease, with about 1 case per 3,000 births in Europe and the United States. This autosomal recessive pathology is related to malfunction or absence of the CF transmembrane conductance regulator (CFTR), a channel transporting chloride ions from the intracellular to the extracellular environment. CFTR is a membrane protein that is primarily expressed by epithelial cells for regulating mucus production. About 2,000 mutations have been identified in CF, including delF508 in nearly 70%–80% of CF cases (www.orpha.net). Fortunately, for this mutation in particular, treatments with two molecules (lumacaftor-ivacaftor, or Orkambi, or tezacaftor-ivacaftor, or Symdeko) or three molecules (elexacaftor-tezacaftor-ivacaftor, or Trikafta) are available to patients from the manufacturer Vertex Pharmaceuticals. As these CFTR modulators restore CFTR folding and CFTR potentiation, there remains a large group of CF patients that do not respond to these treatments due to mutations that result in complete absence of CFTR protein. About 10% of the CF patients carry mutations that result in nonsense mutations. Nonsense mutations are responsible for about 10% of genetic disease cases, including CF [1]. The presence of a nonsense mutation results in low expression levels of the mutant mRNA, due to activation of nonsense-mediated mRNA decay (NMD), an mRNA surveillance mechanism that degrades mRNAs harboring a premature termination codon (PTC) [2, 3, 4, 5, 6, 7]. Strategies for rescuing the expression of genes carrying a nonsense mutation include NMD inhibition [8, 9, 10, 11, 12, 13] gene therapy [14], gene editing [15, 16, 17], antisense oligonucleotides [18, 19, 20] or PTC readthrough, a mechanism leading to the introduction of an amino acid at the PTC position during translation [21, 22, 23]. Molecules stimulating PTC readthrough include aminoglycosides (e.g., G418 or ELX-02) and non-aminoglycosides (e.g., ataluren or amlexanox) [24, 25, 26]. Although ataluren and ELX-02 have reached the clinical trial stage, their efficacy is still debatable [27, 28] and currently there are no treatments available for patients with a nonsense mutation. This underlines the need to identify novel molecules capable of efficiently and safely correcting nonsense mutations in pathological contexts.

Recently, the purine derivative 2,6-diaminopurine (DAP) has been shown to correct UGA nonsense mutations efficiently by activating PTC readthrough [29]. In human cells, DAP rescues the expression and functions of genes carrying UGA nonsense mutations more efficiently than G418. DAP has also been shown to correct UGA nonsense mutations in vivo after oral exposure of mice to DAP [29]. DAP causes readthrough by inhibiting the activity of FTSJ1, a transmethylase that modifies certain tRNAs post-transcriptionally, including that carrying the amino acid tryptophan. Hence, DAP-induced readthrough leads to incorporation of a tryptophan at the position of the PTC UGA [29]. Therefore, DAP is particularly suitable for correcting mutations that convert a tryptophan-encoding codon to a PTC. An example is W1282X, accounting for 18% of CF-causing nonsense mutations [27]. This makes it worthwhile to evaluate the capacity of DAP to correct UGA nonsense mutations in several pathological contexts. Here, in animal models of CF pathology, CF-patient-derived organoids, and patient cells carrying a UGA nonsense mutation in the CFTR gene, we provide evidence in favor of using DAP to restore CFTR function.

Materials and methods

CFTR-NS mouse model

The CFTR-NS mouse was developed at the Institut Clinique de la Souris (ICS). Both point mutations were introduced at the same time, using the Cre-Lox system and homologous recombination in embryonic stem cells before being introduced into embryos with the C57BL/6N genetic background. The leftover LoxP site is located in intron 12 and allowed genotyping. The mouse strain is maintained in the heterozygous state. All in vivo experiments complied with all relevant ethical regulations for animal testing and research and were authorized by the Ethic Committee 075 under the number 12971-2018010815336092.

Collecting primary intestinal epithelial mouse cells

Five centimeters of duodenum was cut into 1-mm pieces after removing all the stool. The pieces were washed five times with PBS before being incubated for 20 min at 37°C in the presence of 200 U/mL collagenase and 100 U/mL hyaluronidase. After 5 min centrifugation at 100 × g and 4°C, the pellet was resuspended in DMEM containing 2% fetal bovine serum (FBS) and 2% sorbitol. The solution was centrifuged for 5 min at 250 × g at room temperature, the pellet was resuspended in DMEM containing 10% FBS, and the cells were placed in culture dishes.

Molecule preparation

DAP was purchased from Sigma-Aldrich (ref. no. 247847) and dissolved at 100 mM in DMSO (cell and organoid treatments) or at 5 mg/mL in 10% DMSO/90% PBS (mouse treatments). ELX-02 was purchased from MedChemExpress (ref. no. HY-114231B) and dissolved in DMSO.

Chapter | 4

Collecting primary epithelial cells from CF patients
All experimentation using human tissues described herein was approved by the medical ethics committee of the University Medical Center Utrecht (UMCU; TcBio 14-008 and TcBio 16-586). Informed consent for tissue collection and for generation, storage, and use of organoids was obtained from all participating patients. Biobanked intestinal organoids are stored and cataloged (https://huborganoids.nl/) at the Hubrecht Organoid Technology foundation (http://hub4organoids.eu) and can be requested from info@hub4organoids.eu. Collection of patient tissues and data was performed according to the guidelines of the European Network of Research Ethics Committees (EUREC) and to European, national, and local law.

Mouse intestinal organoid culture and characterization of CFTR function
Crypts were isolated from small intestinal biopsies of mice as previously described.44 Crypts were plated in 50% Matrigel and developed into organoid structures within 3 weeks. The same medium was used as for the human intestinal organoids, with the exception that the end volume of WNT-conditioned medium was 75% instead of 50%. Organoids were incubated in a humidified chamber with 5% CO2 at 37°C, the medium was refreshed every 2–3 days, and organoids were passaged 1:4 every 5–7 days. For assessing restoration of CFTR function, organoids were preincubated with DAP or G418 for 48 h prior to forskolin addition (5 μM). After 1 h of forskolin stimulation, 10× bright-field pictures were taken using an EVOS inverted microscope. Pictures were assessed in a blinded manner, by quantifying the size of 10 organoids in each picture using ImageJ. For each condition, the average of three replicates was calculated, and results were normalized to the negative control (DMSO treated).

Human intestinal organoid cultures
Crypts were isolated from biopsies of people with CF as previously described [45]. Briefly, organoids were cultured in 50% Matrigel (Corning; 356255) in advanced DMEM/F12 medium supplemented with penicillin and streptomycin, 10 mM HEPES, Glutamax, B27 (all from Invitrogen), 1 μM N-acetylcysteine (Sigma), and the following growth factors: 50 ng/mL mouse epidermal growth factor (mEGF), 50% Wnt3a-conditioned medium (WCM), 10% Noggin-conditioned medium (NCM), 20% Rspo1-conditioned medium (RCM), 10 μM nicotinamide (Sigma), 500 nM A83-01 (Tocris), and 10 μM SB202190 (Sigma). Organoids were incubated in a humidified chamber under 5% CO2 at 37°C. The medium was refreshed every 2–3 days and the organoids were passaged 1:4 every 7–10 days.

Functional assessment of CFTR and measurement of DAP toxicity in PDIOs derived from CF patient cells
Prior to measuring CFTR function in FIS assays, PDIOs were grown for at least 3 weeks after crypt isolation or thawing. They were split as previously described45 and plated in 3-μL basement extract membrane drops on 96-well plates. After a 5-min incubation at 37°C, the medium with DMSO, DAP, or G418 was added to the wells. After a 48-h incubation, forskolin (5 μM) and calcein (3 μM) were added to all wells. PDIO swelling was monitored for 60 min with a Zeiss LSM 710 confocal microscope. Total organoid surface area per well was quantified with Zen software on the basis of calcein staining, and the area under the curve over time was calculated as described in Vonk *et al*.45 After the FIS experiments on PDIOs of donor 1, the medium was replaced with 100 μL alamarBlue stock solution diluted 1:10 in DMEM without phenol red. Plates were incubated at 37°C for 4 h, after which fluorescence (excitation wavelength 470 nm, emission wavelength 530 nm) was measured with a CLARIOstar multimode microplate reader. Viability was normalized to negative controls (PDIOs treated with 0.1% DMSO) and positive controls (PDIOs treated with 10% DMSO for 24 h).

RNA isolation from PDIOs and SYBR-quantitative real-time PCR
Forty-eight hours prior to RNA isolation, DAP and SMG1i were added to the culture medium at 25/50/100 and 0.3 μM, respectively. RNA was isolated for two homozygous W1282X PDIOs, using the NucleoSpin RNA kit (BIOKE) according to the manufacturer's protocol. RNA yield was measured by a NanoDrop spectrophotometer, and extracted mRNA was used for cDNA synthesis using the iScript cDNA synthesis kit (Bio-Rad) according to the manufacturer's protocol. YWHAZ, GAPDH, and CFTR regions were amplified in a two-step quantitative real-time PCR SYBR green reaction (CFX-384 real-time PCR; Bio-Rad) in a total assay volume of 10 μL. Primers sequences were as follows:
YWHAZ (forward, 5'-CTGGAACGGTGAAGGTGACA-3'; reverse, 5'-AAGGGACTTCCTGTAACAATGCA-3'), GAPDH (forward, 5'-TGCACCACCAACTGCTTAGC-3'; reverse, 5'-GGCATGGACTGTGGTCATGAG-3'), and CFTR (forward, 5'-CAACATCTAGTGAGCAGTCAGG-3'; reverse, 5'-CCCAGGTAAGGGATGTATTGTG-3').
Samples were incubated during the PCR as follows: 2 min at 95°C and 39 cycles of 30 s at 95°C, 30 s at 59°C. Relative gene expression of *CFTR* was first normalized against the housekeeping genes GAPDH and YWHAZ, after which *CFTR* expression was normalized against control samples using the comparative 2-ΔΔCT method. Melt peaks were analyzed to confirm amplification of a single product. Two biological replicate experiments were performed with three technical replicates per experiment.

RNA isolation from CFTR-NS mouse lung
Total RNA was extracted from approximately one-fifth of a lung using RNAzol and the supplier-provided protocol. Reverse transcription was done using SuperScript II (Invitrogen) and random hexamers. CFTR cDNA and GAPDH cDNA were then amplified by 35 cycles of PCR using the following oligonucleotides: CFTR sense, 5'-GACGAGTTCTAAAACAAGCC-3'; CFTR antisense, 5'-TACCCATACCCATATGAACG-3'; GAPDH sense, 5'-CATTGACCTCAACTACATGG-3'; GAPDH antisense, 5'-GCCATGCCAGTGAGCTTCC-3'. PCR amplifications were loaded on a 1% agarose gel containing ethidium bromide.

Western blotting
After 24 h of treatment, 2 × 106 Calu-6 cells were harvested and proteins extracted in a lysis buffer containing 5% SDS, 50 mM Tris, and 20 mM EDTA. The equivalent of 2.5 × 105 cells was subjected to 10% SDS-PAGE before transfer of the proteins to a nitrocellulose membrane. The membranes were incubated overnight at 4°C in the presence of a 1/200 dilution

of anti-p53 antibody (DO1; Santa Cruz Biotechnology, Dallas, TX, USA) or 1/1,000 dilution of anti-IMPORTIN9 antibody (Abcam, Cambridge, UK). After three washes of the membrane in TBS Tween, the membranes were exposed to a solution of peroxidase-coupled secondary antibody for detection of mouse- or rabbit-raised antibody (Jackson ImmunoResearch, Suffolk, UK). Antibodies were then detected with SuperSignal West Femto maximum sensitivity substrate (Pierce Biotechnology, Rockford, IL, USA).

Immunohistochemistry

Lung and intestinal tissues were fixed in 4% paraformaldehyde (PFA) or in Carnoy solution (60% methanol, 30% chloroform, 10% acetic acid) before being embedded in paraffin and sectioned into 5-µm lung slices or 10-µm intestine slices. For detection of CFTR in adults and 2-week-old mice, the sections were incubated with blocking buffer consisting of goat serum and anti-mouse IgG before incubating with the anti-CFTR antibody (Abcam ab234037 for lung or LS-Bio LS-C14758 for intestine) at 1:100 dilution. For detection of CFTR in the intestines of newborns, a blocking step with Bloxall (Vector Laboratories) was performed before incubation with the goat serum, and anti-CFTR antibody from Santa Cruz (sc-376683) was used at 1:100 dilution. Mayer's hemalum counterstain was then applied to all slices.

Bioavailability DAP

A PK study was performed using 6-week-old CD-1 mice. A dose of 29 mg/kg DAP solution (10% DMSO/90% PBS) was administered by oral gavage. Blood was taken by intracardiac puncture 0.5, 1, 2, 4, 6, and 24 h after gavage. Blood samples were then placed into an EDTA-coated tube and centrifuged at 4°C, 12,000 × g for 10 min, to collect plasma, which was stored frozen at -80°C until analysis. For this, a volume of 400 µL of plasma was mixed with 1 mL of acetonitrile to precipitate the proteins and extract the DAP. Samples were vortexed for 5 min before being sonicated for 1 min. The proteins were pelletized by centrifugation at 15,000 × g for 5 min at 16°C. One milliliter of supernatant was then evaporated, and the dry matter was resuspended in 100 µL of water containing 1% trifluoroacetic acid before being analyzed by LC-MS/MS mass spectrometry.

Biodistribution DAP

DAP was measured in lung, muscle, and brain from male CD-1 mice. DAP (8.1 mg/kg; maximum solubility in 5% DMSO/95% PBS) was injected intravenously into 18 mice. Three mice were sacrificed at 15, 30, 60, 120, 240, and 360 min. For each time point, plasma, lung, muscles, intestine, and brain were collected and stored at -80°C before proceeding with the analysis. Tissues were collected after perfusion of the mice with 50 mL 0.9% NaCl solution to remove the blood. The lungs, tibialis anterior, small intestine, and brain were crushed in 400 µL water before adding 800 µL acetonitrile. The ground material was vortexed for 5 min and then sonicated for 1 min prior to centrifugation for 5 min at 15,000 × g and 16°C. The supernatant (120 µL) was evaporated and the dry matter resuspended in 120 µL water containing 1% trifluoroacetic acid. The sample was then analyzed by LC-MS/MS. During this experiment, urine was collected from the animal's bladder and stored at -80°C while awaiting analysis. The urine (50–300 µL) was diluted with 200 µL water. Each sample was placed on an SPE cartridge conditioned with 1 mL methanol and then with 1 mL water before washing the cartridge with 1 mL water and eluting with 800 µL methanol. The eluate was vacuum evaporated, the dry matter obtained was resuspended in 500 µL water containing 1% trifluoroacetic acid, and the samples were then treated as described above.

Measurement of DAP in stomach contents

The stomach contents of newborns were collected using a syringe after opening the stomach. The proteins in the samples were precipitated with acetonitrile. The supernatant was analyzed by mass spectrometry after adding 9 vol of water containing 1% trifluoroacetic acid. The samples were analyzed by UHPLC coupled to a Shimadzu LC-MS 8030 triple quadrupole.

Patch-clamp recordings

CFTR activity was acquired using the patch-clamp technique in cell-attached and inside-out configurations. To ensure proper CFTR expression, only cells within confluent islands and completely surrounded by other cells were patched. In some cultures where seals were difficult to make, the cells were treated with trypsin for 30 s. Currents were recorded via an Axopatch 200B amplifier and digitized using the Digidata 1322 digitizer using the pClamp software (Molecular Devices, San Jose, CA, USA). All patch-clamp recordings were made at 20°C–22°C. Patch pipettes were fabricated from borosilicate glass capillaries (World Precision Instruments, Sarasota, FL, USA) on a horizontal puller (Sutter Instruments, Novato, CA, USA) and had a resistance in the range of 3–5 MΩ. The standard bath and pipette solutions contained 150 mM NMDG-Cl, 2.5 mM CaC12, 2.5 mM MgCl2, and 10 mM HEPES, with pH adjusted to 7.3 with HCl. To ensure robust activation of CFTR ion channels, cells were treated with 40 µM forskolin and 400 µM IBMX for 30 min prior to patching. Bath solution was supplemented with 1 mM Mg-ATP to maintain CFTR activity in the excised inside-out patches. In the experiments where online PKA/ATP effects were verified, cells were immersed in the base solution not supplemented by ATP and patched without forskolin/IBMX pretreatment. Instead, 25 nM catalytic domain of PKA + 1 mM Mg-ATP was added to the bath online during data acquisition.

Whole-cell recordings were performed on the cells isolated from the WT and HO DAP- and HO DMSO-treated mice as described above. Isolated cells were immersed in the NMDG-Cl-based solution identical to that used for single-channel recordings. To eliminate K+ and Na+ channel involvement, the pipette solution was also based on the same NMDG-Cl solution, with free Ca2+ buffered to -100 nM by EGTA, resulting in the following composition: 150 mM NMDG-Cl, 2.5 mM MgCl2, 0.2 mM Ca2+, 0.5 mM EGTA, and 10 mM HEPES, with pH adjusted to 7.3 with HCl. Whole-cell recordings were performed using the ramp protocol with cells briefly held (for 50 ms) at -100 mV, followed by ramp from -100 to +100 mV, followed by another brief holding at +100 mV for 50 ms. Such ramps were applied once every second, with cells held at -40 mV between ramps to stabilize their condition. After the whole-cell mode was established, the cells were left undisturbed for 5 min to register basal

current levels, followed by extracellular application of 40 µM forskolin and 400 µM IBMX to stimulate CFTR activity. Under such conditions, with Cl- being the only ion current carrier, current deviation following the forskolin/IBMX application produced symmetric deviation of current at both +100 and -100 mV, with linear IV response during the ramp phase.

Statistics

Data are represented as means ± SD. One-way ANOVAs were performed to compare mean FIS efficacies upon treatment with the various compounds (cocktails). Differences were considered statistically significant at $p < 0.05$. Data analysis was performed with GraphPad Prism 7.0 software (San Diego, CA, USA).

Results

Pharmacokinetics of DAP in mouse

DAP has been shown to correct UGA nonsense mutations in human cells [29]. It is also reported to be stable in hepatic extract, where no degradation was observed even after 4 h of incubation. To evaluate further the possibility of using DAP *in vivo*, several pharmacokinetic parameters were measured. First, the DAP concentration in plasma was measured at different time points after intravenous DAP injection at 8.1 mg/kg **(Figure 1A).** This concentration was found to decrease rapidly, DAP being undetectable 2 h post-injection. These results indicate that DAP is either rapidly degraded in plasma or naturally eliminated. To test these hypotheses, the stability of DAP was measured in plasma **(Figure 1B).** The DAP concentration was found to remain unchanged over a 2-h incubation period, unlike procaine, used as a positive control. As this suggests that DAP could be rapidly eliminated via the urinary tract, its presence in urine was measured at different time points post-injection **(Figure 1C).** The amount of DAP detected in urine samples was found to peak 30 min after intravenous injection, indicating that DAP is cleared very quickly by this route. It was not possible to establish a concentration, because the volume of urine taken from the bladder at the time of sacrifice depended on the last time the animal had urinated. During injection, about 1.35 µmol of DAP was introduced into the body, of which about 40% was found in the urine. This 40% is an underestimate, as we cannot exclude that the mouse might have urinated between two time points. It appears, however, that not all of the DAP is removed by this route and that a certain amount is temporarily retained within different tissues.

Since DAP has previously been shown to correct a nonsense mutation *in vivo* following per os (PO) exposure [29], a very convenient way to administer medication, the DAP plasma level was measured under these exposure conditions **(Figure 1D).** Consistent with the previous results, DAP was detected in plasma after PO exposure. Its blood concentration peaked at about 70 µM 15–30 min after exposure, corresponding to the necessary absorption time. It dropped to 25 µM 1 h after PO exposure and to 1.8 µM 4 h after PO exposure (Table 1). This suggests that readthrough should still be promoted 4 h after PO exposure, since our previously reported results show that DAP readthrough can be measured by western blotting at DAP concentrations as low as 1.6 µM [29].

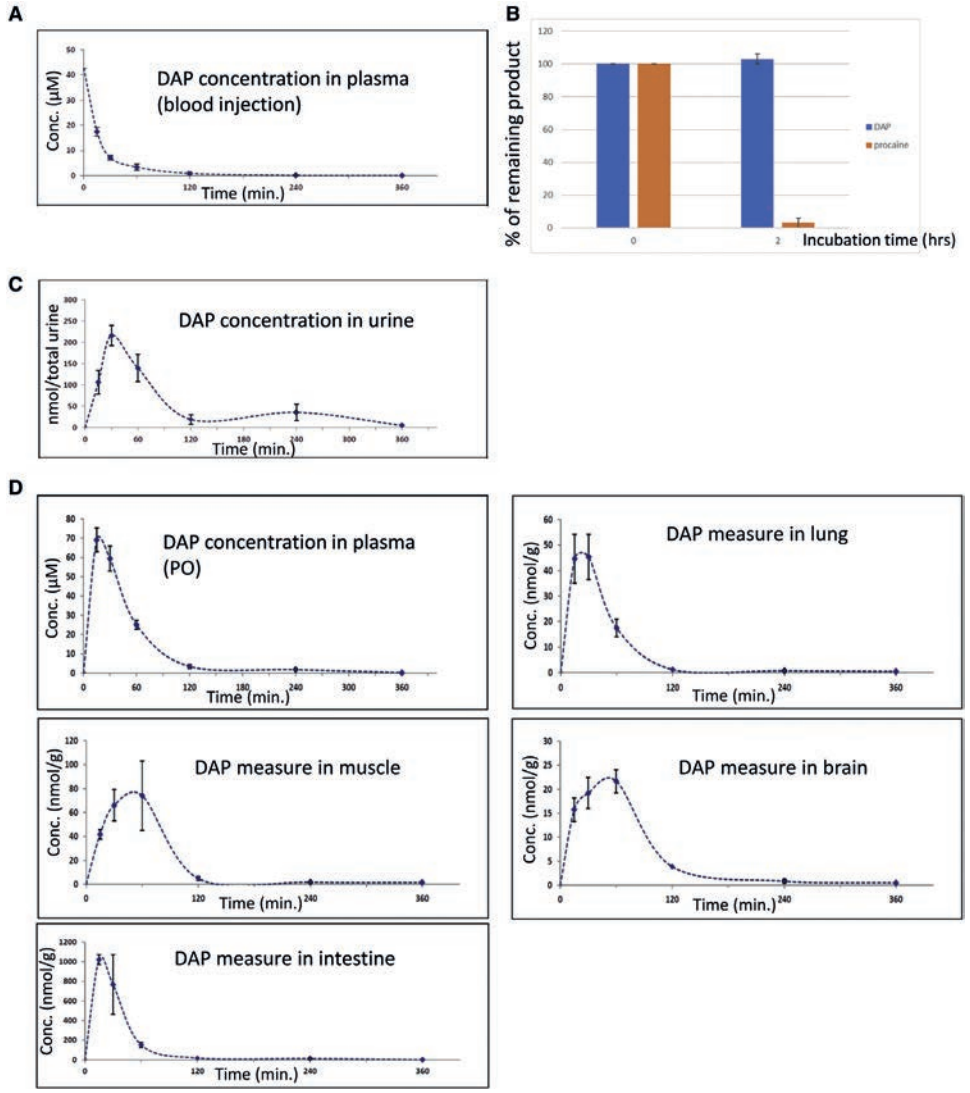

Figure 1. Pharmacokinetic parameters of DAP in CD-1 mouse.
(A) DAP plasma levels after blood injection of DAP at 8.1 mg/kg. Plasma concentrations of DAP were measured 30, 60, 120, 240, and 360 min post-injection. **(B)** Measure of DAP stability in plasma. DAP or procaine (positive control) was incubated for 2 h in plasma to assess its stability. **(C)** Measure by mass spectrometry of the concentration of DAP in urine after DAP injection. **(D)** DAP plasma levels after PO exposure of 29 mg/kg DAP (upper left), and biodistribution of DAP after PO exposure. DAP was measured by mass spectrometry in lung, muscle, brain tissues, and small intestine. Three mice were used for each time point. Error bars show the SD.

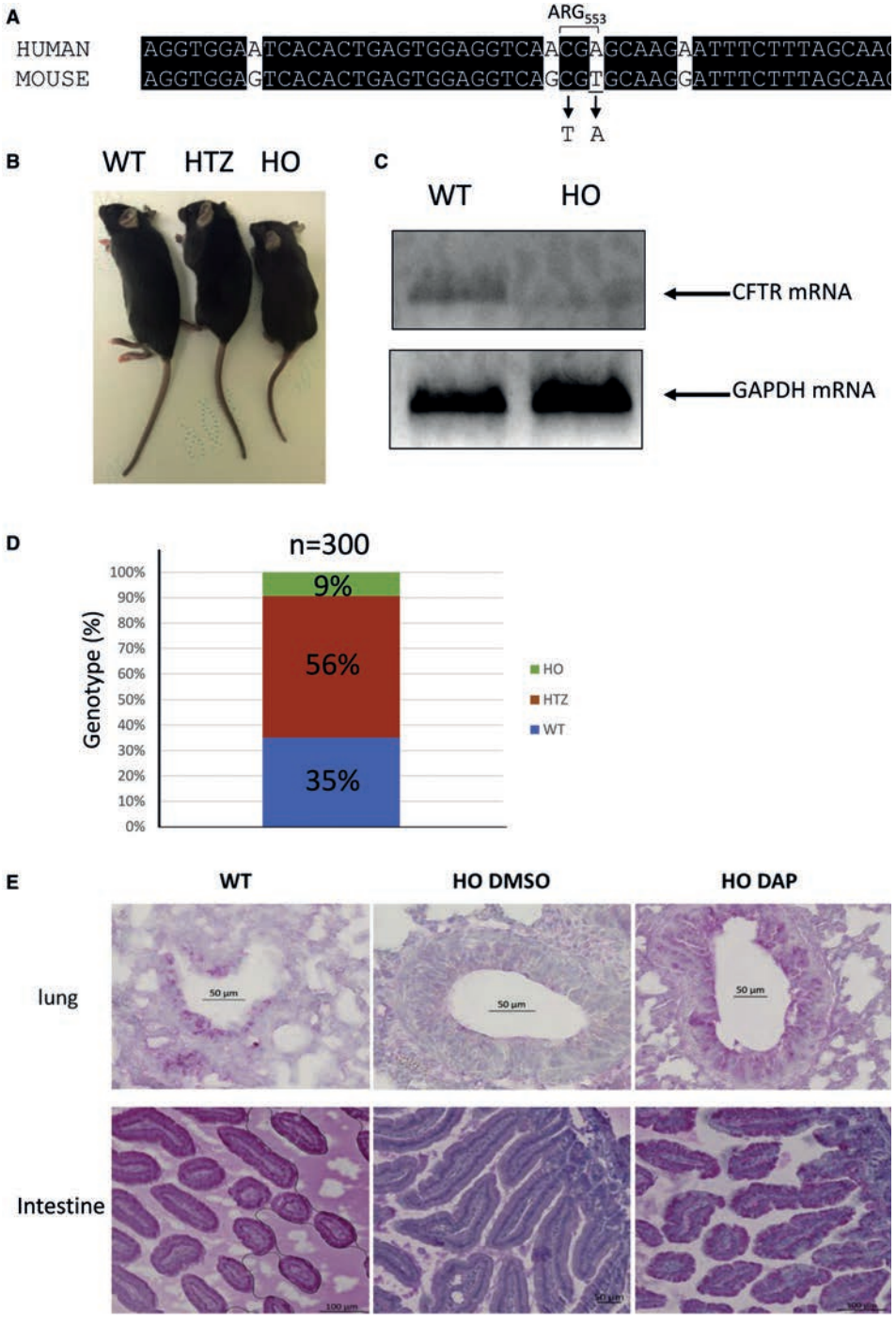

Figure 2. The CFTR-NS mouse model.
(A) Alignment of the human and mouse sequences in the region containing arginine 553. The two nucleotides changed in the murine sequence to generate the UGA stop codon are underlined. **(B)** Picture showing a homozygous wild-type mouse (WT), a mouse heterozygous for the nonsense mutation (HTZ), and a mouse homozygous for the nonsense mutation (HO). **(C)** Measurement of CFTR mRNA level in the lungs of wild-type (WT) and CFTR-NS (HO) mice by RT-PCR. Measurement of the GAPDH mRNA level serves as a loading control. **(D)** Proportion of the three genotypes at weaning. **(E)** Detection of CFTR (in red) by IHC in lung (around the bronchi) and intestinal tissues (duodenum) from WT and HO mice exposed PO to DMSO or DAP. All the IHCs are representative of at least five mice.

The next step was therefore to measure the amount of DAP present in different tissues to assess its biodistribution **(Figure 1D).** The quantity of DAP was thus measured in muscle, lung, brain, and intestine tissues following DAP PO exposure at 29 mg/kg. The quantity of DAP measured in each tissue was divided by the tissue mass. DAP was detected in all four tested tissues, with a very strong exposure of the small intestines. This suggests that DAP undergoes broad tissue distribution. The peak level was reached 15–30 min post-exposure, in keeping with the concentration curve of DAP in plasma **(Figure 1D).** After peaking, DAP decreased rapidly in all tissues but the brain, where the decrease was slower, suggesting transient accumulation in this tissue **(Figure 1D).** The fact that DAP can reach the brain also indicates that it crosses the blood-brain barrier. It should be noted that the biodistribution of DAP measured after PO exposure is closely similar to the biodistribution of DAP measured in the same organs after blood injection, indicating that the route of exposure does not appear to influence the biodistribution of DAP **(Supplemental Figure S1).** Overall, these results show that once introduced into the blood, DAP can reach different tissues without being massively retained there. Overall, the results of Figure 1, in combination with previously reported data, indicate that DAP can be used in vivo to correct nonsense mutations [29].

Characterization of a new mouse model of CF carrying a nonsense mutation in Cftr
As at the start of this project there existed no mouse model carrying an endogenous nonsense mutation in the mouse *CFTR* gene, the Cre-LOX system was used to substitute a UGA nonsense mutation for arginine codon 553 in the mouse Cftr gene30 **(Figure 2A).** This new mouse model was named CFTR-NS. In keeping with previous reports that Cftr-knockout mice are smaller than their heterozygous and wild-type counterparts, we observed this also with the CFTR-NS model **(Figure 2B)** [31,32]. CFTR mRNA is not detectable by RT-PCR in the lung of CFTR-NS mice, unlike wild-type mice, likely due to NMD **(Figure 2C).** In addition, most CFTR-knockout mice die less than 2 months after birth and are reported to develop intestinal obstructions during the first weeks of life. In our model, genotyping performed 2 weeks after birth showed that mice homozygous for the mutation (referred hereafter as HO) were underrepresented: only about 9% showed this genotype, as opposed to the expected 25%. This genotype would thus appear to be lethal **(Figure 2D).** The percentage of pups with a heterozygous genotype was 56%, as expected, and about 35% of the pups displayed a homozygous wild-type genotype, this disequilibrium reflecting the low proportion of HO pups. **Figure S2** shows examples of growth curves of wild-type (WT) and HO mice surviving more than 1 month after birth. The curves show that the ab-

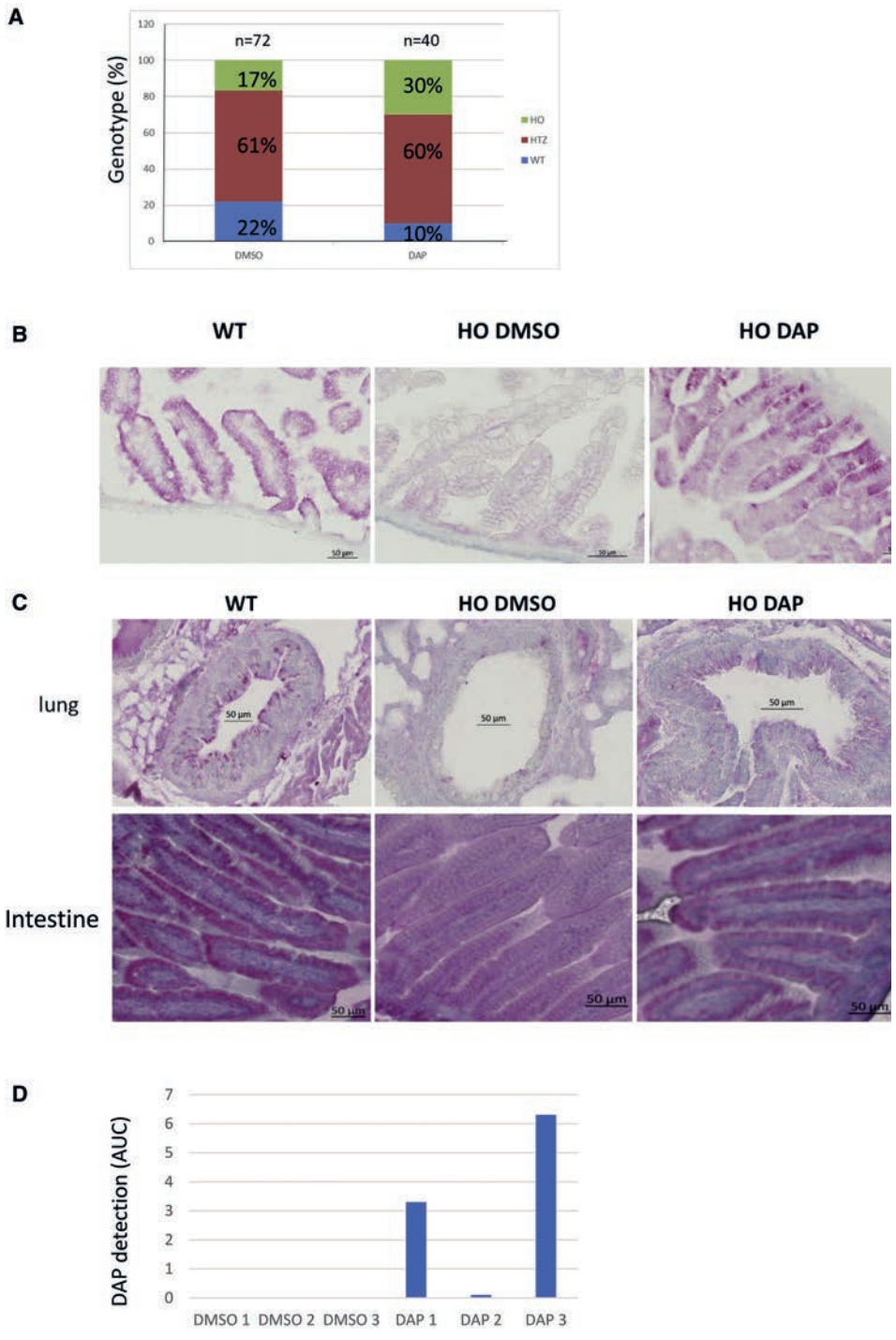

Figure 3. CFTR rescue by DAP in the CFTR-NS mouse model.
(A) Proportions of the three genotypes among live newborns. Mothers were exposed to DMSO or DAP by daily PO exposure during gestation. The counts are from four mothers treated with DMSO and four mothers treated with DAP for one to five litters and the total number of newborn mice analyzed is indicated on the top of each bar. A statistical analysis resulted in a p value lower than 0.01, indicating a strong trust in these results (Monte-Carlo method). **(B)** CFTR (in red) in the intestine (duodenum), detected by IHC applied to tissue from WT and HO newborns, from breastfed pups whose mothers were exposed to DMSO or DAP by daily PO exposure during and after gestation, and from adults (WT and HO) exposed to 3 days of DMSO or DAP by daily PO exposure. **(C)** CFTR (in red) detected by IHC in lung (around the bronchi) and intestinal (duodenum) tissues from 2-week-breastfed WT and HO pups whose mothers were exposed PO daily to DMSO or DAP. All the IHCs are representative of at least five mice. **(D)** Measurement of the presence of DAP in the contents of the stomach of newborns. Each sample is a mix of the contents of the entire litter.

sence of CFTR leads to delayed growth and to a growth reduction of about 30%–40%, as previously reported [31]. Last, the absence of CFTR was assessed by immunohistochemistry (IHC) applied to lung and intestinal tissues, reported to express CFTR [33]. In WT mice, but not HO mice treated with DMSO, CFTR staining was clearly detected in cells forming the bronchi and bronchioles of lung tissue and in cells forming the intestinal villi **(Figure 2E).** Overall, the results of Figure 2 demonstrate that CFTR-NS is a valid mouse model for studying the in vivo efficacy of nonsense mutation correctors.

In CFTR-NS mice, DAP corrects the nonsense mutation in the CFTR gene
A previous report has shown that DAP can rescue expression of a gene carrying a UGA nonsense mutation in xenografted cells in mouse.29 To demonstrate that DAP can correct endogenous nonsense mutations in the Cftr gene, 4-week-old CFTR-NS mice were exposed PO daily to 10% DMSO solution or 1 mg DAP for 3 days before collection of their lungs and intestines to check for Cftr expression **(Figure 2E).** In WT mice, red staining of the CFTR protein appeared highly concentrated around the bronchi and bronchioles, on the central lumen side. CFTR was also detected in cells forming the intestinal villi, again on the side of the central lumen. In contrast, DMSO-treated HO mice displayed no specific labeling. DAP-treated lung and intestinal tissues from HO mice, on the other hand, did show specific staining of CFTR. This result, consistent with the biodistribution data of **Figure 1D,** indicates that in mice exposed PO to DAP for 3 days, DAP can diffuse through their bodies and correct a UGA nonsense mutation in the endogenous *CFTR* gene.

DAP restores Cftr expression in utero
Since nearly all HO CFTR-NS mice die before adulthood, it was necessary to devise a method for testing the ability of DAP to restore CFTR function. **Figure 2D** shows that the HO genotype is underrepresented among pups, indicating that CFTR plays a role during development. **Figure 1D** shows that DAP crosses the blood-brain barrier, and this suggests that it might also cross the placental barrier. The idea was thus to attempt to restore the expected proportion of HO genotypes, i.e., about 25%, by crossing heterozygous (HTZ) mice and treating only the female in each mating pair. Mating female HTZ mice were exposed PO daily to either 10% DMSO solution or 1 mg DAP. Genotyping of the newborn pups showed

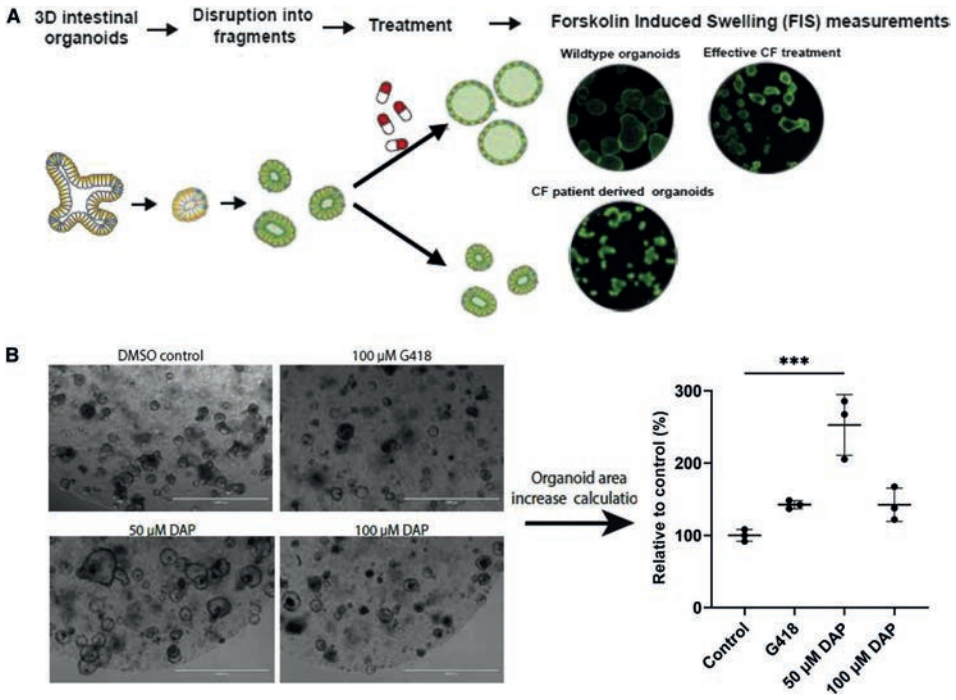

Figure 4. DAP rescues CFTR function in mouse organoids.
(A) Schematic representation of the forskolin-induced swelling (FIS) assay, in which CFTR function can be assessed in mouse- or patient-derived intestinal organoids. **(B)** Organoids derived from CFTR-NS mouse intestinal cells were exposed to DMSO, DAP, or G418, and CFTR function was assessed by FIS. All the results are representative of three experiments. The p values were calculated by one-way ANOVA: ***p < 0.005.

DAP treatment to increase the proportion of pups with the HO genotype from 17% to 30%. This suggests that intrauterine mortality due to the absence of CFTR was prevented by DAP treatment of the mother during gestation **(Figure 3A).** It is interesting to note that these data were obtained from eight pairs, of which the female was treated PO with either DMSO or DAP over a period of approximately 10 months without showing any sign of toxicity. To check that the restored presence of CFTR was responsible for restoring the proportion of HO genotypes to the expected level, an IHC assay was performed on intestinal tissues from pups on their day of birth (their lungs were not yet clearly identifiable at that time) **(Figure 3B).** While no CFTR was detected in HO pups whose mother had been exposed to DMSO, those whose mother had been exposed to DAP showed a staining pattern similar to that of WT newborns. This indicates that DAP can cross the placental barrier and correct a UGA nonsense mutation in utero by allowing Cftr expression. The results in **Figures 3A** and **3B** show that DAP can reach the fetus to restore CFTR protein synthesis and function when the heterozygous mother is exposed PO daily to this compound.

Rescue of CFTR expression in newborns
It remains very challenging to expose mice PO during their first 2 weeks of life. Since DAP can cross both the blood-brain barrier and the placental barrier (**Figure 1** and **3B),** we hypothesized that it might be possible to treat newborns via breastfeeding. For this, PO exposure of heterozygous mothers was prolonged for 2 weeks after birth of their offspring, and then CFTR IHC was performed on lung and intestinal tissues from the pups. Unlike the tissues from pups of DMSO-treated mothers, those obtained from pups of DAP-treated mothers displayed CFTR staining **(Figure 3C).** These results led to the conclusion that newborn mice can be exposed to DAP by treating the nursing mother.

To validate the hypothesis that DAP can be transmitted to newborns through maternal milk, the presence of DAP was sought in maternal milk. For this, six mothers who had never been previously exposed to DAP were exposed PO to DMSO or DAP on the day of the birth of their pups. Newborns were sacrificed 1 h later. The stomach contents of newborns were then collected, pooled by litter, and analyzed by mass spectrometry. The result indicates that DAP is not found in the stomachs of newborns whose mothers have been exposed PO to DMSO but, on the other hand, is detected in the stomachs of newborns whose mothers have been exposed PO to the DAP 1 h before the sacrifice **(Figure 3D).** The variability of the quantity of DAP detected is linked to the fact that the interval between the moment of the last feed and the sacrifice is also very variable and cannot be controlled, since newborn mice drink milk according to their need. This result demonstrates that DAP can be transmitted to newborns via breastfeeding.

DAP restores CFTR synthesis and function in organoids derived from CFTR-NS mouse cells carrying UGA nonsense mutations
The next step was to evaluate the functional rescue of CFTR more directly than by calculating the genotype ratio. For this purpose, organoids derived from CFTR-NS mouse intestinal stem cells were established. Organoid models have been established from many organ types, both healthy and diseased, and have been shown to mimic the tissue from which they were derived [34]. By measuring organoid swelling under specific conditions, the function of CFTR can be quantified **(Figure 4A)** [35, 36]. Murine organoids were incubated in the presence of DMSO, DAP (50 or 100 µM), or 100 µM G418 (positive control) for 48 h before quantifying forskolin-induced swelling (FIS) as a readout for CFTR function **(Figure 4B).** At 100 µM, DAP led to CFTR channel function as efficiently as G418 at the same concentration, which has previously shown to be effective in an organoid model [27]. At 50 µM, however, DAP proved to be about twice as effective as at 100 µM. These results show that CFTR rescued by DAP leads to the synthesis of functional CFTR in a mouse organoid model and that 50 µM is optimal in this test. They importantly confirm, consistent with the results in Figure 3, the ability of DAP to read through the R553X UGA PTC in mouse cells.

DAP restores the function of CFTR in patient cells and in human bronchial epithelial cell lines carrying a UGA nonsense mutation
To test the ability of DAP to rescue CFTR function in yet another preclinical model,

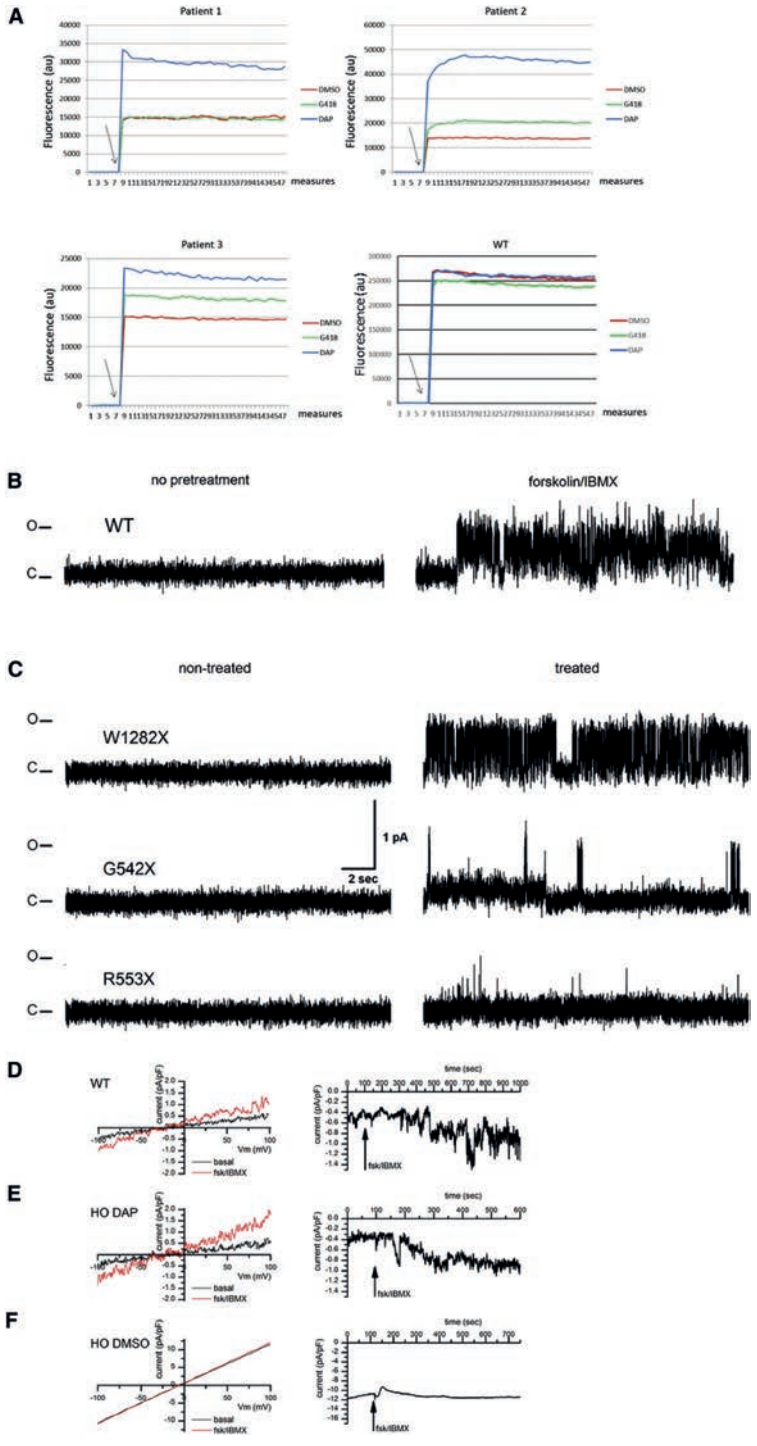

Figure 5. Rescue of CFTR function in CF patient cells and in 16HBE14o_ cells carrying a nonsense mutation in both Cftr alleles.
(A) CFTR function was assessed in CF patient cells by means of an SPQ assay after DMSO (red), G418 (green), or DAP (blue) treatment. Arrows indicate addition of the forskolin-cAMP cocktail to the cell medium. The tested genotypes are W1282X/W1282X (patient 1), G542X/G542X (patients 2 and 3), and WT (lower right). **(B)** Sample single-channel activity of the CFTR Cl_ currents in the 16HBE14o_ expressing wild-type (WT) CFTR without (left) or following pretreatment with 40 μM forskolin and 400 μM IBMX for 30 min, prior to patching the cells (right). Note the absence of activity in patches made to non-stimulated cells and the presence of a characteristic CFTR activity following forskolin/IBMX treatment. **(C)** Single-channel activity of CFTR Cl_ currents in 16HBE14o_ cells expressing mutant CFTR. To stimulate CFTR currents, cells were pretreated with 40 μM forskolin and 400 μM IBMX for 30 min, prior to patching the cells. Sample traces were acquired in excised outside patches of forskolin/IBMX-pretreated cells expressing, from the top to the bottom, W1282X, G542X, and R553X CFTR. Note the absence of activity in the non-treated (left side) cells and presence of the characteristic CFTR activity in the cells treated with DAP. C and O denote closed and open states of the ion channel. **(D–F)** Whole-cell currents in isolated cells from WT **(D)**, HO DAP **(E)**, and HO DMSO **(F)** mice. Whole-cell currents were acquired in NMDG-Cl-based solutions as described. After whole-cell mode was established, the cells were left undisturbed for 5 min to allow replacement of intracellular K+ and Na+ with NMDG, to register basal current levels with Cl_ as the major ion current carrier. This was followed by application of 40 μM forskolin and 400 μM IBMX to stimulate CFTR activity. Panels compare representative IV (current-voltage) relationships (left) as well as the time course of the CFTR activity stimulation with forskolin/IBMX (right). Note an increase in current following forskolin/IBMX application in WT and HO DAP mice and the absence of the effect in the HO DMSO case.

patient cells were collected from the nose epithelium and incubated for 24 h with DMSO, G418 at 600 μM, or DAP at 100 μM (optimal concentration determined previously in cell line29) in an SPQ (6-Methoxy-N-(3-Sulfopropyl)Quinolinium, Inner Salt) assay [37]. Cells homozygous for either G542X or W1282X were tested. In this test, and for both mutations, DAP at 100 μM demonstrated higher functional rescue than G418 at 600 μM **(Figure 5A).** To exclude the possibility that the fluorescence increase observed with DAP in particular might be a non-specific effect, WT nasal cells were incubated with DMSO, DAP, or G418 under the same conditions as the CF cells. When CFTR channel activators (forskolin and IBMX (3-Isobutyl-1-methylxanthine)) were added, the fluorescence increased regardless of the treatment (DMSO, DAP, or G418). This indicates that the variation in fluorescence observed with the CF cells was indeed due to correction of the nonsense mutation and not to a non-specific effect of DAP in particular. It is worth noting that the effect of nonsense mutation correctors differed according to the nonsense mutation (compare the effects on G542X and W1282X) and, for the same mutation, according to the patient from whom the cells were derived (compare patients 2 and 3). An influence of the genetic background on CF treatment efficacy has been reported previously [38, 39]. The results of **Figure 5A** show that DAP restores CFTR function more efficiently than G418 in CF patient cells carrying a UGA nonsense mutation.

To reinforce the previous results on the effect of DAP on the restoration of CFTR channel function, single-channel patch-clamp experiments were undertaken. These types of experiments make it possible to isolate an individual CFTR channel and to evaluate its capacity

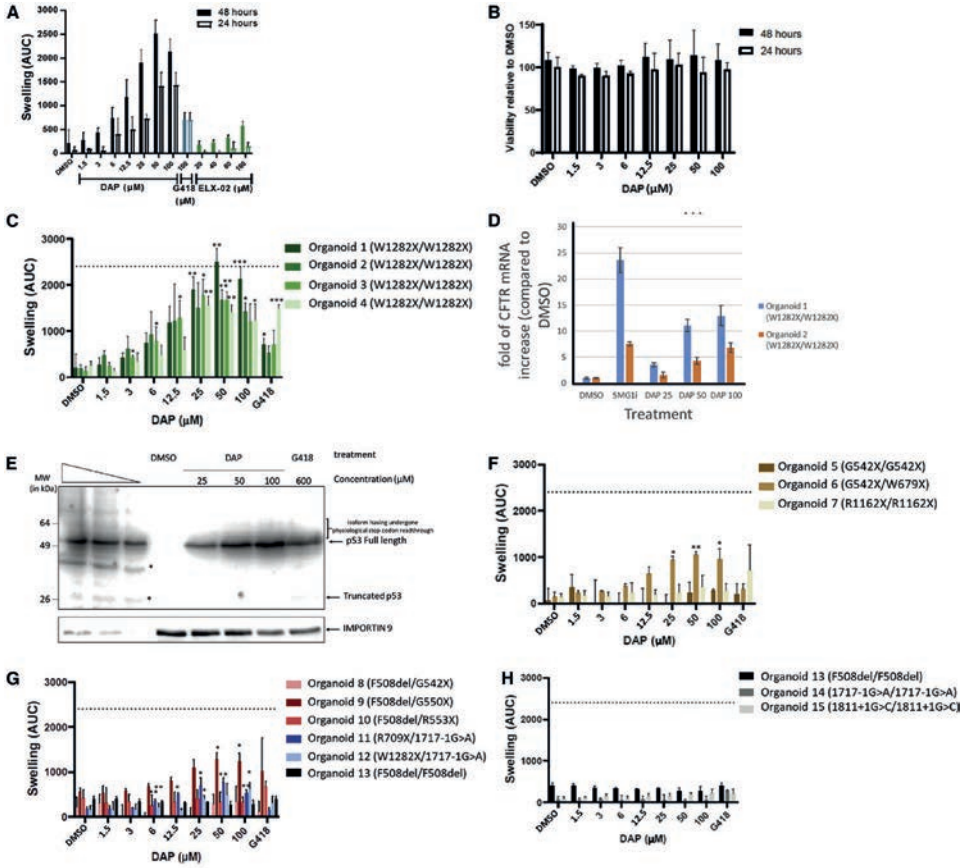

Figure 6. DAP rescues CFTR function in patient-derived intestinal organoids.
(A) FIS assay on organoids derived from rectal cells of CF patients homozygous for the W1282X mutation. Organoids were exposed to DMSO, DAP, G418, or ELX-02 for 24 or 48 h. **(B)** Cell viability measured by alamarBlue incorporation into organoids derived from rectal cells of CF patients homozygous for the W1282X mutation. The organoids were exposed to DMSO or DAP. **(C)** FIS assay on four such organoids exposed to DMSO or DAP. **(D)** Measurement by qRT-PCR of the level of CFTR mRNA in organoids 1 and 2 to evaluate the efficacy of NMD in the presence of DMSO, an inhibitor of NMD (SMG1i), or DAP at 25, 50, or 100 μM. **(E)** Western blot demonstrating the absence of physiological stop codon readthrough by DAP at 25, 50, or 100 μM. Calu-6 cells were exposed to DMSO, DAP, or G418 previously to extract protein and perform a western blot analysis. The three leftmost lanes are serial dilutions of U2OS cell extract. Asterisks show degradation products or non-specific bands. The place to which the isoforms having undergone a readthrough of the physiological stop codon should migrate is indicated on the right side of the gel by a bracket. **(F)** FIS assay on CF patient-cell-derived organoids carrying UGA nonsense mutation on both CFTR alleles. **(G)** FIS assay on CF patient-cell-derived organoids carrying a UGA nonsense mutation on one CFTR allele and a different mutation from a nonsense mutation (F508del or 1717-1G>A) on the other CFTR allele. **(H)** FIS assay on CF patient-cell-derived organoids carrying a mutation different from UGA nonsense mutation on both CFTR alleles (F508del or 1717-1G>A). The dotted line corresponds to the amplitude of swelling obtained with organoids homozygous for the F508del mutation upon treatment with lumacaftor-ivacaftor. Error bar shows the SD, p values were calculated with Student's t test: $*p < 0.05$, $**p < 0.01$, $***p < 0.001$, n.s., not significant. Averages of three experiments with three technical replicates each are shown.

to allow ion transport after stimulation. For this, 16HBE14o- cells, in which a nonsense mutation was introduced by CRISPR-Cas9, were used. The CFTR ion channel is an anionic channel that is known to have a distinctive single-channel activity pattern, characterized by a relatively small single-channel conductance of approximately 9–10 pS, bursting behavior, and sensitivity to ATP, as well as phosphorylation by the PKA catalytic subunit on the cytoplasmic side in order to be gated [40, 41, 42]. First, to confirm the presence of CFTR ion channels, as well as to establish the optimal observation conditions, patch-clamp data were acquired in the WT 16HBE14o- cells. For patch-clamp experiments, cells were immersed in a solution containing 150 mM N-methyl-D-glucamine chloride (NMDG-Cl) as the principal component, with a symmetric composition of the pipette solution. Patches were made to the cells in the middle of the established clusters, surrounded on all sides by other cells. To ensure robust CFTR activity, cells were pretreated with 40 μM forskolin and 400 μM IBMX for 30 min, prior to patching [40,41]. Recordings were made in cell-attached patches, as well as excised inside-out patches, which allowed us to record activity under symmetric ionic conditions, where the only conductive ion present was Cl-, thus allowing us to isolate anionic currents carried by CFTR ion channels. Under such conditions, a characteristic CFTR can be observed in over half of the traces following the forskolin pretreatment in cell-attached as well as excised inside-out patches with a characteristic single-channel conductance of 9.6 ± 0.5 pS (**Figure 5B**, n = 8 of 14 patches). To confirm the sensitivity of the observed activity to ATP, we measured CFTR activity in excised inside-out patches made to cells that were not pretreated with forskolin/IBMX. In such patches CFTR activity could be observed at very low levels following the patch excision, while application to the cytoplasmic side of the patch membrane of 25 nM PKA catalytic subunit + 1 mM Mg-ATP typically restored the characteristic CFTR currents **(Supplemental Figure S3,** n = 7).

Having established the conditions under which robust CFTR activity could be observed in WT 16HBE14o- cells, we performed a series of experiments aimed at determining the presence of such activity in the non-treated 16HBE14o- cells modified via the CRISPR-Cas9 procedure to contain various mutants introducing premature stop codons. **Figure 5C** compares such activity in non-treated modified cells vs. cells treated for 24 h with DAP. While the non-treated cells universally lacked the characteristic CFTR activity, such activity could be restored in the treated W1282X mutant cells, where the treatment was expected to reintroduce the matching amino acid, restoring the proper protein sequence **(Figure 5C).** For the other two mutants, namely G542X and R553X, treatment with DAP restored some functionality of the CFTR channel, since the channel was found alternately in the open or closed state **(Figure 5C).**

Further, to establish the physiological relevance of the restoration of the CFTR expression, we studied whole-cell CFTR currents in cells isolated from the duodenum of 11 CFTR-NS mice under conditions where Cl- was the only ion current carrier (NMDG-Cl-based extracellular and intracellular solutions as described). The recordings done on the cells isolated from control (WT) as well as HO DAP mice showed a small but significant whole-cell current evoked by application of 40 μM forskolin and 400 μM IBMX. Cells isolated from WT

mice yielded 0.81 ± 0.19 pA/pF increase in currents **(Figure 5D,** n = 2), while cells isolated from HO DAP mice yielded an increase of 0.86 ± 0.16 pA/pF (**Figure 5E,** p = 0.0046, n = 4). The HO DMSO-treated mice had a significant amount of tissue degradation, with the isolation procedure yielding a very small number of cells, the majority of which were not viable in culture, consistent with the well-established importance of the CFTR ion channel for cell survival. Repeated attempts to patch these cells yielded only a single successful recording. Application of forskolin/IBMX in this patch did not produce any significant change in the whole-cell current **(Figure 5F).**

DAP restores CFTR synthesis and function in organoids derived from patient cells carrying a UGA nonsense mutation

To complete the demonstration of the ability of DAP to read through UGA PTCs, 15 patient-derived intestinal organoids (PDIOs) were exposed to increasing doses of DAP **(Figures 6**, **Supplemental Figure S4,** and **Supplemental Figure S5).** DMSO was used as a negative control and did not promote any organoid swelling. G418 and ELX-02 were used as positive controls for the correction of nonsense mutations. First, to determine the best experimental conditions for observing a functional effect of DAP on the PDIOs, dose-response curves were constructed after two incubation times (24 and 48 h). To ensure that a positive effect of DAP could be detected, PDIOs homozygous for the nonsense mutation W1282X were used, since DAP causes a tryptophan to be introduced at the site of the nonsense mutation and can thus restore synthesis of a WT CFTR protein. The results show that CFTR function was restored in a dose-dependent manner, becoming significant from 25 µM. The measured effect was also greater when the PDIOs were treated for 48 h than for 24 h **(Figure 6A).** Interestingly, as for murine organoids **(Figure 4),** the concentration causing optimal restoration of CFTR function was 50 µM. The comparison of the effect obtained with DAP compared with G418 or with the molecule in clinical trial, ELX-02, shows that DAP is more effective in correcting the nonsense mutation in this line of organoid. alamarBlue and propidium iodide staining, used to measure viability for each condition in **Figure 4B,** showed the absence of DAP toxicity toward the organoids (Figures 6B and S5). In subsequent assays, a 48-h incubation time was used to optimize the window of opportunity to detect effects.

To further characterize the capacity of DAP to restore CFTR function in W1282X/W1282X PDIOs, FIS was assessed in three additional homozygous W1282X PDIOs **(Figures 6C** and **Supplemental Figure S4).** In all four PDIOs, DAP proved able to induce functional rescue of CFTR in a dose-dependent manner. DAP-induced CFTR rescue even reached the level obtained in F508del/F508del PDIOs with lumacaftor-ivacaftor (dotted line). This is an important benchmark, as lumacaftor-ivacaftor is clinically effective. Within-genotype variation was observed, organoid line 1 being most responsive to DAP and organoid lines 2/3/4 reaching similar areas under the curve. In all organoid lines except organoid line 4, DAP treatment at 50 µM restored CFTR function more effectively than G418. This function-restoring action of DAP in the presence of the W1282X mutation is consistent with its mode of action, which leads to incorporation of a tryptophan at the position of the nonsense mutation. Hence, the protein synthesized after treatment with DAP is the WT protein. Since the concentrations used are greater than those that were previously used in the cell lines and for which no inhibition of NMD had been measured [29]. the effectiveness of NMD was measured in two PDIOs by measuring the level of mRNA CFTR by qRT-PCR **(Figure 6D).** The results show in particular that above 25 µM, DAP induces an inhibition of NMD. This is probably not the main effect of suppression of UGA stop codons, since it is observed that the functional restoration of CFTR at 100 µM is less effective than the effect at 50 µM, even if the inhibition of NMD is greater at 100 µM DAP than at 50 µM DAP **(Figure 6C** and **6D).**

To confirm the physiological stop codon integrity, Calu-6 cells carrying a premature UGA stop codon in the TP53 gene were treated with DMSO, DAP, or G418. The use of Calu-6 cells presents several advantages, including that the analysis of the TP53 gene by western blot is very efficient and that the TP53 gene ends its open reading phase with a physiological stop codon, UGA. A long exposure of the western blot analysis does not result in the detection of isoforms of size greater than the isoform terminating at the physiological stop codon, indicating that DAP does not result in readthrough of physiological stop codons **(Figure 6E).** Other mutations were then tested to assess the ability of DAP to rescue the function of CFTR in PDIOs carrying other UGA nonsense mutations on both CFTR alleles **(Figure 6F)** or on one CFTR allele **(Figure 6G)** or other types of mutations as negative controls **(Figure 6H).** Although the rescue was of lower magnitude than with the W1282X mutation, DAP proved able to restore CFTR function in PDIOs heterozygous for the UGA nonsense mutation G550X, R709X, or W679X. Under these conditions, however, it proved unable to suppress a biallelic R1162X mutation, a biallelic G542X mutation, or a monoallelic G542X or R553X mutation associated with F508del. As expected, DAP failed to suppress a biallelic F508del or 1717-1G>A splice mutation **(Figure 6H).** Overall, the results of Figures 6 and S4 show that DAP can restore CFTR function in PDIOs with various UGA nonsense mutations in the CFTR gene.

Discussion

The study presented here aims to prioritize DAP for further clinical development by studying its efficacy and pharmacokinetics in preclinical models. The models used include a new mouse model of CF, patient cells, PDIOs, and human bronchial epithelial cells. The pharmacokinetic data obtained show that DAP appears in the blood after oral administration and is then rapidly eliminated in the urine, but that a fraction is distributed to various tissues such as the lungs, muscles, and brain **(Figure 1).** This distribution suggests that DAP can correct nonsense mutations in different tissues, which is crucial for a pathology such as CF, in which the absence of the CFTR channel influences the functioning of several epithelia and tissues. Interestingly, DAP crosses the blood-brain barrier. One might thus consider DAP for correcting nonsense mutations involved in neurological diseases. DAP also crosses the placental barrier, as shown in the new mouse model CFTR-NS carrying the R553X nonsense mutation **(Figures 2** and **3).** In this *in vivo* model, DAP is shown here to correct a UGA nonsense mutation in the Cftr gene and to reverse the phenotype associated with it (lethality, absence of CFTR). However, even though DAP clearly crosses the placental bar-

rier and corrects the nonsense mutation *in utero*, treatment *in utero* is probably not possible with this molecule, because the presence of DAP was associated with a reduction in the number of pups per litter, suggesting a possible deleterious effect of DAP during gestation. Yet we have been unable, so far, to verify statistically an influence of DAP on the number of newborns **(Figure 3).**

Another demonstration that DAP might be used therapeutically in CF patient cells or in patients with CF linked to the presence of a UGA nonsense mutation is provided by the present experiments with PDIOs **(Figures 5** and **6).** In these study models, it is possible to measure the function of the CFTR channel and thus to evaluate the ability of DAP to correct functionally a nonsense mutation in the CFTR gene. Importantly, as several UGA nonsense mutations lead to loss of a tryptophan, the use of DAP seems particularly suitable. For example, the W1282X mutation represents 1.2% of the mutations found in CF [43]. On the W1282X mutation, DAP was more effective than G418 or ELX-02. However, it cannot be excluded that the ELX-02 molecule purchased from MedChemExpress may be less active than the molecule from the Eloxx Pharmaceuticals laboratories. A comparison of these two sources of ELX-02 by an independent laboratory would be a good way to verify this point.

In several PDIOs from patients homozygous for the W1282X mutation, DAP was found to rescue the function of the CFTR channel as potently as does lumacaftor-ivacaftor, from Vertex Pharmaceuticals, in the case of the F508del mutation. This result is suggestive of clinical efficacy **(Figure 6C).** On other mutations the effect of DAP is weaker, likely because DAP-promoted introduction of a tryptophan at the PTC position might have an impact, at least partially, on the function of CFTR, consistent with the patch-clamp results obtained on human bronchial epithelial cells **(Figure 5B).**

Each of the four preclinical models used in this study has its specificities and experimental conditions liable to cause variations in responses to molecules. For example, the R553X mutation responds to DAP in mouse organoids, but the same mutation in PDIOs does not. Likewise, the G542X mutation responds to DAP in patient cells or in 16HBE14o- cells but not in PDIOs. These differences can be linked to experimental specificities of each model, the sensitivity of each assay, and the genotype of each individual, previously reported to influence the response to a drug [38, 39]. Overall, the results of this study demonstrate that DAP can be viewed as a good drug candidate, so far, to correct UGA nonsense mutations.

Supplemental Information

Supplemental data can be found online, at https://doi.org/10.1016/j.ymthe.2023.01.014

Acknowledgments

The authors would like to thank Dr. Anne Tsicopoulos and Dr. Quentin Thommen for helpful discussions and advice on IHC and statistical analysis. The authors would also like to deeply thank the Cystic Fibrosis Foundation, for the donation of 16HBE14o- cells carrying nonsense mutations, and Professor Dieter Gruenert for the donation of 16HBE14o- WT cells. F.L. is supported by funding from Vaincre la Mucoviscidose, the Association Française contre les Myopathies, the Agence Nationale de la Recherche, the Fondation Les Ailes, and the Fondation Maladies Rares. Canther Laboratory is part of ONCOLille Institute. This work is supported by a grant from Contrat de Plan Etat-Région CPER Cancer 2015–2020.

Author Contribution Statement

Conceptualization, C.L., S.S., J.B., G.S., and F.L.; methodology, C.L., S.S., N.C.E., V.P., R.K., P.G., S.A., and C. Bailly; investigation, C.L., S.S., V.P., N.C.E., R.K., P.G., S.A., C. Bourban and C. Bailly; funding acquisition, N.P., J.B., and F.L.; project administration, F.L.; supervision, P.G., S.A., C. Bailly, D. Hannebique, A.P., P.R., D. Hubert, M.G., M.C., S.R., J.B., and F.L.; writing – original draft, C.L., S.S., G.S., and F.L.; writing – review & editing, all authors.

Declaration of interests

J.B. is inventor on a patent related to the FIS assay and received financial royalties from 2017 onward. S.A., C. Bailly, S.R., and F.L. are inventors on a patent demonstrating that DAP is a readthrough molecule useful for the treatment of genetic diseases related to nonsense mutations.

Chapter | 4

Supplemental Information

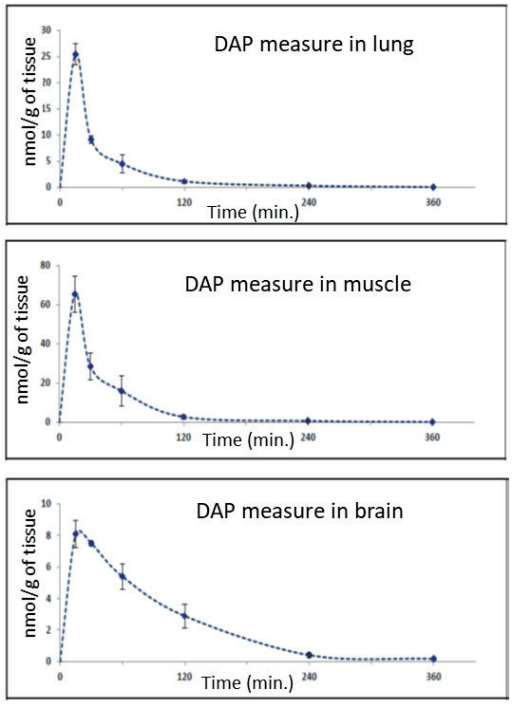

Supplemental Figure S1: Biodistribution of DAP after blood injection in CD-1 mouse. 8.1mg/kg of DAP were injected in blood before measuring the level of DAP in lung (upper panel), muscle (middle panel) or brain (lower panel) at 15, 30, 60, 120, 240 or 360 minutes after exposure. Three mice were used for each time point.

Example 1

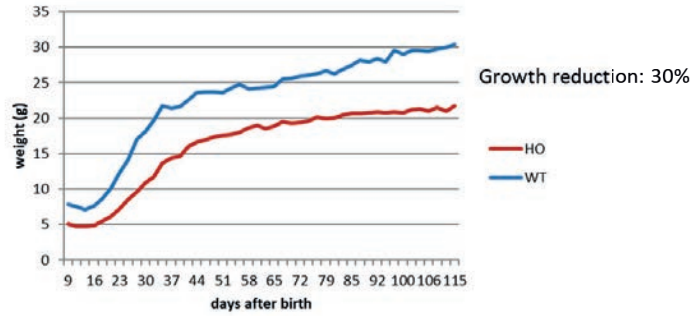

Example 2

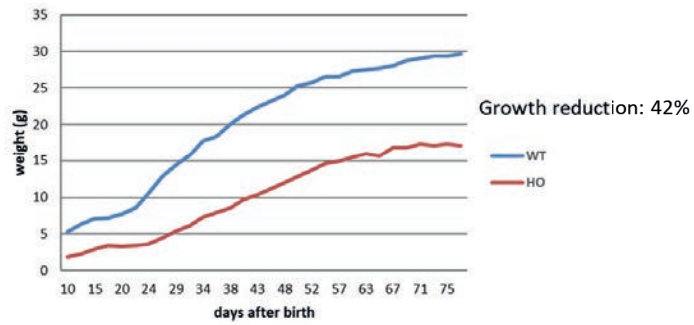

Supplemental Figure S2: The absence of CFTR leads to slowed growth of CFTR-NS mice. Two examples of growth curves of HO mice (homozygous for the R553X mutation) compared to growth curves of WT mice of the same litter.

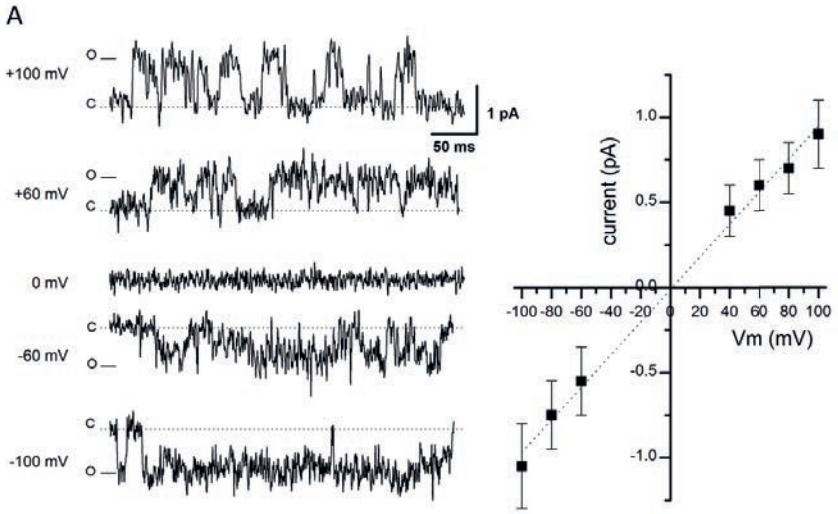

Supplemental Figure S3: Sample activity in the 16HBE14o- cells expressing WT *CFTR*.
(A) Left panel shows sample traces of the CFTR activity in the excised inside-out patches to the fosrkolin/IBMX stimulated cells at the specified membrane potentials. C and O denote closed and open states of the ion channel. Right panel presents an IV plot summarizing the CFTR currents at multiple membrane potentials. Dotted line shows a linear fit to the data, yielding a characteristic conductance of 9.6 ± 0.5 pS (n=6). **(B)** PKA and ATP applied to the intracellular side of the membrane stimulate CFTR activity. 16HBE14o- cells were prepared as described. Cells in the middle of clusters were patched without forskolin/IBMX application. Typically, no or very little CFTR activity could be observed under such conditions in either cell-attached or excised inside-out patched. Figure shows sample activity in the inside out patches, made to untreated cells. Sample trace shows basal activity followed by the application of 25 nM catalitic domain of PKA + 1 mM MgATP to the bath, facing the inner side of the plasma membrane of the excised patches. Note the appearance of the characteristic CFTR activity following the application of PKA + ATP.

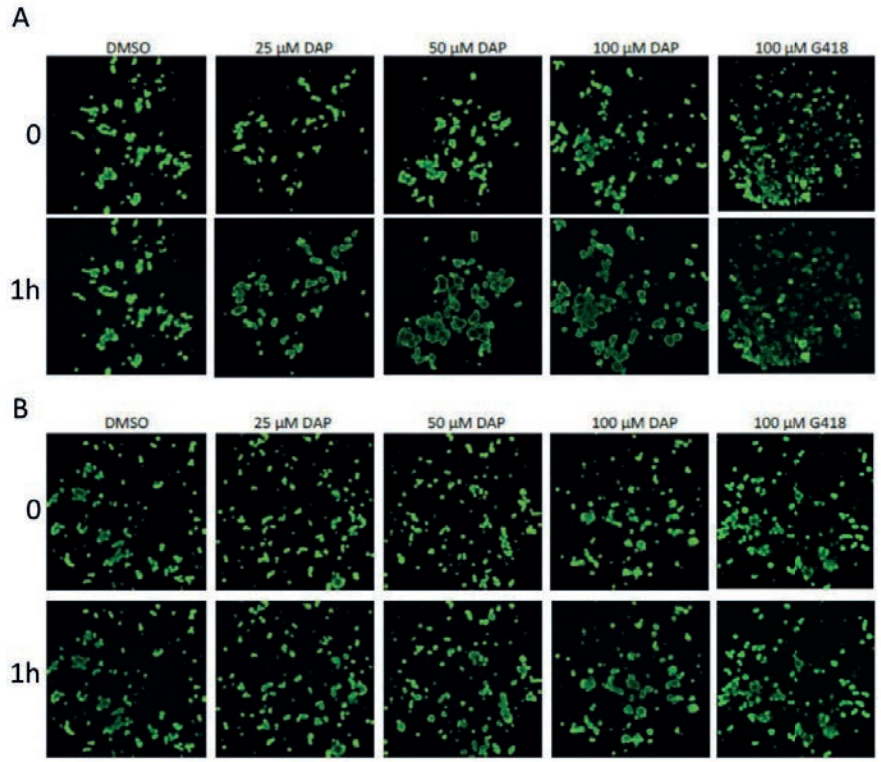

Supplemental Figure S4: DAP promotes swelling of organoids carrying a UGA nonsense mutation but not or organoids carrying an F508del mutation.
(A) Confocal images of DAP-treated organoids (organoid 1, W1282X/W1282X) taken at t=0 and t=1 h after starting treatment with 5 µM FSK. **(B)** Confocal images
of DAP-treated organoids (donor 13, W1282X/1717G>A) taken at t=0 and t=60 min after starting treatment with 5 µM FSK.

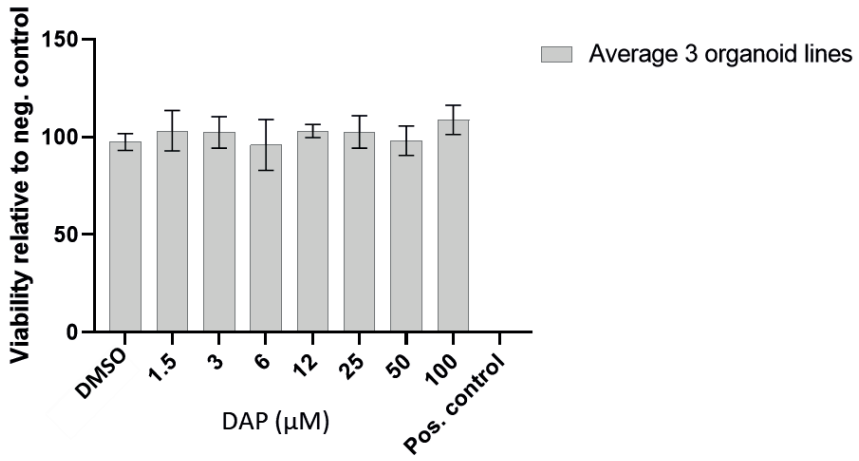

Supplemental Figure S5: Organoid viability after DAP treatment.
The organoid lines used for flow cytometry analysis were grown and collected 48 days after splitting and DAP exposure. Subsequently, isolated cells were obtained by dissociating organoids with TrypLE at 37°C for 15 min. After washing the isolated cells with DMEM +++, the cells were counted and 10 x 105 cells were resuspended in in FACS buffer (PBS containing 5% FBS, 2 mM EDTA) on ice. Dead cells were stained by adding 1 µg/ml PI five minutes prior to FLOW analysis. Unstained and positive controls (cells exposed to 10% DMSO) were included for each line. Measurements were carried out on the BD FACS Canto II (BioRad) with standard filter sets, and the fluorescence intensity of PI was measured in the 488 channel. FlowJo software was used for analysis. Dead cells were excluded on the basis of PI staining and doublets were excluded from analysis on the basis of side scatter height (SSC-H) versus forward scatter height (FSC-H) plots. Positive control conditions were 24 h of incubation with 10% DMSO.

References

1. Mort, M., Ivanov, D., Cooper, D.N., and Chuzhanova, N.A. (2008). A meta-analysis of nonsense mutations causing human genetic disease. Hum. Mutat. 29, 1037–1047.
2. Gupta, P., and Li, Y.R. (2018). Upf proteins: highly conserved factors involved in nonsense mRNA mediated decay. Mol. Biol. Rep. 45, 39–55.
3. Lejeune, F. (2017). Nonsense-mediated mRNA decay at the crossroads of many cellular pathways. BMB Rep. 50, 175–185.
4. Kurosaki, T., and Maquat, L.E. (2016). Nonsense-mediated mRNA decay in humans at a glance. J. Cell Sci. Feb 129, 461–467.
5. Karousis, E.D., Nasif, S., and Muhlemann, O. (2016). Nonsense-mediated mRNA decay: novel mechanistic insights and biological impact. Wiley Interdiscip. Rev. RNA 7, 661–682.
6. Hug, N., Longman, D., and Caceres, J.F. (2016). Mechanism and regulation of the nonsense-mediated decay pathway. Nucleic Acids Res. 44, 1483–1495.
7. Nogueira, G., Fernandes, R., Garcia-Moreno, J.F., and Romao, L. (2021). Nonsense-mediated RNA decay and its bipolar function in cancer. Mol. Cancer 20, 72.
8. Durand, S., Cougot, N., Mahuteau-Betzer, F., Nguyen, C.H., Grierson, D.S., Bertrand, E., Tazi, J., and Lejeune, F. (2007). Inhibition of nonsense-mediated mRNA decay (NMD) by a new chemical molecule reveals the dynamic of NMD factors in P-bodies. J. Cell Biol. 178, 1145–1160.
9. Dang, Y., Low, W.K., Xu, J., Gehring, N.H., Dietz, H.C., Romo, D., and Liu, J.O. (2009). Inhibition of nonsense-mediated mRNA decay by the natural product pateamine A through eukaryotic initiation factor 4AIII. J. Biol. Chem. 284, 23613–23621.
10. Bhuvanagiri, M., Lewis, J., Putzker, K., Becker, J.P., Leicht, S., Krijgsveld, J., Batra, R., Turnwald, B., Jovanovic, B., Hauer, C., *et al*. (2014). 5-azacytidine inhibits nonsense-mediated decay in a MYC-dependent fashion. EMBO Mol. Med. 6, 1593–1609.
11. Martin, L., Grigoryan, A., Wang, D., Wang, J., Breda, L., Rivella, S., Cardozo, T., and Gardner, L.B. (2014). Identification and characterization of small molecules that inhibit nonsense mediated RNA decay and suppress nonsense p53 mutations. Cancer Res. 74, 3104–3113.
12. Gotham, V.J., Hobbs, M.C., Burgin, R., Turton, D., Smythe, C., and Coldham, I. (2016). Synthesis and activity of a novel inhibitor of nonsense-mediated mRNA decay. Org. Biomol. Chem. 14, 1559–1563.
13. Usuki, F., Yamashita, A., Higuchi, I., Ohnishi, T., Shiraishi, T., Osame, M., and Ohno, S. (2004). Inhibition of nonsense-mediated mRNA decay rescues the phenotype in Ullrich's disease. Ann. Neurol. 55, 740–744.
14. Bandara, R.A., Chen, Z.R., and Hu, J. (2021). Potential of helper-dependent Adenoviral vectors in CRISPR-cas9-mediated lung gene therapy. Cell Biosci. 11, 145.
15. Krishnamurthy, S., Traore, S., Cooney, A.L., Brommel, C.M., Kulhankova, K., Sinn, P.L., Newby, G.A., Liu, D.R., and McCray, P.B. (2021). Functional correction of CFTR mutations in human airway epithelial cells using adenine base editors. Nucleic Acids Res. 49, 10558–10572.

16. Santos, L., Mention, K., Cavusoglu-Doran, K., Sanz, D.J., Bacalhau, M., LopesPacheco, M., Harrison, P.T., and Farinha, C.M. (2021). Comparison of Cas9 and Cas12a CRISPR editing methods to correct the W1282X-CFTR mutation. J. Cyst Fibros 21, 181–187.
17. Erwood, S., Laselva, O., Bily, T.M.I., Brewer, R.A., Rutherford, A.H., Bear, C.E., and Ivakine, E.A. (2020). Allele-specific prevention of nonsense-mediated decay in cystic fibrosis using homology-independent genome editing. Mol. Ther. Methods Clin. Dev. 17, 1118–1128.
18. Michaels, W.E., Pena-Rasgado, C., Kotaria, R., Bridges, R.J., and Hastings, M.L. (2022). Open reading frame correction using splice-switching antisense oligonucleotides for the treatment of cystic fibrosis. Proc. Natl. Acad. Sci. USA 119. e2114886119.
19. Kim, Y.J., Sivetz, N., Layne, J., Voss, D.M., Yang, L., Zhang, Q., and Krainer, A.R. (2022). Exon-skipping antisense oligonucleotides for cystic fibrosis therapy. Proc. Natl. Acad. Sci. USA 119. e2114858118.
20. Oren, Y.S., Avizur-Barchad, O., Ozeri-Galai, E., Elgrabli, R., Schirelman, M.R., Blinder, T., Stampfer, C.D., Ordan, M., Laselva, O., Cohen-Cymberknoh, M., *et al*. (2021). Antisense oligonucleotide splicing modulation as a novel Cystic Fibrosis therapeutic approach for the W1282X nonsense mutation. J. Cyst Fibros 21, 630–636.
21. Palma, M., and Lejeune, F. (2021). Deciphering the molecular mechanism of stop codon readthrough. Biol. Rev. Camb Philos. Soc. 96, 310–329.
22. Martins-Dias, P., and Romao, L. (2021). Nonsense suppression therapies in human genetic diseases. Cell Mol. Life Sci. 78, 4677–4701.
23. Venturini, A., Borrelli, A., Musante, I., Scudieri, P., Capurro, V., Renda, M., Pedemonte, N., and Galietta, L.J. (2021). Comprehensive analysis of combinatorial pharmacological treatments to correct nonsense mutations in the CFTR gene. Int. J. Mol. Sci. 22, 11972–11993.
24. Gonzalez-Hilarion, S., Beghyn, T., Jia, J., Debreuck, N., Berte, G., Mamchaoui, K., Mouly, V., Gruenert, D.C., Déprez, B., and Lejeune, F. (2012). Rescue of nonsense mutations by amlexanox in human cells. Orphanet J. Rare Dis. 7, 58.
25. Brasell, E.J., Chu, L.L., Akpa, M.M., Eshkar-Oren, I., Alroy, I., Corsini, R., Gilfix, B.M., Yamanaka, Y., Huertas, P., and Goodyer, P. (2019). The novel aminoglycoside, ELX02, permits CTNSW138X translational read-through and restores lysosomal cystine efflux in cystinosis. PLoS One 14, e0223954.
26. Welch, E.M., Barton, E.R., Zhuo, J., Tomizawa, Y., Friesen, W.J., Trifillis, P., Paushkin, S., Patel, M., Trotta, C.R., Hwang, S., *et al*. (2007). PTC124 targets genetic disorders caused by nonsense mutations. Nature 447, 87–91.
27. de Poel, E., Spelier, S., Suen, S.W.F., Kruisselbrink, E., Graeber, S.Y., Mall, M.A., Weersink, E.J.M., van der Eerden, M.M., Koppelman, G.H., van der Ent, C.K., and Beekman, J.M. (2021). Functional restoration of CFTR nonsense mutations in intestinal organoids. J. Cyst Fibros 21, 246–253.

28. Konstan, M.W., VanDevanter, D.R., Rowe, S.M., Wilschanski, M., Kerem, E., Sermet Gaudelus, I., DiMango, E., Melotti, P., McIntosh, J., and De Boeck, K.; ACT CF Study Group (2020). Efficacy and safety of ataluren in patients with nonsense-mutation cystic fibrosis not receiving chronic inhaled aminoglycosides: the international, randomized, double-blind, placebo-controlled Ataluren Confirmatory Trial in Cystic Fibrosis (ACT CF). J. Cyst Fibros. 19, 595–601.
29. Trzaska, C., Amand, S., Bailly, C., Leroy, C., Marchand, V., Duvernois-Berthet, E., Saliou, J.M., Benhabiles, H., Werkmeister, E., Chassat, T., *et al*. (2020). 2,6- Diaminopurine as a highly potent corrector of UGA nonsense mutations. Nat. Commun. 11, 1509.
30. Sauer, B., and Henderson, N. (1988). Site-specific DNA recombination in mammalian cells by the Cre recombinase of bacteriophage P1. Proc. Natl. Acad. Sci. USA 85, 5166–5170.
31. Snouwaert, J.N., Brigman, K.K., Latour, A.M., Malouf, N.N., Boucher, R.C., Smithies, O., and Koller, B.H. (1992). An animal model for cystic fibrosis made by gene targeting. Science 257, 1083–1088.
32. McHugh, D.R., Steele, M.S., Valerio, D.M., Miron, A., Mann, R.J., LePage, D.F., Conlon, R.A., Cotton, C.U., Drumm, M.L., and Hodges, C.A. (2018). A G542X cystic fibrosis mouse model for examining nonsense mutation directed therapies. PLoS One, e0199573.
33. Doucet, L., Mendes, F., Montier, T., Delépine, P., Penque, D., Férec, C., and Amaral, M.D. (2003). Applicability of different antibodies for the immunohistochemical localization of CFTR in respiratory and intestinal tissues of human and murine origin. J. Histochem. Cytochem. 51, 1191–1199.
34. Drost, J., and Clevers, H. (2018). Organoids in cancer research. Nat. Rev. Cancer 18, 407–418.
35. Dekkers, J.F., Wiegerinck, C.L., de Jonge, H.R., Bronsveld, I., Janssens, H.M., de Winter-de Groot, K.M., Brandsma, A.M., de Jong, N.W., Bijvelds, M.J., Scholte, B.J., *et al*. (2013). A functional CFTR assay using primary cystic fibrosis intestinal organoids. Nat. Med. 19, 939–945.
36. Liu, J., Walker, N.M., Ootani, A., Strubberg, A.M., and Clarke, L.L. (2015). Defective goblet cell exocytosis contributes to murine cystic fibrosis-associated intestinal disease. J. Clin. Invest. 125, 1056–1068.
37. Mansoura, M.K., Biwersi, J., Ashlock, M.A., and Verkman, A.S. (1999). Fluorescent chloride indicators to assess the efficacy of CFTR cDNA delivery. Hum. Gene Ther. 10, 861–875.
38. Cutting, G.R., Kasch, L.M., Rosenstein, B.J., Tsui, L.C., Kazazian, H.H., Jr., and Antonarakis, S.E. (1990). Two patients with cystic fibrosis, nonsense mutations in each cystic fibrosis gene, and mild pulmonary disease. N. Engl. J. Med. 323, 1685–1689.
39. Kerem, B.S., Zielenski, J., Markiewicz, D., Bozon, D., Gazit, E., Yahav, J., Kennedy, D., Riordan, J.R., Collins, F.S., and Rommens, J.M. (1990). Identification of mutations in regions corresponding to the two putative nucleotide (ATP)-binding folds of the cystic fibrosis gene. Proc. Natl. Acad. Sci. USA 87, 8447–8451.
40. Haws, C., Krouse, M.E., Xia, Y., Gruenert, D.C., and Wine, J.J. (1992). CFTR channels in immortalized human airway cells. Am. J. Physiol. 263, L692–L707.

41. Sheppard, D.N., and Welsh, M.J. (1999). Structure and function of the CFTR chloride channel. Physiol. Rev. 79, S23–S45.
42. Winter, M.C., Sheppard, D.N., Carson, M.R., and Welsh, M.J. (1994). Effect of ATP concentration on CFTR Cl- channels: a kinetic analysis of channel regulation. Biophys. J. 66, 1398–1403.
43. Population variation of common cystic fibrosis mutations. The cystic fibrosis genetic analysis consortium (1994). Hum. Mutat. 4, 167–177.
44. Sato, T., and Clevers, H. (2013). Primary mouse small intestinal epithelial cell cultures. Methods Mol. Biol. 945, 319–328.
45. Vonk, A.M., van Mourik, P., Ramalho, A.S., Silva, I.A.L., Statia, M., Kruisselbrink, E., Suen, S.W.F., Dekkers, J.F., Vleggaar, F.P., Houwen, R.H.J., *et al*. (2020). Protocol for application, standardization and validation of the forskolin-induced swelling assay in cystic fibrosis human colon organoids. STAR Protoc. 1, 100019.

Chapter | 4

Chapter | 5

Anticodon engineered transfer RNAs (ACE-tRNAs) as a platform approach for suppressing nonsense mutations

Unpublished data

Wooree Ko[1,*], Joseph J. Porter[1,*], **Sacha Spelier[2,3],** Tyler Couch[1], Isabelle van der Windt[2,3], Priyanka Bhatt[4], Kevin Coote[4], Martin Mense[4], Jeffrey M. Beekman[2,3] and John D. Lueck[1,6,7,*]

**** These authors contributed equally to this work***

1. Department of Pharmacology and Physiology, University of Rochester School of Medicine and Dentistry, Rochester, NY 14642, USA. **2.** Department of Pediatric Respiratory Medicine, Wilhelmina Children's Hospital, University Medical Center, Utrecht University, 3584, EA, Utrecht, The Netherlands **3.** Regenerative Medicine Utrecht, University Medical Center, Utrecht University, 3584, CT, Utrecht, The Netherlands **4.** Cystic Fibrosis Foundation Therapeutics Lab, Cystic Fibrosis Foundation, Lexington, MA US **6.** Department of Neurology, University of Rochester School of Medicine and Dentistry, Rochester, Rochester, NY 14642, USA. **7.** Center for RNA Biology, University of Rochester School of Medicine and Dentistry, Rochester, Rochester, NY 14642, USA.

Summary

Nonsense mutations arise from single nucleotide substitutions that result in premature termination codons (PTCs). PTCs present in mRNA result in activation of the nonsense-mediated mRNA decay (NMD) pathway which degrades most PTC-containing mRNAs, resulting in little to no production of (truncated) protein. We demonstrate that anticodon engineered (ACE) tRNAs efficiently suppress the most prevalent cystic fibrosis (CF) causing PTCs, resulting in functional rescue of cystic fibrosis transmembrane conductance regulator (CFTR) transcript. CFTR functional rescue is further enhanced by combinatorial treatment with CFTR modulators. Interestingly, whilst the codons that give rise to common CF PTCs encode different amino acids, suppression by specifically an ACE-tRNA charged with leucine results in significant rescue of CFTR function in both immortalized airway and primary human intestinal epithelial cells. Together, these results demonstrate that ACE-tRNAs can serve as potential therapeutic approach for CF as well as other nonsense-associated diseases.

Introduction

Approximately 11% of all human genetic diseases are caused by nonsense mutations, in which an alteration of a single nucleotide of an amino acid encoding codon, results into the presence of a premature termination codon (PTC) 5′ of the normal termination codon (NTC). Consequently, a PTC prevents the production of a normal full-length protein by prematurely terminating translation and furthermore activates the nonsense-mediated mRNA decay (NMD) pathway, which initiates degradation of a PTC-containing mRNA transcript [1]. Consequently, genetic disorders caused by nonsense mutations are often associated with severe disease phenotypes. Examples of PTC-associated genetic diseases include cystic fibrosis (CF) [2], [3], Duchenne muscular dystrophy (DMD) [4], spinal muscular atrophy [5] and ß-thalassemia [6].

CF is an autosomal recessive disorder caused by mutations in the cystic fibrosis transmembrane conductance regulator *(CFTR)* gene. This gene encodes the CFTR chloride and bicarbonate channel, which is expressed in the apical membrane of epithelial cells in various organs. Defective CFTR protein function results in the buildup of thick and sticky mucus primarily in the respiratory and digestive systems [2]. In 2022, CF affected about 40,000 people in the United States and 100,000 people worldwide [7], [8]. In the last decades, there have been tremendous efforts to discover and develop therapies to directly target CFTR and restore defective channel function. These efforts resulted in the development of CFTR modulators, correctors and potentiators, which respectively correct folding of CFTR protein and increase potentiation and function of CFTR at the cell membrane. To date, four highly efficient modulator therapies (HEMTs) have been approved for people with CF with specific mutations, encompassing about 90% of the patient population [8]–[12]. However, approximately 10% of all people with CF do not benefit from HEMTs, including those people *CFTR*-PTC mutations.

Several treatment strategies have been explored for diseases caused by PTC mutations. One potential treatment option is stimulating translational readthrough at the PTC by readthrough compounds. First-generation readthrough compounds such as aminoglycosides G418 and gentamicin, have been shown to slow down the ribosome, thereby increasing the chance of incorporating a non-cognate amino acid at the PTC site. Whilst such compounds resulted in a modest level of readthrough-mediated functional protein recovery, their clinical efficacy was limited and off-target toxicity was associated with long-term administration [13]. Next-generation non-aminoglycoside small molecules like ataluren have a relatively good safety profile, yet still questionable readthrough efficiency [14], [15]. The challenging nature of treatments for PTC mutations is further underlined by the fact that at present-day only a single readthrough compound has been approved for clinical use, ataluren in a subset of patients with DMD [16].

Whilst readthrough compound monotherapy has proven challenging, synergetic combinatorial treatment regimens with readthrough compounds, NMD inhibitors and CFTR modulators have been described to be more successful [17]. However, NMD inhibition has been associated with side-effects and at present-day, no NMD inhibitors are tested in a clinical setting. As a consequence, it remains challenging to translate preclinical results of both readthrough compound monotherapy as well as combinatorial treatment regimens build around readthrough compounds into a clinical setting.

For these reasons, it remains valuable to study different non-small-molecule approaches, such as anticodon engineered RNAs (ACE-tRNAs). ACE-tRNAs are anticodon engineered versions of natural tRNAs that bind one of three stop codons, UAA, UAG or UGA, consequently resulting in translation elongation at the PTC site and generation of full-length protein [18], [19]. ACE-tRNAs can be engineered in such a way to faithfully encode the cognate amino acid, allowing restoration of wildtype protein instead of resulting in the production of missense protein variants as is the case for readthrough compounds. Furthermore, based on ribosomal sequencing, ACE-tRNAs selectively result in readthrough at the PTC site in comparison to the NTC site [19]. Whilst ACE-tRNAs offer advantages over other pharmacological readthrough approaches in terms of selectivity and toxicity, one major challenge is efficient delivery to the right cell types across various organs. Recently, liposome-based delivery of ACE-tRNA encoding cDNAs has been shown to promote efficient suppression of endogenous CFTR PTCs in a native genomic context [19]. Although such nonviral gene delivery systems generally have robust safety profiles characterized by low immunogenicity and cytotoxicity, its formulation is complex [20], [21]. Thus, further studies on effective ACE-tRNA delivery to overcome the delivery hurdle and elicit clinically relevant level of functional protein expressions, remain essential.

Here, we investigated the ability of adenovirus (Ad)-mediated ACE-tRNA delivery to suppress and rescue CFTR with PTC mutations. Moreover, we examined whether a single ACE-tRNA subtype, ACE-tRNAleucine, is applicable for the four most prevalent PTC sites originally encoding different amino acids. To further boost the function of the ACE-tRNAs,

we characterize their efficacy in the presence of different compounds with synergistic mode-of-actions, both NMD inhibitors and CFTR modulators. We exploit both immortalized airway cells as well as primary CF-patient derived intestinal organoids. Overall, we report the therapeutic promise of ACE-tRNAs for nonsense mutation-associated diseases.

Methods

Cell culture of HBE cells

16HBE14o- parental cell line and gene-edited 16HBE14o- cell lines (16HBEge) with CFTR nonsense mutations, including CFF-16HBEge CFTR-G542X, CFF-16HBEge CFTR-R553X, CFF-16HBEge CFTR-R1162X and CFF-16HBEge CFTR-W1282X cells, were obtained from the Cystic Fibrosis Foundation Therapeutics Lab (Lexington, MA, USA). Cells were cultured in minimum essential medium (MEM) (Gibco, 11095-080) supplemented with 10% fetal bovine serum (Gibco, 26140-079) and 1% penicillin/streptomycin/glutamine (Gibco, 10378-016) and maintained at 37∞C and 5% CO2. Cells were grown on plates coated with coating solution [LHC-8 basal medium (Gibco, 12677-027), 1.34 µL/mL bovine serum albumin (BSA) 7.5% (Gibco, 15260-037), 10 µL/mL bovine collagen solution, type 1 (Advanced BioMatrix, 5005-100ML) and 10 µL/mL fibronectin from human plasma (Thermo Fisher Scientific, 33016-015)] and dissociated with TrypLE Express (Gibco, 12604-013) for subculturing.

Generation of stable HBE cell lines

Human coxsackievirus and adenovirus (Ad) receptor (hCAR) was stably expressed in HBE cells using the piggyBac (PB) system. PB transposon vector expressing hCAR and PB transposase vector were co-transfected into HBE cells using Lipofectamine LTX and Plus reagent (Invitrogen by Thermo Fisher Scientific, 15338-100) according to manufacturer's guidelines with slight modifications. Briefly, 500,000 cells were plated in each well of a 6-well plate on the day of transfection and incubated in a 37°C/5% CO2 incubator for 20-30 min. The transfection mixture was prepared by combining diluted DNA [5 µg DNA (2.5 µg PB transposon vector and 2.5 µg PB transposase vector) and 2.5 µL PLUS reagent in 125 µL Opti-MEM (Gibco, 51985-034)] and diluted Lipofectamine LTX reagent (5 µL Lipofectamine LTX reagent in 125 µL Opti-MEM), incubated for 5 min at room temperature, and then added to pre-plated cells. Cells were also co-transfected with PB transposon vector and empty vector as a negative control. The media was changed to normal cell culture media 16-24 h post transfection and then to 0.5 µg/mL puromycin (InvivoGen, ant-pr-1) media 48 h post transfection to begin selection. Cells were maintained in puromycin media until complete cell death was observed in the negative control plate.

Adenovirus production

ACE-tRNAs expressing Ads were generated and packaged in Vector Biolabs (Malvern, PA, USA).

Transduction of HBE cells

For Ad transduction of cells plated on the cell culture plate, 500,000 cells were seeded into a 6-well plate and incubated in a cell culture incubator for 4 h. Medium was then replaced with 500 µL of media containing Ad vectors (Ad-4xScr, -4xGly, -4xArg, or -4xLeu) at varying multiplicities of infection (MOIs). The media was replaced 1 day post transduction (DPT).

For Ad transduction of cells plated on Transwells, 100,000-150,000 cells were seeded onto 6.5 mm Transwell permeable support with 0.4 µm polycarbonate membrane inserts (Corning, 3413) pre-coated with collagen from rat tail (Sigma-Aldrich, C7661-25MG). 3 days post seeding, Transwells were flipped upside down to apply 50 µL of Ad-mixed media to the basolateral side and flipped back to the original position after 4 h incubation. Then, 50 µL of Ad-mixed media was added to the apical side followed by media change 24 h after transduction. MOI 100 of Ad vectors (Ad-4xScr, -4xGly, -4xArg or -4xLeu) was used unless otherwise indicated.

Flow cytometry of HBE cells

At 2 DPT, cells were washed with Dulbecco's phosphate-buffered saline (DPBS) (Gibco, 14190-144) and dissociated with TrypLE Express at 37°C for 10 min. Dissociated cells were diluted into 4 mL of FACS buffer, DPBS with 0.3% BSA and 1 mM EDTA, to inactivate the TrypLE and concentrated by centrifugation at 200 x g for 5 min at 4 °C. Cells were resuspended in 250 µL of FACS buffer and run on the BD LSR II (BD Biosciences) until collecting over 20,000 events. GFP was excited with a blue (488 nm) laser, and fluorescence was detected at 505-525 nm. Data were analyzed with FCS Express 7 (De Novo Software, Pasadena, CA, USA). Gating for single cells was accomplished by using forward and side scatter area, height and width parameters. The threshold for GFP positivity was determined with untransduced cells.

RT-qPCR of HBE cells

Total RNA was isolated from cells with the Monarch Total RNA Miniprep Kit (New England BioLabs, T2010S) according to manufacturer's instruction and quantitated with a NanoDrop Onec Spectrophotometer (Thermo Fisher Scientific, Waltham, MA, USA). One-step reverse transcriptase and quantitative PCR (RT-qPCR) was performed using the Luna Universal One-Step RT-qPCR Kit (New England BioLabs, E3006E) according to manufacturer's protocol. Briefly, 10 µl 2x Luna Universal Probe One-Step Reaction Mix, 1 µl 20x Luna WarmStart RT Enzyme Mix, 1 µl 20x CFTR-specific primers and probe, 1 µl TBP-specific primers and probe, 100-500 ng of template RNA and nuclease-free water were mixed in a final volume of 20 µl. Cycle conditions were one cycle of 10 min at 55°C and one cycle of 3 min at 95°C followed by 40 cycles of 15 s at 95°C and 30 s at 60°C. All samples were run in triplicate, and a no-template control (NTC) reaction was included as a negative control. CFTR transcript abundance relative to TBP was calculated using the comparative Ct method, 2-ΔΔCt. Target-specific primers and probes with the final concentration of 500 nM each primers and 250 nM probe were purchased from Integrated DNA technologies (Coralville, IA, USA). RT-qPCR was run on the QuantStudio 3 Real-Time PCR System (Applied Biosystems, Waltham, MA, USA) and analyzed with QuantStudio Design & Analysis Software v1.5.1 (Applied Biosystems, Waltham, MA, USA).

Ussing chamber recordings of HBE cells

Cells were grown and transduced as described above. Where indicated, cells were treated with 0.3 μM SMG1i 48 h before assay and CFTR correctors 3 μM lumacaftor (L, VX-809, Selleck Chemicals, S1565) or 3 μM elexacaftor (E, VX-445, Selleck Chemicals, S8851) and 3 μM tezacaftor (T, VX-661, Selleck Chemicals, S7059) 24 h before assay. CFTR potentiator ivacaftor (I, VX-770, Selleck Chemicals, S1144) was added acutely while running the experiment. Transepithelilal electrical resistance was measured with EVOM2 Epithelial Voltohmmeter (World Precision Instruments, Sarasota, FL, USA) to confirm electrically tight monolayer formation. Transwell inserts were mounted into Ussing chambers (Physiologic Instruments, San Diego, CA, USA) and the short circuit current (Isc) was measured with the VCC MC8 multi-channel voltage current clamp (Physiologic Instruments, San Diego, CA, USA) under voltage clamp condition. Cells were bathed in Ringer's solution (in mM: 135 NaCl, 5 HEPES, 0.6 KH2PO4, 2.4 K2HPO4, 1.2 MgCl2, 1.2 CaCl2, 5 D-Glucose adjusted to pH 7.4) initially on both sides while maintaining the solution at 37 °C and continuously circulating with compressed air. After baseline recordings, 100 μM amiloride was added to block epithelial sodium channels and then 100 μM 4,4′-diisothiocyanostilbene-2,2′-disulfonic acid (DIDS) was added to block Ca2+-activated chloride channels. Then, apical side solution was replaced with low Cl- solution (in mM: 135 Na-Gluconate, 5 HEPES, 0.6 KH2PO4, 2.4 K2HPO4, 1.2 MgCl2, 1.2 CaCl2, 5 D-Glucose adjusted to pH 7.4) to create a transepithelial chloride ion gradient. To assess CFTR-mediated Cl- current, 10 μM forskolin and 100 μM 3-isobutyl-1-methlyxanthine (IBMX) were added to activate CFTR, followed by 20 μM CFTR inhibitor-172 (CFTRInh-172) to inhibit CFTR. Where indicated, vehicle (V, DMSO) or 1 μM ivacaftor (I, VX-770) was added acutely in-between CFTR activators and inhibitor addition for CFTR potentiation. All compounds were added to apical side. Data were acquired with Acquire & Analyze 2.3 software (Physiologic Instruments, San Diego, CA, USA). The area under the curve (AUC) between additions of CFTR activators and CFTR inhibitor was used to determine functional rescue of CFTR activity. Cells were collected after Ussing chamber assay for RT-qPCR experiment described above to measure CFTR transcript level.

Primary intestinal epithelial cell collection and culturing from CF patients

All experiments using human tissues described in this manuscript was approved by the medical ethics committee of the University Medical Center Utrecht (UMCU; TcBio 14-008 and TcBio 16-586). Informed consent for tissue collection and for generation, storage and use of organoids was obtained from all participating patients. Biobanked intestinal organoids are stored and cataloged (https://huborganoids.nl/) at the Hubrecht Organoid Technology foundation (http://hub4organoids.eu) and can be requested from info@hub4organoids.eu. Collection of patient tissues and data was performed according to the guidelines of the European Network of Research Ethics Committees (EUREC) and to European, national and local law. PDIOs were cultured as previously described [22], [23].

Transduction of PDIOs

On the day of transduction, 7-day old PDIO cultures were mechanically disrupted, washed with PBS and subsequently incubated with TrypLE for 20 min at 37°C resulting in structure disintegration into single cells. Cells were counted and incubated at 37°C for 45 min with the adequate amount of pre-titrated Ad vectors diluted in Opti-MEM to result in the desired MOIs. After 45 min, ice-chilled Matrigel was added to the cell-Opti-MEM mix resulting in a 50% final concentration, after which cells were plated in pre-warmed 48-well plates with a density of 1875 cells/μL, where 8 μL of Matrigel-cells solution was added in each well. After a 10-min incubation at 37°C, medium with 10 μM rho-kinase inhibitor (Sigma-Aldrich, 555562) was added to the wells.

Characterization of transduction efficiency in PDIOs by flow cytometry

PDIOs were collected at 2 and 6 DPT and disrupted into single cells using TrypLE. Cells were fixated with 4% PFA during a 30-min incubation and subsequently resuspended in FACS buffer, PBS with 5% FBS and 2 mM EDTA, prior to flow cytometry measurements. Measurements were carried out on the BD LSRFortessa X-20 (BD Biosciences, Franklin Lakes, NJ, USA) 4 laser with standard filter sets. Fluorescence intensity of mCherry was measured on the 610-20 nm channel.

CFTR mRNA level quantification in PDIOs by quantitative PCR

One well of a 24-well plate was collected per condition of W1282X/W1282X PDIOs at 6 DPT after Ad vector transduction or 0.3 μM SMG1i addition. PDIOs were washed once with PBS, and RNA was extracted using RNeasy Mini Kit (Qiagen, 74104) following manufacturers protocol. cDNA was synthesized from 750 ng RNA with IscriptTM (Bio-Rad, 1708890) according to the supplied protocol. qPCR reactions were executed in a 96-well format using IQ SYBR green (Bio-Rad, 1708890) and the following primer sets (Integrated DNA Technologies): YHWAZ forward (CTGGAACGGTGAAGGTGACA), YHWAZ reverse (AAGGGACTTCCTGTAACAATGCA), CFTR forward (CAACATCTAGTGAGCAGTCAGG), CFTR reverse (CCCAGGTAAGGGATGTATTGTG). cDNA was amplified exploiting a Bio-Rad CFX96 PCR cycler, according to the following reaction protocol: one cycle of 3 min at 95°C followed by 39 cycles of 10 s at 95°C and 30 s at 62°C. Relative expression levels of transduced PDIOs were analyzed by means of ΔΔCt calculations, for which YWHAZ served as the housekeeping gene. Two replicate experiments were performed, and two technical replicates per condition were measured. YWHAZ expression was not affected by the different compound therapies. Melt peaks and CT values were analyzed using CFX Maestro Software.

Functional CFTR level assessment in PDIOs

PDIOs derived single cells were transduced and plated as described above. At 3 DPT, medium was refreshed, and forskolin (5 μM) and in some cases CFTR modulators (3 μM) were added to the wells. At 6 DPT, 10x images were acquired using a Leica Thunder microscope (Leica Microsystems). Images were processed using Las X software (Leica Microsystems) and ImageJ, where ImageJ was used for manual quantification in a blinded fashion by 2 different researchers, of total organoid area as well as lumen area. Twenty mCherry positive structures and twenty mCherry negative structures were characterized per condition in each experiment, yet in some cases less structures were present per condition. Each transduction was performed three times.

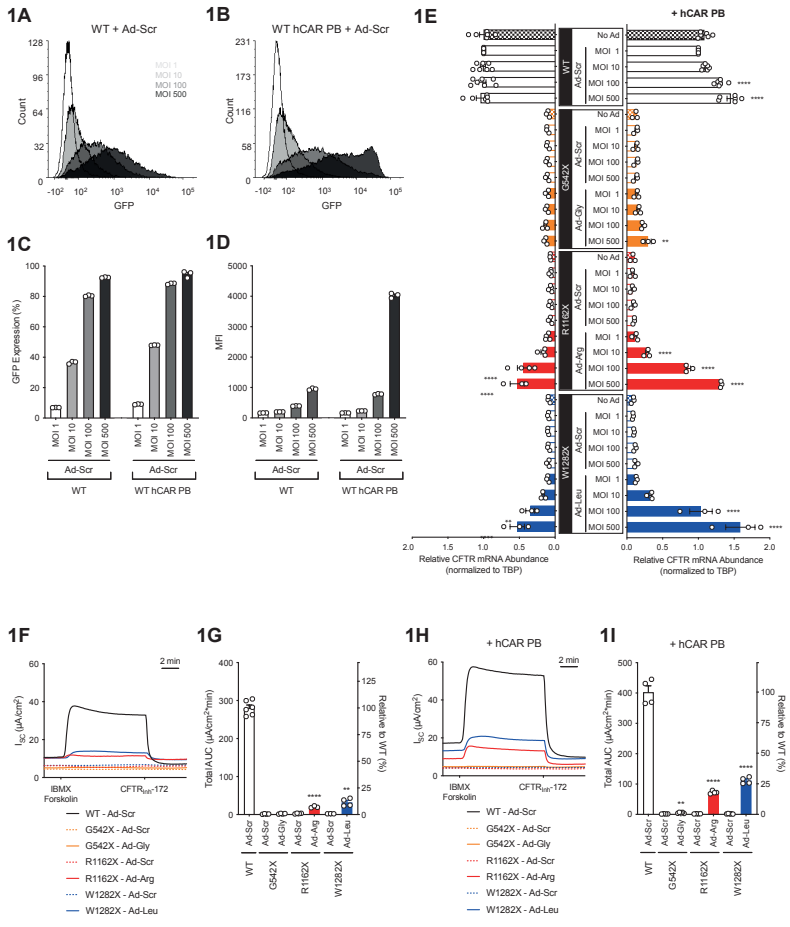

Figure 1. Stable expression of hCAR in 16HBE14o- and 16HBEge cell lines enhances Ad-mediated delivery of ACE-tRNAs.
(A-B) Representative flow cytometry histograms of (A) 16HBE14o- (WT) or **(B)** hCAR expressing WT (WT hCAR PB) cells transduced with MOI 1, 10, 100 and 500 of scrambled (Scr) adenovirus (Ad) that expresses GFP protein as a marker for the identification of transduced cells. **(C)** Quantification of GFP positive cell population and **(D)** median fluorescence intensity (MFI) of the population (n = 3) from flow cytometry data. Data are presented as mean ± SEM for (C) and **(D). (E)** CFTR mRNA abundance normalized to housekeeping gene TBP in WT (black), CFF-16HBEge CFTR-G542X (G542X; orange), CFF-16HBEge CFTR-R1162X (R1162X; red) and CFF-16HBEge CFTR-W1282X (W1282X; blue) cells (left) or same set of cell lines stably expressing hCAR (right) transduced with MOI 1, 10, 100 and 500 of Scr (open bar), ACE-tRNAGly (Gly; orange filled bar), ACE-tRNA^{Arg} (Arg; red filled bar), or ACE-tRNA^{Leu} (Leu; blue filled bar) Ads as indicated in the figure (n = 3-7). Data are presented as mean ± SEM. Significance was determined by one-way ANOVA and Tukey's post-hoc test, where ** p < 0.01 and **** p < 0.0001 vs. Ad-Scr MOI 1 (F-I) Ussing chamber recordings of **(F, G)** original or **(H, I)** hCAR expressing cells transduced with Ads as indicated in the figure in response to addition of CFTR activators, forskolin (10 μM) and IBMX (100 μM), and then CFTR inhibitor, CFTR$_{Inh}$-172 (20 μM). **(F, H)** Representative short-circuit Cl- current (ISC) traces and **(G, I)** total area under the curve (AUC) quantification (n = 3-6). Data are presented as mean ± SEM. Significance was determined by unpaired t-test for **(G)** and (I), where ** p < 0.01 and **** p < 0.0001.

Quantification and statistical analysis
GraphPad Prism 9 software (GraphPad Software, San Diego, CA, USA) was used for all statistical analysis. All of the statistical details of experiments can be found in the figure legends. Data are presented as mean ± standard error of the mean (SEM). Comparisons between two groups were performed using an unpaired Student's t-test. Multiple comparisons were analyzed using a one-way analysis of variance (ANOVA) followed by Tukey's multiple comparisons test. p values < 0.05 were considered statistically significant, with $*p < 0.05$, $**p < 0.01$, $***p < 0.001$ and $****p < 0.0001$.

Results

Adenovirus-mediated ACE-tRNA delivery is enhanced by hCAR expression in cultured airway cells
To evaluate the efficiency of ACE-tRNA technology on PTC mutations, we first utilized the previously developed human bronchial epithelial cell (16HBE) model system, genetically engineered to express various CFTR-PTC variants (HBEge) [24]. HBEge cell lines harboring CFTR nonsense mutations G542X, R1162X or W1282X were selected because of the highest allele frequency of G542X and W1282X PTC mutations and the (CF-overarching) abundance of nonsense mutations arising from the CGA arginine codon to the TGA nonsense codon [1], [25]. We aimed to insert the cognate amino acid at the PTC mutation site, so ACE-tRNAGly and ACE-tRNAArg were delivered to G542X and R1162X cells, respectively. The unavailability of an effective PTC suppressor ACE-tRNATrp limited our effort to insert the cognate tryptophan amino acid at the W1282X mutation site. However, we previously showed that leucine incorporation at the W1282 position of CFTR resulted in substantial CFTR function, so ACE-tRNA^{Leu} was delivered to W1282X cells [25]. ACE-tRNAs were delivered using adenovirus (Ad) which co-expressed a green fluorescent protein (GFP) marker, allowing characterization of transduction efficiency.

We first assessed the effectiveness of Ad-mediated gene delivery in HBE cells using flow cytometry. WT cells were transduced with Ad-scrambled (Ad-Scr) at different multiplicities of infection (MOIs), allowing quantification of GFP signal 2 days post transduction (DPT). Upon transduction with Ad-Scr, GFP fluorescent signal was observed in an MOI dependent manner **(Figure 1A).** We furthermore generated human coxsackievirus and adenovirus receptor (hCAR) stably expressing cell lines using the piggyBac (PB) system, to maximize the transduction efficiency of Ads, as hCAR is the primary receptor for group C of the Ads and group B coxsakieviruses. At similar MOIs, WT hCAR PB cells, compared to original WT cells, transduced with Ad-Scr shifted the GFP positive cell population curve to the right **(Figure 1B).** Further quantification of these flow cytometry data confirmed an increase in GFP signal in hCAR expressing cells, particularly at higher MOIs, confirming an hCAR-dependent increase in Ad transduction **(Figure 1C** and **1D).** Subsequently, original and hCAR expressing G542X, R1162X and W1282X cell lines were transduced with Ad-Scr and Ad-ACE-tRNAs. All transduced cell lines exhibited similar results as Ad-Scr transduced WT and WT hCAR PB cell lines (data not shown).

ACE-tRNA-mediated CFTR PTC suppression enhances PTC-transcript levels and rescues endogenous CFTR channel function in cultured airway cells

When different ACE-tRNAs were tested in HBEge cells harboring CF-causing nonsense mutations, higher MOI (MOI 100 and 500) transduction of Ad-Arg in R1162X cells and Ad-Leu in W1282X cells significantly increased CFTR mRNA levels **(Figure 1E, left),** suggesting efficient delivery of functional ACE-tRNAs using Ad vectors. When hCAR expressing cells were transduced with Ads, significant recovery of CFTR mRNA was detected with Ad-Gly in G542X hCAR cells and close to or over WT level of transcript rescue were evident for higher MOIs of Ad-Arg and Ad-Leu for R1162X hCAR and W1282X hCAR cells **(Figure 1E, right).** This increase in CFTR mRNA indicated a decrease of NMD of CFTR transcripts and consequently efficient Ad-mediated delivery of ACE-tRNAs. Although MOI 500 of Ad vectors elicited the best results, we decided to use MOI 100 in consecutive experiments, to limit the potential toxicity of Ad vectors or ACE-tRNAs (unless otherwise noted).

Next, we determined whether ACE-tRNA-induced PTC suppression translated into endogenous CFTR function recovery. To evaluate this, we performed Ussing chamber assays of cells transduced with ACE-tRNA Ad vectors. ACE-tRNAGly at the G542X site was ineffective at CFTR functional rescue, whereas ACE-tRNAArg at the R1162X site and ACE-tRNALeu at the W1282X site restored 7.2% and 14.9% of WT CFTR activity, respectively **(Figure 1F** and **1G).** In hCAR PB cell lines, CFTR chloride channel function increased as well, 1.3% of WT with ACE-tRNAGly, 18% of WT with ACE-tRNAArg and 27.7% of WT with ACE-tRNA^{Leu} of WT **(Figure 1H** and **1I).** As the expression of hCAR assisted on Ad-mediated delivery of ACE-tRNAs, next studies with HBE cell lines were performed in hCAR expressing cell lines to maximize the ACE-tRNA activity.

CFTR modulators enhance ACE-tRNA mediated functional CFTR rescue in cultured airway cells

However, whilst ACE-tRNAs restored CFTR function to some extent, restored CFTR function did not reach WT levels yet. As it has been described that CFTR modulators, specifically potentiators, can enhance the function of WT CFTR, we hypothesized that ACE-tRNA-mediated recovery of CFTR function also could be further enhanced with CFTR modulators [22], [26]. To test this, we delivered ACE-tRNAs to CFTR PTC cell lines and measured CFTR transcript and function levels in the presence of different CFTR modulator drugs: potentiator ivacaftor (I), the combination of respectively a corrector and potentiator: lumacaftor/ivacaftor (L/I), and the combination of respectively two correctors and one potentiator: elexacaftor/tezacaftor/ivacaftor (E/T/I).

As expected, when R1162X hCAR PB cells were transduced with ACE-tRNAArg Ad, CFTR mRNA did not increase upon CFTR modulator therapies. ACE-tRNAArg delivery resulted in ~40-50% of WT level of CFTR mRNA recovery irrespective of treatment conditions **(Figure 2A).** On a functional level, lumacaftor/ivacaftor treatment resulted in the highest combinatorial effect for functional channel rescue with ACE-tRNAArg delivery at the

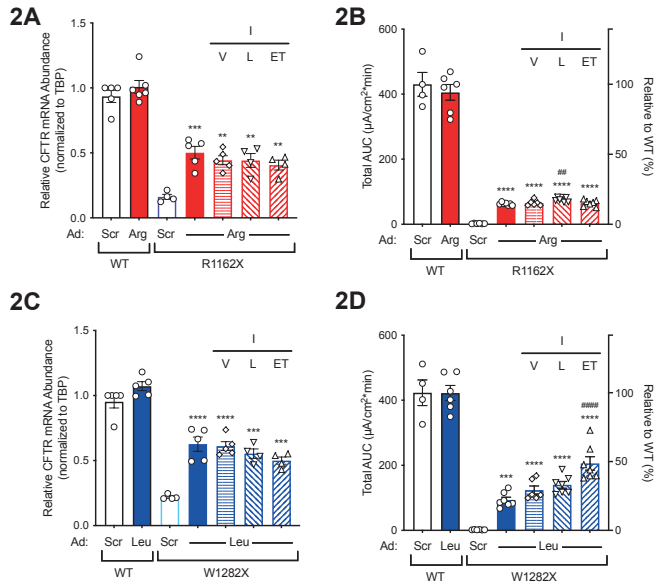

Figure 2. Combination of Ad-delivered ACE-tRNAs with CFTR modulator treatment synergistically improves CFTR channel function.
(A-B) hCAR expressing WT and R1162X cells (WT and R1162X, respectively) were transduced with MOI 100 of Ad-Scr or Arg, pretreated with vehicle (V), lumacaftor (L, 3 μM) or elexacaftor and tezacaftor (ET, 3 μM each) for 24 hours and then acutely treated with vehicle (V) or ivacaftor (I, 1 μM). **(A)** Relative CFTR mRNA expression of cells collected after Ussing chamber experiment (n = 4-6) and **(B)** total AUC quantification (n = 4-7) of Ussing chamber recordings in response to sequential addition of forskolin (10 μM) and IBMX (100 μM), followed by either vehicle (V) or ivacaftor (I, 1 μM), and then by CFTRInh-172 (20 μM). Data are presented as mean ± SEM. Significance was determined by unpaired t-test or one-way ANOVA and Tukey's post-hoc test, where ** $p < 0.01$, *** $p < 0.001$ and **** $p < 0.0001$ vs. Ad-Scr and ## $p < 0.01$ vs. Ad-Arg. **(C-D)** hCAR expressing WT and W1282X cells (WT and W1282X, respectively) were transduced with MOI 100 of Ad-Scr or Leu, pretreated with vehicle (V), lumacaftor (L, 3 μM) or elexacaftor and tezacaftor (ET, 3 μM each) for 24 hours and then acutely treated with vehicle (V) or ivacaftor (I, 1 μM). **(C)** Relative CFTR mRNA expression of cells collected after Ussing chamber experiment (n = 4-5), (and **(D)** total AUC quantification (n = 4-7) of Ussing chamber recordings in response to sequential addition of forskolin (10 μM) and IBMX (100 μM), followed by either vehicle (V) or ivacaftor (I, 1 μM), and then by $CFTR_{Inh}$-172 (20 μM). For **(C)** and **(D),** data are presented as mean ± SEM. Significance was determined by unpaired t-test or one-way ANOVA and Tukey's post-hoc test, where ** $p < 0.01$, *** $p < 0.001$ and **** $p < 0.0001$ vs. Ad-Scr and #### $p < 0.0001$ vs. Ad-Leu.

R1162X mutation site (14.6% for no drug treatment, 15.2% for ivacaftor, 17.8% for lumacaftor/ivacaftor, 15.1% for elexacaftor/tezacaftor/ivacaftor of WT) **(Figure 2B).**

Similarly, in the case of W1282X hCAR PB cells transduced with MOI 100 of Ad-Leu, no significant changes on mRNA level were displayed upon treatment with modulators **(Figure 2C).** CFTR functional evaluation revealed that E/T/I treatment was the best modulator combination to enhance CFTR channel function (22.2% for no drug treatment, 29.3%

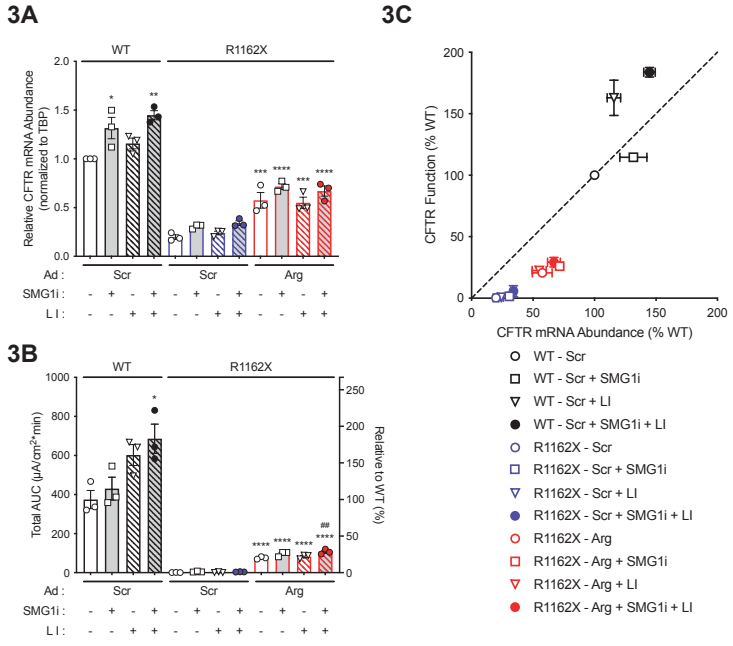

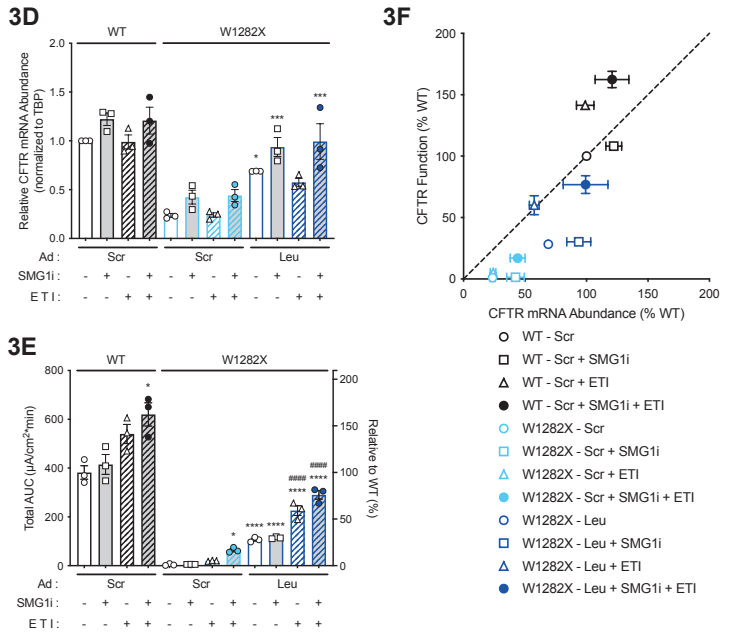

Figure 3. NMD inhibition and CFTR modulation significantly enhance ACE-tRNA rescued CFTR channel function.

(A-C) hCAR expressing WT and R1162X cells (WT and R1162X, respectively) were transduced with MOI 100 of Ad-Scr (black for WT, purple for R1162X) or Arg (red) and pretreated with either vehicle (V) or SMG1i (0.3 μM) for 48 hours and then with either vehicle (V) or lumacaftor (L, 3 μM) for 24 hours. Cells pretreated with lumacaftor were acutely treated with ivacaftor (I, 1 μM). **(A)** Relative CFTR mRNA expression of cells collected after Ussing chamber experiment (n = 3), **(B)** total AUC quantification (n = 3) and (C) functional CFTR level in relation to CFTR mRNA level (n = 3). **(A-C).** Data are presented as mean ± SEM and significance was determined by one-way ANOVA and Tukey's post-hoc test, where * $p < 0.05$, ** $p < 0.01$, *** $p < 0.001$ and **** $p < 0.0001$ vs. Ad-Scr and ## $p < 0.01$ vs. Ad-Arg.
(D-F) hCAR expressing WT and W1282X cells (WT and W1282X, respectively) were transduced with MOI 100 of Ad-Scr (black for WT, light blue for W1282X) or Leu (blue) and pretreated with either vehicle (V) or SMG1i (0.3 μM) for 48 hours and then with either vehicle (V) or elexacaftor and tezacaftor (ET, 3 μM each) for 24 hours. Cells pretreated with elexacaftor and tezacaftor were acutely treated with ivacaftor (I, 1 μM). **(D)** Relative CFTR mRNA expression of cells collected after Ussing chamber experiment (n = 3), **(E)** total AUC quantification (n = 3) and **(F)** functional CFTR level in relation to CFTR mRNA level (n = 3). **(D-F).** Data are presented as mean ± SEM. Significance was determined by one-way ANOVA and Tukey's post-hoc test, where * $p < 0.05$, *** $p < 0.001$ and **** $p < 0.0001$ vs. Ad-Scr and #### $p < 0.0001$ vs. Ad-Leu.

for ivacaftor, 33.1% for lumacaftor/ivacaftor, 48.7% for elexacaftor/tezacaftor/ivacaftor of WT) **(Figure 2D).** Based on these findings, we performed further experiments with L/I for in CFTR-R1162X context and E/T/I in CFTR-W1282X context.

NMD inhibition and CFTR modulation significantly enhance ACE-tRNA rescued CFTR channel function.

Next, we investigated whether NMD inhibitor SMG1i, has a synergistic effect on ACE-tRNA-rescued CFTR function. R1162X hCAR cells were transduced with Ad-Scr or Ad-Arg and pretreated with vehicle or SMG1i as well as lumacaftor/ivacaftor. As expected, SMG1i treatment of R1162X hCAR cells enhanced CFTR mRNA expression level **(Figure 3A).** The best functional recovery was obtained with SMG1i and lumacaftor/ivacaftor treatment (20.3% for no drug treatment, 25.7% for SMG1i, 22.1% for lumacaftor/ivacaftor, 28.5% for SMG1i with lumacaftor/ivacaftor – relative to WT CFTR function) **(Figure 3B).** The relationship between CFTR function and CFTR mRNA abundance is plotted in Figure 3C, which underlines that SMG1i treatment contributes to the availability of CFTR-R1162X mRNA level, yet not so much to the functional CFTR level.

W1282X hCAR cells were transduced with Ad-Leu instead of Ad-Arg and treated with E/T/I. Treatment with SMG1i was effective at recovering PTC containing CFTR mRNA (23.8% to 43.2% of WT for Ad-Scr transduced cells, 63.2% to 96.5% of WT for Ad-Leu transduced cells) **(Figure 3D).** Unlike Ad-Scr transduced R1162X hCAR cells, W1282X hCAR cells transduced with Ad-Scr resulted in reasonable recovery of CFTR function when combined with SMG1i and E/T/I treatment (16.6% of WT) **(Figure 3E).** SMG1i treatment significantly enhanced PTC containing CFTR transcripts but elicited the meaning level of channel function only in combination with ACE-tRNAs or CFTR modulators **(Figure 3F).** Overall, combina-

torial treatment of CF-causing nonsense mutations with ACE-tRNAs, NMD inhibitor and CFTR modulators is most efficient for restoring functional CFTR.

ACE-tRNA^{Leu} and ACE-tRNA^{Arg} rescue function of CFTR with the most prevalent CF-causing PTC mutations

Next, we aimed to characterize whether a single ACE-tRNA sequence may be utilized for multiple CF-causing PTC mutations, as if single ACE-tRNA has a potential to rescue CFTR function for various mutations, clinical application of ACE-tRNA technology could be more practical. To compare their efficacy, three ACE-tRNAs, ACE-tRNA^{Gly}, ACE-tRNA^{Arg} and ACE-tRNA^{Leu}, were delivered using Ad vectors to hCAR expressing 16HBEge cell lines harboring CFTR-G542X, -R553X, -R1162X and –W1282X nonsense mutations, which are the four most prevalent CF-causing nonsense mutations. Surprisingly, ACE-tRNA^{Leu} was the best suppressor for recovering all four CFTR PTCs on mRNA level, followed by ACE-tRNAArg and then ACE-tRNA^{Gly} **(Figure 4A).**

On a functional level, CFTR function improved significantly with ACE-tRNA^{Arg} and ACE-tRNA^{Leu} even without E/T/I treatment for G542X, R553X and R1162X mutations **(Figure 4B).** Interestingly, although both R553X and R1162X mutations are resulted from arginine to nonsense codon mutations, higher CFTR functional recovery was achieved with leucine for the R553X position and arginine for the R1162X position. Uniquely, CFTR function of ACE-tRNA^{Arg} expressing W1282X hCAR cells were only rescued with E/T/I. This result represents that the help of CFTR modulators is essential for CFTR-W1282R channel to be functional. ACE-tRNA^{Leu} with E/T/I treatment was the most effective way of recovering functional CFTR level for W1282X hCAR PB cells, as expected from previous data.

ACE-tRNA^{Leu} significantly increases CFTR function in patient-derived intestinal organoids expressing CF-causing nonsense mutations

Next, we set out to verify ACE-tRNA efficacy in a primary cell setting by using patient-derived intestinal organoids (PDIOs). As characterized by mCherry quantification via flow cytometry, transduction of PDIO derived single cells with ACE-tRNA^{Leu} resulted in an average of 40% efficiency for both MOI 50 and 100 **(Figure 5A).** Prior to functional measurements, we characterized CFTR mRNA levels to investigate ACE-tRNA^{Leu}-mediated inhibition of NMD. As expected, in PDIOs expressing W1282X/W1282X CFTR, CFTR mRNA levels increased ~2.5 fold upon MOI 100 of ACE-tRNA^{Leu} Ad vector transduction, equal to the half of the effect from SMG1i positive control **(Figure 5B).**

To allow the outgrowth of single cells into multicellular structures, CFTR was activated with forskolin at 3 DPT after which CFTR function was characterized by measuring luminal area of PDIO structures at 6 DPT. As shown in Figure 5C, ACE-tRNA^{Leu} resulted in a major increase in lumen area of W1282X/W1282X PDIOs upon forskolin stimulation in a subset of the mCherry positive structures. Indeed, when quantifying lumen area in all conditions for W1282X/W1282X PDIOs, a significant increase in lumen area was present in mCherry positive structures for both MOIs upon stimulation with forskolin **(Figure 5D).** Importantly,

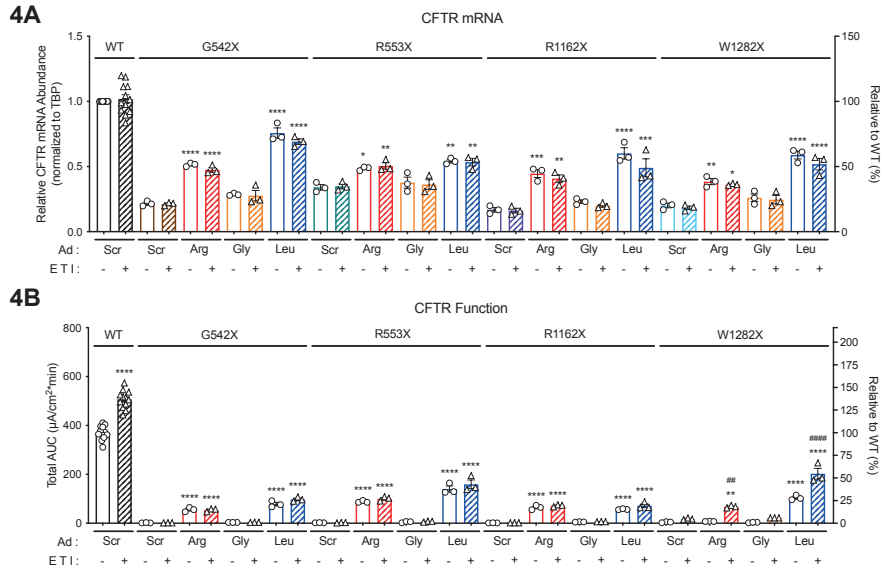

Figure 4. ACE-tRNA^{Leu} and ACE-tRNA^{Arg} significantly rescue function of CFTR with the most prevalent CF-causing nonsense mutations.
(A-C) hCAR expressing WT, G542X, R553X, R1162X, and W1282X cells (WT, G542X, R553X, R1162X, and W1282X, respectively) were transduced with MOI 100 of Scr, Arg (red), Gly (orange) or Leu (blue) Ads. Cells were pretreated with either vehicle (V) or elexacaftor and tezacaftor (ET, 3 μM each) for 24 hours, and elexacaftor and tezacaftor pretreated cells were acutely treated with ivacaftor (I, 1 μM). **(A)** Relative CFTR mRNA expression of cells collected after Ussing chamber experiment (n = 3-12) and **(B)** Total AUC quantification (n = 3-12) of Ussing chamber recordings in response to sequential addition of forskolin (10 μM) and IBMX (100 μM), followed by either vehicle (V) or ivacaftor (I, 1 μM), and then by CFTRInh-172 (20 μM). Data are presented as mean ± SEM. Significance was determined by one-way ANOVA and Tukey's post-hoc test, where * $p < 0.05$, ** $p < 0.01$, *** $p < 0.001$ and **** $p < 0.0001$ vs. Ad-Scr and ## $p < 0.01$, #### $p < 0.0001$ vs. no ETI.

in F508del/F508del PDIOs, ACE-tRNA^{Leu} Ad vector transduction did not result in a significant increase of luminal area in mCherry positive structures **(Figure 5E).** Here, as expected, treatment with CFTR modulators E/T/I did result in a major increase of luminal area upon forskolin stimulation. To further characterize efficacy of ACE-tRNA^{Leu} in restoring CFTR function, we characterized its efficacy for two additional homozygous PTC genotypes, G542X/G542X and R1162X/R1162X, as well as two heterozygous PDIO lines, W1282X/1717-1G>A and G542X/621+1G>T. Increase in luminal area was significant in mCherry positive structures for both MOIs upon stimulation with forskolin and of a similar extent among the three homozygous PTC lines, whereas increase in lumen area of both heterozygous lines was significant exclusively in the highest MOI conditions **(Figure 5F).**

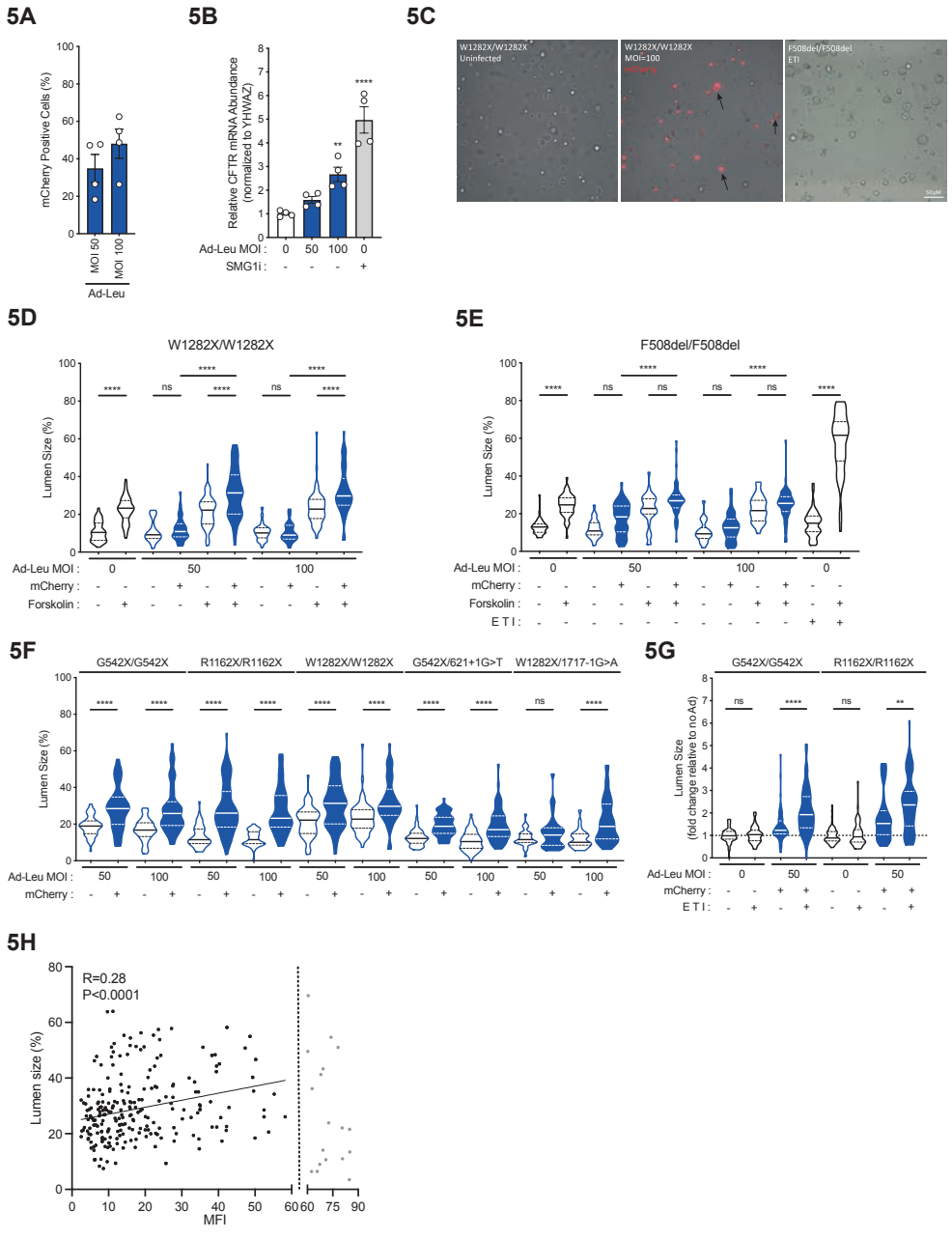

Figure 5. ACE-tRNA^{Leu} significantly increases CFTR function in patient-derived intestinal organoids expressing CF-causing nonsense mutations.
(A) Quantification of mCherry positive cell populations for F508del/F508del and G542X/G542X PIDOs derived single cells transduced with MOI 50 and 100 of Ad-Leu expressing mCherry. Data are presented as mean ± SEM based on two biological replicates per donor. **(B)** Relative CFTR mRNA expression of W1282X/W1282X PDIOs at 6 DPT upon Ad-Leu transduction or SMG1i treatment. Data are presented as mean ± SEM based on two biological replicates, with two technical replicates per condition. Significance was determined by one-way ANOVA and Dunnett's post-hoc test, where ** $p < 0.01$ and **** $p < 0.0001$ vs. Ad-Leu MOI 0. **(C)** Representative images of untransduced W1282X/W1282X PDIOs (left, negative control) or untransduced, ETI-treated F508del/F508del PDIOs (right, positive control), compared to Ad-Leu transduced W1282X/W1282X PDIOs (middle) at 6 DPT. Forskolin (5 μM) was added in all conditions at 3 DPT for CFTR activation. Black arrows represent Ad-Leu transduced W1282X/W1282X PDIOs with cystic structures, indicative of the presence of functional CFTR channel. **(D-E)** Luminal size measurements for F508del/F508del **(D)** and W1282X/W1282X **(E)** PDIOs upon transduction with MOI 50 and 100 of Ad-Leu in the absence and presence of forskolin (5 μM) stimulation. Ad-Leu transduced PDIOs were separated into mCherry negative (ACE-tRNA untransduced, open violin plot) and mCherry positive (ACE-tRNA transduced, blue filled violin plot) organoid populations. Data are represented as violin plots to show distribution of data for organoid structures measured at 6 DPT from three biological replicates. Significance was determined by one-way ANOVA and Tukey's post-hoc test, where **** $p < 0.0001$. **(F)** Luminal size measurements for five different PDIO genotypes [G542X/G542X (n = 38-60), R1162X/R1162X (n = 54-70), W1282X/W1282X (n = 40-60), G542X /621+1G>T (n = 51-61) and W1282X/1717-1G>A (n = 26-54)] upon transduction with MOI 50 and 100 of Ad-Leu. Forskolin (5 μM) was added in all conditions for CFTR activation. Ad-Leu transduced PDIOs were separated into mCherry negative (ACE-tRNA untransduced, open violin plot) and mCherry positive (ACE-tRNA transduced, blue filled violin plot) organoid populations. Data are represented as violin plots to show distribution of data for organoid structures measured at 6 DPT from three biological replicates. Significance was determined by one-way ANOVA and Tukey's post-hoc test, where **** $p < 0.0001$. **(G)** Luminal size relative to untransduced, ETI-untreated condition for G542X/G542X (orange background, n = 54-59) and R1162X/R1162X (red background, n = 59-60) PDIOs upon transduction with MOI 50 of Ad-Leu in the absence and presence of ETI treatment. Forskolin (5 μM) was added in all conditions for CFTR activation. Ad-Leu transduced PDIOs were separated into mCherry negative (ACE-tRNA untransduced, open violin plot) and mCherry positive (ACE-tRNA transduced, blue filled violin plot) organoid populations. Data are represented as violin plots to show distribution of data for organoid structures measured at 6 DPT from three biological replicates. Significance was determined by one-way ANOVA and Tukey's post-hoc test, where ** $p < 0.01$ and **** $p < 0.0001$. **(H)** Relation between MFI per organoid structure and luminal size per organoid structure. When excluding MFI of over 60 (vertical line), a significant positive trend is indicated (R=0.28, P<0.0001).

As leucine incorporation in the three characterized PTC lines results in a missense mutation, we aimed to characterize whether E/T/I modulator treatment further increases functional CFTR in PDIO cells, similar to the HBEge cells. Indeed, both for G542X/G542X as well as R1162X/R1162X, an additive effect was present when E/T/I was added in combination with ACE-tRNA^{Leu}, whilst CFTR modulators alone were not effective **(Figure 5G).** Lastly, we assessed the relation between MFI per organoid structure versus lumen size. We noticed across all experiments that some very bright mCherry positive structures in fact did not show an increased lumen, which could be contributed to Ad vector-associated toxicity upon a high level of transduction. As such, initially no correlation was present when comparing mCherry signal to lumen size for the three homozygous PTC PDIOs for both MOIs

in the presence of forskolin. However, when excluding those structures with the MFI of 60 or over (indicated in gray), a positive linear correlation indicated that higher ACE-tRNA^{Leu} expression resulted in higher level of CFTR function (R=0.28, p<0.0001) **(Figure 5H).**

Discussion

New solutions are needed for the 10-15% of people with CF (pwCF) carrying *CFTR* mutations that are unresponsive to highly efficient modulator therapies (HEMTs). As efforts to discover therapeutic options for PTC-related diseases had limited success in a clinical setting, the study of different non-small molecule approaches remains pivotal [13]. Here, we report the significant nonsense suppression activity of ACE-tRNAs delivered via adenoviral (Ad) vectors and the positive functional outcomes from combinatorial treatment with CFTR modulators.

When we assessed the efficacy of Ad-based gene delivery in HBE cells using Ad vectors expressing fluorescent protein, flow cytometry analyses revealed the effectiveness of Ad-assisted gene delivery to immortalized airway cell lines in a dose dependent manner. The exceptional activity of ACE-tRNAs delivered via Ad vectors was confirmed by their ability to facilitate readthrough of endogenous *CFTR* PTC mutations and increase mRNA abundance, consequently resulting in enhanced protein expression and function. We furthermore generated cell lines stably integrated with hCAR, to understand the safety of Ad-ACE-tRNA delivery system by forcefully increasing transduction rate and evaluate the maximum PTC suppression ability of ACE-tRNAs.

ACE-tRNA technology alone elicited significant level of functional CFTR channel rescue. However, to further increase efficiency we evaluated the combination effect with CFTR modulators and/or NMD inhibitors. Insertion of arginine at CFTR-R1162X mutation site by ACE-tRNAArg synergistically recovered CFTR function with lumacaftor/ivacaftor treatment, while that of leucine at CFTR-W1282X mutation site by ACE-tRNA^{Leu} synergistically increased functional channel level with elexacaftor/tezacaftor/ivacaftor treatment. Interestingly, addition of NMD inhibitor to the ACE-tRNA-CFTR modulator combination increased CFTR mRNA level but minimally enhanced functional channel level. Overall, we achieved the highest rescue of CFTR function with triple combination treatment of ACE-tRNAs, CFTR modulators and NMD inhibitor SMG1i. NMD however is an essential, sophisticated mechanism to maintain cellular homeostasis. Mendell et all found that inhibition of NMD interferes with protein expression levels about 5-10% of the human genes [27]. Previous preclinical studies furthermore suggested that high concentrations of NMD inhibitors are associated with toxicity, further hampering development of NMD-inhibitors as a therapeutic compound [28]. Consequently, circumvention of the need to inhibit NMD for treating nonsense mutations would be preferred. In the context of ACE-tRNA technology, this could be achieved by further improving ACE-tRNA efficacy and stability, as described recently by Porter et al [29].

We further demonstrate that a single ACE-tRNA sequence, ACE-tRNA^{Leu}, can be utilized for various CF-causing PTC mutations. The use of a single ACE-tRNA for a broad spectrum of mutations is very attractive from a therapeutic standpoint, as it will significantly reduce the time and effort for drug discovery and development process. Interestingly, in HBE cells, ACE-tRNA^{Leu} suppressed CFTR-G542X, -R553X, -R1162X and -W1282X mutations, which account for ~73% of all CF-causing PTC mutations, and rescued 16-38% of WT CFTR channel function. Combination treatment with CFTR modulators improved additional 4-27% of WT functional CFTR level, suggesting the potential of leucine ACE-tRNA for multiple PTC mutations, especially in combination with CFTR modulator therapy.

However, particularly in the context of nonsense mutations, a large gap between successful preclinical and disappointing clinical studies has been described recently [13]. As such, whilst results were promising in HBE cells, we aimed to confirm the ability of ACE-tRNA technology in primary epithelial patient-derived intestinal organoid (PDIO) models. Forskolin-induced fluid secretion resulting in luminal size increase and structure swelling has previously been described to be a CFTR-dependent phenotypic readout, allowing quantitative CFTR function measurements in response to different therapies [30], [31]. After transduction optimization based on previous literature, transduction of PDIO derived single cells resulted in an approximately 40% transduction efficiency [32]. Subsequently, by showing forskolin-dependent functional rescue of CFTR upon transduction with ACE-tRNA^{Leu} for homozygous G542X, W1282X and R1162X PDIOs, we confirm that ACE-tRNAs are indeed able to interact with pivotal components of the translational machinery and as such take part in normal translational processes under endogenous conditions.

A main challenge of ACE-tRNA technology is, similar to other gene therapy strategies, optimization of an efficient gene delivery system. However, in comparison to for example delivery of full-length CFTR DNA/mRNA, the small size of the ACE-tRNA expression cassette comes with several advantages. With a minimum size of ~140 nucleotides, ACE-tRNA technology can be easily paired with several non-viral and viral gene delivery systems in the form of both DNA and RNA. Recently, efficient nonsense suppression and functional protein restoration by in vivo delivery of ACE-tRNAs using lipid nanoparticle and adeno-associated virus have been reported. However, the best ACE-tRNA delivery method probably depends on disease-specific target tissue type and indication. Although Ad vectors used in the current study are well-known for triggering strong immune responses and thus raising safety concerns for clinical application, the FDA approved the first Ad vector-based gene therapy for the treatment for bladder cancer on December 16, 2022 [33]. With this first approval and the continued effort for therapeutic indications of the Ad-mediated gene therapy, Ad-based ACE-tRNA delivery may prove feasible in the future. An additional concern of ACE-tRNA technology, similar to other readthrough compounds, is the potential suppressing effect on natural termination codons. ACE-tRNAs, unlike the aminoglycoside G418, have been reported to minimally affect natural termination codon readthrough, displaying the preference for PTCs over natural terminal codons [19], [34].

To summarize, this study demonstrates the discovery of broad spectrum ACE-tRNA for multiple nonsense mutation sites with different PTC contexts as well as native amino acids

Chapter | 5

and the ability of modulator drugs in assisting the functional protein recovery. In combination with an efficient delivery system, ACE-tRNA technology may be a promising therapeutic option for genetic disease caused by nonsense mutations in a CF-overarching manner.

Acknowledgments

We thank members of the Lueck Laboratory and Dr. Amy M. Martin for reading and editing the manuscript and constructive discussion throughout the study. We thank U. Marting with help generating figures. We would like to thank the Cystic Fibrosis Foundation Therapeutics Lab and Dr. Hillary Valley for providing 16HBE14o- and 16HBE14ge cell lines used in this study and Dr. Martina Gentzsch at the University of North Carolina at Chapel Hill and the Cystic Fibrosis Foundation for the CFTR antibody. This work was supported by Emily's Entourage (www.emilysentourage.org) by a grant to S.S, J.M.B. and J.D.L., Cystic Fibrosis Foundation Postdoctoral Fellowship (PORTER20F0) to J.J.P., and a Cystic Fibrosis Foundation Research Grant (LUECK20GO), and NIH grant (1 R01 HL153988) to J.D.L.

Author contributions

W.K., J.J.P., S.S., T.C., P.B., K.C., J.M.B. and J.D.L. designed the study. W.K., J.J.P., S.S., T.C. P.B., I.W. and J.D.L. performed experiments. W.K., J.J.P., S.S., T.C. P.B., I.W. and J.D.L. analyzed the data and constructed the figures. W.K., J.J.P., S.S., T.C., and J.D.L. wrote the manuscript. All authors read and revised the manuscript.

Declaration of interests

J.D.L. is a co-inventor of the technology presented in this study and receives royalty payments related to the licensing of the technology from the University of Iowa. PCT/US2018/059065, filed November 2, 2018; METHODS OF RESCUING STOP CODONS VIA GENETIC REASSIGNMENT WITH ACE-tRNA; Inventors - University of Iowa – Inventors J.D.L. and Christopher A. Ahern pertains to the tRNA sequences used in this study.

References

[1] F. Supek, B. Lehner, and R. G. H. Lindeboom, "To NMD or Not To NMD: nonsense-mediated mRNA decay in cancer and other genetic diseases," *Trends Genet.,* vol. 37, no. 7, pp. 657–668, 2021.

[2] G. R. Cutting, "Cystic fibrosis genetics: from molecular understanding to clinical application," *Nat. Rev. Genet.,* vol. 16, no. 1, pp. 45–56, 2015.

[3] B. Kerem *et al.,* "Identification of mutations in regions corresponding to the two putative nucleotide (ATP)-binding folds of the cystic fibrosis gene.," *Proc. Natl. Acad. Sci.,* vol. 87, no. 21, pp. 8447–8451, 1990.

[4] P. Sicinski, Y. Geng, A. S. Ryder-Cook, E. A. Barnard, M. G. Darlison, and P. J. Barnard, "The molecular basis of muscular dystrophy in the mdx mouse: a point mutation," *Science (80-.).,* vol. 244, no. 4912, pp. 1578–1580, 1989.

[5] B. Wirth *et al.,* "Quantitative analysis of survival motor neuron copies: identification of subtle SMN1 mutations in patients with spinal muscular atrophy, genotype-phenotype correlation, and implications for genetic counseling," *Am. J. Hum. Genet.,* vol. 64, no. 5, pp. 1340–1356, 1999.

[6] J. C. Chang and Y. W. Kan, "beta 0 thalassemia, a nonsense mutation in man.," *Proc. Natl. Acad. Sci.,* vol. 76, no. 6, pp. 2886–2889, 1979.

[7] E. A. Cromwell *et al.,* "Cystic fibrosis prevalence in the United States and participation in the Cystic Fibrosis Foundation Patient Registry in 2020," *J. Cyst. Fibros.,* vol. 22, no. 3, pp. 436–442, 2023.

[8] J. Guo, A. Garratt, and A. Hill, "Worldwide rates of diagnosis and effective treatment for cystic fibrosis," *J. Cyst. Fibros.,* vol. 21, no. 3, pp. 456–462, 2022.

[9] B. W. Ramsey *et al.,* "A CFTR potentiator in patients with cystic fibrosis and the G551D mutation," *N. Engl. J. Med.,* vol. 365, no. 18, pp. 1663–1672, 2011.

[10] C. E. Wainwright *et al.,* "Lumacaftor–Ivacaftor in Patients with Cystic Fibrosis Homozygous for Phe508del CFTR," *N. Engl. J. Med.,* vol. 373, no. 3, pp. 220–231, 2015, doi: 10.1056/nejmoa1409547.

[11] S. M. Rowe *et al.,* "Tezacaftor–Ivacaftor in Residual-Function Heterozygotes with Cystic Fibrosis," *N. Engl. J. Med.,* vol. 377, no. 21, pp. 2024–2035, 2017, doi: 10.1056/nejmoa1709847.

[12] P. G. Middleton *et al.,* "Elexacaftor–tezacaftor–ivacaftor for cystic fibrosis with a single Phe508del allele," *N. Engl. J. Med.,* vol. 381, no. 19, pp. 1809–1819, 2019.

[13] S. Spelier, E. P. M. van Doorn, C. K. van der Ent, J. M. Beekman, and M. A. J. Koppens, "Readthrough compounds for nonsense mutations: bridging the translational gap," *Trends Mol. Med.,* 2023.

[14] E. M. Welch *et al.,* "PTC124 targets genetic disorders caused by nonsense mutations," *Nature,* vol. 447, no. 7140, pp. 87–91, 2007.

[15] E. Kerem *et al.,* "Ataluren for the treatment of nonsense-mutation cystic fibrosis: a randomised, double-blind, placebo-controlled phase 3 trial," *Lancet Respir. Med.,* vol. 2, no. 7, pp. 539–547, 2014.

[16] S. Michorowska, "Ataluren—Promising Therapeutic Premature Termination Codon Readthrough Frontrunner," *Pharmaceuticals,* vol. 14, no. 8. 2021. doi: 10.3390/ph14080785.
[17] E. de Poel *et al.,* "Functional restoration of CFTR nonsense mutations in intestinal organoids," *J. Cyst. Fibros.,* 2021.
[18] W. Ko, J. J. Porter, M. T. Sipple, K. M. Edwards, and J. D. Lueck, "Efficient suppression of endogenous CFTR nonsense mutations using anticodon-engineered transfer RNAs," *Mol. Ther. Acids,* vol. 28, pp. 685–701, 2022.
[19] J. D. Lueck *et al.,* "Engineered transfer RNAs for suppression of premature termination codons," *Nat. Commun.,* vol. 10, no. 1, pp. 1–11, 2019.
[20] M. S. Al-Dosari and X. Gao, "Nonviral gene delivery: principle, limitations, and recent progress," AAPS J., vol. 11, pp. 671–681, 2009.
[21] M. Ramamoorth and A. Narvekar, "Non viral vectors in gene therapy-an overview," *J. Clin. diagnostic Res. JCDR,* vol. 9, no. 1, p. GE01, 2015.
[22] J. F. Dekkers *et al.,* "Characterizing responses to CFTR-modulating drugs using rectal organoids derived from subjects with cystic fibrosis," *Sci. Transl. Med.,* vol. 8, no. 344, pp. 344ra84-344ra84, 2016.
[23] A. M. Vonk *et al.,* "Protocol for Application, Standardization and Validation of the Forskolin-Induced Swelling Assay in Cystic Fibrosis Human Colon Organoids," *STAR Protoc.,* vol. 1, no. 1, p. 100019, 2020, doi: 10.1016/j.xpro.2020.100019.
[24] H. C. Valley *et al.,* "Isogenic cell models of cystic fibrosis-causing variants in natively expressing pulmonary epithelial cells," *J. Cyst. Fibros.,* vol. 18, no. 4, pp. 476–483, 2019.
[25] U. C. F. CFTR2 database, "The Clinical and Functional TRanslation of CFTR (CFTR2); available at http://cftr2.org.," *24-09-2022.*
[26] F. Van Goor, H. Yu, B. Burton, and B. J. Hoffman, "Effect of ivacaftor on CFTR forms with missense mutations associated with defects in protein processing or function," *J. Cyst. Fibros.,* vol. 13, no. 1, pp. 29–36, 2014, doi: 10.1016/j.jcf.2013.06.008.
[27] J. T. Mendell, N. A. Sharifi, J. L. Meyers, F. Martinez-Murillo, and H. C. Dietz, "Nonsense surveillance regulates expression of diverse classes of mammalian transcripts and mutes genomic noise," *Nat. Genet.,* vol. 36, no. 10, pp. 1073–1078, 2004.
[28] D. R. McHugh, C. U. Cotton, and C. A. Hodges, "Synergy between readthrough and nonsense mediated decay inhibition in a murine model of cystic fibrosis nonsense mutations," *Int. J. Mol. Sci.,* vol. 22, no. 1, p. 344, 2020.
[29] J. J. Porter, W. Ko, E. G. Sorensen, and J. D. Lueck, "Optimization of Anticodon Edited Transfer RNAs (ACE-tRNAs) Function in Translation for Suppression of Nonsense Mutations," *bioRxiv,* pp. 2001–2024, 2024.
[30] G. Berkers *et al.,* "Rectal organoids enable personalized treatment of cystic fibrosis," *Cell Rep.,* vol. 26, no. 7, pp. 1701–1708, 2019.
[31] J. F. Dekkers *et al.,* "A functional CFTR assay using primary cystic fibrosis intestinal organoids," *Nat. Med.,* vol. 19, no. 7, pp. 939–945, 2013.
[32] N. Wang *et al.,* "Adenovirus-mediated efficient gene transfer into cultured three-dimensional organoids," *PLoS One,* vol. 9, no. 4, p. e93608, 2014.
[33] S. A. Boorjian *et al.,* "Intravesical nadofaragene firadenovec gene therapy for BCG-unresponsive non-muscle-invasive bladder cancer: a single-arm, open-label, repeat-dose clinical trial," *Lancet Oncol.,* vol. 22, no. 1, pp. 107–117, 2021.
[34] J. Wang *et al.,* "AAV-delivered suppressor tRNA overcomes a nonsense mutation in mice," *Nature,* vol. 604, no. 7905, pp. 343–348, 2022.

Chapter | 6

High throughput functional screen in patient-derived organoids allows drug repurposing for cystic fibrosis

European Respiratory Journal (Open Research), October 2022

Sacha Spelier[1,2,*], Eyleen de Poel[1,2,*], Georgia N. Ithakisiou[1,2], Sylvia W.F. Suen[1,2], Marne C. Hagemeijer[1,2], Danya Muilwijk[1], Annelotte M. Vonk[1,2], Jesse E. Brunsveld[1,2], Evelien Kruisselbrink[1,2],Cornelis K. van der Ent[1] and Jeffrey M. Beekman[1,2]
**** These authors contributed equally to this work***

1. Department of Pediatric Respiratory Medicine, Wilhelmina Children's Hospital, University Medical Center, Utrecht University, Utrecht, The Netherlands. **2.** Regenerative Medicine Utrecht, University Medical Center, Utrecht University, Utrecht, The Netherlands. **3.** Center for Lysosomal and Metabolic Diseases, Department of Clinical Genetics Erasmus University Medical Center, Rotterdam, The Netherlands.

Abstract

Background

Cystic fibrosis (CF) is a rare hereditary disease caused by mutations in the cystic fibrosis transmembrane conductance regulator (*CFTR*) gene. Recent therapies enable effective restoration of CFTR function of the most common F508del *CFTR* mutation. This shifts the unmet clinical need towards people with rare CFTR mutations such as nonsense mutations, of which G542X and W1282X are most prevalent. CFTR function measurements in patient-derived cell-based assays played a critical role in preclinical drug development for CF and may play an important role to identify new drugs for people with rare *CFTR* mutations.

Methods

Here, we miniaturised the previously described forskolin-induced swelling (FIS) assay in intestinal organoids from a 96-well to a 384-well plate screening format. Using this novel assay, we tested CFTR increasing potential of a 1400-compound Food and Drug Administration (FDA)-approved drug library in organoids from donors with W1282X/W1282X CFTR nonsense mutations.

Results

The 384-well FIS assay demonstrated uniformity and robustness based on coefficient of variation and Z'-factor calculations. In the primary screen, CFTR induction was limited overall, yet interestingly, the top five compound combinations that increased CFTR function all contained at least one statin. In the secondary screen, we indeed verified that four out of the five statins (mevastatin, lovastatin, simvastatin and fluvastatin) increased CFTR function when combined with CFTR modulators. Statin-induced CFTR rescue was concentration-dependent and W1282X-specific.

Conclusions

Future studies should focus on elucidating genotype specificity and mode-of-action of statins in more detail. This study exemplifies proof of principle of large-scale compound screening in a functional assay using patient-derived organoids.

Introduction

Cystic fibrosis (CF) is a rare, monogenic disease that is caused by mutations in the cystic fibrosis transmembrane conductance regulator (*CFTR*) gene. Mutations in *CFTR* lead to loss of chloride secretion and deficient fluid transport across tissue epithelium. Subsequently, thick and sticky mucus secretions are produced resulting in chronic bacterial infections, progressive loss of pulmonary function and multiorgan failure [1]. More than 1700 distinct mutations have been characterised, of which 400 are estimated to be disease-causing [2]. The F508del mutation is mainly prevalent, occurring on approximately one allele in 85% of the CF patients. For those patients, increasingly effective treatments called CFTR modulators have been developed in the last decade aiding in proper CFTR protein folding and membrane potentiation [3]. Recently a potent combination of the three CFTR modulators VX-445, VX-661 and VX-770 has been approved by the Food and Drug Administration (FDA) and European Medicines Agency (EMA). However, an urgent need for effective restoration of CFTR function persists for the remaining CF patients that cannot benefit from CFTR modulation.

Approximately 10% of the worldwide CF population carry premature termination codon (PTC) mutations, resulting in production of truncated CFTR protein. Previous preclinical research identified compounds with readthrough (RT) activity that introduce an amino acid at the PTC site and thereby results in full-length protein production [4, 5]. Clinical efficacy of RT approaches is however limited, as demonstrated by for example clinical studies with RT agent Ataluren/PTC-124 [6]. A novel recently developed RT agent, ELX-02 (NB124; Eloxx Pharmaceuticals, Watertown, MA, USA), resulted in production of full-length CFTR protein and restoration of CFTR function in G542X/G542X intestinal organoids [7]. However, in a study characterizing the effect of ELX-02 in a larger set of patient-derived organoids, ELX-02 as single agent resulted in only limited restoration of CFTR function [8]. Altogether, this underlines the need for continuing the search for novel CFTR modulating molecular entities for people with *CFTR* PTC mutations.

Drug development in the context of rare diseases where the numbers of patients are low is challenging. For these patient populations, repurposing of clinically approved drugs could be beneficial. Drug repurposing is an attractive approach that aims to extend the indication of already marketed drugs [9]. A prerequisite for drug repurposing is that the exploited assay is robust and is associated with clinical features of disease, such as therapeutic response. CFTR function measurements in patient-derived intestinal organoids (PDIOs) are associated with clinical features of CF and may enable drug repurposing in a personalised setting. We previously developed a PDIO-based assay for CF based on forskolin-induced swelling (FIS). Forskolin induces fluid secretion into the organoid lumen resulting in CFTR-dependent swelling [10, 11]. CFTR function measurements in PDIOs are associated with 1) disease severity indicators of CF, 2) long-term disease progression and 3) therapeutic response, enabling preclinical drug efficacy and mode-of-action studies [12, 13]. As such, the FIS assay is well suited for identifying and prioritising drugs that influence CFTR function. However, the 96-well format of the assay limits its use when higher throughput screening is required.

Here, we miniaturized the 96-well FIS assay towards a 384-well plate format enabling drug screening in PDIOs at higher throughput. Important factors when validating assay quality are within and between experiment variability, drift and edge effects within plates and comparison of the outcomes of experiments performed with the original 96-well set-up to the novel 384-well set-up [14]. As these validations yielded positive results, Z'-factors were calculated to ultimately summarize assay performance [15]. The 384-well FIS assay was subsequently used to identify compounds from an FDA-approved, commercially available drug library for their capacity to increase CFTR function. The screen was performed in PDIOs harboring W1282X/W1282X *CFTR*, as W1282X encompasses 18% of all PTC mutations, thereby being the most common PTC mutation in CF patients after G542X (CFTR2

database, 2021) [16]. Additionally, W1282X is one of the PTC sites that is closest to the normal termination codon (NTC). As such, W1282X protein is less severely truncated than in other PTC cases, and exploiting PDIOs with this genotype allows potential identification of hits that can improve organoid swelling through various mode of actions, ranging from nonsense-specific effects to more general CFTR-modulating effects.

In brief, we show proof of principle of a high-throughput screening (HTS) assay using PDIOs in a functional assay. By screening a library of FDA-approved compounds, we pave the way for drug repurposing for people with CF for whom no clinical options are available.

Materials and methods

Collection of primary epithelial cells of CF patients

All experimentation using human tissues described herein was approved by the medical ethical committee at University Medical Center Utrecht (UMCU; TcBio#19-831). Informed consent for intestinal tissue collection, generation, storage and use of the organoids was obtained from all participating patients. Biobanked intestinal organoids are stored and catalogued (https://huborganoids.nl/) at the foundation Hubrecht Organoid Technology (http://hub4organoids.eu) and can be requested at info@huborganoids.nl.

Human intestinal organoid culture

Human intestinal organoid culture was executed as described by Vonk *et al*. [11].

Compounds

The FDA library, purchased from Selleck Chemicals GmbH Europe (Z178323-100uL-L1300), was stored at -80°C. All other compounds described in this study were purchased at SelleckChem and dissolved in DMSO at a 20 mM concentration.

384-well FIS assay validation

Differences between the 96-well FIS assay as previously described by Vonk *et al*. [11] and the 384-well FIS assay described in this study are summarised in **Table 1** in the Results section. To characterise FIS in a 384-well format, a quality replicate experiment was performed. Three biological replicate experiments were performed on different days with organoids of different passages, with three technical replicates per condition. The F508del/S1251N organoids were submerged in 8 µL complete culture medium, the F508del/F508del organoids in 8 µL complete culture medium supplemented with 3 µM VX-809. 24 h later, FIS measurements were assessed in the presence of VX-770 (3 µM) and low (0.008 µM) and high (5 µM) forskolin (forskolin) concentrations, resulting in minimum (min) signal values and maximum (max) signal values. Organoid swelling was monitored for 60 min using a Zeiss LSM 710 confocal microscope. Total organoid surface area per well was quantified based on calcein green staining using Zen Blue Software and area under the curve over time was calculated as described by Vonk *et al*. [11]. CV values were calculated according to the following formula: % CV=(sd of means)/(mean of means)×100.

Min and max swelling enabled Z′-factor calculation of each 384-well plate according to the following formula: Z′-factor=1 - (3×(σp + σn)/(µp - µn)), where σp is the standard deviation of the max signal wells (n=128 per plate, +CFTR modulator(s) and 5 µM forskolin), σn is the standard deviation of the min signal wells (n=128 per plate, +CFTR modulator(s) and 0.008 µM forskolin), µp is the mean of the max signal wells and µn is the mean of the min signal wells.

Toxicity screen using 384-well plates

Organoids were plated into 384-well plates and were incubated for 24 h with 8 µL complete culture medium supplemented with a single FDA compound per well at a final concentration of 3 µM.1443 compounds were tested in total, divided over five 384-well plates, on three different PDIO lines (2× F508del/S1251N organoids, 1× F508del/F508del organoids). Bright field images were taken per well, and organoid viability was scored in a binary way (live/apoptotic) by three blinded investigators, based on comparison with positive control PDIOs treated with puromycin, which results in clear phenotypical differences such as cell blebbing. To assess cellular toxicity in a quantitative way, organoids were stimulated with calcein green (7 µM) for 30 min and propidium iodide (0.1 mg·mL-1) for 10 min prior to confocal imaging. Total organoid area per well was determined based on total calcein green staining (Zeiss, excitation at 488 nM) and amount of dead cells per well was determined by total area of PI staining (Zeiss, excitation at 564 nM) using Zen Image analysis software module (Zeiss, Oberkochen, Germany). The ratio of total area calcein green and total area PI (=T - score) was calculated to correct for varying number of organoids between wells. To further correct for the varying organoid sizes among plates the Z-score was calculated between the compound-treated organoids and control DMSO-treated organoids per plate. The Z-score was determined according to the following formula: Z-score = (x - µ)/σ, where x is the calcein/PI ratio of each single FDA compound, µ is the mean calcein/PI ratio of 16 control wells on each plate and σ is the standard deviation of the calcein/PI ratio of the same 16 control wells on each plate. Z-scores of the single FDA compounds were compared to Z-scores of wells treated (n=71) with a toxic concentration of puromycin (24 h, 3 mg·mL-1). Z-scores that were below Q1 - (3×IQR) of all the DMSO-treated wells (Z-score= -2.5) or Z-scores that were above Q3 + (3×IQR) of all puromycin-treated wells (Z-score = 14.8) were excluded. One biological replicate experiment was performed, with one technical replicate per condition.

FDA-screen using 384-well plates

Four W1282X/W1282X organoid lines were plated into 384-well plates and were incubated for 24 h with 8 µL complete culture medium supplemented with two FDA compounds per well (1400 compounds in total, divided over two 384-well plates) as well as VX-809, all tested at 3 µM. The day after plating, FIS measurements were assessed in the presence of VX-770 (3 µM) and 5 µM forskolin. No FDA compounds were added to eight wells per plate as negative control (= min signal), and F508del/S1251N organoids were added to eight wells per plate and treated with VX-770 to serve as positive control (= max signal). Three biological replicate experiments were performed on different days with organoids of different

passages, with one technical replicate per condition. Organoid swelling was monitored as previously described for 180 min using a Zeiss LSM 710 confocal microscope. Additionally, bright field images were taken per well, and organoid morphology was scored in a binary way (no swelling/swelling) by three blinded investigators.

Conventional 96-well format FIS assay

96-well FIS assays were executed as previously described by Vonk *et al*. [11]. FIS of F508del/F508del and F508del/S1251N organoids with or without CFTR modulator(s) and increasing concentration of forskolin performed in 96-well plates was compared to FIS under similar conditions performed in 384-well plates. F508del/F508del organoids were treated with VX-809 (3 μM) for 24 h prior to FIS assays. VX-770 (3 μM) was added simultaneously with forskolin for 1 h. Z′-factors were calculated based on the minimal swelling signals induced with 0.008 or 0.02 μM forskolin + CFTR modulators and the maximum swelling signals induced with 5 μM forskolin + CFTR modulators. For the statin experiments in W1282X/W1282X, F508del/F508del and R334W/R334W donors, compounds were added 24 h prior to FIS measurements with different combinations of CFTR correctors (3 μM). Before FIS measurements, VX-770 (3 μM) and forskolin (5 μM) were added and organoid swelling was monitored during 180 min. Three biological replicate experiments were performed on different days with organoids of different passages, with three technical replicates per condition.

qPCR

PDIOs were treated with statins (3 μM) or nonsense-mediated decay (NMD) inhibitor SMG1i (0.3 μM) during 24 h prior to RNA isolation using a Qiagen RNA isolation kit (Qiagen, Valencia, CA, USA), according to the manufacturer's protocol. The RNA yield was measured by a NanoDrop spectrophotometer (ThermoFisher), and extracted mRNA was used for cDNA synthesis using the iScript cDNA Synthesis Kit (Bio-Rad, Hercules, CA, USA) according to the manufacturer's protocol. A final cDNA concentration of 1000 ng·μL-1 was subjected to a two-step quantitative real-time PCR (qPCR) SYBR green reaction (CFX Connect Real time PCR, CFX-384 Real-time PCR, Bio-Rad) in a total assay volume of 10 μL. Primer sequences for GAPDH, YWHAZ, CFTR, PIAS1 and STAT1 are given in **Table 3**. Expression levels of investigated genes were normalised against mRNA levels of housekeeping genes GAPDH and YWHAZ and thereafter to untreated control samples (ΔΔCT method). Melt peaks were analysed to confirm amplification of a single project. Two biological replicate experiments were performed on different days with organoids of different passages, with three technical replicates per condition.

Table 1. Adaptations in forskolin-induced swelling (FIS) protocol of original 96-well format to allow a 384-well format.

	96-wells format, as described by [11]	384-wells format
1	Plates are prewarmed at 37°C prior to organoid-	Plates are precooled at -20°C, and kept on ice during organoid-matrigel
2	4 µl 50% matrigel organoid suspension is added per well as drops	10 µl 25% matrigel organoid suspension is added per well with an automatic multichannel, to cover the whole surface
3	-	Plate is spun down in a centrifuge to ensure matrigel coverage of the
4	After 10 minutes at 37°C , 50 µl medium per well is	After 10 minutes at 37°C, 8 µl medium per well is added
5	X/Y/Z location is manually set for each well	X/Y/Z is automatically set based on plate lay-out and autofocus of 12

Statistics

Statistical analysis was performed using GraphPad Prism 8.0 (GraphPad Software, La Jolla, CA, USA). Data on the graphs are presented as mean±sem, as experiments were performed in triplicate with three technical replicates per biological replicate. One-way analysis of variance (ANOVA) analyses with Dunnet's post hoc test were performed to analyse the differences in the secondary W1282X/W1282X screen, where a separate test was performed for each compound combination group to compare compound A/compound B or compound combination AB to the Trikafta background. Differences were considered significant at $p<0.05$. Statistical analysis of the primary W1282X/W1282X screen was performed in RStudio, and averages were calculated of the replicate experiments of the four donors combined for all compound combinations. To analyse whether these means increased FIS in comparison to the average of the plate, one-way t-tests were performed, and p-values were adjusted for multiple testing using the Benjamin–Hochberg FDR method.

Results

The 384-well FIS assay is reproducible, spatially uniform and has a comparable dynamic range to the 96-well FIS assay

First, we adapted several practical aspects of the 96-well FIS format which was previously described by Vonk *et al* to allow a higher throughput working method **(Table 1)** [11]. In brief, 384-well plates were precooled prior to organoid addition, a higher volume of a lower matrigel-percentage was added to each well to cover the whole well surface and during image acquisition X/Y/Z locations were based on autofocus.

Using these adjustments, we verified the quality and reliability of the 384-well FIS assay. In **Figure 1A** we summarise the advised steps of assay quality validation when miniaturising a cell-based assay [14]. To demonstrate FIS assay reproducibility, we performed replicate experiments in two organoid lines with different genotypes. FIS was assessed in F508del/S1251N organoids treated with CFTR potentiator VX-770 and in F508del/F508del organoids treated with CFTR potentiator VX-770 and CFTR corrector VX-809. Minimal (min) and maximal (max) signal of swelling was induced with 0.008 and 5 μM forskolin, respectively. The mean as well as the spread of the min and max signals were comparable between the replicate experiments both for F508del/S1251N organoids **(Figure 1B)** and F508del/F508del

organoids **(Figure 1C).** In order to further characterise precision and repeatability within and between these replicate experiments, coefficient of variation (CV) was calculated [17]. For the max signal, the mean intra-assay CV values were 16% and 13% for the F508del/F508del and F508del/S1251N organoids respectively, and the inter-assay CV values were respectively 4% and 8%. CV values should not exceed 20% and CV values under 10% are considered excellent, underlining the reproducibility of the 384-well FIS assay [14].

Next, edge effect for both outer rows and columns as well as overall horizontal or vertical drift on the plates was characterised **(Supplemental Figure S1).** As R2 values reach 0 in both donors for both the row and the column-oriented data, no horizontal or vertical drift across the plates is present. Additionally, the max area under the curve (AUC) values of the outer rows and columns (indicated with red dots) do not differ significantly from the rest of the data in both donors.

We next compared the signal amplitude of the 384-well FIS assay with the conventional 96-well assay. F508del/F508del and F508del/S1251N organoids with or without CFTR modulator(s) were stimulated with an increasing concentration of forskolin **(Figure 1D).** This allows characterisation of "medium" swelling levels in the FIS assay, which is crucial when characterising the capacity of the assay to capture hit compounds during a screen [14]. Medium signal needs to lie between the negative and positive controls, and we show that indeed at 0.128 and at 0.8 µM forskolin the mid-range of the assay is covered.

Table 2: Hits based on mean AUC over all donors (>500)

	Compound 1	Classification Compound 1	Compound 2	Classification Compound 2	Mean AUC	Based on visual analysis
1	**Pitavastatin**	HMG Co-A reductase	Alibendol	Choleretic	862.9	26
2	**Simvastatin**	HMG Co-A reductase	Tamoxifen Citrate	Estrogen antagonist	712.1	9
3	Fenspiride HCl	PDE4 inhibitor	**Mevastatin**	HMG Co-A reductase	671.8	25
4	Guaifenesin	Expectorant	**Fluvastatin Sodium**	HMG Co-A reductase	658.3	24
5	Valsartan	Angiotensin II antagonist	**Lovastatin**	HMG Co-A reductase	599.2	33
6	Carvedilol	B2 antagonist	Formoterol	B2 agonist	574.7	1
7	CO-1686	TRK	Palbociclib	CDK4/6 inhibitor	569.8	2
8	Tivantinib	c-Met inhibitor	Darifenacin HBr	Muscarinic antagonist	566.2	1
9	Sofosbuvir	HCV polymerase inhibitor	Sertaconazole nitrate	Anti-fungal	536.6	0
10	Deoxycholic acid	Cytolytic agent	Riociguat	GC stimulator	532.8	0
11	Voxtalisib	mTor inhibitor	L-Glutamine	Amino acid	527.6	3
12	Butoconazole	Inflammation blocker	Ketotifen Fumarate	Antihistamin	518.7	0
13	LEE011	CDK4/6 inhibitor	Heparin sodium	Glycosaminoglycan	510.5	0
14	Albendazole	Antlemintic	Diclazuril	Coccidiostaticum	507.7	3
15	Levobupivacaine	Neuronal NA channel inhibitor	Chlorquinaldol	Antiseptic	504.8	0
16	Nilotinib	BCR-Abl inhibitor	Dienogest	Progesteron	503.5	0
17	Dovitinib	RTK inhibitor	Letrozole	Aromatase inhibitor	500.5	0

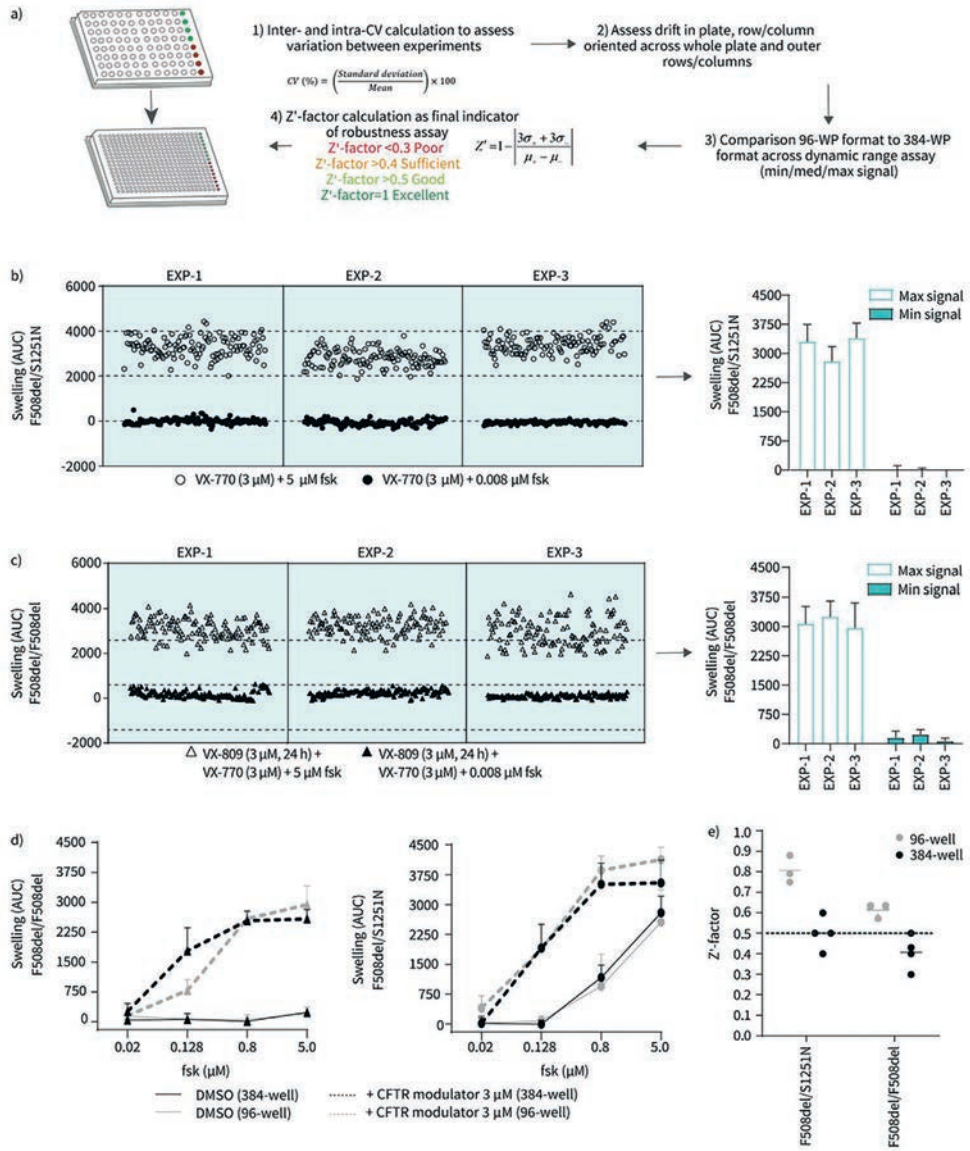

Figure 1. The 384-well forskolin-induced swelling (FIS) assay is reproducible, spatially uniform and has a similar dynamic range to the 96-well FIS-assay.
(A) Summary of optimisation steps for assay development, specifically for miniaturising a cell-based assay from 96-well format to 384-well format. **(B)** and **(C)** Replicate experiments of three 384-well plates with respectively F508del/S1251N and F508del/F508del patient-derived intestinal organoids (PDIOs), performed on three different culturing days. VX-770 (3 µM) and forskolin (0.008 µM) were added to 128 wells of each 384-well plate to induce minimal swelling (=min signal wells). Maximum swelling was achieved by the addition of 5 µM forskolin and VX-770 (3 µM) to another 128 wells (=max signal wells). The mean±sd swelling of all min and max signal wells of each plate depicted in b and c are summarised in the bar graphs. **(D)** Swelling of F508del/F508del PDIOs treated with VX-770/VX-809 and

F508del/S1251N PDIOs treated with VX-770 and in presence of an increasing concentration of forskolin, measured in 96-well plates and 384-well plates (data points represent mean±sd, n=3 for the 96-well experiments, n=1 for the 384-well experiments). **(E)** Z'-factors calculated for each replicate experiment plate included in b, c and d. CV: coefficient of variation; WP: well plate; fsk: forskolin; AUC: area under the curve.

Differences between the 96-well and 384-well assay are negligible, except for 0.128 µM forskolin in the F508del/F508del organoids. Lastly, Z'-factors were calculated as an indicator of assay quality. The Z'-factor is a parameter based on positive and negative control that ranges between 0 and 1, with 1 indicating a perfect assay and Z'-factors larger than 0.4 considered acceptable [14]. Whilst mean Z'-factors from the 96-well format experiments were higher compared to those of the 384-well format experiments **(Figure 1E)**, the mean Z'-factor of the F508del/S1251N organoids was 0.4 and the mean Z'-factor of the F508del/F508del organoids was 0.5, indicating adequate assay robustness.

43 out-of 1443 FDA-approved compounds induce toxicity in PDIOs

Prior to assessing the effect of compounds on CFTR function restoration, we assessed potential toxicity of the 1443 FDA-approved compounds. Organoid viability was determined by a dual live cell staining approach in which calcein was used to stain metabolically active cells and propidium iodide (PI) to visualise dead cells, a toxicity assay that has previously been performed on intestinal organoids [18, 19]. The ratio of total calcein green area and total PI area was calculated to correct for varying number of organoids between wells, after which values were normalised to Z-scores facilitating comparisons between plates **(Figure 2A)**. Z-scores beyond 2, indicating toxicity, were found for 41 compounds **(Figure 2B)**. Additionally, organoid morphology was verified by three blinded observers. This led to a further exclusion of two additional compounds. The majority of the toxic compounds (81%), listed in supplementary table S1, are described as anti-cancer drugs. All 43 compounds were excluded from further screening.

FDA-approved drugs increase FIS in homozygous W1282X/W1282X organoid lines

We next set out to identify FIS-increasing compounds. A schematic of the workflow is shown in figure 3a. Four organoid lines homozygous for W1282X-CFTR were pretreated with VX-809 and VX-770 to increase baseline function of W1282X/W1282X, facilitating hit detection. Two FDA-approved compounds were combined in each well. F508del/S1251N organoids treated with VX-770 were used as positive control on each plate, allowing CV value and Z'-factor calculation for quality control purposes. Inter- and intra-assay CV values were 17% and 14% respectively, averaged over the four donors, highlighting robustness of the assay. For each donor two 384-well plates were measured in triplicate, resulting in six Z'-factors for donor 1 and five Z'-factors for donors 2–4 due to technical errors. Mean Z'-factors for all plates approximated 0.4, ranging between 0.3 and 0.5 **(Figure 3B).**

17 compound combinations resulted in a mean increase of at least 500 AUC **(Figure 3C).** The top five compound combinations reaching the highest AUC values were verified by visual analysis **(Figure 3D** and **Table 2).** Subsequently, p-values were calculated for the

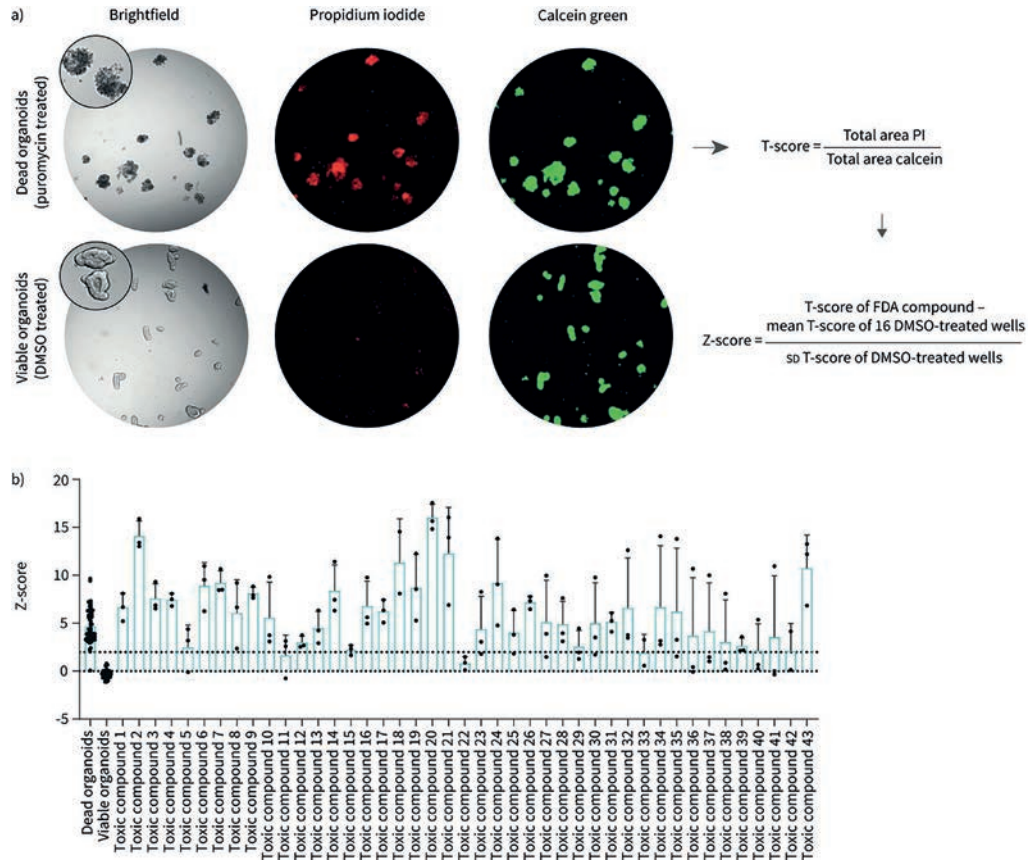

Figure 2. 43 out of 1443 Food and Drug Administration (FDA)-approved compounds induce toxicity in patient-derived intestinal organoids (PDIOs).
(A) Schematic of toxicity assessment pipeline. The ratio of total area calcein green and total area propidium iodide (PI) (T-score) was calculated to correct for varying number of organoid structures between wells. To further normalise to the negative control organoids, the Z-score was calculated between the compound-treated PDIOs and control (DMSO-treated) PDIOs. **(B)** Z-scores of the compounds labelled as toxic based on brightfield image scoring, compared to Z-scores of dead PDIOs (treated for 24 h with puromycin 3 mg·mL–1) and viable PDIOs not exposed to compounds. Bars represent mean±sd, n=3 for toxic compounds, n=71 for dead and healthy controls.

difference between the mean of each plate and the FDA-compound treated wells. Prior to multiple testing correction of the p-values by the Benjamin–Hochberg false discovery rate (FDR) method, 40 compound combinations resulted in a significant increase ($p<0.05$) in AUC compared to the mean of the plate **(Supplemental Table S2)**. Included in these 40 compound combinations were the top five hits based on AUC values and nine out of 12 of the rest of the top 17. However, after FDR correction, only the positive controls remained significantly different. Still, interestingly one of each of the compounds of the top five compound combinations is a statin, suggesting a statin-induced effect on organoid swelling. Altogether the results provided sufficient rationale to confirm whether these statins have indeed potential to increase CFTR function.

To assess whether the statins of the compound combinations were responsible for AUC increase, the top five different compound combinations were repurchased from an independent supplier and tested on W1282X/W1282X donors 1 and 3. Compounds were tested in combination with VX-445/VX-661/VX-770 to further maximise the window of opportunity to detect effects in comparison to the primary screen **(Figure 4B).** The data of both donors combined confirmed that simvastatin, mevastatin, fluvastatin and lovastatin further induced organoid swelling, yet not significantly in both donors. Alibendol additionally resulted in a significant increase in AUC. In the absence of CFTR modulator treatment no simvastatin- or mevastatin-induced CFTR response was observed in both W1282X/W1282X donors **(Figure 4B).** AUC values, however, do not reach the values of positive control-treated PDIOs which were treated with RT agent ELX-02, NMD inhibitor SMG1i and Trikafta. By assessing swelling induction with a concentration range of simvastatin and mevastatin, we observed a concentration-dependent increase in AUC levels **(Figure 4C).** Concentrations above 3 μM resulted in decreased AUC values due to compound-induced toxicity (data not shown). Using 3 μM as maximal value, EC50s were respectively 1.35 and 2.96 μM for simvastatin and mevastatin, whereas a higher maximum swelling was induced with mevastatin than with simvastatin. To evaluate whether the statins increased FIS of specifically W1282X-CFTR, we assessed statin-induced swelling in organoid cultures homozygously expressing F508del/F508del and R334W/R334W in combination with VX-809/VX-770 and VX-770, respectively. For these genotypes, we did not observe a further increase of FIS by mevastatin and simvastatin **(Figure 4D).**

Statins have been described to interact with many pathways additional to cholesterol synthesis, including STAT1/3, p38, MAPK and Akt phosphorylation. Firstly, we investigated whether 6-fluoromevalonate (6F), a compound that inhibits cholesterol synthesis further down the synthesis pathway than statins do, also results in rescue of CFTR function. However, 6F did not result in further rescue of CFTR in the W1282/W1282X PDIOs, indicating that the observed CFTR rescue upon statin treatment is not cholesterol mediated **(Supplemental Figure S2A).** We subsequently investigated whether statins inhibit NMD, the process in which PTC harbouring mRNAs are recognised and degraded. As statins were combined with CFTR modulators, NMD inhibition could result in a pool of truncated CFTR protein that could be partially rescued by CFTR modulators. Additional to CFTR

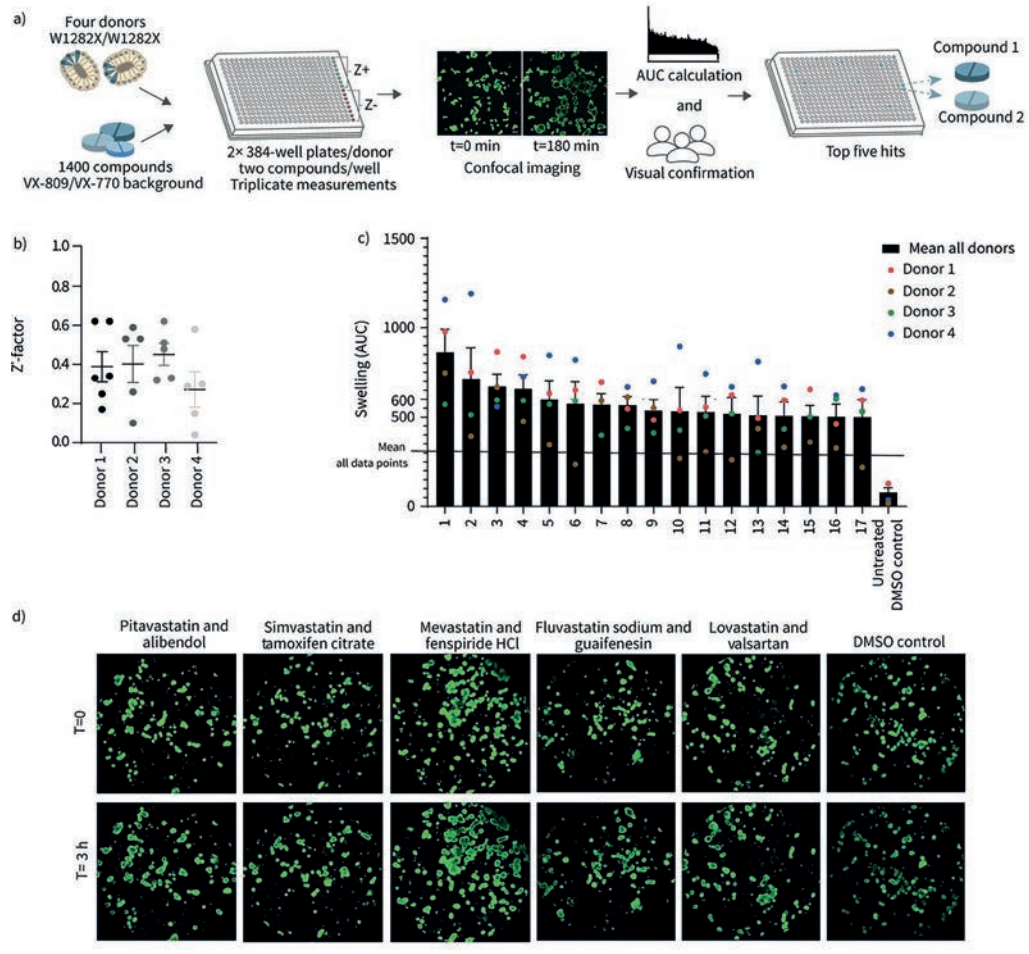

Figure 3. Food and Drug Administration (FDA)-approved drugs increase forskolin-induced swelling (FIS) in homozygous W1282X/W1282X patient-derived intestinal organoids (PDIOs). **(A)** Schematic of workflow of FDA-approved drug library testing on W1282X/W1282X PDIOs. **(B)** Z'-factor for each 384-well plate for the four PDIOs. F508del/S1251N PDIOs treated with VX-770 served as positive control. **(C)** Area under the curve (AUC) values of the top 17 compound combinations, means of the triplicate experiments of all PDIOs are shown with the different PDIOs indicated by the four different coloured dots. **(D)** Pictures of the PDIO line 1, of the primary screen, for the top five compound combinations and the DMSO control (t=0 h and t=3 h).

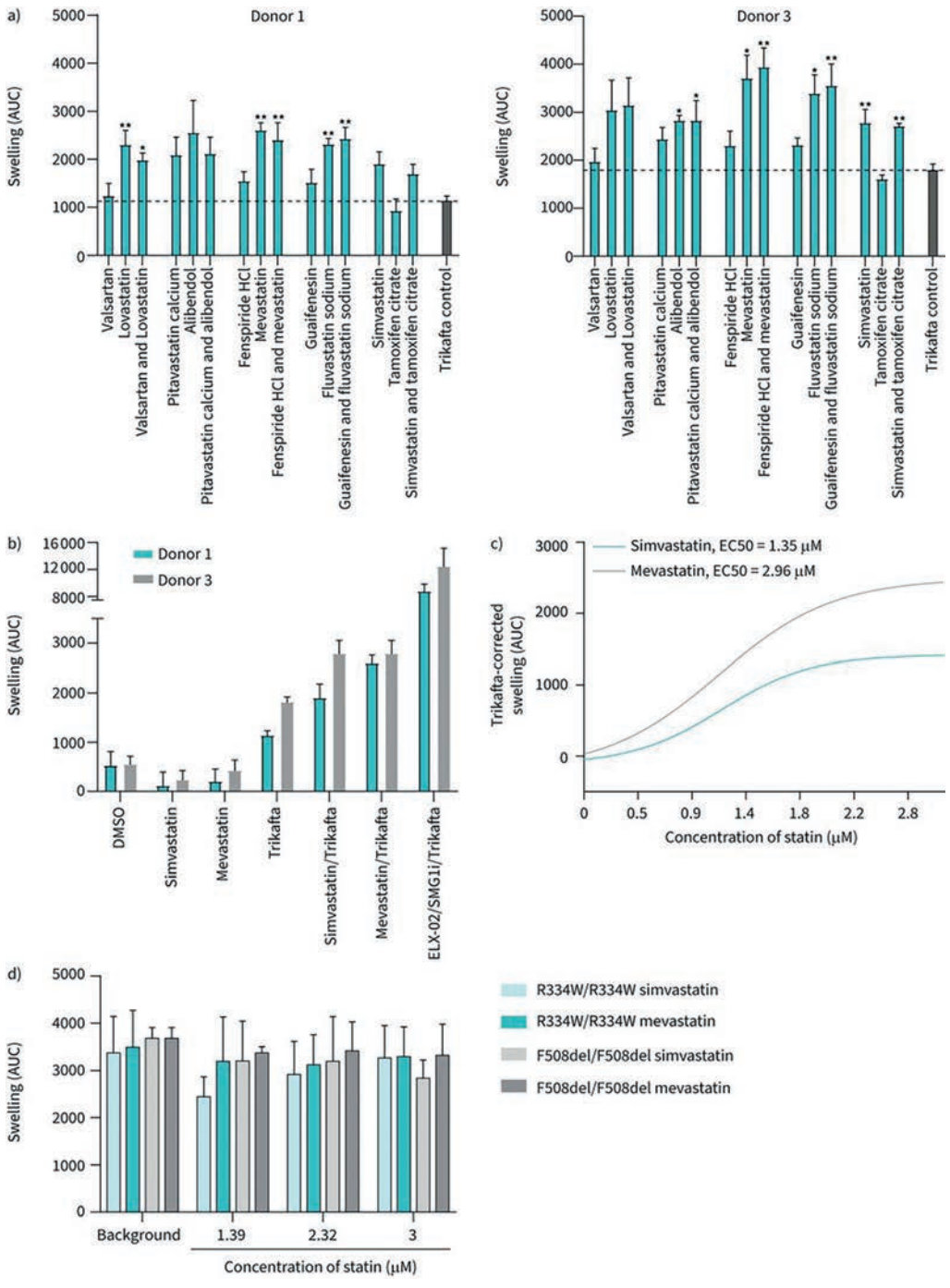

Figure 4. Statins increase forskolin-induced swelling (FIS) in homozygous W1282X/W1282X patient-derived intestinal organoids (PDIOs) in a concentration-dependent manner.
(A) Area under the curve (AUC) values of the secondary FIS screen for two W1282X/W1282X PDIOs, in which compounds of the primary screen top five were tested separately and as original combination. Trikafta (CFTR modulators VX-445/VX-661/VX-770) was used as background. **(B)** AUC values for two W1282X/W1282X PDIOs upon treatment with the statins and CFTR modulators separately (all at 3 µM), as well as the combination and a positive control consisting of 80 µM ELX-02, 0.3 µM SMG1i and 3 µM VX-445/VX-661/VX-770 (Trikafta). Means are shown of three biological replicate experiments with three technical replicates per condition; sem is indicated by error bars. **(C)** Curve-fitting line for AUC values of W1282X/W1282X PDIO line 1 upon a mevastatin and simvastatin concentration gradient, corrected for Trikafta-induced baseline swelling. **(D)** AUC values for R334W/R334W and F508del/F508del PDIOs upon simvastatin and mevastatin treatment, with respectively VX-770 and VX-770/VX-809 as background (all at 3 µM). Means are shown of three biological replicate experiments with three technical replicates per condition; sem is indicated by error bars.

mRNA levels, we investigated PIAS1 and STAT1 mRNA levels, as reduction of PIAS1 upon statin treatment has been linked to normalised STAT1 activation and CFTR function [20]. However, whilst NMD inhibitor SMG1i indeed resulted in an increase of CFTR mRNA levels, CFTR, PIAS1 and STAT1 mRNA levels did not increase upon statin treatment **(Supplemental Figure S2B).**

Discussion

Whilst potent compounds have been developed for the most common F508del-CFTR mutation, there's a lack of medication for other genotypes and an urgent need to improve therapy for these CF patients. Approximately 10% of the worldwide CF population carry PTC mutations that result in production of truncated CFTR protein with severe loss-of-function. Developing new drugs is a time-consuming and expensive process. In this regard, drug repurposing is an attractive solution providing economical and time-wise benefits. In this study, we developed a 384-well version of the FIS assay, exemplifying the feasibility of large-scale compound screening with a functional read-out using patient-derived organoids.

We adapted several steps compared to the previously described 96-well FIS assay [11]. Importantly, medium replacement steps are not needed in this experimental pipeline, enabling a straightforward working scheme. To ensure successful screening, quality and reliability of the 384-well FIS assay was characterised. We show that replicate experiments yield similar results with low intra- and inter-assay CV values and without outer row- or column-associated effects. Overall, assay performance of the 384-well FIS assay was adequate with Z'-factors reaching 0.4 or higher [14]. Z'-factors were robust in the W1282X/W1282X screen as well; however, the positive control here consisted of F508del/S1251N organoids treated with VX-770 as a more suitable positive control specifically for W1282X/W1282X organoids was not available. Potentially in future studies the recently described RT agent 2,6-diaminopurine (DAP) can be used for this [21] or a combination of compounds that together result in higher levels of CFTR rescue [8]. The gain of throughput did result in lower Z'-factors for 384-well plates than obtained for 96-well plates in the FIS assay. In the future, additional automation such as automated organoid dispensers, drug printers and centrifugal washers

might further reduce technical variability, whereas biological robustness could be improved by incorporating a proper positive control for the PDIO's genotype of interest. Such improvements could aid in increasing the Z'-factor. Yet, so far, mainly small-scale screenings using PDIOs have been performed, e.g. <100 compounds [22, 23]. Although recent work showed the implementation of organoid cultures in 3D matrix in a 384- and 1536-well format for HTS, exploited read-outs such as fluorescence-based viability analyses were relatively simple and exhibited lower Z'-factors [24]. Jiang *et al*. [25] performed high-throughput experiments in the context of CFTR, using induced pluripotent stem cells (IPSCs) differentiated into early-stage lung progenitor cells in a fluorescence-based assay of CFTR channel activity, y*et al*so with a lower Z'-factor (0.34). Berg *et al*. [26] describe a 96-well screening assay using 3D-cultured primary airway cells with a disease-relevant read-out consisting of liquid secretion quantification, yet Z'-factors were not described in this study. The clinical relevance of the exploited FIS assay in our study in combination with the robust Z'-factors in a 384-well plate format, underline the strength of this study.

Whilst toxicity testing was not the main focus in our study, we exploited the 384-well screening pipeline to analyse potential toxicity of the FDA library. Indeed, 43 compounds induced toxicity and were excluded for further characterisation. This approach could be translated to different PDIO systems, for example when comparing compound-induced toxicity in tumour and wild-type organoids derived from the same patient. Notably, we could miss potential efficacies of compounds that act at a nanomolar range that were excluded based on toxic effects observed at a micromolar range testing. However, we expect that compound efficacies are not completely abolished at higher concentrations. As such, we assumed that this risk was acceptable in the context of workload. The effect of the 1400 FDA-approved compounds on CFTR-mediated fluid secretion was assessed in W1282X/W1282X PDIOs. Using a statistical approach, after multiple testing correction, only the positive controls remained significantly different. However, 17 compound combinations resulted in an mean increase of at least 500 AUC. An important remark is that in this work, we push towards highest sensitivity by measurement of swelling at a high forskolin concentration (5 μM)in a 3-h measurement, as we anticipated that such assay conditions were needed to be able to detect the marginal effects that are needed for detection of responses of single drugs in the context of stop codons. Organoid assay conditions that are associated with disease severity indicators are mostly observed at 0.8 μM forskolin in 1 h swell conditions [27], whereas therapeutic responses are mostly analysed at 0.128 μM forskolin and 1 h swell conditions [13, 28]. The amount of rescue we observe under the assay conditions in this study is below levels associated with the studies cited above, and thus are anticipated to have less clinical impact. However, we previously found that disease severity in a clinical setting for patients with F508del/F508del CFTR could be linked to variation in organoid function under conditions where organoids were stimulated with 5 μM forskolin and 3 h stimulation [27]. We therefore cannot rule out that these small changes we observe have no impact on long-term disease progression. The AUC analysis of the FIS experiments, the results based on visual analysis of PDIO swelling and the statistical analysis in which statins merely reached statistical significance, all pointed in the same direction concerning the top five compound combinations. Interestingly, one of each of the compounds of this top five compound combinations was a statin, suggesting a statin-induced effect on organoid swelling. Indeed, in the subsequent confirmation screen four out of five statins significantly increased AUC values as separate compound as well as in the original combination in which the statins were tested. Importantly, in this secondary screen CFTR modulators VX-445/VX-661/VX-770 were used as a background instead of VX-809/VX-770 due to its higher potency to increase CFTR function, thereby further maximising the window of opportunity to detect effects, whilst additionally possessing a more favourable safety profile and a more clinically robust benefit [29].

In order to assess whether the statins increased CFTR function only in W1282X/W1282X organoid cultures, we assessed the effect of simvastatin and mevastatin on R334W/R334W and F508del/F508del organoid cultures, in combination with VX-770 and VX-809/VX-770 respectively. However, here no further increase in CFTR function was observed. This points in the direction that the effect is W1282X/W1282X or PTC specific. Interestingly, a HTS study using Fischer rat thyroid (FRT) cells stably expressing F508del-CFTR with a yellow fluorescent protein flux assay as read-out, did reveal atorvastatin calcium and fluvastatin as hits [30]. In future studies, assessing the effect of statins on a large panel of organoid with different genotypes will be valuable to draw firm conclusions on this.

Additionally, in combination with genotype specificity studies, more research is needed to elucidate the mode-of-action (MoA) of statins with respect to CFTR elevating function. Statins are generally known for their potential to inhibit HMG-CoA reductase, thereby inhibiting the production of cholesterol and isoprenoids [31, 32]. As such their potential to increase CFTR function is in fact contradictory to previous studies. By contributing to the creation and maintenance of the lipid rafts in which CFTR resides, cholesterol has been described to positively impact CFTR levels and function [33]. However, in this study more fundamental techniques were exploited, and results were not verified in primary patient-derived cells. Statins additionally have previously been described to have nanomolar median inhibitory concentration (IC50) as HMG-CoA reductase inhibitors in human cell lines [34]. The fact that we observe IC50 values that are higher could have two potential explanations: 1) the difference in model system and read-out – primary patient-derived cells used in a 3D Matrigel context versus cell background and the 2D systems in which statins' IC50 was previously assessed; or 2) the effect is not mediated via HMG-CoA reductase inhibition but via another MoA. To assess whether the MoA of statins could be linked to their influence on cholesterol synthesis, we investigated the effect of 6F, a compound that also inhibits cholesterol synthesis. As no effect was observed, however, it is unlikely that the effect of the statins can be attributed to their inhibitory effect on cholesterol synthesis. Statins additionally have been described to interfere with PIAS1 and STAT1, which both have been linked to CFTR function [20], and Akt phosphorylation [35], which has recently been linked to NMD inhibition [36]. However, we did not observe differences in mRNA levels of PIAS1/STAT1 and CFTR upon statin treatment, indicating that the statin-mediated CFTR rescue is not achieved by NMD inhibition nor via statin-mediated correction of the STAT1 pathway. More elaborate studies should be performed to understand the exact MoA.

In conclusion, we have miniaturised our FIS assay into a robust 384-well plate high-throughput screen and used it to assess toxicity as well as CFTR increasing potential of an FDA-approved drug library. We found that statins increased CFTR function in CF PDIOs harbouring nonsense mutations. This finding can serve as an important starting point for developing novel treatment regimens for those CF patients that are left behind without a treatment regimen at present. Altogether, the developed pipeline in this study shows the potential of performing high-throughput, functional screenings assays on primary, patient-derived organoids.

Supplemental Information

Supplemental data can be found online, at https://doi.org/10.1183/23120541.00495-2022

Acknowledgements

We would like to thank the people with cystic fibrosis who gave informed consent for generating and testing their individual organoids; all members of the research teams of the Dutch CF clinics that contributed to this work; all colleagues of the HUB Organoid Technology for their help with generating intestinal organoids; and we thank Prof. Rene Eijkemans (Department of Biostatistics and Research Support, Utrecht University) for his valuable statistical advice and help.

Author Contribution Statement

S. Spelier and E. de Poel contributed to the design of the study, the acquisition, verification, analysis and interpretation of the data, and drafted the manuscript. G.N. Ithakisiou, S.W.F. Suen, A.M. Vonk, J.E. Brunsveld, E. Kruisselbrink, D. Muilwijk and M.C. Hagemeijer contributed to the acquisition of study data and revised the manuscript. C.K. van der Ent and J.M. Beekman made substantial contributions to the conception and design of the study, and interpretation of data, and revised the manuscript.

Conflict of interest

C.K. van der Ent reports grants from GSK, Nutricia, TEVA, Gilead, Vertex, ProQR, Proteostasis, Galapagos NV and Eloxx, outside the submitted work; in addition, he has a patent (number 10006904) with royalties paid. J.M. Beekman reports personal fees from Vertex Pharmaceuticals, Proteostasis Therapeutics, Eloxx Pharmaceuticals, Teva Pharmaceutical Industries and Galapagos, outside the submitted work; in addition, he has a patent related to the FIS assay with royalties paid. All other authors have nothing to disclose.

Support statement

This work was funded by grants of the Dutch Cystic Fibrosis Foundation (NCFS) as part of the HIT-CF Program and by ZonMW grant number 91214103. Funding information for this article has been deposited with the Crossref Funder Registry.

Supplementary Table 1. List of 43 compounds excluded for further screening, based on toxicity assay.

Compound number	Compound name	In vivo application
1	ABT-263 (Navitoclax)	Anti-cancer drug
2	YM155 (Sepantronium Bromide)	Anti-cancer drug
3	Bortezomib (PS-341)	Anti-cancer drug
4	Panobinostat (LBH589)	Anti-cancer drug
5	CEP-18770 (Delanzomib)	Anti-cancer drug
6	17-AAG (Tanespimycin)	Anti-cancer drug
7	Ganetespib (STA-9090)	Anti-cancer drug
8	Saracatinib (AZD0530)	Anti-cancer drug
9	Onalespib (AT13387)	Anti-cancer drug
10	Dasatinib (BMS-354825)	Anti-cancer drug
11	Docetaxel (RP56976)	Anti-cancer drug
12	Ispinesib (SB-715992)	Anti-cancer drug
13	Paclitaxel (NSC 125973)	Anti-cancer drug
14	Rigosertib (ON-01910)	Anti-cancer drug
15	Epothilone B (EPO906, Patupilone)	Anti-cancer drug
16	Flavopiridol (Alvocidib)	Anti-cancer drug
17	Topotecan (NSC609699) HCl	Anti-cancer drug
18	Epirubicin (IMI 28) HCl	Anti-cancer drug
19	Tamoxifen (ICI 46474)	Anti-cancer drug
20	Vincristine (NSC-67574)	Anti-cancer drug
21	Rufinamide	Anti-epileptic/seizure drugs
22	Volasertib (BI 6727)	Anti-cancer drug
23	Neratinib (HKI-272)	Anti-cancer drug / Inhibits Xenograph growth
24	Ixazomib (MLN2238)	Anti-cancer drug
25	Crystal Violet	triarylmethane dye
26	Omipalisib (GSK2126458, GSK458)	Anti-cancer drug
27	Carfilzomib (PR-171)	Anti-cancer drug
28	Daunorubicin (RP 13057) HCl	Anti-cancer drug
29	Cabazitaxel (XRP6258)	Anti-cancer drug
30	Bisacodyl	Laxative drug
31	Dinaciclib (SCH727965)	Anti-cancer drug
32	Vinorelbine Tartrate	Anti-cancer drug
33	Digoxin	Atrial fibrillation and heart failure drug
34	Puromycin (CL13900) 2HCl	Aminonucleoside antibiotic
35	Vinblastine (NSC-49842) sulfate	Anti-cancer drug
36	Birinapant (TL32711)	Anti-cancer drug
37	Dasatinib Monohydrate	Anti-cancer drug
38	Docetaxel Trihydrate	Anti-cancer drug
39	Riociguat (BAY 63-2521)	Pulmonary hypertension drug
40	Mebendazole	Anthelmintic drug
41	Gemcitabine (LY-188011) HCl	Anti-cancer drug
42	Vancomycin HCl	Antibacterial agent
43	Fosbretabulin (Combretastatin A4 Phosphate (CA4P)) Disodium	Anti-cancer drug

Supplementary Table 2. List of p-values and adjusted p-valued (Benjamin-Hochberg method) of top 40 compound combinations in the W1282X/W1282X screen, based on a one-sided T-test where the average AUC value per condition over the 4 donors was compared to the average of the plate.

Compound_ID	p	p_adjusted	Compound 1	Compound 2
Pos. Control plate A	0	0		
Pos. Control plate B	0	0		
1	0.000341	0.084206	Fenspiride HCl (S4090)	Mevastatin (S4223)
2	0.000683	0.126271	Pitavastatin Calcium (S1759)	Alibendol (S1928)
3	0.002352	0.348096	Simvastatin	Tamoxifen Citrate (S1972)
4	0.003027	0.365673	CO-1686 (AVL-301)	Palbociclib (PD-0332991) HCl
5	0.003459	0.365673	Valsartan (S1894)	Lovastatin (S2061)
6	0.008797	0.758291	Guaifenesin (S1740)	Fluvastatin Sodium (S1909)
7	0.010058	0.758291	Nilotinib (AMN-107)	Dienogest
8	0.010525	0.758291	Carvedilol	Formoterol Hemifumarate
9	0.016278	0.758291	Butoconazole nitrate	Ketotifen Fumarate
10	0.017213	0.758291	Droperidol	Fluorometholone Acetate
11	0.017866	0.758291	Sotrastaurin	Ethynodiol diacetate
12	0.018242	0.758291	Linezolid	Acetylcysteine
13	0.020269	0.758291	S- (+)-Rolipram (S2127)	Naphazoline HCl (S2519)
14	0.022949	0.758291	Varlitinib	Entacapone
15	0.0233	0.758291	Cabazitaxel	Pergolide mesylate
16	0.025466	0.758291	Pravastatin sodium	Mirabegron
17	0.025704	0.758291	Voxtalisib (XL765, SAR245409)	L-Glutamine
18	0.026123	0.758291	Levobupivacaine HCl	Chlorquinaldol
19	0.026898	0.758291	Idasanutlin (RG-7388)	Lypressin Acetate
20	0.031113	0.758291	Cobicistat (GS-9350)	Eletriptan HBr
21	0.031239	0.758291	Triciribine	Cilostazol
22	0.03282	0.758291	Rosuvastatin Calcium	Secnidazole
23	0.033328	0.758291	Foretinib (GSK1363089)	Cilnidipine
24	0.033605	0.758291	TH-302	Estradiol valerate
25	0.035348	0.758291	Cilengitide	Empty
26	0.035555	0.758291	Sofosbuvir (PSI-7977, GS-7977)	Sertaconazole nitrate
27	0.037549	0.758291	Probucol	Spectinomycin HCl
28	0.038516	0.758291	Marbofloxacin	Monobenzone
29	0.041068	0.758291	Griseofulvin	Florfenicol
30	0.041323	0.758291	Lomerizine HCl	Amoxapine
31	0.041537	0.758291	VX-680 (Tozasertib, MK-0457)	Celecoxib
32	0.04302	0.758291	Edoxaban	Nafarelin Acetate
33	0.044306	0.758291	Bendamustine HCl	Omeprazole
34	0.046228	0.758291	Licofelone	Sulfadoxine
35	0.046428	0.758291	Albendazole Oxide	Diclazuril
36	0.047365	0.758291	KPT-330	Oxytocin (Syntocinon)
37	0.048372	0.758291	Retapamulin	Tiratricol
38	0.049341	0.758291	Sorafenib Tosylate	Rufinamide

References

1. Ehre C, Ridley C, Thornton DJ. Cystic fibrosis: an inherited disease affecting mucin-producing organs. Int J Biochem Cell Biol 2014; 52: 136–145.
2. Sosnay PR, Siklosi KR, Van Goor F, *et al*. Defining the disease liability of variants in the cystic fibrosis transmembrane conductance regulator gene. Nat Genet 2013; 45: 1160–1167.
3. Lopes-Pacheco M, Pedemonte N, Veit G. Discovery of CFTR modulators for the treatment of cystic fibrosis. Expert Opin Drug Discov 2021; 16: 897–913.
4. Nudelman I, Rebibo-Sabbah A, Cherniavsky M, *et al*. Development of novel aminoglycoside (NB54) with reduced toxicity and enhanced suppression of disease-causing premature stop mutations. J Med Chem 2009 52: 2836–2845.
5. Welch EM, Barton ER, Zhuo J, *et al*. PTC124 targets genetic disorders caused by nonsense mutations. Nature 2007; 447: 87–91.
6. Kerem E, Konstan MW, De Boeck K, *et al*. Ataluren for the treatment of nonsense-mutation cystic fibrosis: a randomised, double-blind, placebo-controlled phase 3 trial. Lancet Respir Med 2014; 2: 539–547.
7. Crawford DK, Mullenders J, Pott J, *et al*. Targeting G542X CFTR nonsense alleles with ELX-02 restores CFTR function in human-derived intestinal organoids. J Cyst Fibros 2021; 20: 436–442.
8. de Poel E, Spelier S, Suen SWF, *et al*. Functional restoration of CFTR nonsense mutations in intestinal organoids. J Cyst Fibros 2022; 21: 246–253.
9. Ashburn TT, Thor KB. Drug repositioning: identifying and developing new uses for existing drugs. Nat Rev Drug Discov 2004; 3: 673–683.
10. Dekkers JF, Wiegerinck CL, De Jonge HR, *et al*. A functional CFTR assay using primary cystic fibrosis intestinal organoids. Nat Med 2013; 19: 939–945.
11. Vonk AM, van Mourik P, Ramalho AS, *et al*. Protocol for application, standardization and validation of the forskolin-induced swelling assay in cystic fibrosis human colon organoids. STAR Protoc 2020; 1: 100019.
12. Berkers G, van Mourik P, Vonk AM, *et al*. Rectal organoids enable personalized treatment of cystic fibrosis. Cell Rep 2019; 26: 1701–1708.e3.
13. Muilwijk D, de Poel E, van Mourik P, *et al*. Forskolin-induced organoid swelling is associated with long-term CF disease progression. Eur Respir J 2022; 60: 2100508.
14. Chai SC, Goktug AN, Chen T. Assay validation in high throughput screening: from concept to application. In: Vallisuta O, Olimat S, eds. Drug Discovery and Development – From Molecules to Medicine. London, IntechOpen, 2015; pp. 221–239.
15. Zhang JH, Chung TDY, Oldenburg KR. A simple statistical parameter for use in evaluation and validation of high throughput screening assays. J Biomol Screen 1999; 4: 67–73.
16. CFTR2. Database UCF. The Clinical and Functional TRanslation of CFTR (CFTR2). http://cftr2.org Date last updated: 29 April 2022. Date last accessed: 24 September 2022.
17. Reed GF, Lynn F, Meade BD. Use of coefficient of variation in assessing variability of quantitative assays. Clin Vaccine Immunol 2002; 9: 1235–1239.
18. Grabinger T, Luks L, Kostadinova F, *et al*. Ex vivo culture of intestinal crypt organoids as a model system for assessing cell death induction in intestinal epithelial cells and enteropathy. Cell Death Dis 2014; 5: e1228.
19. van Rijn JM, Ardy RC, Kuloğlu Z, *et al*. Intestinal failure and aberrant lipid metabolism in patients with DGAT1 deficiency. Gastroenterology 2018; 155: 130–143.e15.
20. Kreiselmeier NE, Kraynack NC, Corey DA, *et al*. Statin-mediated correction of STAT1 signaling and inducible nitric oxide synthase expression in cystic fibrosis epithelial cells. Am J Physiol Cell Mol Physiol 2003; 285: L1286–L1295.
21. Trzaska C, Amand S, Bailly C, *et al*. 2, 6–Diaminopurine as a highly potent corrector of UGA nonsense mutations. Nat Commun 2020; 11: 1.
22. Sachs N, de Ligt J, Kopper O, *et al*. A living biobank of breast cancer organoids captures disease heterogeneity. Cell 2018; 172: 373–386.e10.
23. Schütte M, Risch T, Abdavi-Azar N, *et al*. Molecular dissection of colorectal cancer in pre-clinical models identifies biomarkers predicting sensitivity to EGFR inhibitors. Nat Commun 2017; 8
24. 24 Du Y, Li X, Niu Q, *et al*. Development of a miniaturized 3D organoid culture platform for ultra-highthroughput screening. J Mol Cell Biol 2020; 12: 630–643.
25. Jiang JX, Wellhauser L, Laselva O, *et al*. A new platform for high-throughput therapy testing on iPSC-derived lung progenitor cells from cystic fibrosis patients. Stem Cell Rep 2021; 16: 2825–2837.
26. Berg A, Hallowell S, Tibbetts M, *et al*. High-throughput surface liquid absorption and secretion assays to identify F508del CFTR correctors using patient primary airway epithelial cultures. SLAS Discov 2019; 24: 724–737.
27. de Winter-de Groot KM, Janssens HM, van Uum RT, *et al*. Stratifying infants with cystic fibrosis for disease severity using intestinal organoid swelling as a biomarker of CFTR function. Eur Respir J 2018; 52: 1702529.
28. Dekkers JF, Berkers G, Kruisselbrink E, *et al*. Characterizing responses to CFTR-modulating drugs using rectal organoids derived from subjects with cystic fibrosis. Sci Transl Med 2016; 8: 344ra84.
29. Heijerman HGM, McKone EF, Downey DG, *et al*. Efficacy and safety of the elexacaftor plus tezacaftor plus ivacaftor combination regimen in people with cystic fibrosis homozygous for the F508del mutation: a double-blind, randomised, phase 3 trial. Lancet 2019; 394: 1940–1948.
30. Lin S, Sui J, Cotard S, *et al*. Identification of synergistic combinations of F508del cystic fibrosis transmembrane conductance regulator (CFTR) modulators. Assay Drug Dev Technol 2010; 8: 669–684.
31. Bansal AB, Cassagnol M. HMG-CoA Reductase Inhibitors. In: StatPearls [Internet]. Treasure Island, FL, StatPearls Publishing. Available from: www.ncbi.nlm.nih.gov/books/NBK542212/ Date last updated: 4 July 2022.
32. Zhao W, Zhao SP. Different effects of statins on induction of diabetes mellitus: an experimental study. Drug Des Devel Ther 2015; 9: 6211–6223.

Chapter | 6

33. Chin S, Ramjeesingh M, Hung M, *et al*. Cholesterol interaction directly enhances intrinsic activity of the cystic fibrosis transmembrane conductance regulator (CFTR). Cells 2019; 8: 804.
34. Slater EE, MacDonald JS. Mechanism of action and biological profile of HMG CoA reductase inhibitors. Drugs 1988; 36: Suppl 3, 72–82.
35. Bonifacio A, Sanvee GM, Bouitbir J, *et al*. The AKT/mTOR signaling pathway plays a key role in statin-induced myotoxicity. Biochim Biophys Acta 2015; 1853: 1841–1849.
36. Palma M, Leroy C, Salomé-Desnoulez S, *et al*. A role for AKT1 in nonsense-mediated mRNA decay. Nucleic Acids Res 2021; 49: 11022–11037.

Chapter | 7

FDA-approved drug screening in patient-derived organoids demonstrates potential of drug repurposing for rare cystic fibrosis genotypes

Journal of Cystic Fibrosis, May 2023, Volume 22, Issue 3

E. de Poel [1,2,*], **S. Spelier [1,2,*],** M.C. Hagemeijer[1,2,3], P. van Mourik[1], S.W.F. Suen[1,2], A.M. Vonk[1,2], J.E. Brunsveld[1,2], G.N. Ithakisiou[1,2], E. Kruisselbrink[1,2], H. Oppelaar[1,2], G. Berkers[1], K.M. de Winter de Groot[1], S. Heida-Michel[1], S.R. Jans[1], H. van Panhuis[1], M. Bakker[4], R. van der Meer[5], J. Roukema[6], E. Dompeling[7], E.J.M. Weersink[8], G.H. Koppelman[9,10], A.R. Blaazer[11], J.E. Muijlwijk-Koezen[11], C.K. van der Ent[1] and J.M. Beekman[1,2,12]

**** These authors contributed equally to this work***

1. Department of Pediatric Respiratory Medicine, Wilhelmina Children's Hospital, University Medical Center, Utrecht University, Utrecht, EA 3584, the Netherlands **2.** Regenerative Medicine Utrecht, University Medical Center, Utrecht University, Utrecht, CT 3584, the Netherlands **3.** Center for Lysosomal and Metabolic Diseases, Department of Clinical Genetics, Erasmus University Medical Center, Rotterdam, GD 3015, the Netherlands **4.** Department of Pulmonology, Erasmus MC, University Medical Center, Rotterdam, GD 3015, the Netherlands **5.** Haga Teaching Hospital, The Hague, CH 2545, the Netherlands **6.** Radboud University Medical Center, Radboud Institute for Health Sciences, Nijmegen, XZ 6525, the Netherlands **7.** Maastricht University Medical Center, Maastricht, HX 6229, the Netherlands **8.** Amsterdam University Medical Center, location AMC, Amsterdam, AZ 1105, the Netherlands **9.** University of Groningen, University Medical Center Groningen, Beatrix Children's Hospital, Department of Pediatric Pulmonology and Pediatric Allergology, Groningen, the Netherlands **10.** University of Groningen, University Medical Center Groningen, Groningen Research Institute for Asthma and COPD (GRIAC), Groningen, the Netherlands **11.** Division of Medicinal Chemistry, Vrije Universiteit Amsterdam, Amsterdam, HZ 1081, the Netherlands **12.** Centre for Living Technologies, Alliance TU/e, WUR, UU, UMC Utrecht, Princetonlaan 6, Utrecht, CB 3584, the Netherlands

Highlights

- We implemented a high-throughput 384-wells version of the functional FIS assay to screen a large number of PDIOs for compounds that enhance CFTR function.
- We found that PDE4 inhibitors are potent CFTR function inducers when residual CFTR function is either present or created by additional compound exposure.
- We show that CFTR modulators can be beneficial for CF patients with CFTR mutations that are not eligible for CFTR modulators at present-day.
- Our study demonstrates how preclinical studies using PDIOs can be used to initiate drug repurposing efforts, paving the way for patient stratification in the upcoming era of personalized medicine.

Abstract

Background

Preclinical cell-based assays that recapitulate human disease play an important role in drug repurposing. We previously developed a functional forskolin induced swelling (FIS) assay using patient-derived intestinal organoids (PDIOs), allowing functional characterization of CFTR, the gene mutated in people with cystic fibrosis (pwCF). CFTR function-increasing pharmacotherapies have revolutionized treatment for approximately 85% of people with CF who carry the most prevalent F508del-*CFTR* mutation, but a large unmet need remains to identify new treatments for all pwCF.

Methods

We used 76 PDIOs not homozygous for F508del-*CFTR* to test the efficacy of 1400 FDA-approved drugs on improving CFTR function, as measured in FIS assays. The most promising hits were verified in a secondary FIS screen. Based on the results of this secondary screen, we further investigated CFTR elevating function of PDE4 inhibitors and currently existing CFTR modulators.

Results

In the primary screen, 30 hits were characterized that elevated CFTR function. In the secondary validation screen, 19 hits were confirmed and categorized in three main drug families: CFTR modulators, PDE4 inhibitors and tyrosine kinase inhibitors. We show that PDE4 inhibitors are potent CFTR function inducers in PDIOs where residual CFTR function is either present, or created by additional compound exposure. Additionally, upon CFTR modulator treatment we show rescue of CF genotypes that are currently not eligible for this therapy.

Conclusion

This study exemplifies the feasibility of high-throughput compound screening using PDIOs. We show the potential of repurposing drugs for pwCF carrying non-F508del genotypes that are currently not eligible for therapies.

Introduction

Preclinical cell-based assays that recapitulate human disease play an important role in the first steps of drug development. Drug repurposing is the process of using clinically approved drugs outside their original disease-indication [1]. Pharmacokinetic and safety data that is readily available for existing drugs can enable a rapid use in clinical studies, which is particularly relevant in the context of rare diseases and personalized medicine where small patient populations enlarge economic and technical complexities. It has been estimated that 75% of known drugs could potentially be repositioned for various diseases [2].

Cystic fibrosis (CF) is a rare hereditary disease caused by mutations in the *CFTR* gene. Pharmacotherapies termed CFTR modulators that rescue CFTR function have revolutionized treatment for approximately 85% of people with CF (pwCF) who carry the most prevalent F508del-CFTR mutation [3], but a large unmet need remains to identify new and affordable treatments for patients with *CFTR* mutations that are non-eligible or non-responsive for CFTR modulators. CFTR function measurements in patient-derived intestinal organoids (PDIO's) associate with clinical features of CF and may enable drug repurposing in a personalized setting [4], [5], [6], [7]. These CFTR function measurement are performed by means of the forskolin-induced (FIS) assay, in which forskolin induces fluid secretion into the PDIO lumen resulting in rapid organoid swelling in a (near-to) complete CFTR-dependent manner. As found by us and others, CFTR function measurements in PDIOs associate with disease severity indicators of CF and CFTR modulator response, thereby enabling drug discovery efforts [8,9]. The established correlation between the FIS assay and clinical response furthermore allows theratyping: the matching of patients to beneficial compounds based on laboratory results of the patient-derived cells [10]. The fact that the FIS assay is well characterized in regards to translation of results to the pwCF in the clinic, indicates its potential for drug repurposing experiments.

Other prerequisites for drug repurposing are that the exploited assay is high-throughput and robust. We recently succeeded in establishing a high-throughput screening version of the FIS assay, allowing testing of compounds that directly or indirectly influence CFTR function in a 384-wells plate based, high-throughput manner on CF patient-derived material [11]. We screened 76 non-homozygous F508del PDIOs using this miniaturized FIS assay, aiming to identify CFTR function enhancing drugs in a 1400-compound FDA-approved drug library. Three main hit families were distinguished: existing CFTR modulators, PDE4 inhibitors and tyrosine kinase inhibitors (TKIs). Due to the anti-cancer, toxic nature of the latter category and the fact that PDE4 inhibitors are already used for treatment of the airway disease COPD [12,13], we argued that PDE4-inhibitor repurposing and CFTR modulator label extension for non-approved genotypes, hold most potential. We investigated those families in the rest of this study in several manners.

This study exemplifies the feasibility of high-throughput compound screening using PDIOs in an assay with a functional read-out. We show the potential of repurposing drugs for pwCF that are currently not eligible for modulator therapies, underlining the need for label

expansion. Additionally, we describe the potential therapeutic benefit of PDE4 inhibitors for pwCF with residual functional *CFTR* mutations. Altogether, this study underlines the potential and importance of identification of potential treatments and responsive patients, paving the way for patient stratification in the upcoming era of personalized medicine.

Material and methods

Collection of primary epithelial cells of CF patients (pwCF)

All experimentation using human tissues described herein was approved by the medical ethical committee at University Medical Center Utrecht (UMCU; TcBio#14-008 and TcBio#16-586). Informed consent for tissue collection, generation, storage, and use of the organoids was obtained from all participating patients. Biobanked organoids are stored and catalogued (https://huborganoids.nl/) at the foundation Hubrecht Organoid Technology (http://hub4organoids.eu) and can be requested at info@hub4organoids.eu

Human intestinal organoid culture and forskolin selection

Patient-derived intestinal organoid (PDIO) culturing was executed as previously described [4]. Prior to the FIS-assay, residual function levels of CFTR were determined during culture by visual analysis. Each PDIO culture was incubated with 0.02, 0.128, 0.8 and 5.0 μM forskolin for 1h, after which PDIO swelling was checked visually with a light-microscope. The forskolin concentration that resulted in lowest levels of residual swelling was chosen for subsequent screenings.

Compounds

The FDA library, purchased from SelleckChem (Z178323-100uL-L1300), was stored at -80°C. All other compounds used in this study are listed in **Supplemental Table 5**.

384-wells FIS assay

384-wells FIS-assays were performed according to previously described protocols [4], [5], with minor adaptations allowing a 384-wells screening setting as summarized in [9]. PDIOs of 76 different donors were seeded in 25% matrigel on two 384-wells plates/donor (7 μL/well). Organoids were subsequently submerged in 8 μL complete culture media supplemented with two FDA compounds/well (3 μM). The bottom 8 wells of the last column of each plate were not supplemented with FDA-compounds and served as negative control as well as minimal signal for Z'-factor calculations. The top 8 wells of the last column of each plate contained F508del/S1251N organoids that were treated with VX-770 (3 μM, acute addition) and forskolin (5 μM, acute addition), serving as a positive control and maximal signal for Z'-factor calculations. After 24 hours, 30 minutes prior to confocal imaging, organoids were fluorescently labeled with 5 μL calcein green (7 μM). 50 μL DMEM-F12 supplemented with forskolin and VX-770 for the positive controls, was added. Organoid swelling was monitored during 1 hour and total organoid surface area per well was quantified. Additional to fluorescent confocal images, brightfield images were taken of each well for visual analysis of organoid swelling. We removed outliers in the included plates based on interquartile range (IQR) calculations where wells with AUC values above Q3+(3xIQR) (=5963) of all positive control wells or below Q1-(3xIQR) (=-452) of all negative control wells were excluded. AUC values above 5963 (=Q3+(3xIQR) of all positive control wells of all plates with a Z'-factor > 0.5) and AUC values below -452 (=Q1-(3xIQR) of all negative control wells were excluded. Plates with an outlier percentage above 2% were excluded for hit selection resulting in exclusion of 11 plates, mostly due to calcein-staining related artefacts. Six additional plates were not measured or excluded after image acquisition due to poor organoid culture quality.

Wells were selected as hit when AUC values were higher than the mean+3xSD of the 8 negative control wells (DMSO treated) on each individual plate. The top 5% hits that increased AUC above the threshold in most patients and that were a hit in at least 2 PDIOs based on visual analysis resulted in 33 compound combinations. The total number of hits we investigated in a secondary screen was 30 as three of the identified hits were the positive controls (VX-770, VX-809 and VX-770/VX-809). Since in the primary screen two compounds per well were combined, the secondary screen consisted of in total 60 individual compounds. The primary and secondary screen were performed once with one technical replicate per condition, except for negative and positive controls (8 replicates each).

For questions outside the scope of this manuscript concerning practical challenges, timelines or costs of high-throughput screenings on PDIOs, we encourage the reader to contact us.

96-wells FIS assay

96-wells FIS assays were conducted as previously described [4]. For the secondary FDA screen, PDIOs derived from 9 donors were seeded into 96-wells plates within 50% matrigel. PDIOs were submerged in complete culture medium supplemented with one of the FDA compounds (3 μM), except for three wells (only DMSO). Z-scores of the secondary screen were determined according to the following formula: z-score = $(x-\mu)/\sigma$, where x is the AUC value of each condition, μ is the mean AUC value of the 3 control wells on each plate, and σ is the standard deviation of the same 3 control wells on each plate. Besides the negative controls, each plate contained two positive control wells with F508del/S1251N organoids that were treated with VX-770 and 5 μM forskolin. For each donor, a suboptimal forskolin concentration was used, i.e. a forskolin concentration that resulted in minimal PDIO swelling. Organoid swelling was monitored during 1 hour and total organoid surface area per well was quantified [7].

For all follow-up FIS experiments on PDE4 inhibitors after the primary/secondary screen, PDE4 inhibitors were added acutely prior to the FIS measurement in combination with 0.128 μM forskolin prior to a 2hr measurement FIS assay, except when stated otherwise. Three biological replicate experiments were performed with three technical replicates per condition.

The screening of 107 different organoid cultures upon roflumilast treatment was assessed with 24h of roflumilast preincubation, and a donor-dependent suboptimal forskolin concentration (either 0.128, 0.8 or 5.0 μM) was used for the FIS-assay. This screen was performed once with one technical replicate per condition.

For the CFTR modulator screen, CFTR modulators VX-770 (3 μM, simultaneously added with forskolin), VX-809 (3 μM, 24h) and VX-770/VX-809 were tested on an additional 236 cultures, covering 167 different genotypes. Prior to the 1h FIS measurements, CFTR activation was stimulated by addition of 0.128 μM forskolin for all genotypes. Screening was performed once with one technical replicate per condition.

PDIO viability

Cell viability was assessed by means of an Alamar Blue assay performed on the PDIOs in the FIS assay plate, after the FIS assay ended. Organoids were treated with the PDE4 inhibitors or salbutamol at the indicated concentrations and incubation times. PDIOs were incubated with Alamar Blue (1:10 diluted in DMEM/F12 phenol-red free) for 4h at 37°C. Fluorescence intensity of the Alamar Blue solution was measured with a photo spectrometer at 544/570 nm. Viability was normalized to the averages of the positive (10% DMSO) and negative controls. Three biological replicate experiments were performed with three technical replicates per condition.

PDIO lumen size

Confocal images obtained in the FIS assay results were used for the quantification of organoid lumen area and subsequently drug-induced swelling prior to the FIS assay. The luminal area as well as the total area was quantified manually using ImageJ, in a blinded fashion by 2 researchers. Results from three wells were averaged prior to calculation of the percentage of luminal organoid surface area of the total organoid surface area. Three biological replicate experiments were performed in which 10 organoid structures were characterized per condition.

PDE4 quantative RT-qPCR

Prior to qPCR, total RNA was isolated from the airway and intestinal organoids using 350 μl RNeasy lysis buffer. RNA extraction was performed using the RNeasy Kit according to the manufacturer's instructions and RNA yield was determined by a Nanodrop spectrophotometer. Subsequently, cDNA was synthesized using an iScript cDNA synthesis kit according to the manufacturer's protocol. Next, 10 μl qRT-PCR reactions were executed using BIO-RAD I-Cycler 96 wells-plates with iQ™ SYBR Green Supermix and 10 μM forward and reverse primers. The samples were incubated for 3 minutes at 95 °C and 39 cycles at 10 seconds at 95 °C and 30 seconds at 62 °C. For the expression levels of PDE4 enzymes, ΔCt values were calculated while for the treated PTC organoids ΔΔCt values were calculated. The Ct values were normalized with the mean of mRNA expression of YWHAZ and GAPDH that served as housekeeping genes. Averages were calculated from the three technical replicates corresponding to one biological replicate. Melting peaks were analyzed to confirm specific primer binding. Details of primers used for qPCR are listed in **Supplemental Table 6**.

Primary airway organoid FIS

FIS of primary airway organoids was performed as previously described [36]. In brief, human nasal epithelial cells of early passage were cultured on 12-transwell inserts, previously coated with PureCol (1:100; 30 μg/ml) in expansion medium. When confluency was reached, culture medium was changed to air-liquid interface (ALI) differentiation medium supplemented with A83-01 in submerged condition for 2-3 days. Next, cells were air-exposed and further differentiated as ALI-cultures, refreshed at the basolateral side with ALI-diff medium supplemented with A83-01 and neuregulin-1β (NR, 0.5 nM). After 2-4 days, cells were refreshed with ALI-diff medium only with NR and without additional A83-01 and were differentiated for 3 weeks. The apical side of the cultures was washed with PBS once per week while the medium was refreshed twice a week. Upon 3 weeks of differentiation, organoid swelling was assessed in FIS assays, similar to the 96-wells PDIO FIS assays as described above. Averages were calculated from three technical replicates derived of three biological replicates.

Statistical analysis

Statistical analyses were performed using GraphPad Prism®. For analysis of qPCR, One-Way ANOVAs were performed for the CF/WT/intestinal/airway groups separately to compare PDE4-subtype expression to the average expression of all PDE4 subtypes, followed by Dunnetts post-hoc analysis. For analysis of the PDE screen, a One-Way ANOVA was performed to compare swelling to DMSO control, followed by Dunnetts post-hoc analysis. Unless stated otherwise, graphs represent the average of 3 biological replicates which are obtained by averaging 3 technical replicates. To calculate statistical significance in the PDE4-screen, One-Way ANOVAs were performed per PDIO to compare compound-incuded swelling to baseline swelling, followed by Dunnetts post-hoc tests. When comparing two groups to each other, unpaired two-tailed T-tests were performed unless otherwise specified.

Results

FDA-approved drugs increase FIS in non-homozygous F508del PDIOs

We set out to study rescue of CFTR function by 1400 FDA-approved compounds in PDIO cultures of 76 different donors, covering 58 different *CFTR* genotypes. PDIOs from 47 donors were compound heterozygous for the F508del allele **(Supplemental Table 1)**. Genotypes were stratified into different categories based on a recent publication [9]. Most mutations included in this study were large deletions or splicing mutations in close proximity of the splice site and were therefore categorized as Class I mutations, except for mutation A559T that was recently described to result in poor apical trafficking due to a defective folding of the CFTR protein and was therefore categorized as Class II [14]. PDIOs from 22 donors were compound heterozygous for a premature termination codon (PTC) mutation and PDIOs from 24 donors were compound heterozygous for a missense mutation Addi-

tionally, 51 alleles of all PDIOs were characterized by a splice mutation, deletion or insertion and PDIOs from 5 donors had an insertion or an unclassified mutation **(Figure 1A,** left). All CFTR mutation classes are represented in our cohort except for Class III mutations and 6% of all alleles were unclassified **(Figure 1A,** right).

A challenge with screening a large variety of PDIOs is variation in baseline FIS due to differences in residual CFTR function. To compensate for this variability, we first determined the appropriate forskolin concentration per individual PDIO that resulted in the lowest detectable level of baseline swelling, as to increase the chance of detecting compound-induced FIS per PDIO **(Figure 1B).** As such, PDIOs with high (25%), moderate (15%) or absent (60%) residual CFTR function were measured with 0.128, 0.8 or 5 μM forskolin respectively.

The screening pipeline consisted of **a)** preparation of two full 384-wells per PDIO, **b)** addition of two compounds per well for 24 h, **c)** addition of forskolin directly before FIS measurements and **d)** confocal FIS measurements to visualize organoid swelling **(Figure 1C).** Positive and negative controls allowed CV value calculation, Z' factor calculation and outlier percentage calculation. CV values should not exceed 20% and CV values under 10% are considered excellent [15]. The average CV value of 12.4% of all plates underlined assay robustness **(Figure 1D).** Additionally, Z'-factors were calculated as indicator of assay quality. The Z'-factor is a parameter based on positive and negative control that ranges between 0 and 1, with 1 indicating a perfect assay and Z'-factors larger than 0.4 considered acceptable [15]. The average Z'-factor over all donors was 0.49, underlining the overall assay robustness **(Figure 1E).** Out of the 152 plates, six plates were not measured or excluded after image acquisition due to poor organoid culture quality. Subsequent calculation of outlier percentages of the remaining plates resulted in a median outlier percentage of 0.3% per plate and an additional exclusion of 11 plates that comprised outlier percentages above 2%. **(Figure 1F).**

Positive hits were selected based on FIS values that were higher than the mean+3SD of the 8 negative control wells within the identical plate **(Figure 1G).** In **Figure 1H,** outcomes for 30 top compound combinations and the three positive controls consisting of CFTR modulators are listed, complete selection criteria are described in Figure 1C and the Materials and Methods. We observed large differences between PDIOS with respect to response to compound combinations **(Supplemental Table 2).** Overall, the median number of hits differed per mutation category, ranging from 10.5 hits in Class II/Class V PDIOs to a median of 73 hits for Class II/Na or unclassified PDIOs **(Supplemental Figure S1).** Additionally, the mean number of hits in the Class I/Class I category was significantly lower than the mean averaged number of hits of all categories combined ($p = 0.0173$).

Identification of three main compound families that increase CFTR function

We next set out to determine which of the two compounds of the selected wells was associated with the observed efficacy, for which we selected 9 genotypically different PDIOs to represent the different *CFTR* mutation classes as well as the three different forskolin concentrations. PDIOs were treated with the individual 60 FDA compounds from the 30 original compound combinations. For most compound combinations, one of each compounds clearly resulted in a higher increase of FIS than the other compound. Z-scores were calculated in order to correct for differences between plates, compound with a Z-score higher than 1.5 in at least two donors were considered a hit, resulting in confirmation of 19 hits **(Figure 2A).** As anticipated, donor variation was observed between the selected hits, Rolipram for example (plate 1, compound 11) reached high Z-scores particularly in PDIOs with high residual CFTR function. Four compounds reached a Z-factor of 1.5 only in one donor, and in 9 compound combinations neither of both compounds was identified as hit. Average DMSO-corrected AUC levels of these 19 confirmed hits were calculated for the PDIOs in which the compound was defined as hit **(Figure 2B).** Overall, 3 main compound families could be identified: CFTR modulators, phosphodiesterase (PDE) inhibitors and tyrosine kinase inhibitors (TKIs). Due to the toxic nature of the latter category and the fact that PDE4 inhibitors are already used for airway disease COPD [12,16], we argued that PDE4 inhibitors and CFTR modulators hold most potential and continued with follow-up characterization of these two families.

Potential of label expansion of CFTR modulators for rare CFTR genotypes

In the primary and secondary screen, CFTR modulators elevated CFTR function to a high degree and in a large number of PDIOs, suggesting a high potential for label extension of CFTR modulators. To further characterize genotypes that would potentially benefit from CFTR modulator therapy, we screened 197 PDIOs representing 127 genotypes, that carried at least one *CFTR* mutation that is present in <1% of the European and American population and a maximum one of the following alleles: F508del/G542X/G551D/R117H/N1303K/W1282X/3849+10kbC>T/R553X/17171G>A/621+1G>T/2789+5G>A/3120+1G>A/CFTRdele2,3 **(Supplemental Table 3).** Response to CFTR modulators from of another 109 PDIOs **(Supplemental Table 4)** representing 34 different genotypes were additionally screened, to obtain an overview of reference AUC levels allowing characterization of the correlation between FIS data and clinical data at group level. Importantly, allele-based dose response, e.g. a doubling in FIS when two responsive alleles are expressed in comparison to one responsive allele, has previously been described [6].

The 197 PDIOs were treated with VX-770 or VX-809/VX-770. FIS data are shown for PDIOs carrying at least one F508del allele in **Figure 3A**, and FIS data for non-F508del PDIOs are shown in **Figure 3B**. At present-day, both the FDA and EMA have approved the most recently developed modulator therapy Trikafta for CF patients with at least one F508del allele. Additionally, the FDA has extended eligibility for several rare genotypes **(Figure 3B).** As done before in a smaller dataset [7], we investigated the association between average FIS values in PDIOs and the average FEV1 response in clinical trials **(Table 1)** in 7 representative genotype-stratified subgroups **(Figure 3C & Supplemental Table 4).** Consistent with previous findings [8], we found a significant correlation ($R2=0.53$, $p<0.0001$) between the level of CFTR-modulator induced swelling of the PDIOs and the treatment effect expressed in absolute change in FEV1pp of reported clinical studies.

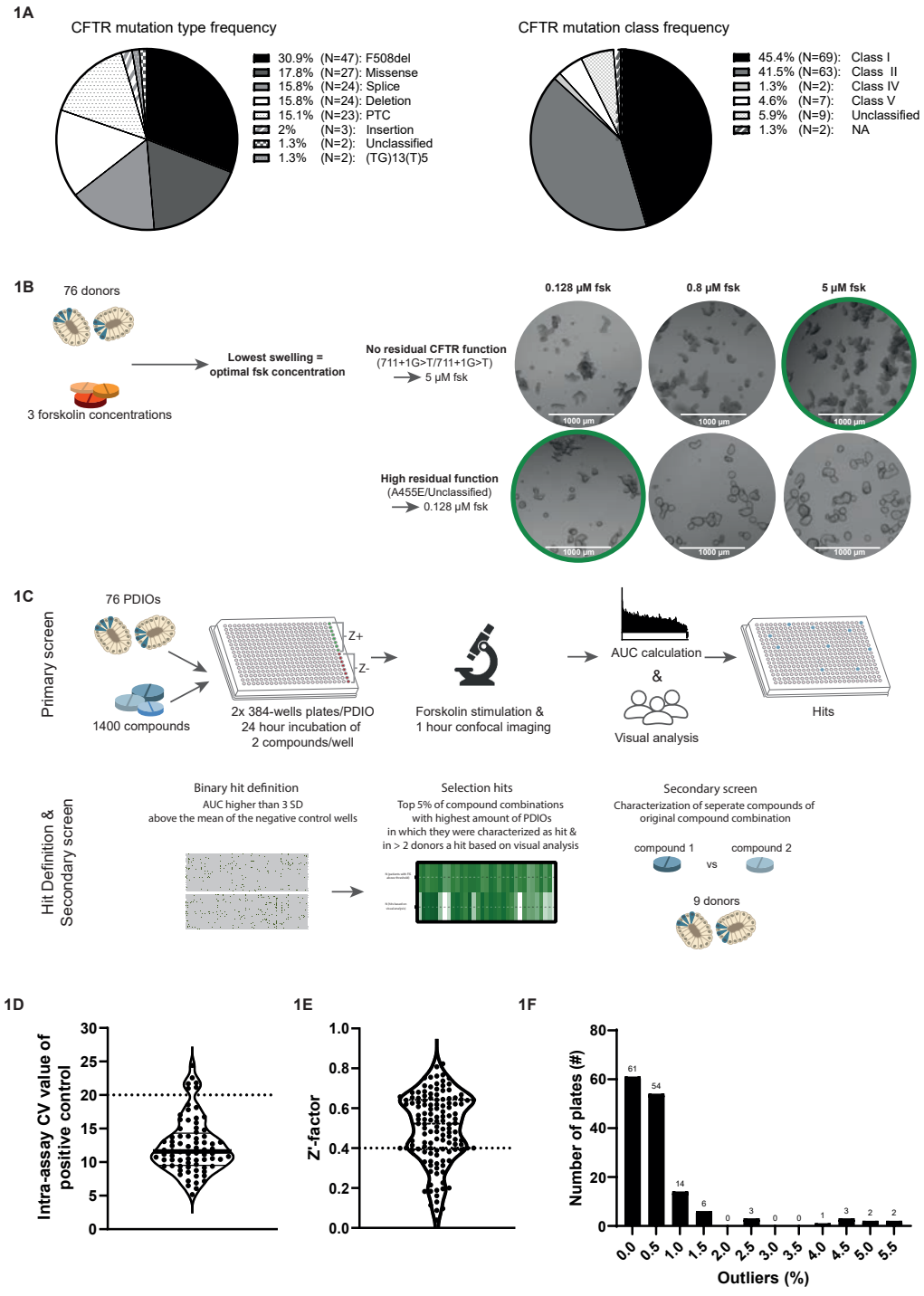

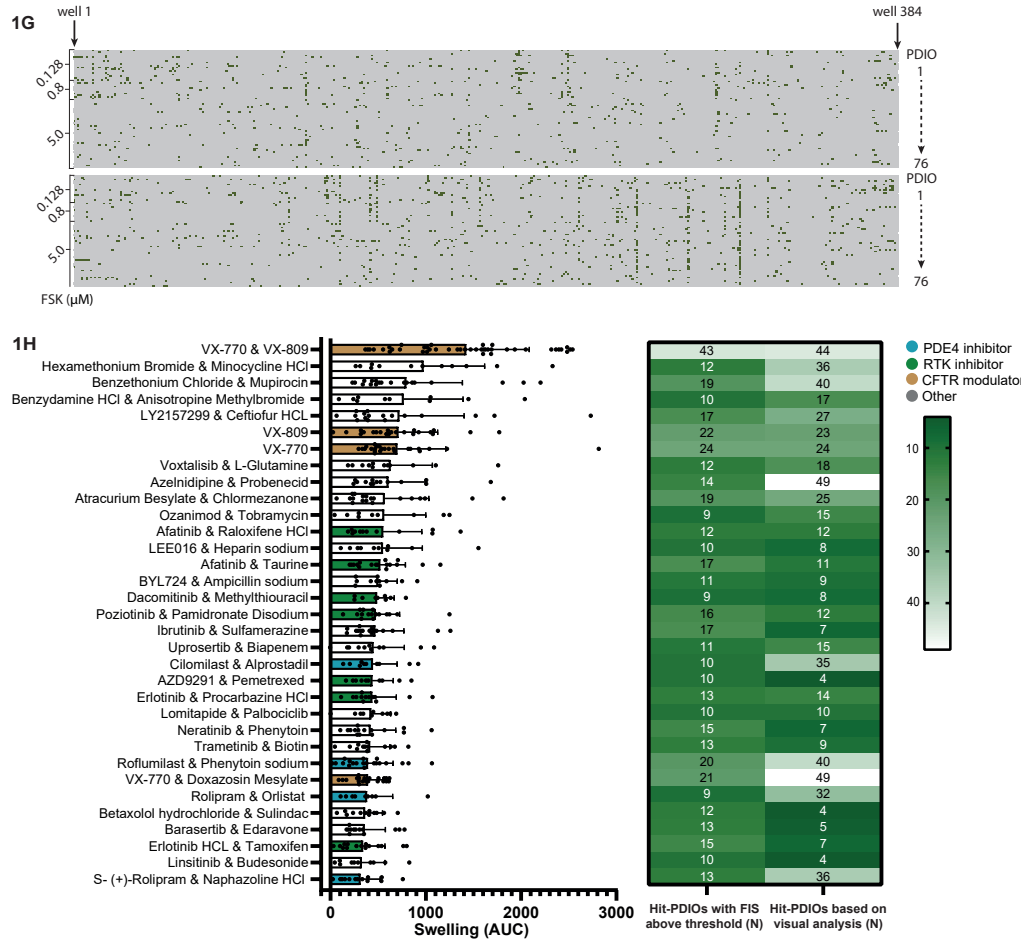

Figure 1. FDA-approved drugs increase FIS in non-homozygous F508del PDIOs.
(A) Frequency of represented CFTR mutation types (left) and classes (right) of the 76 PDIOs included in the primary FDA screen. **(B)** Schema of selection pipeline of forskolin concentration, based on residual CFTR function. Two PDIOs are shown as example that hold low (top) or low (bottom) residual CFTR function resulting in respectively a high or low forskolin concentration during the FIS assays. **(C)** Schematic of primary FDA screen describing PDIO plating, data analysis and decision pipeline for inclusion in secondary screen. **(D)** The intra-assay CV values of all plates, based on the Z+ values of all plates. The dotted line at 20 represent the upper limit value that indicates sufficient assay robustness. **(E)** The mean Z'-factor of all plates. The dotted line at 0.4 indicates a robust Z'-factor. **(F)** Outlier percentage of all measured plates with adequate organoid quality. AUC values above >Q3+(3xIQR) (=5963) of all positive control wells or below Q1-(3xIQR) (=-452) of all negative control wells of the plates with a Z'-factor >0.5, were defined as outlier. **(G)** Binary outcome (hit or no hit) of all wells (from left to right) and PDIOs (from top to bottom) divided over the two 384-wells plates. A well was selected as hit if the AUC was higher than the mean+3SD of the 8 negative control wells (DMSO treated) per 384-wells plate. Wells that were defined as hit are highlighted in green. **(H)** Overview of AUC values of the top 30 compound combinations and the three positive controls in primary screen, depicted for

the PDIOs in which the compound combination was defined as hit. In the heatmap, numbers of PDIOs in which the compound combination was scored as hit based on AUC calculations are stated on the left, whereas numbers of PDIOs in which the compound combination was scored as hitbased on visual analysis are stated on the right. Bars represent the means of all donors based on one technical replicate in one experiment.

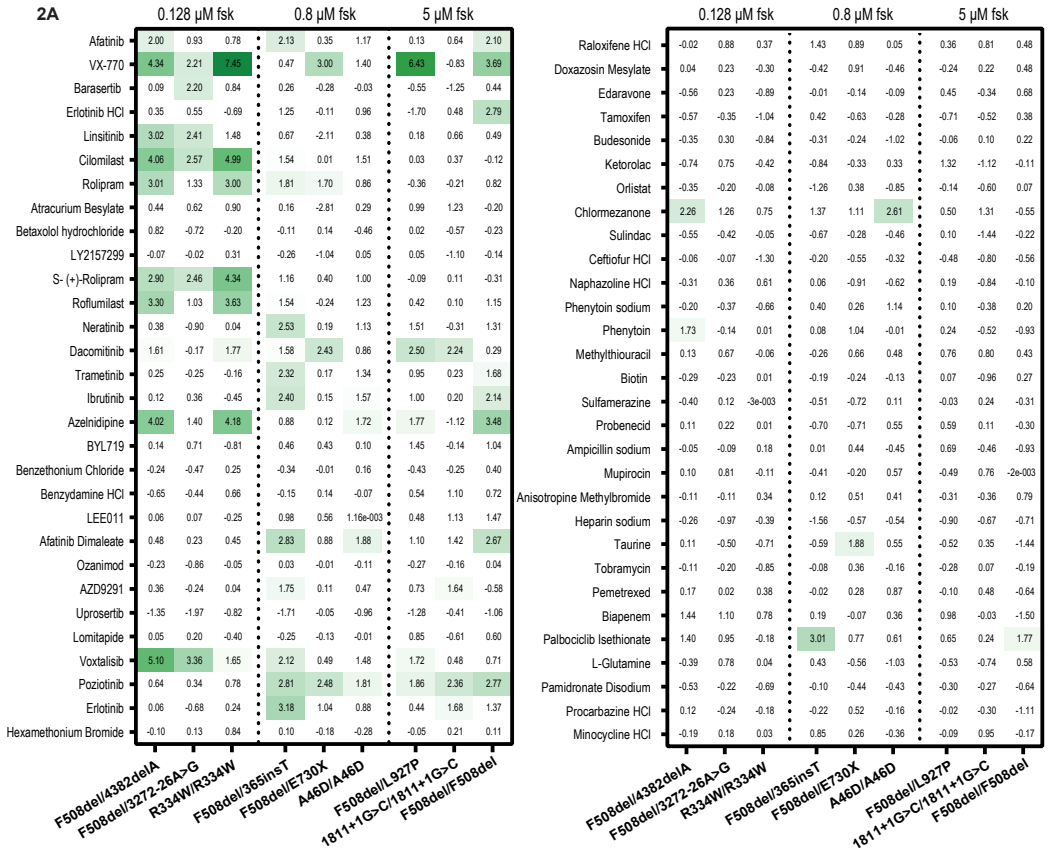

Figure 2. Identification of three main compound families that increase CFTR function.
(A) Z-scores of secondary FIS screen of 9 PDIOs treated separately with the compounds of the top 30 compound combinations, based onthree biological replicate experiments with three technical replicate. **(B)** The number of PDIOs in which FIS led to a Z-score above a threshold of 1.5 (left) and DMSO normalized AUC values of those PDIOs in which the compound was classified as a hit (right). Compound class is indicated by color, distinguishing between PDE4 inhibitors, RTK inhibitors, CFTR modulators and compounds with a distinct MoA.

Table 1. Overview of clinical trials with CFTR-correcting treatments in subjects expressing different CFTR mutations.
For the R117H trial, only data from CF subjects aged >18 were used, because subjects aged 6 to 18 had a different mean baseline FEV1 compared to those in the other trials. The numbers correlate with the numbers in Fig. 5C. NS: not significant, NA: statistical analysis not performed due to small numbers for individual mutations, RF: residual function, MF: minimal function.

Treatment	Genotype	Absolute change in FEV1pp versus placebo
1. VX-770	F508del/F508del	1.72 (NS) [35]
2. VX-770/VX-809	F508del/MF	0.6 (NS) [36]
3. VX-770	F508del/RF_splice	5.4 (NA) [37]
4. VX-770	F508del/RF_missense	3.6 (NA) [37]
5. VX-770/VX-809	F508del/F508del	2.8 (p<0.001) [38]
6. VX-770	R117H/other	5 (p = 0.01) [39]
7. VX-770	S1251N/other	9 (NA) [40]

These data indicate that 31 of the 127 genotypes had VX-770-responses beyond that of VX-770 treated F508del/splice PDIO and that 36 genotypes of the 127 genotypes had VX-770/VX-809 responses beyond that of VX-770/VX-809-treated F508del/F508del PDIO, indicating a clinical benefit based on the correlation described in **Figure 3C**. Furthermore, PDIOs with *CFTR* mutations that are currently not categorized into one of the *CFTR* mutation classes, can be classified based on these data.

We observed a strong correlation (R2=0.7) between baseline swelling (DMSO) at 5 µM forskolin and swelling increase with VX-770 and 0.128 µM forskolin **(Figure 3D).** A similar relation between residual CFTR function and VX-770/VX-809-mediated increase in swelling was observed, however with a lower R2 (R2=0.4). Only two organoid cultures (E92K/E92K and A455E/(TG)13(T)5) showed an increase in CFTR function upon VX-809 treatment, and correlation between VX-809 induced swelling and DMSO-induced swelling was absent.

Acute PDE4 inhibition increases CFTR function at a low nanomolar EC50
Phosphodiesterases (PDEs) comprise enzymes that catalyze the hydrolysis of phosphodiester bonds of second messengers, cAMP and cyclic guanosine monophosphate (cGMP), thereby regulating many downstream signaling processes [17]. PDE4 inhibitors act by blocking the catalytic site of PDE4, thereby suppressing cAMP degradation which results in an increase of PKA activation, subsequently increasing CFTR phosphorylation and function

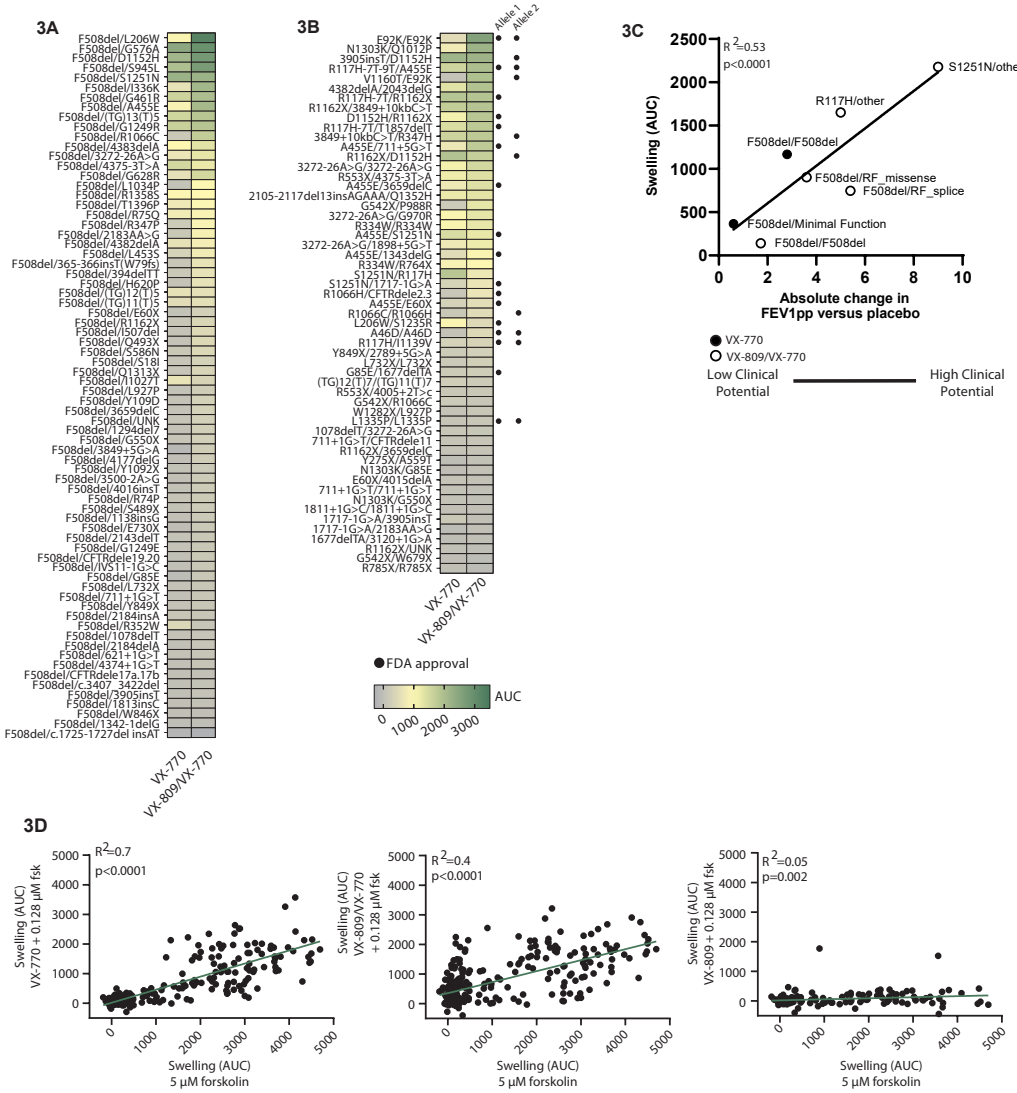

Figure 3. Potential of label expansion of CFTR modulators for rare CFTR genotypes.
(A-B) VX-770 or VX-809/VX-770 induced swelling of PDIOs at 0.128 µM forskolin for (A) PDIOs expressing a F508del mutation on one allele and a rare CFTR mutations on the other allele and **(B)** PDIOs expressing two rare CFTR variants. Swelling is normalized for residual CFTR function by subtraction of DMSO-induced FIS. Values are based on one technical replicates, derived of one biological replicates. **(C)** Pearson correlation of drug-corrected PDIO swelling versus lung function increase (FEVpp). CFTR modulator swelling was measured at 0.128 µM forskolin and corrected for DMSO-induced swelling and is presented per CFTR genotype group. VX-770-treated PDIOs are represented by white dots whereas VX-809/VX-770 treated PDIOs are represented by black dots. FEV1pp versus placebo values are based on clinical trials, summarized in **Table 1**. **(D)** Pearson correlation of PDIO swelling upon modulator therapy (VX-770, VX-809 or VX-809/VX770) and 0.128 µM forskolin versus 5 µM forskolin and DMSO-treated PDIOs.

(Figure 4A). RNA expression analysis of the four PDE4 subtypes indicates (highly) similar expression between wild-type and CF (F508del/F508del) intestinal PDIOs. When comparing the PDE subtypes, higher expression of specifically PDE4D was observed in primary airway epithelial cells **(Figure 4B).**

We first studied selectivity of PDE subtypes for modulating FIS in R334W/R334W PDIOs, one of the PDIOs that was most responsive to PDE4 inhibitors based on the results of the secondary screen. Comparison of different PDE inhibitors that target cAMP or cGMP as well as three pan-PDE inhibitors, indicate that inhibition of mainly PDE4D results in a large increase of CFTR function **(Figure 4C).** Inhibition of other cAMP-mediated PDEs or cGMP-mediated PDEs did not increase of CFTR function. Surprisingly, pan-PDE inhibitors were less efficacious than PDE4-selective inhibitors, potentially due to a low PDE4 specificity in comparison to the selective PDE4 inhibitors. We continued with optimizing the dynamic range to detect effects of PDE4 inhibitors and observed that PDE4 inhibitor-induced swelling was at its maximum after two hours of incubation **(Figure 4D).** In the primary and secondary screen, all compounds were preincubated for 24 h prior to FIS measurements. Acute addition and longer exposures of PDE4 inhibitors however all resulted in similar increases in FIS, consistent with the established mode-of-action of PDE4i as direct inhibitor of cAMP degradation **(Figure 4D).** This is distinct from β2 adrenergic receptors (β2AR)-agonists that increase cAMP levels and downregulate PDIO responses to forskolin. Especially upon longer exposure it has been shown that B2AR-agonist salbutamol pretreatment can result in reduced CFTR activity [18]. We also detected a decrease in organoid swelling after 72 h of pre-incubation with both salbutamol and roflumilast when compared with PDIO swelling induced by acute administration (**Supplemental Figure 2A**). We however observed forskolin-independent PDIO preswelling prior to the FIS assay, indicated by an increase of steady-state lumen area (SLA) **(Supplemental Figure S2B).** This potentially explains a decrease of PDIO swelling during the FIS assay. We subsequently calculated ratios between FIS decrease and SLA increase, where ratios larger than 1 indicate that the decrease of PDIO swelling after 72 h incubation with salbutamol is larger than what is caused by PDIO preswelling. Whilst this is the case for salbutamol, this is not the case for especially the lower concentration of roflumilast **(Supplemental Figure S2C).** This indicates that PDE4 inhibition, opposed to B2AR-agonist, does not result in downregulation of CFTR activity.

Without forskolin induced cAMP increase, PDE4 inhibition did not result in increased CFTR function. Additionally, when stimulating with a high concentration of forskolin, the difference between residual CFTR function and PDE4 induced CFTR function was not detectable due to high swelling in both conditions **(Figure 4E).** This underlines the forskolin dependency of the effect of PDE4 inhibitors as well as that 0.128 µM forskolin results in the optimal dynamic range to detect effects of PDE4 inhibition. Additionally, FIS was measured with increasing concentrations of roflumilast and a clear concentration-dependent effect was observed (EC50 = 65 nM) **(Figure 4F).**

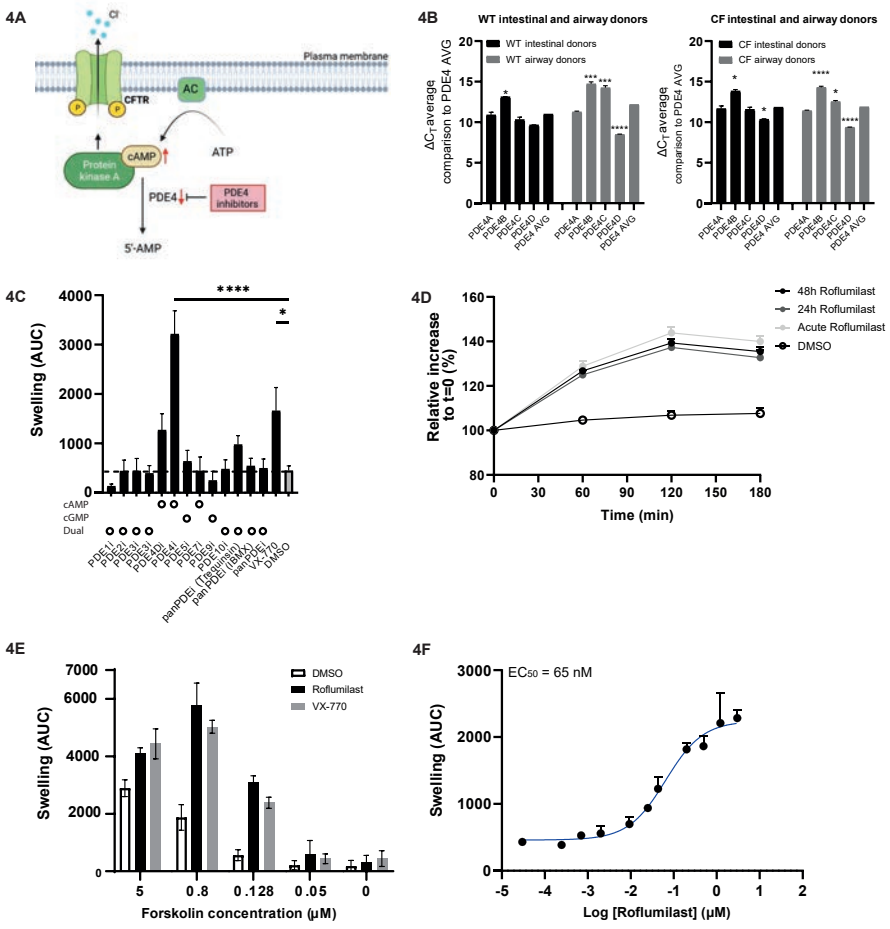

Figure 4. Acute PDE4 inhibition increases CFTR function at a low nanomolar EC50.
(A) Schematic of mode of action of PDE4 inhibitors, that by suppressing cAMP degradation, result in subsequent elevation of intracellular cAMP, PKA activation and increase of CFTR phosphorylation and function. (**B)** Delta-CT values obtained via RT-qPCR of the different PDE4 subtypes, normalized for CT values of housekeeping gene GAPDH, for WT and CF (F508del/F508del) donors in PDIOs and patitient-derived, differentiated nasal epithelial cells. To calculate which PDE4 subtypes differed significantly from the average of all PDE subtypes, One-Way ANOVAs were performed for the CF/WT/intestinal/airway samples separately, followed by Dunnetts post-hoc analysis. Significance indicated by one asterisk corresponds to a p-value <0.05, significance indicated by three or four asterisks correspond to p<0.005 and p<0.0001, respectively. Bars indicate the mean of three technical replicates, derived of one biological replicate with errorbars indicating the SD. **(C)** FIS levels (AUC) of R334W/R334W PDIOs upon treatment with a range of PDE inhibitors. To assess significance, a One-Way ANOVA was performed followed by Dunnetts post-hoc analysis. Significance indicated by one asterisk corresponds to a p-value <0.05, significance indicated by four asterisks corresponds to a p-value <0.0001. Bars indicate the mean of three technical replicates, derived of three biological replicates with errorbars indicating the SEM. **(D)** Relative size increase during a FIS assay overtime for R334W/R334W PDIOs upon preincubation or acute treatment with PDE4 inhibitor roflumilast (RF). Dots indicate the mean of three technical replicates, derived of three biological replicates with errorbars indicating the SEM. **(E)** FIS levels (AUC) of R334W/R334W PDIOs, upon acute treatment of RF and VX-770 and a titration range of forskolin. Bars indicate the mean of three technical replicates, derived of three biological replicates with errorbars indicating the SEM. **(F)** FIS levels (AUC) of R334W/R334W PDIOs, upon a concentration range of acute stimulation with RF. The EC50 was calculated based on logarithmic curve-fitting using GraphPad Prism and corresponds to 65 nM. Bars indicate the mean of three technical replicates, derived of three biological replicates with errorbars indicating the SEM..

PDE4 inhibition efficacy depends on residual CFTR function

To compare whether different PDE4 inhibitors result in differences in CFTR function increase, we compared 5 different PDE4 inhibitors: rolipram, roflumilast, cilomilast, piclamilast and apremilast. To further characterize genotype-specific effect, the PDE4 inhibitors were screened on a panel of 14 PDIOs. 8 PDIOs expressed different Class II/Class III mutations, 4 PDIOs were homozygous for the F508del/F508del *CFTR* mutation and 2 PDIOs homozygously expressed W1282X *CFTR*. Prior to characterizing CFTR function increase, we confirmed absence of toxicity of those PDE4 inhibitors **(Supplemental Figure S3).** PDE4 inhibitors were tested alone or in combination with additional compounds. We compared compound-induced swelling to background-induced swelling **(Figure 5A & Supplemental Figure S4).** Correlations were significant and positive for all compounds, with the highest for VX-770 (R2=0.95, p<0.0001) in comparison to roflumilast (R2=0.68, p<0.0001) and rolipram (R2=0.73, p<0.0001). Whilst this underlines that PDE4 inhibition efficacy is positively correlated to baseline CFTR function, we observed large variation in PDE4 inhibitor response between PDIOs with low residual function.

In total, in 6-out-of-8 non-Class I and non-F508del PDIOs, at least one PDE4 inhibitor significantly elevated CFTR function, in some cases resulting in AUC values similar or higher than VX-770 **(Supplemental Figure S5A).** W1282X/W1282X PDIOs treated with PDE4 inhibitors were tested in combination with readthrough (RT) agent DAP, a compound that induces incorporation of an amino acid at the site of the PTC site thereby resulting in ribosomal readthrough at the PTC site and as such production of full-length protein. Interestingly, response was better than predicted based on the correlation **(Figure 5B).** The large additional effect of PDE4 inhibitors when combined with DAP indicates compound synergy, which could be attributed to the MoA of DAP which results in tryptophan incorporation at the PTC site and therefore WT restoration of the CFTR protein in case of W1282X/W1282X [19]. This is not the case for RT-agent ELX-02, for which we observed a less prominent increase in CFTR function when combined with PDE4 inhibitors & CFTR modulators Trikafta (VX-445/VX-661/VX-770). In this combination however, the combination of roflumilast/ELX-02/CFTR modulators reached PDIO swelling levels that were comparable to the combination of ELX-02/Trikafta/SMGi, the latter inhibiting nonsense-mediated mRNA decay (NMD). PDIOs that respond less to PDE4 inhibitors than predicted based on background/compound-induced swelling correlation, are PDIOs homozygous for F508del CFTR that were tested in combination with CFTR modulators VX-809/VX-770 **(Supplemental Figure S5B).** All responses are summarized in Figure 5C, in which we show background-corrected AUC values upon PDE4 inhibitor treatment. The effect of PDE4 inhibition varies greatly between PDIOs, underlining genotype-associated differences in response.

Figure 5. PDE4 inhibition efficacy depends on residual CFTR function.
(A) Roflumilast, rolipram or VX-770-induced swelling (AUC) versus background (DMSO/other) induced swelling (AUC), for 14 PDIOs indicated by the different colored dots. Dots indicate the mean of three technical replicates, derived of three biological replicates. **(B)** W1282X-/W1282X PDIO swelling upon treatment with a panel of PDE4 inhibitors, in combination with ELX-02 (E), VX-445/VX-661/VX-770 (T) or SMG1i (S) (left) or DAP (right). Bars indicate the mean of three technical replicates, derived of three biological replicates with errorbars indicating the SEM. **(C)** A heatmap of compound-induced PDIO swelling, normalized to background compounds or DMSO. To calculate statistical significance, One-Way ANOVAs were performed per PDIO to compare compound-incuded swelling to baseline swelling, followed by Dunnetts post-hoc tests. Values are the mean of three technical replicates, derived of three biological replicates and significant differences are depicted by one/two/three/four asterisks, corresponding to p-values smaller than 0.05, 0.01, 0.001 or 0.0001 respectively. **(D)** DMSO-corrected swelling of A445E/S1251N airway organoids upon treatment with roflumilast and a concentration range of forskolin. Bars indicate the mean of three technical replicates, derived of three biological replicates with errorbars indicating the SEM.

Overall, among all included PDIOs, a similar trend was observed regarding the effect of the different PDE4 inhibitors, with piclamilast, roflumilast and rolipram resulting in the highest increase in CFTR function.

We subsequently investigated the effect of PDE4 inhibition in primary airway organoids harboring A445E/S1251N CFTR, as these mutations have previously been recognized as Class II/III mutations respectively and possess some residual CFTR function. Corresponding to the results in the PDIOs, roflumilast elevates CFTR function in a forskolin dependent manner, where maximum efficacy is observed at mainly 0.128 µM forskolin **(Figure 5D).**

Discussion

Preclinical cell-based assays that recapitulate human disease can play an important role in the first steps of drug repurposing. We previously developed a robust, functional in vitro assay in the context of CF, using PDIOs that express CFTR as only ion channel allowing fluid secretion measurements that are entirely CFTR dependent under standard conditions [6,7]. Whilst the expression of alternative ion channels as in for example airway organoids can be beneficial in some cases, the CFTR dependency in PDIOs is advantageous when the goal is to characterize compounds that specifically enhance CFTR-mediated fluid secretion. Additionally, the usage of PDIOs, as opposed to airway organoids, allows comparison of individual FIS results to clinical parameters. As such it has been shown that outcomes of the FIS assay correlate with disease severity indicators of CF, long-term disease progression and therapeutic response, underlining the potential clinical value of identified preclinical hits [8,9]. Using a high-throughput version of this assay, we screened 76 non-homozygous F508del-CFTR PDIOs to measure the efficacy of 1400 FDA-approved drugs on improving CFTR function as measured by FIS. Here, we show that PDE4 inhibitors are potent CFTR inducers in PDIOs where residual CFTR is either present, or created by additional compound exposure. Additionally, upon CFTR modulator treatment (VX-809/VX-770), we show rescue of PDIOs that are currently not eligible for this therapy.

Previous optimization of several steps in 96-wells FIS assay [4]enabled scaling to 384-wells format [11]. Whilst patient-derived organoid screening has received much attention, many studies in this context are lower-throughput screenings, in which read-outs are often centered around viability [20], [21], [22]. Whereas viability can be quantified in a straightforward fashion, for example by luminescence measurements, increasing throughput of functional assays with a more complicated read-out is exceedingly challenging. A few recent studies reported higher throughput screenings on 2D patient-derived material in the context of CF [23,24] and one recent publication describes a 384-wells function assay for airway organoids [25] Robustness of exploited assays was however either lower than in our study or not reported. Additionally, PDIO characteristics are robust and scalable in terms of cell culture and experimental pipeline, making them highly suitable for the high-throughput character of our study. This remains unparalleled by for example airway organoids and their lengthy, demanding culture protocols. Overall, robustness of our screening assay was confirmed and underlined by 70% of the plates reaching Z'-factors of 0.4 or higher and the

average of all plates reaching a Z'-factor of 0.5. As the Z'-factor positive signal on each plate however consisted of F508del/S1251N PDIOs stimulated with VX-770 and forskolin, we did not use Z' calculations to exclude individual plates from the analysis.

A challenge we encountered, is that PDIOs differ in baseline residual CFTR function, thereby limiting the opportunity to detect positive hits for individual PDIOs with high forskolin (optimal for low baseline CFTR) and low forskolin (optimal for high baseline CFTR) stimulation. PDIO-specific forskolin concentrations were thus selected, introducing an extra variable in the FIS assay as well as preventing the use of a uniform assay for all PDIOs. As cAMP is a second messenger affecting a variety of pathways, this could affect other molecular mechanisms than solely CFTR-mediated fluid secretion. However, as fluid secretion in the FIS assay is entirely CFTR dependent, hits that do not target CFTR directly still eventually increase fluid secretion via modulation of the CFTR-dependent fluid secretion.

The primary screen resulted in a list of 30 top compound combinations. Large differences between PDIOs were observed, as expected, PDIOs with two Class I mutations were least responsive. In the secondary screen, we showed that 19 compounds out of the 30 compound combinations resulted in an increase in FIS, amongst which CFTR modulators and PDE4 inhibitors. In the results of the secondary screen, a different challenge of the FIS assay was underlined by detection of hits based on the Z-scores in the homozygous splice donor. Whilst it could be an intriguing finding connected to manipulation of splicing ór the induction of expression of alternative ion channels, rechecking the raw image data as well as the absolute AUC quantification indicated an absence of clear swelling and as such a false positive identity of hits such as dacomitinib and poziotinib. Presumably, in PDIOs with severe Class I mutations where hardly any response is observed, hits are more likely to be false positive. A reason for this is that a small increase in AUC could result in a Z-score indicative of a hit, whilst this observation is biologically less meaningful due to the low absolute AUC value. As such, extra caution should be taken in case of interpreting the response of Class I PDIOs.

Among all FDA hits, CFTR function modulators were most effective. Importantly, as CFTR modulators are already approved for specific mutations causing CF, it would be a matter of label extension instead of drug repurposing, which could result in an even faster translation into the clinic. Consistent with a previous study investigating this correlation [7], we found a significant correlation between the level of the DMSO-corrected drug-induced swelling of the PDIOs with 0.128 µM forskolin and the treatment effect expressed in absolute change in FEV1pp of available clinical trial data of mutations present in our study. By choosing a single forskolin concentration, we here did not differentiate F508del/minimal function genotypes based on residual function. As such, we cannot exclude the possibility that certain PDIOs with high residual function and lower levels of FIS than expected based on the linear correlation, in fact exhibited compound-induced, forskolin-independent pre-swelling prior to the FIS assay. This preswelling in case of PDIOs with residual function or in case of highly effective treatments, remains a challenge in our FIS assay set-up at present-day. As such, the development of novel assays which take this phenomenon into account will prove valuable.

Based on the association between FIS data and clinical data, 17 out of 54 or 23 out of 54 PDIOs included in this dataset could have a moderate clinical benefit of respectively VX-770 or VX-809/VX-770 therapy. The mutations in the N1303K/Q1012P, 4382delA/2043delG and R334W/R334W genotypes are particularly interesting as these mutations are currently not approved for VX-770 therapy. These results underline the relevance of continuing to screen non-eligible non-F508del-CFTR genotypes with CFTR modulators and to potentially expand the label of these compounds based on the FIS assay. Additionally, our results and screening pipeline overall can aid in theratyping CFTR mutations of unknown consequence into a mutation category. For example, CF0823 (G542X/P988R) responds well to the combination of VX-770/VX-809 whilst swelling is not increased upon VX-770 treatment alone, indicating that mutation P988R is a CFTR mutation that results in improper CFTR folding and trafficking. Recently, the triple combination of CFTR modulators VX-445/VX-661/VX-809 has been approved by the FDA and EMA for all non-homozygous F508del genotypes and, specifically by the FDA, for several rare genotypes [26]. Future studies in which CFTR restoration by this newest combination of CFTR modulators is compared to CFTR restoration by VX-809/VX-770 will be valuable. It is expected that trends for genotypes described in this manuscript will be similar to results obtained with VX-445/VX-661/VX-809, yet that the triple therapy will be more potent overall.

PDEs catalyze the hydrolysis of phosphodiester bonds of second messengers, cAMP and cyclic guanosine monophosphate (cGMP), thereby regulating many downstream signaling processes such as smooth muscle activation and inflammation associated pathways [17]. We verified that PDE4 is indeed the main PDE variant whose inhibition is related to CFTR function elevation and found also higher expression of this PDE variant than of the other PDE variants in both PDIOs as well as primary nasal epithelial cells differentiated at air-liquid interface. Whilst PDE4 inhibition can increase CFTR activation due to higher levels of cAMP and subsequent PKA activation and increased CFTR channel opening, PDE4 inhibition does not restore CFTR function directly. This is underlined by the absence of PDE4i-mediated increase in CFTR function in W1282X/W1282X PDIOs when no other compounds are combined with the PDE4 inhibitors. Among all included PDIOs, piclamilast, roflumilast and rolipram elevated CFTR function to the highest extent. The difference between those PDE4 inhibitors and apremilast and cilomilast could be related to differences in the potency as well as PDE4 subtype selectivity. Roflumilast and piclamilast have previously been characterized by high subnanomolar potency [12,27], whereas apremilast and cilomilast were characterized as less potent [28,29]. We additionally set out to verify our results in PDIOs in a different, relevant model system. Whilst CFTR modulators such as VX-809 and VX-770 have been tested in airway-based models in prior studies [30], PDE4 inhibitor mediated CFTR rescue has not previously been described. Indeed, PDE4 inhibitor roflumilast efficiently restores CFTR function in a patient-derived, primary airway-organoid model, further highlighting the effectiveness of PDE4 inhibition.

Of the different PDIOs characterized in this study, several genotypes benefited from PDE4 inhibition as single compound, such as R334W, 3849+10kbC>T and G461R. We addition-

ally assessed the effect of PDE4 inhibition in combination with additional compounds. We show that large synergistic effects can be achieved by combination of PDE4 inhibitors and compounds with different MOAs, such as DAP and roflumilast in W1282X/W1282X PDIOs. Strikingly, PDE4 inhibition did not further increase CFTR function in F508del/F508del PDIOs. Differences in intracellular characteristics such as low cAMP levels or the lack of window of opportunity to increase CFTR function due to highly effective modulator treatment in the context of F508del CFTR, might explain this absence of the PDE4 inhibitor-related effects.

Additional to PDE4 inhibitors and CFTR modulators, we found several other hit families that may reveal new targets and pathways acting on CFTR and that could be further characterized in the future. In the secondary screen, several TKIs were found to elevate CFTR function, such as afatinib and erlotinib. Interactions between CFTR and TKIs such as afatinib have indeed previously been described, for example in the context of RTK inhibitor induced diarrhea [31]. A recent study additionally describes that EGFR TKIs potentiated the activity of potassium and CFTR chloride channels in T84 cell monolayers and rat models [32].TKIs are mainly used as anti-cancer therapeutics and are known for severe side-effects, making rapid translation of these results to the clinic challenging. Interestingly however, some TKIs have been described in the context of respiratory diseases, e.g. Nintedanib improved clinical manifestations in patients with idiopathic lung fibrosis [33]. Voxtalisib, a PI3kinase and mTOR inhibitor additionally increased organoid swelling. Inhibitors of the PI3K/Akt/mTOR pathway have previously been shown to improve F508del-*CFTR* stability and function by stimulating autophagy in CFBE cells [34]. Whether voxtalisib acts with a similar MoA remains unclear for now.

In conclusion, we implemented a high-throughput 384-wells version of the functional FIS assay to screen a large number of PDIOs for compounds that enhance CFTR function. We characterized PDE4 inhibitors as novel CFTR elevating compound family and furthermore show that CFTR modulators such as VX-809 and VX-770 might be beneficial for CF patients with *CFTR* mutations that are not eligible for CFTR modulators at present-day. As next step, we believe it is of great interest to conduct clinical studies to test the effects of roflumilast and existing CFTR modulators for those patients who could benefit from either or both based on preclinical data described in this study. Overall, our study demonstrates how preclinical studies using PDIOs can be used to initiate drug repurposing efforts. It facilitates the identification of potential treatments and responsive patients, thereby paving the way for patient stratification in the upcoming era of personalized medicine.

Supplemental Information

Supplemental data can be found Volume 63, Issue 1, at https://doi.org/10.1016/j.jcf.2023.03.004

Data availability

Overviews of the tested FDA library and the subsequentially obtained AUC data in the primary screen, are available online as respectively Supplemental File 2 & 3. All other data is available upon request.

Financial support

This work was funded by grants of the Dutch Cystic Fibrosis Foundation (NCFS) as part of the HIT-CF Program and by ZonMW grant number: 91214103.

Author Contribution statement

E.d.P. and S.S: conceptualization, methodology, investigation, formal analysis, data curation, writing - original draft & reviewing/editing, visualization. P.V.M., G.N.I., S.W.F.S., A.M.V., J.E.B., E.K., H.O., M.C.H., G.B., K.M.d.W-d.G., S.H.-M., S.R.J., H.v.P., M.M.v.d.E., R.v.d.M., J.R., E.D., E. J.M.W., A.R.B., J.M.K. and G.H.K: resources, review. C.K.v.d.E and J.M.B.: conceptualization, supervision, project administration, funding acquisition, writing - original draft & reviewing/editing.

Declaration of Competing Interest

J.M.B. reports personal fees from Vertex Pharmaceuticals, Proteostasis Therapeutics, Eloxx Pharmaceuticals, Teva Pharmaceutical Industries and Galapagos, outside the submitted work; In addition, J.M.B. has a patent(s) related to the FIS-assay with royalties paid. C.K.v.d.E. reports grants from GSK, grants from Nutricia, TEVA, Gilead, Vertex, ProQR, Proteostasis, Galapagos NV and Eloxx outside the submitted work; In addition, C.K.v.d.E. has a patent 10006904 with royalties paid. G.H.K. reports grants from Lung Foundation of the Netherlands, Vertex Pharmaceuticals, UBBO EMMIUS foundation, GSK, TEVA the Netherlands, ZON-MW (Vici-grant), European Union (H2020), outside the submitted work; and he has participated in advisory boards meetings to GSK and PURE-IMS outside the submitted work (Money to institution). All other authors have nothing to disclose.

Acknowledgments

We would like to thank the people with CF who gave informed consent for generating and testing their individual organoids; all members of the research teams of the Dutch CF clinics that contributed to this work; and all colleagues of the HUB Organoid Technology for their help with generating intestinal organoid lines.

Sup. Fig. 1

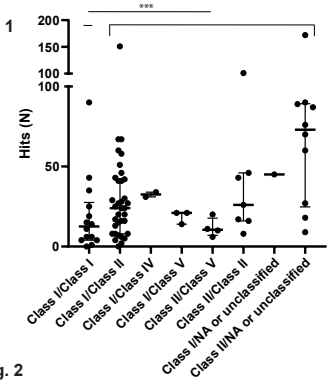

Sup. Fig. 2

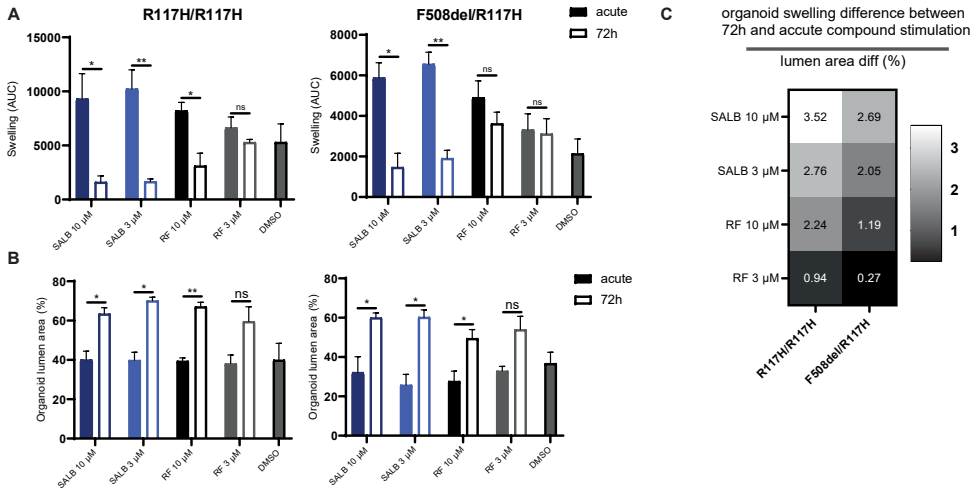

Sup. Fig. 3

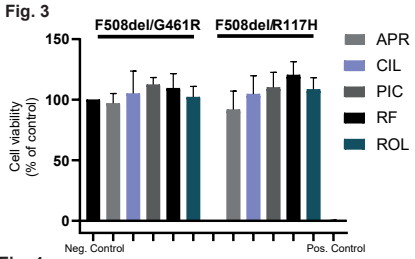

Sup. Fig. 4

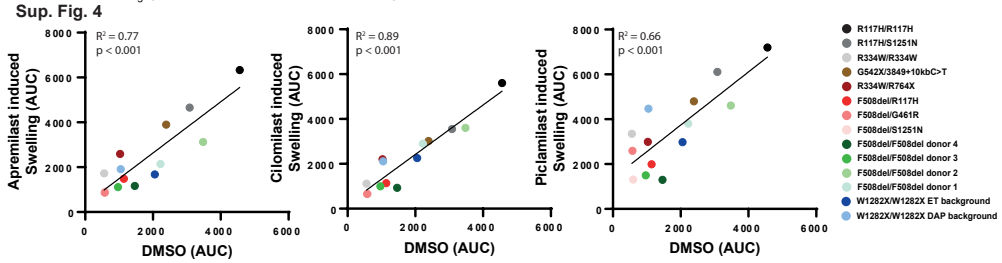

Supplemental Figure 1. Number of hits in the primary screen for each mutation class.
Medians and interquartile ranges are indicated by stripes and errorbars and are based on one technical replicate derived of one biological replicate. As data was not normally distributed, the Class I/Class I category was compared to the "other data" category, using a Mann Whitney U test underlining a significant difference (p=0,0173).

Supplemental Figure 2. Pre-incubation with roflumilast and salbutamol can result in forskolin-indepedent swelling
(A) PDIO swelling for two PDIOs upon treatment with salbutamol and roflumilast at different incubations, preincubated for 72 hours or added acutely. Bars indicate the mean of three technical replicates, derived of three biological replicates. **(B)** PDIO lumen size for the PDIOs corresponding to A, upon treatment with salbutamol and roflumilast at different incubations, preincubated for 72 hours or added acutely. Bars indicate the mean of three technical replicates, derived of three biological replicates. **(C)** Calculation of differences of organoid swelling (AUC) in response to 72hr prestimulation and acute compound treatment, divided by the lumen area (%) prior to FIS measurements. Data is shown for two PDIOs and four compounds, a value over 1 indicating that the decrease in AUC between 72hr and acute stimulation is larger than expected based on the increase of the lumen area.

Supplemental Figure 3. Viability of PDIOs treated with the different PDE4 inhibitors
Viability was normalized to vehicle-treated negative controls and and 10% DMSO treated positive controls PDIOs. Bars indicate the mean of three technical replicates, derived of three biological replicates, with errorbars indicating the SEM.

Supplemental Figure 4. Cilomilast, apremilast or piclamliast induced swelling correlates with residual CFTR function

Cilomilast (left), apremilast (middle) or piclamliast (right) induced swelling (AUC) versus background (DMSO/other) induced swelling (AUC), for 14 PDIOs indicated by the different colored dots. Dots indicate the mean of three technical replicates, derived of three biological replicates.

Supplemental Figure 5. Compound-induced swelling of PDIOs with residual function and F508del/F508del-CFTR PDIOs
(A) PDIO swelling (AUC) of 8 PDIOs upon treatment with the various PDE4 inhibitors. Bars indicate the mean of three technical replicates, derived of three biological replicates, with errorbars indicating the SEM. **(B)** PDIO swelling (AUC) of 4 F508del/F508del PDIOs upon treatment with the various PDE4 inhibitors. Bars indicate the mean of three technical replicates, derived of three biological replicates, with errorbars indicating the SEM.

Supplemental Table 1: Overview genotypes and corresponding CFTR classes of PDIOs included in primary screen, according to reference in table. Mutation categories were summarized by A: Class I/Class I, B: Class I/Class II, C: Class I/Class IV, D: Class I/Class V, E: Class II/Class V, F: Class II/Class II, G: Class I/NA or Unclassified, H: Class II/NA or Unclassified

Donor number	Genotype	Forskolin (µM)	Allele 1 Class	Allele 2 Class	Reference Allele Class	Mutation category
donor 01	1677delTA/3120+1G>A	5	I	I	Muijlwijk (2022)	A
donor 02	1717-1G>A/2183AA>G	5	I	I	Muijlwijk ((2022))	A
donor 03	1717-1G>T/3905insT	5	I	I	Muijlwijk (2022)	A
donor 04	1811+1G>C/1811+1G>C	5	I	I	Muijlwijk (2022)	A
donor 05	1811+1G>C/1811+1G>C	5	I	I	Muijlwijk (2022)	A
donor 06	1811+1G>C/1811+1G>C	5	I	I	Muijlwijk (2022)	A
donor 07	1811+1G>C/1811+1G>C	5	I	I	Muijlwijk (2022)	A
donor 08	2789+5G>T/711+1G>T	0.128	V	I	Muijlwijk (2022)	D
donor 09	3272-26A->G/G970R	0.128	V	I	Muijlwijk (2022)	D
donor 10	579+1G>T/CFTRdele11	5	I	I	Muijlwijk (2022)	A
donor 11	711+1G>T/711+1G>T	5	I	I	Muijlwijk (2022)	A
donor 12	A455E/1343delG	0.8	II	I	-	B
donor 13	A455E/E60X	0.128	II	I	Muijlwijk (2022)	B
donor 14	A455E/NA	0.128	II	NA	Muijlwijk (2022)	H
donor 15	A46D/A46D	0.8	II	II	Muijlwijk (2022)	F
donor 16	E60X/4015delATTT	5	I	I	-	A
donor 17	E92K/E92K	0.128	II	II	Muijlwijk (2022)	F
donor 18	F508del/(TG)13(T)5	0.128	II	V	Muijlwijk (2022)	E
donor 19	F508del/(TG)13(T)5	5	II	V	Muijlwijk (2022)	E
donor 20	F508del/1078delT	5	II	I	Muijlwijk (2022)	B
donor 21	F508del/1294del7	5	II	I	Niet in CFTR2	B
donor 22	F508del/1813insC	5	II	I	Muijlwijk (2022)	B
donor 23	F508del/2143delT	5	II	I	-	B
donor 24	F508del/2143delT	5	II	I	-	B
donor 25	F508del/2183AA>G	0.8	II	I	Muijlwijk (2022)	B
donor 26	F508del/2184delA	5	II	I	Muijlwijk (2022)	B
donor 27	F508del/3272-26A>G	0.128	II	V	Muijlwijk (2022)	E
donor 28	F508del/3500-2A->G	5	II	I	-	B
donor 29	F508del/ 365-366insT(W79fs)	0.8	II	I	Muijlwijk (2022)	B
donor 30	F508del/3659delC	5	II	I	Muijlwijk (2022)	B
donor 31	F508del/394delTT	0.8	II	I	Muijlwijk (2022)	B
donor 32	F508del/4374+1G>T	5	II	I	Muijlwijk (2022)	B
donor 33	F508del/4382delA	5	II	V	Muijlwijk (2022)	E
donor 34	F508del/711+1G>T	5	II	I	Muijlwijk (2022)	B
donor 35	F508del/711+1G>T	5	II	I	Muijlwijk (2022)	B
donor 36	F508del/711+1G>T	5	II	I	Muijlwijk (2022)	B
donor 37	F508del/CFTRdele17a.17b	5	II	I	Muijlwijk (2022)	B
donor 38	F508del/CFTRdele17a.17b	5	II	I	Muijlwijk (2022)	B
donor 39	F508del/CFTRdele19.20	5	II	I	Muijlwijk (2022)	B
donor 40	F508del/CFTRdele2.3	5	II	I	-	B
donor 41	F508del/CFTRdele2.3	5	II	I	-	B
donor 42	F508del/E60X	5	II	I	Muijlwijk (2022)	B
donor 43	F508del/E730X	0.8	II	I	Muijlwijk (2022)	B
donor 44	F508del/G1249R	5	II	Unclassified	Muijlwijk (2022)	H
donor 45	F508del/G461R	0.128	II	Unclassified	Muijlwijk (2022)	H
donor 46	F508del/G461R	0.128	II	Unclassified	Muijlwijk (2022)	H
donor 47	F508del/G461R	0.128	II	Unclassified	Muijlwijk (2022)	H
donor 48	F508del/G550X	5	II	I	Muijlwijk (2022)	B
donor 49	F508del/G550X	5	II	I	Muijlwijk	B

donor 52	F508del/L927P	5	II	Unclassified	Muijlwijk (2022)	H
donor 53	F508del/R1066C	0.8	II	II	Muijlwijk (2022)	F
donor 54	F508del/R347P	0.128	II	II	Muijlwijk (2022)	F
donor 55	F508del/R347P	0.128	II	II	Muijlwijk (2022)	F
donor 56	F508del/R347P	0.128	II	II	Muijlwijk (2022)	F
donor 57	F508del/R74P	0.8	II	Unclassified	Muijlwijk (2022)	H
donor 58	F508del/S489X	5	II	I	Muijlwijk (2022)	B
donor 59	F508del/W1282X	5	II	I	Muijlwijk (2022)	B
donor 60	F508del/W1282X	5	II	I	Muijlwijk (2022)	B
donor 61	F508del/Y1092X	5	II	I	Muijlwijk (2022)	B
donor 62	F508del/Y1092X	0.8	II	I	Muijlwijk (2022)	B
donor 63	F508del/Y1092X	5	II	I	Muijlwijk (2022)	B
donor 64	F508del/Y109D	0.8	II	Unclassified	Muijlwijk (2022)	H
donor 65	G542X/CFTRdele2.3	5	I	I	-	A
donor 66	G542X/G542X	5	I	I	Muijlwijk (2022)	A
donor 67	G542X/R1066C	5	I	II	-	B
donor 68	N1303K/G550X	5	II	I	Muijlwijk (2022)	B
donor 69	R1162X/3539del16	5	I	I	-	A
donor 70	R1162X/3659delC	5	I	I	Muijlwijk (2022)	A
donor 71	R117H-7T/T1857delT	0.128	IV	I	-	C
donor 72	R334W/R334W	0.128	II	II	Muijlwijk (2022)	F
donor 73	R334W/R764X	0.128	IV	I	Muijlwijk (2022)	C
donor 74	R553X/NA	0.128	I	NA	Muijlwijk (2022)	G
donor 75	Y275X/A559T	0.8	I	II	Shishido, 2020	B
donor 76	Y849X/2789+5G>A	0.128	I	V	Muijlwijk (2022)	D

Supplemental Table 2: Overview of hits in primary FDA screen per mutation category, including mean number of hits, the top-responders and the lowest responders.

Category	Median number of hits	Hits of Top Responders (N)		Hits of Top Non-Responders (N)	
Class I/Class I	12.5	90 43 35	R1162X/3659delC donor 70 579+1G>T/CFTRdele11 donor 10 711+1G>T/711+1G>T donor 11	4 1 0	R1162X/3539del16 donor 69 1811+1G>C/1811+1G>C donor 04 1811+1G>C/1811+1G>C donor 06
Class I/Class II	24	151 67 67	F508del/394delTT donor 31 F508del/Y1092X donor 63 F508del/CFTRdele19.20 donor 39	4 2 0	F508del/3500-2A->G donor 28 F508del/711+1G>T donor 35 F508del/711+1G>T donor 34
Class I/Class IV	32.5	34	R117H-7T/T1857delT donor 71	31	R334W/R764X donor 73
Class I/Class V	21	21 21	3272-26A->G/G970R donor 09 Y849X/2789+5G>A donor 76	14	2789+5G>T/711+1G>T donor 08
Class II/Class V	10.5	11 20	F508del/(TG)13(T)5 donor 18 F508del/(TG)13(T)5 donor 19	10 6	F508del/3272-26A>G donor 27 F508del/4382delA donor 33
Class II/Class II	26	101 46 43	F508del/R347P donor 54 F508del/R347P donor 56 F508del/R1066C donor 53	17 16 8	E92K/E92K donor 17 A46D/A46D donor 15 R334W/R334W donor 72
Class I/NA or unclassified	45	45	R553X/NA donor 74		
Class II/NA or unclassified	73	172 90 89	F508del/G461R donor 47 F508del/L927P donor 52 F508del/L927P donor 51	27 18 9	F508del/G1249R donor 44 F508del/R74P donor 57 F508del/Y109D donor 64

Supplemental Table 3: Overview of genotypes of PDIOs included in the CFTR modulator screen, corresponding to **Figure 3A & 3B**

CF-number	Genotype
CF0008, CF0354, CF0239, CF0355	F508del/L927P
CF0012	E60X/4015delATTT
CF0031	R117H-7T-9T/A455E
CF0033, CF0315, CF0314, CF0394, CF0250	F508del/Y1092X
CF0035, CF0609, CF0025, CF0024, CF0021	F508del/(TG)13(T)5
CF0044	R117H-7T/R1162X
CF0049	F508del/2183AA>G
CF0050, CF0543, CF0351	F508del/E60X
CF0055, CF0170, CF0169	F508del/G461R
CF0060, CF0007, CF0011, CF0046	F508del/A455E
CF0063	R117H-7T/T1857delT
CF0068	F508del/3500-2A->G
CF0073, CF0161	F508del/G1249R
CF0077, CF0076, CF0211, CF0040, CF0212	F508del/R1162X
CF0088	A455E/S1251N
CF0092	R334W/R764X
CF0122	R117H/I1139V

CF0134, CF0135, CF0517,CF0291, CF0304, CF0594	F508del/711+1G>T
CF0138	F508del/(TG)12(T)5
CF0139	1677delTA/IVS16+1G>A(3120+1G>A)
CF0140	S1251N/R117H
CF0141	F508del/S945L
CF0160	A455E/E60X
CF0167, CF0126, CF0196, CF0124, CF0099, CF0190, CF0154, CF0067, CF0109, CF0216, CF0061, CF0141, CF0053, CF0114, CF0112	F508del/S1251N
CF0171	F508del/Gly1349fs
CF0174	2105-2117del13insAGAAA/Q1352H
CF0175	F508del/365-366insT(W79fs)
CF0181	1717-1G>A/2183AA>G
CF0191	F508del/4374+1G>T
CF0198	R553X/c.4375-3T>A
CF0217	F508del/E730X
CF0219, CF0238, CF0176	F508del/R347P
CF0224	711+1G>T/711+1G>T
CF0225	F508del/L1034P
CF0227	3272-26A>G/G970R
CF0231, CF0228, CF0607, CF0606	F508del/3272-26A>G
CF0236	711+1G>T/CFTRdele11
CF0253	F508del/Q1313X
CF0256	R334W/R334W
CF0262	F508del/D1152H
CF0269	F508del/G85E
CF0270	F508del/2184delA
CF0271, CF0168, CF0271, CF0188	1811+1G>C/1811+1G>C
CF0272	E92K/E92K
CF0278	F508del/W846X
CF0289	R1162X/3659delC
CF0296	N1303K/G550X
CF0297	F508del/1294del7
CF0303	A455E/3659delC
CF0307	F508del/3849+5G->A
CF0308	F508del/621+1G>T
CF0317	F508del/CFTRdele19.20
CF0328	F508del/2184insA
CF0334	R1066H/CFTRdele2.3
CF0335, CF0593	F508del/1078delT
CF0340	F508del/Y109D
CF0341	F508del/S489X

CF0342, CF0375	F508del/2143delT
CF0346	F508del/1813insC
CF0348	F508del/R74P
CF0349	F508del/4382delA
CF0357	R1162X/3539del16
CF0358	F508del/c.1725-1727del insAT
CF0359	F508del/394delTT
CF0360, CF0361	A46D/A46D
CF0373, CF0520	F508del/Y849X
CF0378	F508del/3905insT
CF0388	F508del/G550X
CF0391 CF0822	G542X/R1066C
CF0392	W1282X/L927P
CF0396	Y849X/2789+5G>A
CF0398	1717-1G>A/3905insT
CF0400	R1066C/R1066H
CF0401	3849+10kbC>T/R347H
CF0406	F508del/4383delA
CF0412	Y275X/A559T
CF0414	1078delT/3272-26A>G
CF0419	A455E/1343delG
CF0422, CF0458, CF0215	F508del/G628R
CF0432, CF0403	F508del/R1066C
CF0437	F508del/IVS11-1G>C
CF0442	F508del/4016insT
CF0460	F508del/L732X
CF0477	F508del/3659delC
CF0478	3905insT/D1152H
CF0480	F508del/R75Q
CF0487	F508del/L206W
CF0488	F508del/Q493X
CF0489	G542X/W679X
CF0523, CF0623, CF0326	F508del/S18I
CF0534	F508del/I1027T
CF0551	F508del/1342-1delG
CF0556	F508del/c.4243-3T>A
CF0563	N1303K/c.3035A>C
CF0570	(TG)12(T)7/(TG)11(T)7
CF0572, CF0597	R1162X/D1152H
CF0574	F508del/G576A
CF0576	3272-26A>G/1898+5G>T

CF0579	N1303K/G85E
CF0583	F508del/1682dup
CF0588	L732X/L732X
CF0592, CF0248, CF0384, CF0621, CF0433	F508del/CFTRdele17a.17b
CF0596	F508del/I507del
CF0600	F508del/R1158X
CF0608	R785X/R785X
CF0610	F508del/R1358S
CF0612	3272-26A>G/3272-26A>G
CF0641	G85E/1677delTA
CF0645	R1162X/3849+10kbC>T
CF0665	F508del/I336K
CF0667	F508del/S586N
CF0669	L1335P/L1335P
CF0671	F508del/H620P
CF0696	R553X/4005+2T-c
CF0699	F508del/L453S
CF0705	F508del/T1396P
CF0706, CF0187	F508del/(TG)11(T)5
CF0710	S1251N/1717-1G>A
CF0712	F508del/G1249E
CF0715	4382delA/2043delG
CF0733	L206W/S1235R
CF0744	V1160T/E92K
CF0754	F508del/Ile336fs
CF0823	G542X/P988R
CF0829	A455E/711+5G>T
CF0841	F508del/R352W
CF0844	F508del/c.3407_3422del

Supplemental Table 4: Overview of genotypes and corresponding mutation category of reference PDIOs included in CFTR modulator screen, corresponding to **Figure 3C.**

Category	Genotype	N
F508del/RF_splice	F508del/2789+5G>A	3
	F508del/3272-26A>G	4
	F508del/3849+10kbC>T	5
F508del/RF_missense	F508del/G551D	2
	F508del/D1152H	1
	F508del/L206W	1
	F508del/S945L	1
	F508del/A445E	4
S1251N/other	S1251N/F508del	15
	S1251N/1717-1G>A	1
R117H/other	R117H/F508del	6
	R117H/R1162X	1
	R117G/R553X	1
	R117H/T1857delT	1
	R117H/W1282X	1
F508del/minimal	F508del/W1282X	5
	F508del/R1066C	2
	F508del/Y1092X	5
	F508del/N1303K	5
	F508del/G85E	2
	F508del/1078delT	1
	F508del/1717-1G>A	4
	F508del/2184delA	2
	F508del/I507del	1
	F508del/R553X	1
	F508del/1078delT	1
	F508del/2143delT	2
	F508del/2183AA>G	1
	F508del/3659delC	2
	F508del/3905insT	1
	F508del/394delTT	1
	F508del/CFTRdele2.3	3
	F508del/G542X	1
F508del/F508del	F508del/F508del	1

Supplemental Table 5: List of compounds used in this study, corresponding to **Materials & Methods.**

Compound	Final concentration	Incubation time	Manufacturer	Product number
Vinpocetine (PDE1i)	3 µM	24h	Sigma	V6383
BAY 60-7550 (PDE2i)	3 µM	24h	Cayman	10011135
Milrinone (PDE3i)	3 µM	24h	Cayman	13357
Cilostazol (PDE3i)	3 µM	24h	Supelco	PHR1503
Trequinsin (PDE3/4i)	3 µM	24h	Cayman	17217
D159687 (PDE4Di)	3 µM	24h	MedChem Express	HY-15444
Sildenafil (PDE5i)	3 µM	24h	MedChem Express	HY-15025A
BRL-50481 (PDE7i)	3 µM	24h	Cayman	16899
BAY 73-6691 (PDE9i)	3 µM	24h	SantaCruz	SC-252407
PF-2545920 (PDE10i)	3 µM	24h	Cayman	18266
IBMX (panPDEi)	3 µM	24h	Sigma	I7018
Zaprinast (panPDEi)	3 µM	24h	Alfa Aesar	J63326.MA
apremilast	0.493 µM	Acute	Toronto Research Chemicals	A729700
cilomilast	0.493 µM	Acute	SelleckChem	S1455
piclamilast	0.493 µM	Acute	SelleckChem	SML0585
roflumilast	0.493 µM	Acute	SelleckChem	S2131
rolipram	0.493 µM	Acute	SelleckChem	S1430
Valsartan	3 µM	24h	SelleckChem	S1894
Lovastatin	3 µM	24h	SelleckChem	S2061
Pitavastatin calcium	3 µM	24h	SelleckChem	S1759
Alibendol	3 µM	24h	MedChem Express	HY-B0326
Fenspiride HCl	3 µM	24h	TargetMoi	T0383
Mevastatin	3 µM	24h	Cayman	10010340
Guaifenesin	3 µM	24h	SelleckChem	S1740
Fluvastatin Sodium	3 µM	24h	Cayman	10010337
Simvastatin	3 µM	24h	Cayman	10010344
Tamoxifen Citrate	3 µM	24h	SelleckChem	S1972
VX-770	3 µM	Acute	SelleckChem	S1144
VX-445, VX-661, VX-809	3 µM	24h	SelleckChem	S8851, S7059, S1565
ELX-02ds	80 µM	48h	MedChem Express	HY-114231B
DAP	50 µM	48h	Gift of Fabrice Lejeune lab	
SMGi1	0.3 µM	24h	Gift of CFF	

Supplemental Table 6: List of primers used in this study, corresponding to **Materials & Methods.**

Primer Target	Primer sequence
PDE4A FW	GTGGCTCCGGATGAGTTCTC
PDE4A REV	GGGCTGCTGTGGCTTACAG
PDE4B FW	CCGATCGCATTCAGGTCCTTCGC
PDE4B REV	TTTCCATTCCCCTCTCCCGCT
PDE4C FW	ACTCTGGAGGAGGCAGAGGAA
PDE4C REV	AGGCAACTCCAAGGCCTCTT
PDE4D FW	TGCTCAGGTCTTGGCCAGTCTGC

References

1. Ashburn TT, Thor KB. Drug repositioning: identifying and developing new uses for existing drugs. Nat Rev Drug Disco. 2004;3(8):673–83.
2. Huang F, *et al*. Identification of amitriptyline HCl, flavin adenine dinucleotide, azacitidine and calcitriol as repurposing drugs for influenza A H5N1 virus-induced lung injury. PLoS Pathog 2020;16(3):e1008341.
3. Despotes KA, Donaldson SH. Current state of CFTR modulators for treatment of cystic fibrosis. Curr Opin Pharmacol 2022;65:102239.
4. Vonk AM, *et al*. Protocol for application, standardization and validation of the forskolin-induced swelling assay in cystic fibrosis human colon organoids. STAR Protoc 2020;1(1):100019. doi:10.1016/j.xpro.2020.100019.
5. de Winter-de Groot KM, *et al*. Stratifying infants with cystic fibrosis for disease severity using intestinal organoid swelling as a biomarker of CFTR function. Eur Respir J 2018;52(3).
6. Dekkers JF, *et al*. A functional CFTR assay using primary cystic fibrosis intestinal organoids. Nat Med 2013;19(7):939–45.
7. Dekkers JF, *et al*. Characterizing responses to CFTR-modulating drugs using rectal organoids derived from subjects with cystic fibrosis. Sci Transl Med 2016;8(344) 344ra84-344ra84.
8. Berkers G, *et al*. Rectal organoids enable personalized treatment of cystic fibrosis. Cell Rep 2019;26(7):1701–8.
9. Muilwijk D, *et al*. Forskolin-induced Organoid Swelling is Associated with Long-term CF Disease Progression. Eur Respir J 2022.
10. Clancy JP, *et al*. CFTR modulator theratyping: current status, gaps and future directions. J Cyst Fibros 2019;18(1):22–34.
11. Spelier S, *et al*. High-throughput functional assay in cystic fibrosis patient-derived organoids allows drug repurposing. Biorxiv 2022.
12. Garnock-Jones KP. Roflumilast: a review in COPD. Drugs 2015;75(14):1645–56. doi:10.1007/s40265-015-0463-1.
13. Mauro MJ. Lifelong TKI therapy: how to manage cardiovascular and other risks. Hematology 2021;2021(1):113–21.
14. Shishido H, Yoon JS, Yang Z, Skach WR. CFTR trafficking mutations disrupt co–translational protein folding by targeting biosynthetic intermediates. Nat Commun 2020;11(1):1–11.
15. Chai SC, Goktug AN, Chen T. Assay validation in high throughput screening–from concept to application. Drug Discov Dev Mol Med 2015.
16. Pottier C, Fresnais M, Gilon M, Jérusalem G, Longuespée R, Sounni NE. Tyrosine kinase inhibitors in cancer: breakthrough and challenges of targeted therapy. Cancers (Basel) 2020;12(3):731.
17. Keravis T, Lugnier C. Cyclic nucleotide phosphodiesterase (PDE) isozymes as targets of the intracellular signalling network: benefits of PDE inhibitors in various diseases and perspectives for future therapeutic developments. Br J Pharmacol 2012;165(5): 1288–305.
18. Brewington JJ, *et al*. Chronic β2AR stimulation limits CFTR activation in human airway epithelia. JCI Insight 2018;3(4).
19. Trzaska C, *et al*. 2, 6-Diaminopurine as a highly potent corrector of UGA nonsense mutations. Nat Commun 2020;11(1):1–12.
20. Driehuis E, *et al*. Oral mucosal organoids as a potential platform for personalized cancer therapy. Cancer Discov 2019.
21. Folkesson E, *et al*. High-throughput screening reveals higher synergistic effect of MEK inhibitor combinations in colon cancer spheroids. Sci Rep 2020;10(1):1–14.
22. Schütte M, *et al*. Molecular dissection of colorectal cancer in pre-clinical models identifies biomarkers predicting sensitivity to EGFR inhibitors. Nat Commun 2017;8(1): 1–19.
23. Jiang JX, *et al*. A new platform for high-throughput therapy testing on iPSC-derived lung progenitor cells from cystic fibrosis patients. Stem Cell Rep 2021;16(11):2825–37.
24. Berg A, *et al*. High-throughput surface liquid absorption and secretion assays to identify F508del CFTR correctors using patient primary airway epithelial cultures. SLAS Discov Adv Life Sci R&D 2019;24(7):724–37.
25. Rodenburg LW, *et al*. Drug repurposing for Cystic Fibrosis: identification of drugs that induce CFTR-independent fluid secretion in nasal organoids. Int J Mol Sci 2022;23(20):12657.
26. Vertex, Trikafta Prescribing Information (2021), https://www.accessdata.fda. gov/drugsatfda_docs/label/2021/212273s004lbl.pdf.
27. Zhao YU, Zhang H-T, O'Donnell JM. Inhibitor binding to type 4 phosphodiesterase (PDE4) assessed using [3H] piclamilast and [3H] rolipram. J Pharmacol Exp Ther 2003;305(2):565–72.
28. Huai Q, *et al*. Enantiomer discrimination illustrated by the high resolution crystal structures of type 4 phosphodiesterase. J Med Chem 2006;49(6):1867–73.
29. Schafer PH, *et al*. Apremilast, a cAMP phosphodiesterase-4 inhibitor, demonstrates anti-inflammatory activity *in vitro* and in a model of psoriasis. Br J Pharmacol 2010;159(4):842–55.
30. Amatngalim GD, *et al*. Measuring cystic fibrosis drug responses in organoids derived from 2D differentiated nasal epithelia. Life Sci Alliance 2022;5(12).
31. Yokota H, *et al*. Relationship between plasma concentrations of afatinib and the onset of diarrhea in patients with non-small cell lung cancer. Biology (Basel) 2021;10(10):1054.
32. Duan T, Cil O, Thiagarajah JR, Verkman AS. Intestinal epithelial potassium channels and CFTR chloride channels activated in ErbB tyrosine kinase inhibitor diarrhea. JCI insight 2019;4(4).
33. Brown KK, *et al*. Lung function outcomes in the INPULSIS® trials of Nintedanib in idiopathic pulmonary fibrosis. Respir Med 2019;146:42–8.
34. Reilly R, *et al*. Targeting the PI3K/Akt/mTOR signalling pathway in Cystic Fibrosis. Sci Rep 2017;7(1):1–13. doi:10.1038/s41598-017-06588-z.
35. Flume PA, *et al*. Ivacaftor in subjects with cystic fibrosis who are homozygous for the F508del-CFTR mutation. Chest 2012;142(3):718–24. doi:10.1378/chest. 11-2672.

36. Rowe SM, *et al*. Lumacaftor/ivacaftor treatment of patients with cystic fibrosis heterozygous for F508del-CFTR. Ann Am Thorac So. 2017;14(2):213–19. doi:10. 1513/ AnnalsATS.201609-689OC.
37. Rowe SM, *et al*. Tezacaftor–ivacaftor in residual-function heterozygotes with cystic fibrosis. N Engl J Med 2017;377(21):2024–35. doi:10.1056/ nejmoa1709847.
38. Wainwright CE, *et al*. Lumacaftor–ivacaftor in patients with cystic fibrosis homozygous for Phe508del CFTR. N Engl J Med 2015;373(3):220–31. doi:10.1056/nejmoa1409547.
39. Moss RB, *et al*. Efficacy and safety of ivacaftor in patients with cystic fibrosis who have an Arg117His-CFTR mutation: a double-blind, randomised controlled trial. Lancet Respir Med 2015;3(7):524–33. doi:10.1016/S2213-2600(15) 00201-5.
40. K DB, *et al*. Efficacy and safety of ivacaftor in patients with cystic fibrosis and a non-G551D gating mutation. J Cyst Fibros 2014;13(6):674–80.

Chapter | 8

Organoid-guided synergistic treatment of minimal function CFTR mutations with CFTR modulators, roflumilast and simvastatin: a personalized approach

European Respiratory Journal, January 2024, Volume 63, Issue 1

Sacha Spelier[1,2], Karin de Winter-de Groot[1], Natascha Keijzer-Nieuwenhuijze[1,2], Yves Liem, Kors van der Ent[1], Jeffrey Beekman[1,2], Lieke S. Kamphuis[4]

1. Department of Pediatric Respiratory Medicine, Wilhelmina Children's Hospital, University Medical Center, Utrecht University, Utrecht, The Netherlands **2.** Regenerative Medicine Utrecht, University Medical Center, Utrecht University, Utrecht, The Netherlands **3.** Department of Clinical Pharmacy, Wilhelmina Children's Hospital, University Medical Center, Utrecht University, Utrecht, The Netherlands **4.** Department of Respiratory Medicine, Erasmus University Medical Center, Rotterdam, The Netherlands.

Introduction

Highly effective cystic fibrosis transmembrane conductance regulator (CFTR) protein-targeting modulator therapies (HEMTs) facilitate strong clinical improvements in a large proportion of people with CF (pwCF) [1,2]. More specifically, the EMA and FDA approved combination of the CFTR modulators elexacaftor/tezacaftor/ivacaftor (ETI) for pwCF with at least one F508del allele, whilst the FDA extended eligibility for several rare genotypes [3,4]. However, 10-15% of pwCF carry CFTR mutations that are unresponsive to HEMTs as monotherapy [1]. Furthermore, some pwCF suffer from HEMT intolerance or HEMTs are not accessible due to practical challenges such as lack of access due to high costs or legislation and approval challenges. Consequently, the focus in the CF research field has shifted towards filling the unmet clinical need for the pwCF that will not benefit from HEMTs.

We previously carried out large drug repurposing screens using patient-derived intestinal organoids (PDIOs) from pwCF with rare *CFTR* variants using forskolin-induced (FIS) assays, allowing characterization of functional CFTR [5,6]. FIS outcomes associate with clinical features of CF and treatment response, enabling compound testing in a personalized setting [3]. Three FDA-approved compound families, with favorable safety and pharmacokinetic profiles, were identified to increase CFTR function. We found that CFTR modulators have a large treatment potential for *CFTR* mutations that are not eligible for these compounds at present-day [6]. We characterized two additional FDA-approved compound families, which were not previously described to increase CFTR function. Phosphodiesterase 4 (PDE) inhibitors such as roflumilast, which is approved for obstructive lung disease treatment, presumably increase CFTR function by elevating intracellular cAMP levels, thereby increasing opening of available CFTR [6]. We additionally identified statins such as simvastatin to increase CFTR function in the context of W1282X/W1282X *CFTR*, when combined with CFTR modulator pretreatment [5]. The molecular mechanism connecting statin treatment to increased W1282X *CFTR* function remains unclear and previous clinical studies of statins as monotherapy did not show effects in pwCF (NCT00255242) [5].

Due to the diverse molecular working mechanisms of ETI, roflumilast and statins, the combination could synergistically restore CFTR function. Here, we tested this hypothesis in PDIOs using the FIS assay for 2 different *CFTR* genotypes that are not eligible for ETI at present-day and have previously been characterized as unresponsive to ETI monotreatment: L927P/W1282X and W1282X/W1282X [7,8][4]– [6]. L927P is a rare missense mutation (c.2780C>T; pLeu927Pro; allele frequency of 0,02% in CFTR2), that is overrepresented in the Belgium CF population with a 2.4% incidence rate [9,10]. L927P is a complex allele ,due to the presence of an additional 1110delGAAT mutation in cis which impacts splicing and thereby potentially masksresponse to CFTR modulators[8]. W1282X is the most prevalent premature termination codon (PTC) mutation after G542X (c.3846G>A; p.Trp128X; 1,2% allele frequency in CFTR2) with an incidence of 61% in Jewish Ashkenazi pwCF [11,12]. PTC mutations result in low levels of truncated CFTR protein and associate with severe clinical manifestations [13].The main preclinical treatment strategy for PTC mutations, is inducing translational readthrough at the PTC, yet in clinical settings results of such readthrough compounds are disappointing [14].

Here, we describe preclinical data of the drug combination of ETI, roflumilast and simvastatin in PDIOs and present a case study where an individual with L927P/W1272X *CFTR* with a severe, deteriorating clinical status received this drug combination under a compassionate use setting covered by the patients' own hospital **(Figure 1A).**

Results

Preclinical functional CFTR restoration upon combinatorial ETI, roflumilast and statin treatment

CFTR restoration was studied in PDIOs of an individual with W1282X/L927P *CFTR* and four W1282X/W1282X PDIOs. All PDIOs showed no baseline residual CFTR function. Compounds used as monotherapy or in dual combinations were mostly ineffective, yet the complete drug combination resulted in significant FIS for both genotypes, which is most clear in 3-hour measurements **(Figure 1B & Figure 1C).** Individual variation was observed between the four W1282X/W1282X PDIOs, yet trends across the various drug combinations were identical. Rescue of CFTR with the complete compound combination was higher than lumacaftor/ivacaftor FIS in F508del/minimal function (MF) for both genotypes, similar to lumacaftor/ivacaftor in F508del/F508del PDIOs and reached approximately 40% of the effect of ETI in F508del/MF PDIOs.

Case study highlights clinical improvements upon combinatorial ETI, roflumilast and simvastatin treatment

As the patient with L927P/W1282X *CFTR* experienced rapid clinical deterioration, we initiated treatment with the complete drug combination in a clinical N-of-1 setting. The 51-year old male patient colonized with a multiresistent Pseudomonas aeruginosa, received an average of four annual antipseudomonal antibiotics per year for exacerbations and received no previous CFTR modulators. Other major CF comorbidities were CF-related diabetes, pancreatic insufficiency and polyposis nasi. In recent years, his rapidly deteriorating clinical condition resulted in permanent incapacitation for work.

A trial period with simvastatin (40 mg daily), roflumilast (250 µg daily) and ETI treatment was started. Dosages were selected based on labeled indications for use in people without CF , and together with a pharmacist a drug safety monitoring plan was designed [3,15,16]. Baseline measurements of the patient were a predicted FEV1 of 74%, corresponding to an absolute FEV1 of 2.52L (day 0 of therapy start). During evaluation with his pulmonologist a week after treatment, the patient reported a major decrease of productive cough and fatigue. After 4 weeks, sweat chloride (SwCl) concentrations lowered from 106 mM to 58 mM and decrease persisted at 16 weeks of treatment (67 mM, -39 mM compared to baseline) **(Figure 1D).** Pulmonary function measurements improved considerably after 16 weeks, underlined by an absolute FEV1 of 2.85L, corresponding to an absolute increase of 9% **(Figure 1E).** The Cystic Fibrosis Questionnaire-Revised (CFQ-R) respiratory domain improved after 4 weeks treatment with 61 points (MCID 4 points) and 67 points in the vitality domain on the 100 point scale (no MCID available), but also on other subdomains **(Figure 1F)** [17,18].

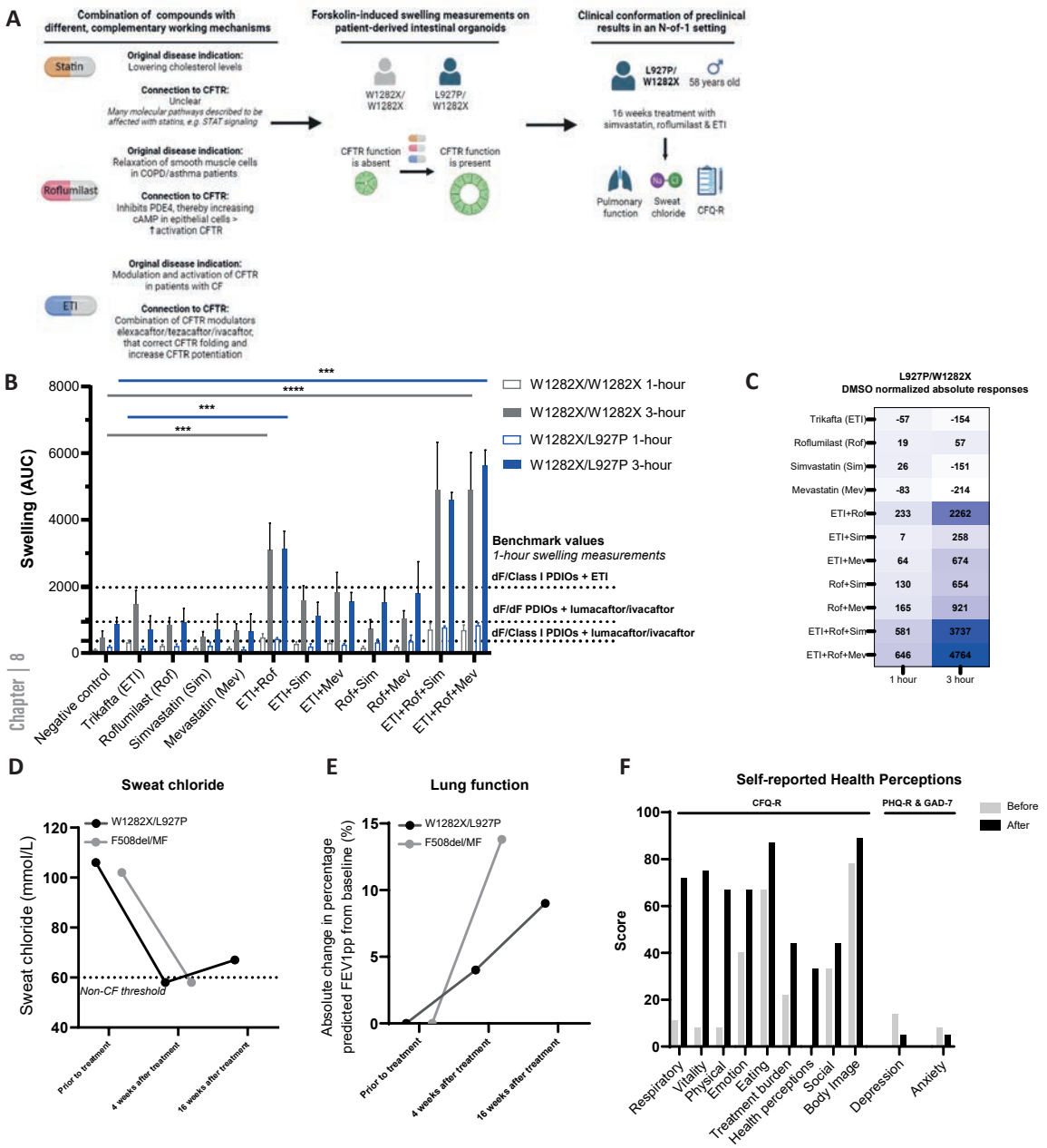

Trikafta (ETI)	-57	-154
Roflumilast (Rof)	19	57
Simvastatin (Sim)	26	-151
Mevastatin (Mev)	-83	-214
ETI+Rof	233	2262
ETI+Sim	7	258
ETI+Mev	64	674
Rof+Sim	130	654
Rof+Mev	165	921
ETI+Rof+Sim	581	3737
ETI+Rof+Mev	646	4764

Figure 1. Preclinical studies guide a successful personalized clinical treatment regimen in a person with minimal function *CFTR*, upon synergistic treatment with CFTR modulators, a cholesterol synthase inhibitor and a phosphodiesterase 4 inhibitor.
(A) Schematic pipeline of this study. We characterized synergetic effect of statins/roflumilast/ETI in a preclinical setting on patient-derived intestinal organoids (PDIOs) using the functional forskolin-induced swelling (FIS) assay, after which we characterized efficacy of simvastatin/roflumilast/ETI in a clinical N-of-1 setting in the patient with L927P/W1282X *CFTR*. **(B)** CFTR function indicated as area under the curve (AUC), as characterized by FIS in PDIOs with genotypes W1282X/L927P (indicated in blue) or W1282X/W1282X (indicated in grey), measured during 1 hour or 3 hours. Different compound combinations are indicated on the x-axis. Bars indicate the average of 3 biological replicates based on 3 technical replicates with error bars indicating the SEM. Significance was calculated using a two-way ANOVA followed by Dunnett's multiple comparisons test and is indicated by asterixis (* = P < 0.05, ** = P < 0.01, *** = P < 0.001, **** = P < 0.0001). Dotted lines indicate benchmark 1-hour FIS values for F508del (dF)/minimal function (MF) or dF/dF PDIOs treated with indicated CFTR modulators. **(C)** Absolute responses normalized for DMSO response for L927P/W1282X PDIOs. **(D)** Sweat chloride concentration at day 0 of treatment and after 4 or 16 weeks of treatment in the N-of-1 trial of a CF patient with L927P/W1282X CFTR (black line), compared to data of F508del/MF CF patients as published by Middleton et al (grey line). The dotted line indicates the threshold of non-CF sweat chloride levels. **(E)** Overview of lung function of the treated patient at day 0 of treatment and after 4 or 16 weeks upon treatment with ETI/roflumilast/simvastatin (black line), compared to data of F508del/MF CF patients as published by Middleton et al (grey line). Lung function is depicted as absolute change in percentage predicted FEV1pp. **(F)** Overview of self-reported health perceptions before (grey bars) and 4 weeks after treatment (black bars), based on CFQ-R (Cystic Fibrosis Questionnaire–Revised) domain score; range 0 to 100. High scores indicating a higher patient-reported quality of life with regard to the concerning domain, PHQ-9 (personal health questionnaire) depression score; range 0 to 27, with higher scores indicating a depressive disorder. GAD-7 (generalized anxiety disorder) questionnaire; range 0 to 21, with higher scores indicating a generalized anxiety disorder.

The self-report depression screening (PHQ-9) and anxiety questionnaires improved considerably as well **(Figure 1G)**. Importantly, over the course of the treatment, no adverse effects were detected and drug safety indicators, such as liver function, showed no anomalies.

Discussion

Here, we report that a personalized drug testing effort led to a successful clinical intervention with a novel drug combination consisting of the FDA-approved compounds, ETI, roflumilast and simvastatin in a person with two minimal function *CFTR* mutations. The potential for the individual drugs to increase CFTR function was based on previous observations, but the novel combinatory regimen was verified here using PDIOs prior to clinical intervention.

In PDIOs, FIS data highlighted that the drugs interact in a synergistic manner. Whilst single drugs were not effective, restoration of CFTR function with the complete compound combination was similar to lumacaftor/ivacaftor induced FIS in homozygous F508del PDIOs. This points into the direction of its clinical potential as lumacaftor/ivacaftor yields moderate results in homozygous F508del pwCF a clinical setting as well [19]. The observed synergy between the compounds is likely due to the different molecular mechanisms of the compounds. ETI directly interacts with the produced CFTR protein leading to improved folding, trafficking and gating of CFTR protein and PDE4 inhibitors like roflumilast can result in increased activation of CFTR by elevating intracellular cAMP levels. The exact working mechanism of simvastatin in terms of restoring CFTR function is unclear and future studies on the exact MoA of statins are warranted. FIS effects were more clear when measuring swelling during 3 hours. Whilst previous studies established optimal in vitro-in vivo correlations with 1-hour measurements, 3-hour measurements can enable better signal-over-noise measurements for *in vitro-in vivo* correlations if FIS at 1-hour measurement is low [20].

Clinically, the magnitude of response is exciting and strongly supports individual clinical benefit, but additional studies are needed. SwCl decrease was similar to observations in F508del/MF ETI treated pwCF, suggesting drug-induced effects beyond well beyond individual technical variation [21,22]. FEV1pp reaches two-third of the increase as measured in F508del/MF ETI treated PwCF, yet in absolute numbers the 9% increase in FEV1pp is substantial and beyond the 5% threshold that is considered clinically relevant [22]. The major improvements in self-reported health perceptions furthermore underline major health improvements for the patient. Whilst it could be argued that the increase in FEV1pp is partially due to roflumilast-mediated smooth muscle relaxation and as such bronchovasodilation, the change in SwCl concentration and the preclinical PDIO data, support direct modulation of CFTR in vivo. Although the magnitude of response is encouraging for this individual, a washout period showing subsequent decline is missing. As such, this single case observation needs to be interpreted with care and points to a need for additional studies. Future studies in larger subgroups with placebo-controlled cohorts should investigate the contribution of the different drugs in the context of different genotypes, such as homozygous W1282X *CFTR*.

Overall, our study shows that personalized drug testing effort can result in identification of novel treatment regimens and successful individual clinical intervention. Proceeding with further clinical studies on the combination of ETI, roflumilast and simvastatin is essential to identify how more pwCF can benefit from this therapeutic regimen.

Declaration of competing interest

JM Beekman and CK van der Ent are inventors on patent(s) related to organoid swelling, and received royalties from 2017 onwards. LK received royalties by Vertex for participation in the advisory board for psychosocial wellbeing in CF patients in 2022. All other authors declare no competing interests.

Chapter | 8

References

1. McBennett, K. A., Davis, P. B., & Konstan, M. W. (2022). Increasing life expectancy in cystic fibrosis: Advances and challenges. Pediatric Pulmonology, 57, S5–S12.
2. Riordan, J. R., Rommens, J. M., Kerem, B., Alon, N. O. A., Rozmahel, R., Grzelczak, Z., Zielenski, J., Lok, S. I., Plavsic, N., & Chou, J.-L. (1989). Identification of the cystic fibrosis gene: cloning and characterization of complementary DNA. Science, 245(4922), 1066–1073.
3. Kaftrio EMA approval. (2023). https://www.ema.europa.eu/en/medicines/human/EPAR/kaftrio#assessment-historysection
4. Kaftrio FDA approval. (2023). https://www.accessdata.fda.gov/scripts/cder/daf/index.cfm?event=overview.process&Appl No=212273
5. Spelier, S., de Poel, E., Ithakisiou, G. N., Suen, S. W. F., Hagemeijer, M. C., Muilwijk, D., Vonk, A. M., Brunsveld, J. E., Kruisselbrink, E., & van der Ent, C. K. (2023). High-throughput functional assay in cystic fibrosis patient-derived organoids allows drug repurposing. ERJ Open Research, 9(1).
6. de Poel, E., Spelier, S., Hagemeijer, M. C., van Mourik, P., Suen, S. W. F., Vonk, A. M., Brunsveld, J. E., Ithakisiou, G. N., Kruisselbrink, E., Oppelaar, H., Berkers, G., de Winter de Groot, K. M., Heida-Michel, S., Jans, S. R., van Panhuis, H., Bakker, M., van der Meer, R., Roukema, J., Dompeling, E., ... Beekman, J. M. (2023). FDA-approved drug screening in patient-derived organoids demonstrates potential of drug repurposing for rare cystic fibrosis genotypes. Journal of Cystic Fibrosis.
7. Burgel, P.-R., Sermet-Gaudelus, I., Durieu, I., Kanaan, R., Macey, J., Grenet, D., Porzio, M., Coolen-Allou, N., Chiron, R., & Marguet, C. (2023). The French compassionate programme of elexacaftor/tezacaftor/ivacaftor in people with cystic fibrosis with advanced lung disease and no F508del CFTR variant. European Respiratory Journal, 61(5).
8. Ramalho, A. S., Cuyx, S., Boon, M., Proesmans, M., Dupont, L., De Boeck, K., Verhulst, S., De Wachter, E., Van Biervliet, S., & Vermeulen, F. (2022). The importance of CFTR mRNA testing to uncover other variants in CF genotype that affect CFTR expression.
9. Levring, J., Terry, D. S., Kilic, Z., Fitzgerald, G., Blanchard, S. C., & Chen, J. (2023). CFTR function, pathology and pharmacology at single-molecule resolution. Nature, 616(7957), 606–614.
10. Storm, K., Moens, E., Vits, L., De Vlieger, H., Delaere, G., D'Hollander, M., Wuyts, W., Biervliet, M., Van Schil, L., & Desager, K. (2007). High incidence of the CFTR mutations 3272- 26A→ G and L927P in Belgian cystic fibrosis patients, and identification of three new CFTR mutations (186-2A→ G, E588V, and 1671insTATCA). Journal of Cystic Fibrosis, 6(6), 371–375.
11. Kalman, Y. M., Kerem, E., Darvasi, A., DeMarchi, J., & Kerem, B. (1994). Difference in frequencies of the cystic fibrosis alleles, ΔF508 and W1282X, between carriers and patients. European Journal of Human Genetics, 2(2), 77–82.
12. Shoshani, T., Augarten, A., Gazit, E., Bashan, N., Yahav, Y., Rivlin, Y., Tal, A., Seret, H., Yaar, L., & Kerem, E. (1992). Association of a nonsense mutation (W1282X), the most common mutation in the Ashkenazi Jewish cystic fibrosis patients in Israel, with presentation of severe disease. American Journal of Human Genetics, 50(1), 222
13. 13. de Poel, E., Spelier, S., Suen, S. W. F., Kruisselbrink, E., Graeber, S. Y., Mall, M. A., Weersink, E. J. M., van der Eerden, M. M., Koppelman, G. H., & van der Ent, C. K. (2021). Functional restoration of CFTR nonsense mutations in intestinal organoids. Journal of Cystic Fibrosis.
14. Spelier, S., van Doorn, E. P. M., van der Ent, C. K., Beekman, J. M., & Koppens, M. A. J. (2023). Readthrough compounds for nonsense mutations: bridging the translational gap. Trends in Molecular Medicine.
15. Daxas EMA approval. (2023). https://www.ema.europa.eu/en/medicines/human/EPAR/daxas
16. Simvastatin EMA approval. (2023) https://www.ema.europa.eu/en/medicines/human/referrals/simvastatin-vale
17. Quittner, A. L., Modi, A. C., Wainwright, C., Otto, K., Kirihara, J., & Montgomery, A. B. (2009). Determination of the minimal clinically important difference scores for the Cystic Fibrosis Questionnaire-Revised respiratory symptom scale in two populations of patients with cystic fibrosis and chronic Pseudomonas aeruginosa airway infection. Chest, 135(6), 1610–1618.
18. Sutharsan, S., Mondéjar-Lopez, P., Duckers, J., Pastor-Vivero, D., Barr, H., McKinnon, C., Menon, P., Heyne, M., Jennings, M., & Vega-Hernandez, G. (2023). P117 A longitudinal study on the impact of elexacaftor/tezacaftor/ivacaftor treatment on quality of life in people with cystic fibrosis in the real world. Journal of Cystic Fibrosis, 22, S99–S100.
19. Muilwijk, D., Bierlaagh, M., van Mourik, P., Kraaijkamp, J., van der Meer, R., van den Bor, R., Heijerman, H., Eijkemans, R., Beekman, J., & van der Ent, K. (2021). Prediction of real-world long-term outcomes of people with CF homozygous for the F508del mutation treated with CFTR modulators. Journal of Personalized Medicine, 11(12), 1376.
20. de Winter-de Groot, K. M., Janssens, H. M., van Uum, R. T., Dekkers, J. F., Berkers, G., Vonk, A., Kruisselbrink, E., Oppelaar, H., Vries, R., & Clevers, H. (2018). Stratifying infants with cystic fibrosis for disease severity using intestinal organoid swelling as a biomarker of CFTR function. European Respiratory Journal, 52(3).
21. Vermeulen, F., Lebecque, P., De Boeck, K., & Leal, T. (2017). Biological variability of the sweat chloride in diagnostic sweat tests: A retrospective analysis. Journal of Cystic Fibrosis, 16(1), 30–35.
22. Middleton, P. G., Mall, M. A., Dřevínek, P., Lands, L. C., McKone, E. F., Polineni, D., Ramsey, B. W., Taylor-Cousar, J. L., Tullis, E., & Vermeulen, F. (2019). Elexacaftor–tezacaftor–ivacaftor for cystic fibrosis with a single Phe508del allele. New England Journal of Medicine, 381(19), 1809–1819.

Chapter | 9

CFTR rescue in intestinal organoids with GLPG/ABBV-2737, ABBV/GLPG-2222 and ABBV/GLPG-2451 triple therapy

Frontiers Molecular Biosciences, September 2021, Volume 8

Eyleen de Poel[1,2,*], **Sacha Spelier[1,2,*],** Ricardo Korporaal[3], Ka Wai Lai[3], Sylvia F. Boj[3], Katja Conrath[4], Cornelis K. van der Ent[1] and Jeffrey M. Beekman[1,2]

**** These authors contributed equally to this work***

1. Department of Pediatric Respiratory Medicine, Wilhelmina Children's Hospital, University Medical Center, Utrecht University, Utrecht, Netherlands **2.** Regenerative Medicine Utrecht, University Medical Center, Utrecht University, Utrecht, Netherlands **3.** Hubrecht Organoid Technology (HUB), Utrecht, Netherlands **4.** Galapagos NV, Mechelen, Belgium

Abstract
Cystic fibrosis transmembrane conductance regulator (CFTR) modulators have transformed the treatment of cystic fibrosis (CF) by targeting the basis of the disease. In particular, treatment regimen consisting of multiple compounds with complementary mechanisms of action have been shown to result in optimal efficacy. Here, we assessed the efficacy of combinations of the CFTR modulators ABBV/GLPG-2222, GLPG/ABBV2737 and ABBV/GLPG-2451, and compared it to VX-770/VX-809 in 28 organoid lines heterozygous for F508del allele and a class I mutation and seven homozygous F508del organoid lines. The combination ABBV/GLPG-2222/ABBV-2737/ABBV/GLPG-2451 showed increased efficacy over VX-770/VX-809 for most organoids, despite considerable variation in efficacy between the different organoid cultures. These differences in CFTR restoration between organoids with comparable genotypes underline the relevance of continuing to optimize the ABBV/GLPG-Triple therapy, as well as the in vitro characterization of efficacy in clinically relevant models.

Keywords
Cystic fibrosis – CFTR - F508del - forskolin induced swelling assay - intestinal organoids - personalized medicine - CFTR modulator therapy

Background
Cystic fibrosis (CF) is a monogenetic, autosomal, recessive disease caused by mutations in the cystic fibrosis transmembrane conductance regulator (*CFTR*) gene [1]. Various mutations in *CFTR* have been characterized that result in dysfunction or complete absence of CFTR, which is followed by ion misbalance and subsequent aberrant fluid secretion in multiple organ systems such as the intestine, airways and pancreas [1]. For patients with common mutations, like F508del and G5551D multiple CFTR modulating compounds have been developed that rescue the mutation specific defects. These first generation CFTR modulating drugs however do not restore CFTR function in CF patients with one F508del mutation sufficiently [2]. In line with these clinical observations, *in vitro* experiments still detect the presence of immature (B-band) CFTR after treatment with CFTR corrector VX-809 treated F508del cells [3], providing the rationale for combining two correctors with a complementary mode of action that collectively further restore the trafficking defect. The recent discovery of the triple combination of VX-445/VX-661/VX-770 clearly shows that indeed a combination of two correctors with a potentiator is required to obtain high efficacy CFTR modulation [4]. However, recent clinical studies showed great variation in triple treatment efficacy, highlighting the need for expanding the pool of treatment options [5]. One such new triple therapy that showed effective rescue of CFTR in human bronchial epithelial cells is developed by Abbvie and consists of the Abbvie/GLPG correctors ABBV/GLPG-2222 and GLPG/ABBV-2737 and potentiator ABBV/GLPG-2451 [6, 7, 8]. ABBV/GLPG-2222 and ABBV/GLPG-2451 exhibit similarities in biological activity with respectively VX-809 and VX-770, but rescue F508del-CFTR more potently [9]. In an effort to further increase the efficacy of the combination of ABBV/GLPG-2222/ABBV/GLPG-2451, another corrector with a complementary mode of action, termed GLPG/ABBV-2737 was developed that exerted functional synergy with ABBV/GLPG-2222 and VX-809 [7]. Combining these modulators into a triple therapy resulted in a two-fold increase in Cl– current in F508del/F508del HBE cells compared to VX770/VX809 treatment.

In this report we compare the efficacy of single, dual or triple combinations of ABBV/GLPG-2222, GLPG/ABBV-2737 and ABBV/GLPG-2451 to VX-809/VX-770 using intestinal organoids and the forskolin (FSK) induced swelling (FIS) assay [10]. In vitro FIS response of patient-derived intestinal organoids upon modulator therapy has been shown to predict in vivo response to therapy, making this model a relevant model in the context of preclinical drug discovery and lead selection [11, 12]. To assess efficacy and between-patient variability of the ABBV/GLPG-compounds on rescuing F508del-CFTR, we measured FIS in 35 intestinal organoid cultures, seven expressing F508del/F508del-CFTR and 28 expressing F508del/minimal function CFTR. All organoids cultures did not exhibit swelling when exposed to solely forskolin, indicating the absence of residual CFTR function for all organoid cultures. Ultimately, the aim of this report is to assess the preclinical efficacy of a newly developed triple therapy and to identify people with CF likely to benefit from modulator therapy.

Materials and Methods
Collection of primary epithelial cells
All experimentation using human tissues described herein was approved by the medical ethical committee at University Medical Center Utrecht (UMCU; TcBio#14-008) and performed following the guidelines of the European Network of Research Ethics Committees (EUREC) following European, national, and local law. Informed consent for tissue collection, generation, storage, and use of the organoids was obtained from all study participants. Biobanked intestinal organoids are stored and catalogued at the foundation Hubrecht Organoid Technology (HUB, http://hub4organoids.eu).

Organoid culture and FIS assay
Crypts were isolated from rectal biopsies of subjects with cystic fibrosis as previously described (Dekkers *et al*., 2013). In brief, biopsies were washed with cold DMEM/F12 and incubated with 10 mM EDTA for 30 min. After harvesting the crypts containing supernatant, EDTA was washed away and crypts were seeded in 50% matrigel in 24 well plates (–10–30 crypts in three 10 ml Matrigel droplets per well). Growth medium (Paranjapye *et al*., 2020) was further supplemented with Primocin (1:500; Invivogen). Organoids were incubated in a humidified chamber with 5% CO2 at 37°C. Medium was refreshed every 2–3 days, and organoids were passaged 1:4 every 7 days. Prior to conducting FIS assays, organoids were cultured at least 3 weeks after thawing or crypt isolation. To quantify the organoid size increase over time, organoids are stained with calcein green (10 µM) which is added 30 min prior to the addition of forskolin and CFTR potentiators ABBV/GLPG-2451 and VX-770. All CFTR correctors ABBV/GLPG-2222 and GLPG/ABBV-2737 were added during plating of the organoids, 24 h prior to the FIS-assay. Forskolin was used at a 5 µM concentration, except in the FIS assay on F508del/F508del donors in which forskolin was used at 0.8 µM.

Chapter | 9

All CFTR modulators were used at a 3 μM, with the exception of the FIS assay on F508del/F508del donors in which all ABBV/GLPG2451 and GLPLG/ABBV-2737 were used at 1 μM and ABBV/GLPG-2222 at 0.15 μM. Organoid swelling was measured using a confocal microscope, followed by quantification of total organoid surface area per well based on calcein staining. To correct for well to well differences in total organoid area, increase of organoid surface area over time was normalized to the organoid surface area of the first time point for each well as earlier described [11]. All experiments with GLPG/ABBV compounds were conducted with two to three technical replicates. Orkambi stimulated FIS served as a positive control, while FIS with only forskolin served as negative control.

Results

Rescue of minimal-function and residual-function CFTR mutations with ABBV/GLPG-2222, GLPG/ABBV-2737 and ABBV/GLPG-2451

New therapies under development for F508del should be sufficiently efficacious for people with a single F508del allele. For this reason, we first compared the efficacy of compounds on three organoid cultures with F508del in compound heterozygosity with established and characterized non-functional class I alleles so that impact of treatment on a single F508del was established **(Figure 1, Supplemental Table 1).** Whereas single compounds did not result in increased levels of organoid swelling in F508del/R1162X and F508del/711 + 1G > T, it resulted in a mild increase in swelling (± 1000 AUC) for the F508del/W1282x organoid culture. The two dual combinations of one corrector (ABBV/GLPG-2222 or GLPG/ABBV-2737) and the potentiator ABBV/GLPG-2451, resulted in substantial swelling. For two organoid cultures, expressing F508del/R1162X and F508del/711+1G > T CFTR, the combination of all three ABBV/GLPG compounds resulted in a further increased AUC. Interestingly, the combination of one corrector and ABBV/GLPG-2451 resulted in similar swelling levels as the ABBV/GLPG-Triple in the W1282X organoid culture.

Next, the ABBV/GLPG-Triple as well as VX-809/VX-770 were tested on 28 organoid cultures harboring F508del/minimal function genotypes **(Figure 2A, Supplemental Table 1).** Upon exposure to the ABBV/GLPG-Triple substantial AUC values were observed (AUC >2000 for 19/28 lines). Although the efficacy of the triple therapy greatly varied between the different organoid cultures, organoid swelling increased on average by 297% with the ABBV/GLPG-Triple compared to VX-809/VX-770 **(Figure 2B, Supplemental Table 1).** Not only did we observe large variation in CFTR function rescue between organoids expressing distinct F508del/minimal function genotypes, we also observed variation in treatment response between organoids expressing F508del/F508del-CFTR **(Figure 2C, Supplemental Table 1).** Moreover, we compared Orkambi response and ABBV/GLPG-Triple response in the panel of 28 organoid lines and observed a linear positive correlation (R = 0.57) indicating that organoid cultures that respond to Orkambi are likely to regain CFTR when treated with the ABBV/GLPG-Triple **(Figure 2D, Supplemental Table 1).**

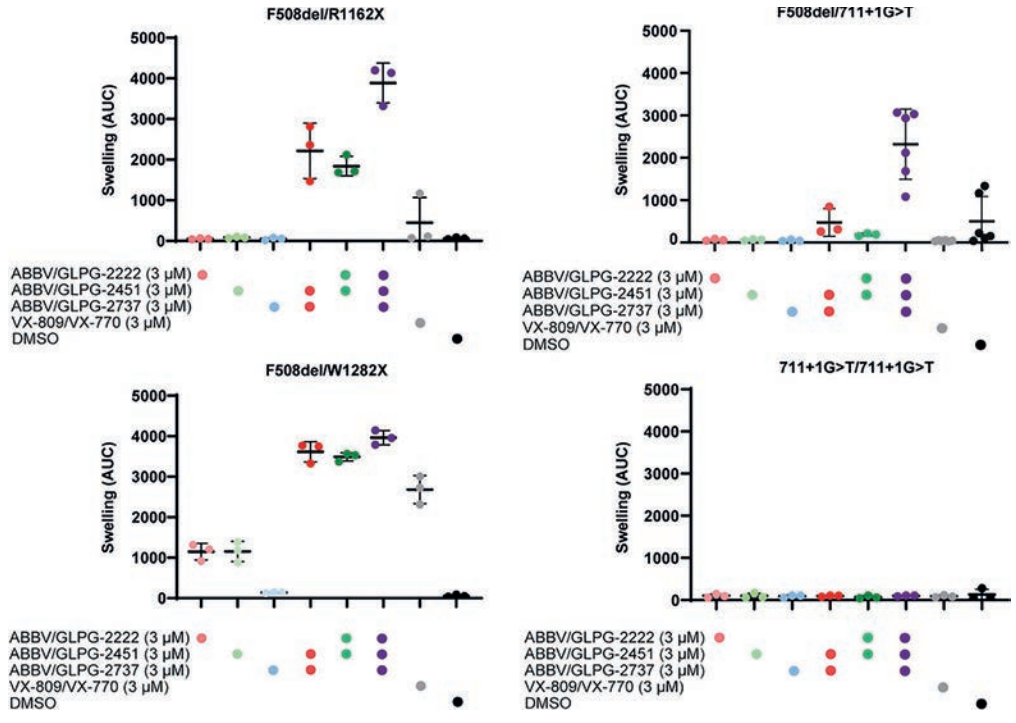

Figure 1. CFTR function rescue with single, dual and triple ABBV/GLPG modulator therapy in intestinal organoids.
FIS responses of three organoid cultures expressing F508del/minimal function genotypes and one organoid culture homozygous for 711+1G > T, stimulated with 5.0 μM forskolin for 1h. FIS responses were measured upon treatment with ABBV/GLPG compounds, VX-809/VX-770 and DMSO. n = 3 or n = 6, each bar represents mean ± SD.

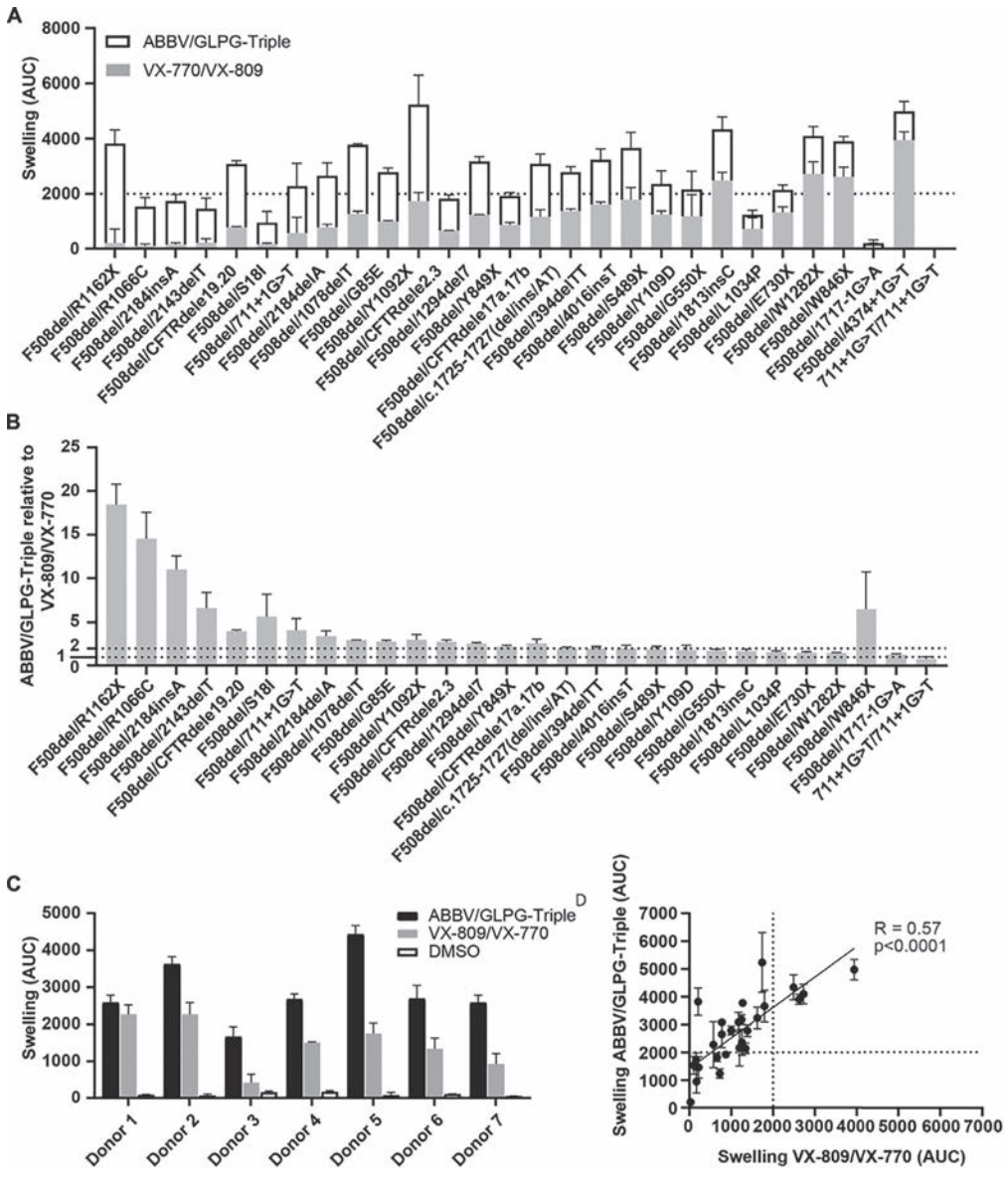

Figure 2. FIS response of F508del/minimal function organoid cultures upon ABBV/GLPG-Triple therapy.

A. FIS response upon VX-770/VX-809 (3 μM, gray bars) and Abbvie-Triple (ABBV/GLPG-2222 3 μM + GLPG/ABBV-2737 3 μM + ABBV/GLPG-2451 3 μM,white bars, stacked) treatment, corrected for the DMSO condition. n = 3, each bar represents mean + SD. CFTR correctors were added 24h prior to FIS measurements, CFTR potentiators were simultaniously added with 5 μM FSK.

B. FIS reponse upon the ABBV/GLPG-Triple (3 μM) relative to VX-770/VX-809 (3 μM) treatment, both corrected for the DMSO condition. n = 3, each bar represents mean + SD. Similar raw data was used in A and B, yet differentially illustrated. **C.** FIS response of seven F508del/F508del organoid cultures upon treatment with ABBV/GLPG-Triple (ABBV/GLPG-2222 1 μM + GLPG/AB BV-2737 1 μM + ABBV/GLPG-2451 1 μM) or VX-809/VX-770 (1 μM) and 0.8 μM FSK. n = 3, bars represent mean + SD.

D. Correlation of FIS responses upon the ABBV/GLPG-Triple (3 μM) and VX-770/VX-809 (3 μM) treatment, n = 3, each datapoint represents mean ± SD.

Discussion

The objective of this study was to assess efficacy of CFTR-F508del restoration by the single ABBV/GLPG modulators (ABBV/GLPG-2222/GLPG/ABBV-2737/ABBV/GLPG-2451) and all combinations thereof in comparison to VX-809/VX-770 by measuring FIS in organoids carrying at least one single F508del allele. We observed highest CFTR-restoring efficacy with the ABBV/GLPG-Triple, which is consistent with previous studies showing the additive effect on CFTR function rescue with three compounds with complementing working mechanisms [4]. In 19 organoid cultures, AUC values of over 2000 were observed with the ABBV/GLPG-Triple. Comparable AUC values are obtained with VX-809/VX-770 and F508del/F508del organoids [around 2500 AUC, [11]], indicating that clinical efficacy of the ABBV/GLPG-Triple for pwCF compound heterozygous for F508del might be similar to the clinical effect of VX-809/VX-770 for pwCF homozygous for F508del-*CFTR*.

Interestingly, despite this general high efficacy, we observed great variation in response between both F508del/minimal function as well as between the F508del/F508del organoid cultures. The latter observation might indicate the presence of other cis-mutations in the CFTR gene or other genetic modifiers affecting CFTR-mediated fluid transport, two processes summarized in an excellent recent review [13]. Another possible explanation for the variation in drug efficacy between the F508del/minimal function organoids might be partial rescue of the minimal function allele with the ABBV/GLPG-modulators. We observed for example in the F508del/W1282X organoid culture some swelling response when pretreated with only one corrector, and hardly a difference between the dual ABBV/GLPG combinations and the triple ABBV/GLPG combination. This could be explained by the fact that the premature termination codon (PTC) mutation occurs late in the *CFTR* gene, resulting in only a minor truncation of the W1282X CFTR variant allowing further rescue by CFTR modulators, such as VX-770 as earlier described by [12]. This illustrates the potential contribution of the compound heterozygous mutations to the observed differences. In order to assess whether the variation in drug efficacy among pwCF is the result of rescue of the minimal function allele, future drug efficacy studies should also include allele specific biochemical analysis. Additional to the observed variation, two F508del/minimal function organoid cultures (expressing F508del/W846X and F508del/44374+1G > T CFTR) hardly responded to either VX-770/VX-809 or ABBV/GLPG-Triple, which corresponds to the results obtained with the VX-659/VX-661/VX-770 study, also showing two study participants not improving in mean change in FEV1 upon VX-659/VX-661/VX-770 therapy [5]. Despite the overall variation, response to VX-770/VX-809 correlated in a linear positive manner with response to the ABBV/GLPG-Triple. This especially underlines the benefit of ABBV/GLPG-Triple therapy for patients that are mildly responsive to VX-770/VX-809.

Whether the ABBV/GLPG-Triple therapy is specifically effective for pwCF currently not benefitting from VX-445/VX-661/VX-770 therapy remains unclear, as the clinical trial reports did not share genotypes [14]. Future research should therefore investigate efficacy of the VX-445/VX-661/VX-770 in a large panel of F508del/minimal function organoids. In addition, it would be interesting to compare these results to the results obtained with the ABBV/GLPG-Triple. In future studies, it could be interesting to assess the efficacy of the GLPG/ABBV compounds in nasal/bronchial epithelial cells to confirm that rescue of CFTR is also achievable in airway-derived primary cells. Intestinal organoids are however superior over nasal or bronchial epithelial organoids when assessing function of CFTR by means of organoid swelling, as swelling of intestinal organoids is completely CFTR dependent whilst additional ion channels present in airway organoids also influence swelling. The effect of CFTR-mediated airway organoid swelling could therefore be underestimated. Finally, it should be noted that the absolute swelling values obtained in this manuscript cannot be directly compared to other published drug-induced FIS data, as experiments were performed with 5 μM or 0.8 μM forskolin instead of 0.128 μM forskolin [11, 12].

In summary, we confirm that combining compounds with complementary working mechanisms is a valuable approach for restoring CFTR function. We also show that characterizing compound efficacy in a personalized manner is required, as we observe great variation in drug efficacy between organoid cultures with comparable and even identical genotypes. Identifying individuals with a high modulator-responsive genotype ultimately will help in better understanding which genetic or cellular processes influence response to therapy and in defining personalized treatment regimes.

Supplemental Information

Supplemental data can be found online, at https://doi.org/10.3389/fmolb.2021.698358

Ethics Statement

The studies involving human participants were reviewed and approved by the medical ethical committee at University Medical Center Utrecht (UMCU; TcBio#14-008). The patients/participants provided their written informed consent to participate in this study.

Author Contribution Statement

EDP Conceptualization, Formal analysis, Visualization, Writing - original draft, Writing - review and editing; SS Conceptualization, Formal analysis, Visualization, Writing - original draft, Writing - review and editing; RK Data collection, Data analysis; KL Data collection, Data analysis; SB Conceptualization, Data curation, Formal analysis, Investigation, Methodology, Project administration; Resources; KC Conceptualization, Methodology, Supervision; CE Funding acquisition; JB Conceptualization, Funding acquisition, Methodology, Supervision.

Funding

This study is powered by Health – Holland, Top Sector Life Sciences & Health. Health-Holland (40-41200-98-9296). Organoid experiments performed at HUB were funded by Galapagos.

Conflict of Interest

HUB is a foundation which holds the exclusive rights to Organoid Technology patents. JB and CE are inventors on patent(s) related to the FIS-assay and received financial royalties from 2017 onward. KC is employed by Galapagos NV and may own stock in the company. JB and CE report receiving research grant(s) and consultancy fees from various industries, including Vertex Pharmaceuticals, Proteostasis Therapeutics, Eloxx Pharmaceuticals, Teva Pharmaceutical Industries and Galapagos outside the submitted work. The authors declare that this study received funding from Galapagos. The funder had the following involvement with the study: Conceptualization, Methodology, Supervision. The remaining authors declare that the research was conducted in the absence of any commercial or financial relationships that could be construed as a potential conflict of interest.

References

1. Sosnay, P. R., Siklosi, K. R., Van Goor, F., Kaniecki, K., Yu, H., Sharma, N., *et al*. (2013). Defining the disease liability of variants in the cystic fibrosis transmembrane conductance regulator gene. Nat. Genet. 45 (10), 1160–1167. Available from. doi:10.1038/ng.2745
2. Rowe, S. M., McColley, S. A., Rietschel, E., Li, X., Bell, S. C., Konstan, M. W., *et al*. (2017). Lumacaftor/ivacaftor treatment of patients with cystic fibrosis heterozygous for F508del-CFTR. Ann. Am. Thorac. Soc. 14 (2), 213–219. doi:10.1513/AnnalsATS.201609-689OC
3. Van Goor, F., Hadida, S., Grootenhuis, P. D. J., Burton, B., Stack, J. H., Straley, K. S., *et al*. (2011). Correction of the F508del-CFTR protein processing defect in vitro by the investigational drug VX-809. Proc. Natl. Acad. Sci. 108 (46), 18843–18848. doi:10.1073/pnas.1105787108
4. Veit, G., Roldan, A., Hancock, M. A., da Fonte, D. F., Xu, H., Hussein, M., *et al*. (2020). Allosteric folding correction of F508del and rare CFTR mutants by elexacaftor-tezacaftor-ivacaftor (Trikafta) combination. JCI Insight 5 (18), 1–14. doi:10.1172/jci.insight.139983
5. Davies, J. C., Moskowitz, S. M., Brown, C., Horsley, A., Mall, M. A., McKone, E. F., *et al*. (2018). VX-659-Tezacaftor-Ivacaftor in Patients with Cystic Fibrosis and One or Two Phe508del Alleles. N. Engl. J. Med. 379 (17), 1599–1611. doi:10.1056/nejmoa1807119
6. Wang, X., Liu, B., Searle, X., Yeung, C., Bogdan, A., Greszler, S., *et al*. (2018). Discovery of 4-[(2R,4R)-4-({[1-(2,2-Difluoro-1,3-benzodioxol-5-yl) cyclopropyl] carbonyl}amino)-7-(difluoromethoxy)-3,4-dihydro-2h-chromen2-yl] benzoic Acid (ABBV/GLPG-2222), a Potent Cystic Fibrosis Transmembrane Conductance Regulator (CFTR) Corrector for the Treatment of Cystic Fibrosis
7. de Wilde, G., Gees, M., Musch, S., Verdonck, K., Jans, M., Wesse, A.-S., *et al*. (2019). Identification of GLPG/ABBV-2737, a novel class of corrector, which exerts functional synergy with other CFTR modulators. Front. Pharmacol. 10, 514. doi:10.3389/fphar.2019.00514
8. Van der Plas, S. E., Kelgtermans, H., Mammoliti, O., Menet, C., Tricarico, G., De Blieck, A., *et al*. Discovery of GLPG2451, a Novel Once Daily Potentiator for the Treatment of Cystic Fibrosis. J. Med. Chem.
9. Singh, A. K., Alani, S., Balut, C., Fan, Y., Gao, W., Greszler, S., *et al*. (2016). Discovery and characterization of ABBV/GLPG-2222, a novel first generation CFTR corrector, 51. Pediatr Pulmonology
10. Boj, S. F., Vonk, A. M., Statia, M., Su, J., Vries, R. R., Beekman, J. M., *et al*. (2017). Forskolin-induced Swelling in Intestinal Organoids: An In Vitro Assay for Assessing Drug Response in Cystic Fibrosis Patients. J. Vis. Exp. 120, 1–12. doi:10.3791/55159
11. Dekkers, J. F., Berkers, G., Kruisselbrink, E., Vonk, A., De Jonge, H. R., Janssens, H. M., *et al*. (2016). Characterizing responses to CFTR-modulating drugs using rectal organoids derived from subjects with cystic fibrosis. Sci. Transl Med. 8 (344), 344ra84–84. doi:10.1126/scitranslmed.aad8278
12. Berkers, G., van Mourik, P., Vonk, A. M., Kruisselbrink, E., Dekkers, J. F., de Winter-de Groot, K. M., *et al*. (2019). Rectal Organoids Enable Personalized Treatment of Cystic Fibrosis. Cel Rep. 26 (7), 1701–1708. e3. Available from. doi:10.1016/j.celrep.2019.01.068
13. Paranjapye, A., Ruffin, M., Harris, A., and Corvol, H. (2020). Genetic variation in CFTR and modifier loci may modulate cystic fibrosis disease severity. J. Cystic Fibrosis 19, S10–S14. doi:10.1016/j.jcf.2019.11.001
14. Middleton, P. G., Mall, M. A., Dřevínek, P., Lands, L. C., McKone, E. F., Polineni, D., *et al*. (2019). Elexacaftor-Tezacaftor-Ivacaftor for Cystic Fibrosis with a Single Phe508del Allele. N. Engl. J. Med. 381 (19), 1809–1819. doi:10.1056/nejmoa1908639

Chapter | 9

Chapter | 10

General discussion

Sacha Spelier, Cornelis K. van der Ent and Jeffrey M. Beekman

New solutions are needed for the 10-15% of people with CF (pwCF) carrying *CFTR* mutations that are unresponsive to highly efficient modulator therapies (HEMTs). In this thesis, we explored different strategies for filling the unmet clinical needs of those pwCF, particularly focusing on characterizing therapeutic strategies for *CFTR* nonsense mutations. We aimed to optimize preclinical-to-clinical translation by exploiting patient-derived intestinal organoids (PDIOs) in functional assays, allowing stratification of pwCF who could benefit from specific treatments. In this chapter, I summarize and discuss the promises and challenges of the research described throughout this thesis.

Therapeutic regimens for nonsense mutations

We touch upon the most important overarching challenges for the development of therapeutic regimens for nonsense mutations in **chapter 2.** In the next section, I expand on the conclusions drawn in that chapter and further reflect on therapeutic regimens for nonsense mutations, pointing out various results and conclusions described throughout this thesis.

Readthrough and associated challenges

The main studied treatment regimen for treating nonsense mutations is based on compounds that induce translational readthrough. Such readthrough compounds act through various mode-of-actions to promote the incorporation of non-cognate amino acids (AAs), which consequently results in translation beyond the PTC site. Since the characterization of aminoglycosides as first class of compounds that stimulate ribosomal readthrough by slowing down the ribosome [1], over 30 compounds with readthrough potential have been identified and characterized in preclinical studies [2]. However, as described in **chapter 2,** preclinical studies often show contradictory results when comparing different PTC mutations, genetic diseases, model systems and read-outs. Additionally, whilst preclinical studies showed promising results in many cases, clinical studies, in a CF-overarching context, on readthrough compounds are so far disappointing. In fact, ataluren is the only readthrough compound that received conditional approval in July 2018 from the European Medicines Agency (EMA) for treating a subset of patients with Duchenne Muscular Dystrophy (DMD) (pediatric, ambulatory, >2 years) [3], [4].

We further underline the challenging nature of readthrough compound monotherapy in **chapter 3, chapter 6 and chapter 8.** Three major factors that contribute to this are presumably **a)** the degradation of PTC harboring mRNAs by nonsense-mediated decay (NMD), **b)** the incorporation of non-cognate amino acids (AAs) at the PTC site upon translational readthrough, resulting in production of protein variants with missense mutations and **c)** readthrough compound associated toxicity. The association between readthrough compounds and cellular toxicity is based on two aspects. First, treatment with first-generation readthrough compounds aminoglycosides is associated with cellular toxicity such as nephrotoxicity, presumably due to interference with the mitochondrial ribosome [5]. Subsequent chemistry studies however resulted in optimization of these compounds, by decreasing the toxicity of aminoglycoside derivatives, leading to the development of for example ELX-02, originally a G418 derivative [6]. A second readthrough-associated concern, is readthrough of the normal termination codon (NTC) which could result in hazardous, C-terminal elongated protein variants with novel loss- or gain-of-function characteristics. In this context, recent studies indicate that intrinsic, genetic differences between NTC and PTC sites allow for distinguishment between them. In particular, the increased distance of PTCs, in comparison to NTCs, from the 3′-end of mRNAs results in reduced interaction with translation termination agonists such as poly(A) tail-binding proteins (PABPs). The absence of such NTC quality-control mechanisms at PTC sites, provides a rationale for the development of therapies that can selectively increase readthrough at PTCs over NTCs. Furthermore, multiple alternative stop codons are often present downstream of the NTC, further decreasing the chance of extensive readthrough of the 3′-untranslated region (UTR) of mRNAs [7]–[9]. In this thesis, we did not confirm the absence of NTC-readthrough in our experiments. A technique to precisely investigate this is by means of ribosomal sequencing, which allows characterization of the (undesired) presence of ribosomes downstream of the NTC in the 3′ UTR [10]. It is strongly recommended to characterize NTC readthrough of the most potent compounds discussed in this thesis via ribosomal sequencing, such as DAP **(chapter 4).** Performing ribosomal sequencing on patient-derived cells under physiologically relevant conditions is especially relevant and novel. Lastly, it is pivotal to underline that readthrough compound efficacy differs between PTC identities, as described in **chapter 2.** Readthrough susceptibility differs between stopcodon identity, where UGA is most susceptible to readthrough and UAA least susceptible [9]. Furthermore, the localization of the PTC mutation also influences how severe its implications are. A PTC mutation relatively close to the NTC results in the production of CFTR protein variants with a relatively small C-truncation that might hold some residual function. The opposite however, PTC mutations in close proximity to the 5′ end of the mRNA, could also be advantageous in comparison to PTC mutations right in the middle of *CFTR*, due to alternative translation initiation at start codons downstream of the original start codon [11].

Whilst we compare PDIOs with different PTC genotypes in **chapter 3,** we cannot conclude whether the observed differences in FIS outcomes are indeed due to their different PTC identities, as the location of the PTC site differed between the PDIOs.

Combination treatment strategy for treating PTC mutations

Our first approach to improve functional restoration with readthrough compounds, was aimed at tackling the two main challenges of readthrough compound therapy: NMD of PTC harboring mRNA and the production of missense CFTR protein variants due to incorporation of non-cognate AAs. We hypothesized that PTC functional restoration could be improved by combining readthrough compounds with compounds with complementary mode-of-actions that **a)** inhibit NMD, resulting in a larger pool of mRNAs that can be targeted by the readthrough compound and **b)** modulate CFTR on a protein level, e.g. correctors and potentiators, improving function of CFTR protein if missense mutations are present [12], [13]. Indeed, in **chapter 3**, we show that inhibition of NMD-1 by SMG1 in combination with stimulation of readthrough by ELX-02 and CFTR protein modulation by elexacaftor/tezacaftor/ivacaftor (ETI), results in efficient CFTR rescue. FIS levels of ELX-02/

SMG1/ETI treated homozygous PTC PDIOs, were higher than lumacaftor/ivacaftor treated F508del/F508del PDIOs. As lumacaftor/ivacaftor is effective at improving lung function in pwCF homozygous for F508del, this comparison indicates that the observed effect of ELX-02/SMG1/ETI is in a potentially clinically relevant range [14]. The dual combinations of ELX-02/ETI or ELX-02/SMG1i were significantly less effective, underlining that especially the combination of enhancing translational readthrough, inhibiting NMD and CFTR protein modulation could provide a powerful combined approach. In contrast to our results on the limited efficacy of ELX-02 in preclinical assays, Crawford *et al* demonstrated efficacy of ELX-02 as monotherapy in G542X/G542X PDIOS as measured by FIS [15]. However, in these experiments a high forskolin concentration and a prolonged imaging period were exploited in order to increase the assay sensitivity to allow detection of low CFTR function. Whilst such alterations can be beneficial to detect effects of lower effective compounds, the translational value allowing preclinical-clinical translation decreases. Indeed, when comparing preclinical data of ELX-02 to clinically available data, results with ELX-02 are disappointing. ELX-02 is currently being evaluated in two Phase 2 trials (NCT04126473 and NCT04135495) in CF patients with at least one PTC allele. Preliminary results showed a minor decrease in sweat chloride concentration, indicating only limited treatment efficacy [16]. ELX-02 is additionally being investigated in combination with the CFTR modulator ivacaftor (NCT04135495); however, a first press release reported no significant improvement upon this dual therapy [17].

To NMD or not to NMD

Whilst inhibition of NMD in combination with ELX-02 mediated readthrough and ETI mediated CFTR modulation yielded promising results, NMD is an essential, sophisticated mechanism to maintain cellular homeostasis. Mendell *et all* found that inhibition of NMD interferes with protein expression levels about 5-10% of the human genes [18]. This, rightfully, underlines the need for caution and explains the hesitance of industry to proceed with further development of NMD inhibitors. Previous preclinical studies furthermore suggested that high concentrations of NMD inhibitors are associated with toxicity, further hampering development of NMD-inhibitors as a therapeutic compound [19]. In **chapter 3** however, we observed no toxicity upon inhibition of SMG1i when used at a low micromolar concentration. Consequently, in a combinatorial approach, concentration of NMD inhibitors could be lowered to such an extent that the toxic side-effects might be minimal. I believe additional (safety) studies on NMD inhibitors such as SMG1i are therefore still of interest. Furthermore, NMD is a complex process involving more interactors than SMG1. Potentially, inhibition of different NMD-associated proteins results in a more favorable therapeutic window than inhibition of the NMD-associated proteins described in this thesis. Tan *et al* recently reviewed clinical potential of NMD inhibition, highlighting that knockdown of the NMD factor SMG8 causes less deleterious effects than knockdown of other NMD factors [20]. In another recent study, FDA-approved drugs were profiled for their potential to inhibit NMD [21]. Zhao and colleagues found that some compounds inhibited NMD in a dose-dependent manner, such as the drug homoharringtonine (HHT) [21]. Whilst the original dose of HHT is associated with side-effects, lowering of the dose facilitated by the synergistic treatment approach earlier described could yield beneficial results. Another interesting approach to inhibit NMD is by means of synthetic antisense oligonucleotides (ASOs) designed to prevent binding of exon junction complexes (EJC) downstream of premature termination codons (PTCs) [22]. EJCs mark the exon-exon junction on the mRNA after splicing and are consequently absent 3′ of the NTC, which resides in the last exon. As PTCs are located more upstream, one or more introns are often present 3′ of the NTC. As a consequence, it is possible that translation termination in transcripts with PTCs takes place while one or more EJCs remain attached to the mRNA. These EJCs can interact with the ribosome during translation termination and initiate NMD of the mRNA. As ASOs are designed to bind to specific sequences, they could attenuate NMD in a gene-specific manner and therefore result in a decrease in unwanted side-effects.

Lastly, similarly to differences in readthrough efficacy for different types of PTC mutations, it is important to note that not all PTC mutations result in the production of mRNAs with a similar NMD probability. As recently shown in an elegant fashion on a single-cell level, NMD probability is highly variable between different transcripts and depends on several factors, particularly the PTC-to-intron distance, the number of introns both upstream and downstream of the PTC and the surrounding exon sequence downstream of the PTC [23]. That the probability of NMD depends on the presence of introns, is related to the presence of downstream EJCs 3′ of the PTC as just introduced. Consequently, it is expected that different PTC mutations in *CFTR* will result in differences in NMD probability of the corresponding mRNA transcripts. Whilst we compared the effect of SMG1i in PDIOs with different PTC mutations in **chapter 3,** we cannot draw firm conclusions on the influence of NMD probability in relation to PTC identity, as the patient-derived identity of the PDIOs results in more differences between PDIOs than PTC identity alone. Future studies on NMD probability of different CFTR PTC-mRNAs in a more isogenic context are warranted.

Whilst research on NMD inhibition holds potential, we also describe approaches in this thesis in which NMD inhibition was not a necessary component of a therapeutic regimen for nonsense mutations. In **chapter 7,** we describe that the combination of ELX-02/ETI and roflumilast is almost as potent for restoring CFTR function of W1282X-CFTR as ELX-02/ETI and SMG1i, circumventing the need for an NMD inhibitor. In **chapter 8,** we describe a therapeutic regimen with neither a readthrough compound nor an NMD inhibitor. Here, we show that the combination of ETI, simvastatin and roflumilast yielded a beneficial outcome in both a heterozygous (L927P/W1282X) as well as a homozygous (W1282X/W1282X) context. The success of this combinatorial regimen could be contributed to the characteristics of W1282X, which is a PTC mutation relatively close to the NTC that consequently results in the production of CFTR protein variants with a relatively small C-truncation. As such, in contrast to W1282X, we presume that PTC mutations early in the *CFTR* gene which result in a larger truncation, will not benefit from this approach. We further discuss this approach and the associated case study in a later section.

Monotherapy regimens for treating PTC mutations
Clearly, we envisioned that readthrough compound monotherapy would be challenging if not impossible, and mainly focused on characterizing potent combination treatment regimens. However, upon starting a collaboration with dr. Fabrice Lejeune to thoroughly characterize a novel readthrough compound developed in his lab, DAP, we found that readthrough compound monotherapy might be achievable.

In **chapter 4,** we describe that DAP is incredibly potent specifically in the context of rescuing W1282X/W1282X CFTR. If we compare data shown in **chapter 3** to data shown in **chapter 6,** DAP is as potent as the combination of ELX-02/SMG1i and ETI. This can likely be attributed to the underlying molecular mechanism of DAP, which specifically inhibits FTSJ1, a transmethylase that modifies $tRNAs^{Tryptophan}$ post-transcriptionally. As a consequence, $tRNAs^{Tryptophan}$ also recognize a UGA-PTC site in addition to its cognate UGG tryptophan codon. This decrease in fidelity of $tRNAs^{Tryptophan}$ results in tryptophan incorporation at the UGA-PTC site and production of full-length protein. In case of W1282X CFTR, WT-CFTR protein is produced, circumventing the need for additional CFTR modulators [24]. Surprisingly, in contrast to previous preclinical studies as well as different experiments in the same chapter, DAP was not able to restore CFTR function in PDIOs with G542X-CFTR [25]. Here, functional restoration of G542X was shown for CF patient-derived nasal cells by means of SPQ measurements. SPQ is a chemical chloride or indicator that quenches upon contact with iodides [26]. Whilst this assay holds advantages such as the ease of read-out and a limited required amount of input material, challenges associated with its use are a limited reproducibility of the assay due to leakage of dyes from the cells, photobleaching of the dye when prolonged periods of illumination are used and a limited dynamic range of the assay. In case of G542X, more studies indeed point into the direction that G542W is not functional, presumably due to a partial defect in maturation and reduced stability at the cell membrane resulting in total absence of fully glycosylated CFTR based on western blot [1]. Based on the robustness and characteristics of the FIS assay in PDIOs, we expect that this model is more likely to be indicative of the *in vivo* situation. In addition to DAP, recent studies describe that readthrough compounds NV848/N914/NV930 hold a similar FTSJ-1 inhibitory working mechanism [27]. As all these compounds yielded promising preclinical results in relevant model systems and additionally showed a favorable safety profile in animal models [28], clinical trials are expected to start soon. Aside from this, future studies specifically searching for inhibitors of other tRNA-modifying proteins resulting in incorporation of cognate-AAs at different PTC sites, are of great interest. Potentially, tRNA modifying enzymes could be found for different tRNAs, allowing a mix-and-match approach for restoring different PTC products to the originally wildtype protein version.

Additionally, novel studies that focus on identification of new readthrough compounds or pharmacological optimization of older generation readthrough compounds, could result in promising results with an optimized safety-efficiency trade-off. For instance, recent high-throughput screenings using cellular reporter models allowed the selection of novel compounds with not earlier described readthrough mechanisms, such as the inhibition of translation termination factor ERF1 by NVS1 and SRI-41315, or the inhibition of ERF3 by CC-90009 [29]–[31].

Non-small molecule readthrough strategies
Alternative non-small molecule readthrough approaches moreover warrant further attention. As described in **chapter 5**, ACE-tRNA technology could prove beneficial in terms of specific AA incorporation. Whilst we show proof-of-principle data confirming their efficacy in PDIOs, future studies on efficacy as well as off-targets effects of ACE-tRNAs such as impact on cell viability and ribosomal readthrough of the NTC is pivotal. Further assessment of ACE-tRNAs in primary cell models as well as additional studies on ACE-tRNA delivery will help to prioritize ACE-tRNAs for further clinical development.

Readthrough strategies in a nutshell
Overarching, based on the results of this thesis, multiple strategies that hold potential for treating PTC mutations can be discriminated **(Figure 1).** Further broad characterization of these different therapeutic regimens is needed for a wide range of different PTC genotypes at different positions in the *CFTR* gene, to fully recapitulate the potential of these treatment strategies for all pwCF with PTC mutations. Furthermore, elaborate characterization of potential NTC-readthrough associated toxicity by means of analyses such as ribosomal sequencing, should confirm the absence of hazardous side-effects.

FIS in PDIOs: boosting translational preclinical research

The described gap between efficacy of readthrough compounds in a preclinical setting and results obtained in a clinical setting **(chapter 2),** underlines two readthrough-biology overarching considerations. First, whilst simplified assays in cell models where CFTR is ectopically expressed are highly valuable in context of compound discovery, it is essential to rapidly switch to more biologically relevant cell models and assays for follow-up validation experiments. By prioritizing functional assays on endogeneous patient-derived cell models of which the outcomes correlate with clinical parameters, results of these preclinical experiments hold increased translational value in terms of potential clinical benefit. Secondly, the use of patient-derived cell models could allow for prediction of drug efficacy in a clinical setting and as such stratification of patients or patient groups who could benefit from a specific therapy. This is highly relevant, as the progression and clinical phenotype of pwCF varies highly between subjects, where allelic variation in *CFTR* has been described to not fully explain phenotypic variability [32]. Likewise, treatment response varies strongly between pwCF with the same *CFTR* genotype. As such, preclinical stratification of potential responders could result in substantial prevention of ineffective treatment regimens and associated exhaustion of resources such as money and time.

In this thesis, we particularly studied CFTR function in adult stem-cell based patient-derived intestinal organoids (PDIOs) by means of FIS. The FIS assay has been optimized in our lab in previous studies, and proved highly useful for quantification of CFTR function in CF PDIOs and characterization of CFTR restoring potential of different treatment regimens.

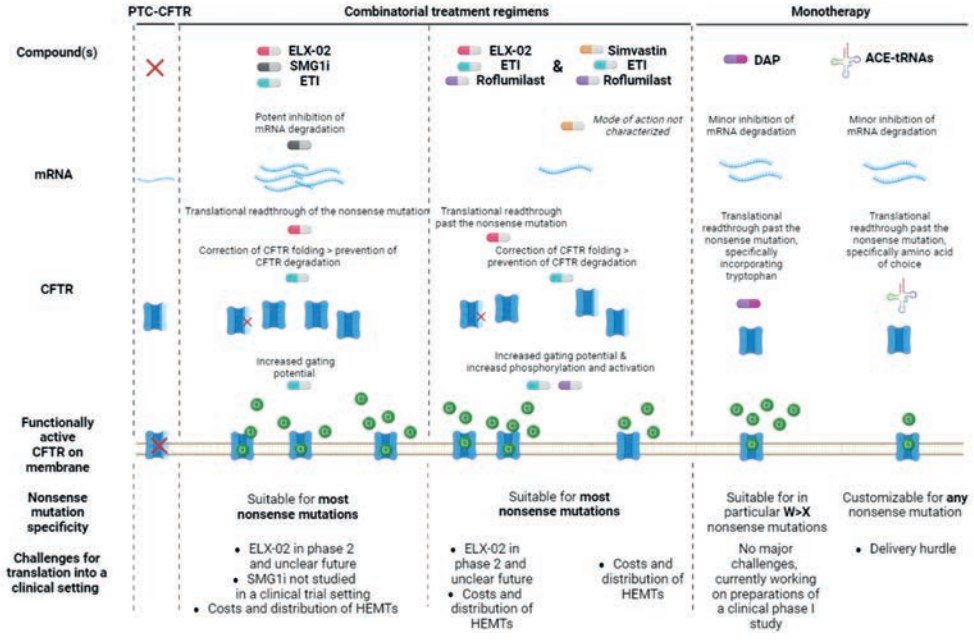

Figure 1. Summary of readthrough strategies described in this thesis.
In this thesis we describe multiple strategies for treating PTC mutations, which can be discriminated in combinatorial treatment strategies and monotherapies. In this figure, we summarize and compare these strategies in the context of biological mode-of-action, nonsense mutation specificity and their potential for rapid translation into a clinical setting.

The CFTR dependency under standard assay condition, and the robustness and scalability of the FIS-assay, as described in **chapter 6,** allow robust characterization of efficacy of therapeutic regimens at a preclinical stage, as described in **chapter 6 and 7.** How preclinical FIS assays can allow identification of potential responders and guide validation of a treatment regimen in a clinical setting, is underlined in **chapter 8.** We describe particular findings of these chapters in other sections of this discussion. Here, we will discuss the promises, challenges and future applications of the FIS assay itself in more details.

The dynamic window of the FIS assay
The dynamic range of the FIS assay is dependent on two conditions: the concentration of forskolin and the length of FIS-imaging. When efficacy of the tested treatment is expected to be low, e.g. when performing drug screens with novel compounds ór in the context of severe *CFTR* mutations, increasing the forskolin concentration and prolonging the time of imaging can increase the dynamic window to detect organoid swelling. "Pushing the system" in these manners can aid in hit identification and hypotheses testing, which would otherwise

be impossible due to the lower detection limits. Throughout this thesis, we performed FIS experiments under different conditions, which has to be kept in mind when comparing data.

Importantly, increasing the dynamic window is not desired under all circumstances. So far, studies have described that FIS measurements and clinical parameters correlate in particularly at low forskolin concentration (0.128-0.8 uM) during short (1-hour) measurements [33], [34]. The validity of prediction of clinical benefit based on 3-hour FIS measurements or high (0.8-5 uM) forskolin concentrations, remains to be demonstrated. This hampers direct translation of preclinical results to a potential clinical setting. Furthermore, an additional advantage of adhering to the more standard FIS-assay settings of 0.128 uM forskolin and 1-hour measurements, is that this allows for comparison of obtained results to benchmark data. Benchmark data in this context, means FIS data of compound treated PDIOs of which the compounds in question have shown to be effective in a clinical setting for a specific genotype. In this thesis, we frequently compared our data to 1-hour swelling data of ETI and lumacaftor/ivacaftor treated F508del/F508del and F508del/minimal function (MF) PDIOs, as these are currently regarded as, respectively, the highest responders or borderline responders to these HEMTs. This comparative benchmark data is not available for 3-hour FIS assays, as within that timeframe HEMT treated F508del/F508del organoid structures swell so excessively that structures eventually collapse. Importantly, the preclinical results described in **chapter 3 and 4,** on ETI/roflumilast/simvastatin combinatorial therapy and DAP as monotherapy respectively, were obtained under standardized FIS assay settings. As swelling levels of treated PTC PDIOs were similar to lumacaftor/ivacaftor treated F508del/F508del PDIOs, this presumably indicates that observed effects are in the range of potential clinical benefit. In brief, "pushing the system" by increasing forskolin concentration and FIS stimulation can be beneficial to detect effects of lower effective compounds, yet the translational value allowing preclinical-clinical translation decreases. A relevant example underlining this, is ELX-02. Contrary to our results, Crawford *et al* demonstrated efficacy of ELX-02 as monotherapy for restoring CFTR function in G542X/G542X PDIOS as measured by FIS [15]. In this study however, the high forskolin concentration and prolonged imaging period is likely the reason for impaired preclinical-to-clinical translation as later emphasized by disappointing clinical trial results.

In summary, when performing exploratory proof-of-principle studies, it can be beneficial to increase the dynamic window by increasing the forskolin concentration and length of imaging after forskolin stimulation. At a later research stage however, we advocate to stick to the more standardized FIS assay settings of 0.128 uM forskolin and 1-hour measurements, to increase the preclinical-to-clinical translational value of the obtained results.

Further improving the FIS assay
In **chapter 6,** we developed a 384-well plate (WP) version of the FIS assay. To our knowledge, we are the first to exemplify the feasibility of large-scale compound screening based on a functional read-out using PDIOs. However, whilst assay performance of the 384 wells FIS assay was decent underlined by Z'-factors reaching 0.4 or higher, assay quality was

lower than for 96 wells FIS assays. If in the future more high-throughput FIS screens are to be performed, additional changes that improve assay robustness and standardization are recommended. On this note, currently, the FIS assays on PDIOs is not yet recognized by the EMA as preclinical model for the identification of prospective treatment responsive *CFTR* genotypes. First interactions with the EMA indeed resulted in emphasis on the need for further improving assay robustness and overall pipeline standardization, in order for the FIS assay to be recognized as preclinical model valid for the stratification of potential treatment responders. Consequently, alterations that hold potential for reducing technical and biological variability, deserve attention in future studies.

From a technical perspective, improvements can come from a) replacing manual steps in the FIS assay by automated actions and b) improving the FIS analysis pipeline. Further automatization is worthwhile if not essential, as work described in for example **chapter 6 and 7** is highly labor intensive and prone to human errors. The relative straightforward set-up of the FIS assay allows for automatization of practically every step along the assay, ranging from printer-mediated compound addition to automated plate-handling and imaging. Additional to these wet-lab improvements of the FIS assay, the analysis of FIS-data could be further improved. In this thesis, PDIO structures were visualized by calcein staining prior to the assay and analyses were performed per well, grouping all organoid structures of that well. Switching from this calcein-based analysis to brightfield-based analysis would decrease calcein-associated fluorescent noise and background, which can hamper image analysis. Additionally, instead of analyzing FIS-results per well, recognition and analysis of separate structures based on AI-mediated labeling could further decrease noise by only including viable, healthy structures. This could allow a switch from technical replicates in the form of wells, to technical replicates in the form of individual organoid-structures in one well, allowing a further increase in throughput. Recent efforts from our lab resulted in such bright-field based analyses, which we will further discuss in a later section in this chapter.

From a biological perspective, the strength of representing biological complexity of our assay, also results in challenges in terms of assay robustness. Increased biological robustness of the performed FIS assays could be achieved by additional standardization of the PDIO culture pipeline. Such standardization could come from switches in growth medium, in particular replacing animal-derived products such as FBS and Matrigel for similar animal-free products. Furthermore, a pivotal element of the PDIO medium is WNT3A, which is a main ligand for WNT/ β-catenin signaling which regulates the expression of genes involved in cell differentiation, survival, proliferation and migration [35]. Moreover, Pablo *et al* identified CFTR as a direct downstream target gene of Wnt/β-catenin signaling, underlining the importance of WNT3A in the medium. Currently, we exploit WNT3A-producing cell-conditioned media for culturing the PDIOs, which holds batch-to-batch differences. Potentially, switching to WNT-surrogate could further standardize PDIO growth and behavior.

Altogether, these improvements could aid in increasing standardization, robustness and the dynamic window of the FIS assay, thereby making it even more suitable for future (ultra)-high-throughput drug screening efforts and preclinical stratification of potential treatment responders.

Preclinical-to-clinical translation of results obtained in the FIS assay
Throughout this thesis we show that that our drug testing efforts can result in identification of novel treatment regimens. Additionally, due to exploiting patient-derived cells in an assay for which preclinical-clinical correlations are established, we point out that such compound characterizations could guide successful, individual clinical interventions. At present-day, the FDA approves modulator therapy for specific mutations based on preclinical FRT data [36]. However, our results throughout this thesis show that the PDIO model might be more suitable or could be used as complementary model in the identification of prospective responders allowing label-expansion. However, some challenges concerning preclinical-to-clinical translation remain.

First, as mentioned often throughout this thesis, various studies indicate correlations on a group level between FIS outcome or baseline residual CFTR function in PDIOs, and clinical parameters such as sweat chloride and FEV1pp [33], [34], [37]. We furthermore confirm the presence of a correlation on a group level between FIS data (1-hour, 0.128 uM forskolin) and published clinical data in **chapter 7.** However, some other studies contradict the presence of such a correlation, such as a recent study where clinical response indicators only poorly correlate with FIS measurements of lumacaftor/ivacaftor treated F508del/F508del PDIOs on a group level [38]. Furthermore, preclinical-clinical correlations on a group level do not necessarily interpolate to a preclinical-clinical correlation on an individual level, which is underlined by studies describing contradictory results on such individual correlations. One study demonstrated that clinical response to CFTR modulators ivacaftor or ivacaftor/lumacaftor did correlate on an individual level based on preclinical data for a heterogeneous CFTR genotype setting [34]. Later studies with lumacaftor/ivacaftor on homozygous F508del and A455E pwCF however, did not confirm individual preclinical-clinical correlations [39]–[41]. Similarly, whilst Lefferts *et al* describe a preclinical-clinical correlation on a group level for ETI treated F508del PDIOs, preclinical-clinical correlations on an individual level were not significant [42]. As such, additional studies characterizing correlation on an individual level between FIS response and clinical parameters are warranted. In order to draw firm conclusions on the presence of group ánd individual correlations, it is essential that such studies represent the heterogenous population of pwCF, including non-responders. An example of such an approach is the HIT-CF organoid study, where potential responders are selected based on preclinical FIS assays and subsequently treated in a clinical setting, and where non-responders will be included as presumably negative controls [43]. If in such studies robust preclinical-clinical correlations are found, it is pivotal that the FIS assay obtains an official EMA-approved status as preclinical model valid for the stratification of potential treatment responders. This would subsequently result in pwCF who are considered responsive to CFTR treatments regimens based on preclinical testing of their own PDIOs, to be eligible for subsequent testing in a clinical settings.

Chapter | 10

On the aspect of preclinically guided clinical interventions, the question of what *exactly* defines a responder in the FIS assay arises. The decision for an exact cut-off swelling level is challenging, in particular due to the contradicting results on individual preclinical-clinical correlations. Consequently, a decision for a particular cut-off has not been made in the field. A future study in which preclinical-clinical correlations are assessed in a large, diverse cohort as described above could aid in the decision-making for an exact cut-off value. This is however a challenging and complex task due to the high costs of HEMTs, further discussed in a later section. It could be argued that a cut-off value should be on the low side, for example the average swelling levels of lumacaftor/ivacaftor treated F508del PDIOs, in order to avoid missing potential responders. However, there is a trade-off between individual patient gain and social welfare where healthcare systems need to deal with budget constraints. Navigating this ethical terrain is complex and asks for discussions between all involved stakeholders.

Novel assays on PDIOs to complement FIS

Although the FIS assay has been invaluable in previous studies and the studies described in this thesis, it remains important to question whether the FIS assay is suitable for characterization of all treatment regimens. In the FIS assay, quantification of CFTR function by means of quantification of swelling is based on relative size increase of organoid structures. This implies that when comparing different donors or treatment regimens, it is essential that the organoids' baseline of absolute luminal areas are identical at the start of each experiment. This is generally the case, except for two notable exceptions: WT-CFTR structures and CFTR-deficient structures that are highly responsive to specific treatment regimens, which results in a WT phenotype prior to forskolin addition. As WT-CFTR PDIOs exhibit large fluid-filled lumens under steady-state culture conditions, the dynamic range to swell upon forskolin stimulation is small and as such, absolute FIS of WT-CFTR PDIOs is low. Similarly, highly effective treatments can induce fluid transport and organoid swelling in a forskolin-independent manner. Consequently, at the time of forskolin stimulation and FIS measurements, such structures have begun to swell and phenotypically resemble, to some extent, WT-CFTR PDIOs, again resulting in low absolute FIS and as such an underestimation of the efficacy of the treatment regimen. This is observed for example for ETI treated F508del/F508del-CFTR PDIOs, presumably due to elexacaftor which possesses both corrector and potentiator function. In **chapter 3,** we also observed that the EST combination resulted in PDIO swelling prior to the addition of forskolin, underlining that this combinatorial regimen in fact was highly effective.

A way to quantify such forskolin-independent PDIO preswelling prior to the FIS assay is by means of quantification of drug-induced swelling (DIS), as described recently by Lefferts *et al* [79]. In the DIS assay, swelling is monitored directly after compound exposure independent of forskolin stimulation. The DIS assay allowed characterization of functional CFTR restoration in response to ETI treatment, without underestimating effect as observed in homozygous F508del PDIOs in a conventional FIS assay. Validating the DIS assay in a larger cohort is pivotal to further investigate the relation between DIS measurements and clinical parameters upon drug treatment. Whereas the DIS assay, similarly to the FIS assay, is based on relative size increase of structures, various other methods to characterize CFTR function have been developed as well. In **chapter 7,** we characterize steady-state lumen area (SLA) of treated PDIOs, a method previously described by Dekkers *et al* [37]. SLA can be quantified by measuring the lumen area as a percentage of total organoid area, and thereby allows for comparisons of drug response between WT-*CFTR* and CF PDIOs. Whilst SLA measurements did correlate with clinical parameters, its dynamic window was smaller than the dynamic window of the FIS assay and consequently less suitable for characterization of CFTR function in the lower region of the assay, e.g. for more severe *CFTR* mutations or less effective compounds. Additionally, the manual analysis is time-consuming and relatively low in accuracy. To improve on these aspects, our lab is currently optimizing an automated way of analyzing SLA. Lastly, whereas SLA measurements are less sensitive than FIS measurements, SLA can also be characterized after forskolin induction, enabling a highly sensitive characterization of drug effect. We exploited this in **chapter 5** for characterization of ACE-tRNAs, allowing characterization of ACE-tRNA mediated functional CFTR restoration. However, whilst this is valuable for characterization of potential compounds, translational value is expected to be low as only luminal area increased opposed to swelling of the entire structure.

Strength and future applications of drug repurposing

Developing new drugs is exceptionally time-consuming and expensive, especially in the context of rare diseases. In this regard, drug repurposing is an attractive solution that holds economical and time-wise benefits. For proper drug repurposing assays it is essential that the preclinical assay has a sufficient dynamic window and is robust, and preferably of high translational value to really speed up translating preclinical results into a clinical setting. The fact that the FIS assay is well characterized in terms of its preclinical-to-clinical translational value, indicates its potential for drug repurposing experiments. Furthermore, screening in a high-throughput fashion is essential to increase the odds of finding hits. As such, in **chapter 6,** we established a 384 wells version of the FIS assay, allowing testing of compounds that directly or indirectly influence CFTR function in a high-throughput manner. Although recent work showed the implementation of organoid cultures in 384- and 1536-WP format for HTS, exploited read-outs were relatively simple in comparison to the functional read-out of the FIS assay and exhibited lower Z'-factors [45]–[47]. We subsequently exploited the 384-WP FIS assay in **chapter 6 and 7** to screen 1443 FDA-approved compounds in 80 PDIOs recapitulating a wide range of genetic contexts, resulting in over 60 00 datapoints in the primary screens. To our knowledge, such a tremendous (team) effort has not earlier been described in the context of primary cells in a functional assay.

Statins

First, in **chapter 6,** we set out to identify FIS-increasing compounds in PDIOs homozygous for W1282X-CFTR, pretreated with lumacaftor/ivacaftor to increase baseline CFTR function and facilitate hit detection. Prior to assessing the effect of compounds on functional CFTR restoration, we assessed toxicity of all compounds by means of PI-calcein analysis. Whilst this allowed for exclusion of 43 toxic compounds, we recommend a different analysis type

in future studies. For example, viability in 3D organoids is at present-day often assessed by means of cell titer glo (CTG), which is less time-consuming and has a larger dynamic window to assess effects [48], [49].

Subsequential, we found that in the presence of CFTR modulators, statins significantly increased swelling of PDIOs with PTC-CFTR. Statins are generally known for their cholesterol and isoprenoid-lowering effects, yet have been described to interact with many pathways including STAT1/3, p38, MAPK and Akt phosphorylation [50]–[52]. Interestingly, previous studies described a negative association between cholesterol depletion and CFTR function. As cholesterol is essential for lipid raft formation where CFTR preferentially resides, cholesterol depletion had a negative impact on CFTR levels and function [53]. This possibly points into the direction of a different non-cholesterol related mode-of-action, further underlined by the fact that inhibition of cholesterol synthesis by 6F, did not yield an observable effect. Statin treatment moreover did not result in NMD inhibition, as shown by an absence of effect on CFTR mRNA levels. To fully elucidate the statins' mode-of-action in CFTR rescue, more comprehensive investigations are warranted. Additionally, genotype-specificity should be further elucidated. Whilst we describe an absence of effect in F508del and R334W context, assessing the effect of statins on a larger panel of organoid with different genotypes will be valuable to draw firm conclusions on this.

CFTR modulators and PDE4 inhibitors

Next, in **chapter 7,** we screened 76 non-homozygous F508del PDIOs using the miniaturized FIS assay, aiming to identify CFTR function enhancing drugs in a 1400-compound FDA-approved drug library. Among all tested compounds, the positive control consisting of CFTR modulators lumacaftor/ivacaftor resulted in the highest increase in FIS in most donors. Importantly, as CFTR modulators are already approved for specific CF mutations, it would be a matter of label extension instead of drug repurposing to treat pwCF with modulators, resulting in an even faster translation into the clinic. Based on the association between FIS data and clinical data, 17 out of 54 or 23 out of 54 PDIOs included in this chapter could have a moderate clinical benefit of respectively VX-770 or VX-809/VX-770 therapy. Recently, a similar repurposing study with the more effective HEMT combination ETI was performed by Lefferts *et al* [79]. This study further confirms that screening CFTR restoring potential of CFTR modulators for non-eligible *CFTR* genotypes is constructive, as a considerable amount of pwCF with non-eligible genotypes could indeed benefit from CFTR modulator treatment.

Additional to CFTR modulators, we show that PDE4 inhibitors are potent CFTR function inducers in PDIOs when residual CFTR is either present, or created by additional compound exposure. PDEs catalyze the hydrolysis of phosphodiester bonds of second messengers such as cAMP by PDE4, thereby regulating many downstream signaling processes such as smooth muscle activation [54], [55]. Consequently, the inhibition of PDE4 results in an increase of cAMP levels, connecting PDE4 inhibitors such as roflumilast to smooth muscle relaxation and accordingly its use in obstructive airway diseases such as COPD [56]. In the context of CFTR, PDE4 mediated increase in cAMP supposedly results in subsequent PKA activation and increased CFTR channel opening. Importantly, PDE4 inhibition does not restore CFTR function directly. This is underlined by the absence of PDE4 inhibitor monotherapy mediated increase in CFTR function in W1282X/W1282X PDIOs. For some CFTR mutations however, such as R334W, PDE4 inhibitors could serve as monotherapy. For this genotype, roflumilast restored CFTR function to a similar extend as lumacaftor/ivacaftor. Furthermore, large synergistic effects can be achieved by combination of roflumilast with compounds with different molecular working mechanisms. We describe that the combination of ELX-02/ETI and roflumilast is almost as potent as ELX-02/ETI and SMG1i in the context of restoring W1282X-CFTR function, circumventing the need for an NMD inhibitor. Additionally, in a clinical setting where PDE4 inhibitors act systemically, non-CFTR related side-effects of PDE4 inhibitors could be of additional benefit. For COPD, PDE4 associated smooth muscle relaxation and anti-inflammatory characteristics have been associated with improving lung function and decreasing the annual rate of exacerbations, which could prove useful in the context of CF as well [56]. On a last note, a daily dose of simvastatin is estimated to cost $1428 on an annual basis in the UK, compared to $250,000 for CFTR modulators [57], [58]. This further highlights that characterization of roflumilast in a clinical trial setting is warranted, both as monotherapy as well as part of a combinatorial treatment regimen. We summarize our drug repurposing approach and corresponding next steps in **Figure 2**.

Figure 2. Drug repurposing allows characterization of CFTR increasing potential of novel compound families.

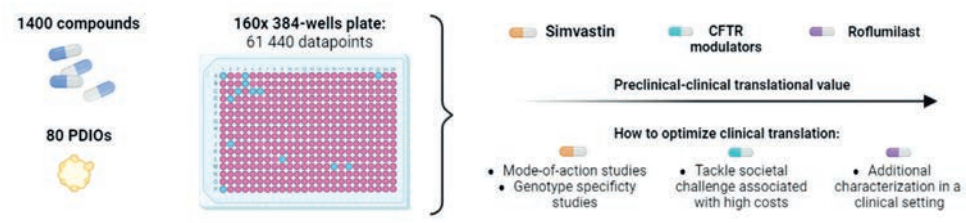

In **chapter 6, 7** and **8** we describe work on repurposing FDA-approved drugs for CF. We approximately screened 1400 compound on 80 PDIOs resulting in roughly 60 000 datapoints, of which three compound families particularly proved promising: statins, CFTR modulators and PDE4 inhibitors such as roflumilast. To optimize preclinical-to-clinical translation, certain follow-up steps are recommended for each compound family.

From bench to bedside based on drug repurposing studies

Based on the results of **chapter 6 and 7,** we hypothesized that a combination of ETI, roflumilast and statins could synergistically restore CFTR function. We tested this in **chapter 7** in PDIOs using the FIS assay for two different *CFTR* genotypes that are not eligible for ETI at present-day and that have previously been characterized as unresponsive to ETI monotreatment: L927P/W1282X and W1282X/W1282X. Rescue of CFTR with the complete compound combination indeed showed significant rescue of FIS, whilst single compounds or dual combinations were mostly ineffective. As noted in an earlier section, it is striking that this treatment regimen yielded beneficial for the homozygous PTC mutation, W1282X-CFTR. W1282X however is a PTC mutation relatively close to the NTC, that consequently results in the production of CFTR protein variants with a relatively small C-truncation. For that reason, we can envisage that W1282X could benefit to some extent from CFTR modulation, presumably in particular through potentiation provided by elexacaftor and ivacaftor. Additionally, the low amount of "corrected" W1282X-*CFTR* that ends up at the plasma membrane could be activated by roflumilast.

Comparison of the results of the entire compound combination for both genotypes to benchmark data of lumacaftor/ivacaftor and ETI treated F508del/F508del PDIOs, indicated that the effects of the complete compound combination were in a clinically relevant range. As the patient with L927P/W1282X *CFTR* experienced rapid clinical deterioration, we therefore initiated treatment with the complete drug combination in a clinical N-of-1 setting. Clinically, the magnitude of response was major and strongly supports individual clinical benefit underlined by a SwCl decrease similar to observations in F508del/MF ETI treated pwCF, suggesting drug-induced effects [59]. Additionally, lung function improved significantly which was demonstrated by an FEV1pp increase similar to two-third of the increase as measured in F508del/MF ETI treated pwCF and the improvements in self-reported health perceptions furthermore emphasize major health improvements for the patient. The change in SwCl concentration and the preclinical PDIO data support direct modulation of CFTR *in vivo*, yet potentially roflumilast-mediated smooth muscle relaxation further increased FEV1pp. Whilst promising, this single case observation needs to be interpreted with care as a washout period showing subsequent decline is missing and no firm conclusions can be drawn about the contribution of the separate compounds. Future studies in larger subgroups with placebo-controlled cohorts should further investigate genotype-specificity as well as the contribution of the different drugs.

All in all, drug repurposing studies yield many advantages and can tremendously speed up the conventional drug development pipeline, in particular when the repurposing study is performed in patient-derived cell models in functional assays. Potentially, repeating this study using different FDA approved compounds could yield additional insights into novel compounds that hold CFTR elevating potential.

Leaving no one behind

We describe several promising strategies related to combinatorial approaches using HEMTs. In this thesis, we however do not describe the large societal challenges related to HEMTs, particularly its pricing, legislation and reimbursement approval. In this context, recent studies estimated costs of production for elexacaftor/tezacaftor/ivacaftor at $5,676 per year, which is 97% lower than the US list price of $250 000 [72]. Consequently, this current pricing model restricts access to the best available therapy, thereby exacerbating existing inequalities in CF care. Cost-associated barriers to and solutions for CFTR modulator equity were recently well summarized by Taylor-Cousar *et al* [59]. Based on preclinical results presented throughout this thesis in **chapter 3, 6, 7 and 8,** it is clear that more pwCF can be benefit from HEMTs as monotherapy, or as part of combinatorial treatment regimen. However, whilst promising preclinical or even clinical data is a first step needed for success stories for all pwCF who could benefit from HEMTs, this is not enough. This is additionally emphasized by our case study **(chapter 8).** Preclinical FIS characterization guided a successful clinical intervention, which additionally resulted in success from a scientific point of view due to subsequential publication in the highly valued scientific journal European Respiratory Journal (ERJ). However, the health insurance company was not willing to reimburse the costs of ETI specifically. Consequently, the patient stopped receiving the treatment regimen after this study, resulting in detoriating health immediately after. Together with his treating physician and the Dutch Cystic Fibrosis Patient Association (Nederlandse Cystic Fibrosis Stichting, NCFS), the patient filed a complaint against this decision at the Health Insurance Disputes Committee. I am content to have added the next sentence as very last change in my thesis: in December 2023, the Health Insurance Disputes Committee made the binding decision that the health insurance company has to reimburse the costs of ETI, based on the positive, persuasive preclinical and clinical data, allowing the patient to continue with the full treatment regimen [60]. Whilst this is very good news and the efforts of his treating physicians as well as the NCFS should be acclaimed, the process between obtaining positive (pre)clinical results and final continuation with a specific treatment regimen, clearly should be improved. This case furthermore underlines the large associated need and consequentially major goal for the CF community to increase availability of triple combination treatment worldwide and obtaining access to CFTR modulators for all pwCF that could benefit from them. To achieve this, societal attention for and discussion on HEMT costs and insurance acceptance is pivotal [59].

In this context, a potential approach to improve modulator access is to continue studies on different CFTR modulators, despite the existence of HEMTs. Currently, the compounds produced by Vertex are the only regulatory approved CFTR modulators, but several others are progressing through preclinical studies and clinical trial pipelines. In this context, Abbvie (ABBV) acquired a portfolio of CFTR modulating drugs initially developed by Galapagos (GLPG), which we studied preclinically in **chapter 9.** Here, we characterize efficiency of ABBV/GLPG-Triple therapy consisting of 2 CFTR modulators and 1 CFTR potentiator, and compare this to the approved modulator regimen lumacaftor/ivacaftor. ABBV/GLPG-Triple therapy was higher than lumacaftor/ivacaftor in homozygous F508del/F508del PDIOs, in-

dicating potential clinical efficacy, albeit comparison between FIS upon ABBV/GLPG-Triple therapy to recent data of ETI treated PDIOs underlines that ETI is superior at increasing CFTR function (Lefferts, 2023). The effects of the modulators of ABBV/GLPG-Triple therapy have been assessed in clinical trials as monotherapies [61], [62], yet the full combination with the additional potentiator is not yet under investigation in a clinical setting. Further optimization of such treatment regimens, comparison to established HEMTs and final characterization of efficacy in a clinical setting is pivotal and could aid in stimulating competition between different manufacturers, thereby improving cost-effectiveness of CFTR modulator regimens.

Genotype-overarching strategies for all pwCF

Whilst we describe promising strategies for some CFTR mutations, we do not touch upon how to restore function of other severe *CFTR* mutations such as large deletions or splice mutations. For these mutations, genotype-overarching treatment regimens that could work for all pwCF are particularly attractive. Whilst not studied in this thesis, two genotype-overarching treatment regimens are in particular on the rise and deserve mentioning: gene/mRNA therapy and modulation of alternative chloride channels. Firstly, classic gene therapy aims to introduce WT copies of *CFTR* DNA into the patient in the desired organ. Whilst preclinical studies show promising results, several challenges remain that need to be tackled for application in a clinical setting [63]. One particular challenge is the efficient and safe delivery into the ASC population of the different affected organs, circumventing the need for repeated rounds of gene therapy. Furthermore, ensuring a 100% safety remains challenging as insertional mutagenesis could occur due to unpredictable genomic incorporation of the *CFTR* copies. A strategy that circumvents permanent off-target effects, is the introduction of CFTR mRNA copies offering a temporary correction. This means that frequent re-administration is required to maintain therapeutic benefits. Similarly to gene therapy, the major hurdle of mRNA therapy is delivery. Various delivery methods such as lipid nanoparticles and viral vectors are being investigated, and their effectiveness, safety, and efficiency need to be carefully evaluated. First results recently published of the RESTORE-CF phase I/II trial (NCT03375047) in which pwCF were treated with LNP-formulated aerosols with CFTR mRNA, which reported mild side-effects and unfortunately no improvement of FEV1 [64]. The study however was not powered or intended to detect a change in FEV1 and participants were permitted to be on a stable dose of ETI, potentially masking beneficial effects of the study drug. Future studies of efficacy of inhaled CFTR mRNA are warranted for drawing firm conclusions on efficacy. Additional to the non-specific introduction of wildtype CFTR DNA/RNA copies, gene-editing techniques can allow partial correction or full replacement of the mutated *CFTR* gene. CRISPR-CAS has showed to be an efficient, customizable tool for restoring wildtype CFTR in preclinical studies [65]. However, efficiency and safety challenges remain, due to delivery-hurdles and potential off-target effects. Future studies performed in the coming decade(s) will elucidate whether gene therapy really will prove itself as genotype-overarching treatment regimen for all pwCF.

Encountering and challenging new complications for ageing pwCF

Evidently, the last decade of CF research resulted in major progress and influenced the lives of many pwCF. As such, life expectancy of HEMT treated pwCF is expected to increase massively, approaching the average age of individuals without CF [66]. Despite this tremendous progress, the aging CF population faces new difficulties. First off, a large subset of pwCF received HEMTs when tissue was already damaged and remodeled, resulting in overrepresentation of fibrotic tissue hampering organ function. Future studies that further investigate how such damage can be repaired will be useful for the ageing CF population [67]. Additionally, a third of all adult CF patients suffer from a range of co-morbidities, such as an increased chance of developing a variety of epithelial cancers such as breast cancer, head and neck cancer, pancreatic cancer, ovarian cancer, lung cancer and colorectal cancer (CRC) [68]–[71]. The increase in prevalence of CRC has been described in particular, whilst its prevalence is 2-5% in the non-CF population between 40-49 years old, its prevalence is around 23% in CF patients [72]–[76]. Increasing our understanding of the effects of dysregulated CFTR in a wide context, will be an essential challenge to tackle to improve the lives of all pwCF.

Concluding remarks

New solutions are needed for the last 10-15% of pwCF carrying *CFTR* mutations that are unresponsive to HEMTs. We explored different strategies for fulfilling the unmet clinical needs of those pwCF, particularly in the context of nonsense mutations. We exploited state-of-the-art functional experiments in PDIOs, allowing preclinical-clinical translation of the novel combinatorial therapies that furthermore allow guidance of personalized treatment strategies.

An interesting question, is whether findings in this thesis can be extrapolated to different diseases. In this context, I believe that our work on nonsense mutations is to some extent CF-overarching, in particular the main conclusion of the need to characterize combinatorial treatment regimens instead of finding a golden bullet. This approach applies for treating nonsense mutations of other diseases as well such as DMD, for which readthrough compounds could be combined with proteasome inhibitors and heat shock activators, as well as cancers with mutations in for example the tumor-suppressor gene P53, for which various compounds correcting structural defects also have been described [77], [78]. Additional to our work on nonsense mutations, our developed pipelines and lines of thoughts concerning preclinical-clinical translation presented in this thesis, hold value for other disease-areas as well. One of the elements that I personally valued highly about the research performed in our lab, is the extent to which focus on the importance of preclinical-to-clinical translation of data generated in our studies. Whilst fundamental studies are pivotal to fully understand the underlying molecular defects and consequently to elucidate potential targets for precision therapies, subsequential follow-up in endogenous, functional assays on patient-derived material is invaluable, as we hope to have underlined in this thesis.

Whilst many challenges need to be tackled, we envisage that the work presented in this thesis aids in advancing precision medicine for CF and that concepts we explore here can be transferred to other diseases. We hope and expect that additional ongoing and future studies, that build on the work presented here, will further pave the way towards therapy development and availability for all people with CF.

References

[1] B. Roy *et al.,* "Ataluren stimulates ribosomal selection of near-cognate tRNAs to promote nonsense suppression," *Proc. Natl. Acad. Sci.,* vol. 113, no. 44, pp. 12508–12513, 2016.

[2] S. Spelier, E. P. M. van Doorn, C. K. van der Ent, J. M. Beekman, and M. A. J. Koppens, "Readthrough compounds for nonsense mutations: bridging the translational gap," *Trends Mol. Med.,* 2023.

[3] E. Mercuri *et al.,* "Safety and effectiveness of ataluren: comparison of results from the STRIDE Registry and CINRG DMD Natural History Study," *J. Comp. Eff. Res.,* vol. 9, no. 5, pp. 341–360, 2020.

[4] C. M. McDonald *et al.,* "Ataluren in patients with nonsense mutation Duchenne muscular dystrophy (ACT DMD): a multicentre, randomised, double-blind, placebo-controlled, phase 3 trial," *Lancet,* vol. 390, no. 10101, pp. 1489–1498, 2017.

[5] Y. Qian and M.-X. Guan, "Interaction of aminoglycosides with human mitochondrial 12S rRNA carrying the deafness-associated mutation," *Antimicrob. Agents Chemother.,* vol. 53, no. 11, pp. 4612–4618, 2009.

[6] I. Nudelman *et al.,* "Development of novel aminoglycoside (NB54) with reduced toxicity and enhanced suppression of disease-causing premature stop mutations," *J. Med. Chem.,* vol. 52, no. 9, pp. 2836–2845, 2009.

[7] I. Behm–Ansmant, D. Gatfield, J. Rehwinkel, V. Hilgers, and E. Izaurralde, "A conserved role for cytoplasmic poly (A)–binding protein 1 (PABPC1) in nonsense–mediated mRNA decay," *EMBO J.,* vol. 26, no. 6, pp. 1591–1601, 2007.

[8] M. Cassan and J.-P. Rousset, "UAG readthrough in mammalian cells: effect of upstream and downstream stop codon contexts reveal different signals," *BMC Mol. Biol.,* vol. 2, no. 1, pp. 1–8, 2001.

[9] M. T. Howard, B. H. Shirts, L. M. Petros, K. M. Flanigan, R. F. Gesteland, and J. F. Atkins, "Sequence specificity of aminoglycoside–induced stop codon readthrough: Potential implications for treatment of Duchenne muscular dystrophy," *Ann. Neurol. Off. J. Am. Neurol. Assoc. Child Neurol. Soc.,* vol. 48, no. 2, pp. 164–169, 2000.

[10] J. R. Wangen and R. Green, "Stop codon context influences genome-wide stimulation of termination codon readthrough by aminoglycosides," *Elife,* vol. 9, 2020.

[11] A. Bowling *et al.,* "Downstream Alternate Start Site Allows N-Terminal Nonsense Variants to Escape NMD and Results in Functional Recovery by Readthrough and Modulator Combination," *J. Pers. Med.,* vol. 12, no. 9, p. 1448, 2022.

[12] O. Laselva *et al.,* "Functional rescue of c. 3846G> A (W1282X) in patient-derived nasal cultures achieved by inhibition of nonsense mediated decay and protein modulators with complementary mechanisms of action," *J. Cyst. Fibros.,* vol. 19, no. 5, pp. 717–727, 2020.

[13] A. Venturini *et al.,* "Comprehensive Analysis of Combinatorial Pharmacological Treatments to Correct Nonsense Mutations in the CFTR Gene," *Int. J. Mol. Sci.,* vol. 22, no. 21, p. 11972, 2021.

[14] C. E. Wainwright *et al.,* "Lumacaftor–Ivacaftor in Patients with Cystic Fibrosis Homozygous for Phe508del CFTR," *N. Engl. J. Med.,* vol. 373, no. 3, pp. 220–231, 2015, doi: 10.1056/nejmoa1409547.

[15] D. K. Crawford, J. Mullenders, J. Pott, S. F. Boj, S. Landskroner-Eiger, and M. M. Goddeeris, "Targeting G542X CFTR nonsense alleles with ELX-02 restores CFTR function in human-derived intestinal organoids," *J. Cyst. Fibros.,* vol. 20, no. 3, pp. 436–442, 2021.

[16] J. Woolford, "Eloxx Pharmaceuticals Reports Positive Topline Results from Monotherapy Arms of Phase 2 Clinical Trial of ELX-02 in Class 1 Cystic Fibrosis Patients," 2021. [Online]. Available: https://investors.eloxxpharma.com/node/11986/pdf

[17] J. Woolford, "Eloxx Pharmaceuticals Reports Topline Results from Phase 2 Combination Clinical Trial of ELX-02 in Class 1 Cystic Fibrosis (CF) Patients," 2022. [Online]. Available: https://investors.eloxxpharma.com/news-releases/news-release-details/eloxx-pharmaceuticals-reports-topline-results-phase-2?fbclid=IwAR31GRojriXkl1njErqm3qQCY6-Cw4bgmqP-hzogmDAz58cY9C 2xnjZeXw

[18] J. T. Mendell, N. A. Sharifi, J. L. Meyers, F. Martinez-Murillo, and H. C. Dietz, "Nonsense surveillance regulates expression of diverse classes of mammalian transcripts and mutes genomic noise," *Nat. Genet.,* vol. 36, no. 10, pp. 1073–1078, 2004.

[19] D. R. McHugh, C. U. Cotton, and C. A. Hodges, "Synergy between readthrough and nonsense mediated decay inhibition in a murine model of cystic fibrosis nonsense mutations," *Int. J. Mol. Sci.,* vol. 22, no. 1, p. 344, 2020.

[20] K. Tan, D. G. Stupack, and M. F. Wilkinson, "Nonsense-mediated RNA decay: an emerging modulator of malignancy," *Nat. Rev. Cancer,* vol. 22, no. 8, pp. 437–451, 2022.

[21] J. Zhao *et al.,* "Molecular profiling of individual FDA-approved clinical drugs identifies modulators of nonsense-mediated mRNA decay," *Mol. Ther. Acids,* vol. 27, pp. 304–318, 2022.

[22] Y. J. Kim, T. Nomakuchi, F. Papaleonidopoulou, L. Yang, Q. Zhang, and A. R. Krainer, "Gene-specific nonsense-mediated mRNA decay targeting for cystic fibrosis therapy," *Nat. Commun.,* vol. 13, no. 1, p. 2978, 2022.

[23] T. A. Hoek *et al.,* "Single-molecule imaging uncovers rules governing nonsense-mediated mRNA decay," *Mol. Cell,* vol. 75, no. 2, pp. 324–339, 2019.

[24] C. Leroy *et al.,* "Use of 2,6-diaminopurine as a potent suppressor of UGA premature stop codons in cystic fibrosis," *Mol. Ther..*

[25] C. Trzaska *et al.,* "2, 6-Diaminopurine as a highly potent corrector of UGA nonsense mutations," *Nat. Commun.,* vol. 11, no. 1, pp. 1–12, 2020.

[26] A. S. Ramalho, M. Boon, M. Proesmans, F. Vermeulen, M. S. Carlon, and K. De Boeck, "Assays of CFTR function in vitro, ex vivo and in vivo," *Int. J. Mol. Sci.,* vol. 23, no. 3, p. 1437, 2022.

[27] P. S. C. Lentini *et al.,* "Inhibition of FTSJ1, a tryptophan tRNA-specific 2'-O-methyltransferase as possible mechanism to readthrough premature termination codons (UGAs) of the CFTR mRNA," *Abstract FISV Conference 2022,* 2022. https://iris.unipa.it/handle/10447/569426

[28] I. Pibiri, R. Melfi, M. Tutone, A. Di Leonardo, A. Pace, and L. Lentini, "Targeting nonsense: optimization of 1, 2, 4-oxadiazole trids to rescue cftr expression and functionality in cystic fibrosis cell model systems," *Int. J. Mol. Sci.,* vol. 21, no. 17, p. 6420, 2020.

[29] L.-A. Gurzeler *et al.,* "Drug-induced eRF1 degradation promotes readthrough and reveals a new branch of ribosome quality control," *Cell Rep.,* vol. 42, no. 9, 2023.

[30] J. Sharma *et al.,* "A small molecule that induces translational readthrough of CFTR nonsense mutations by eRF1 depletion.," *Nat. Commun.,* vol. 12, no. 1, p. 4358, Jul. 2021, doi: 10.1038/s41467-021-24575-x.

[31] A. Baradaran-Heravi, A. D. Balgi, S. Hosseini-Farahabadi, K. Choi, C. Has, and M. Roberge, "Effect of small molecule eRF3 degraders on premature termination codon readthrough," *Nucleic Acids Res.,* vol. 49, no. 7, pp. 3692–3708, 2021.

[32] C. F. G.-P. Consortium, "Correlation between genotype and phenotype in patients with cystic fibrosis," *N. Engl. J. Med.,* vol. 329, no. 18, pp. 1308–1313, 1993.

[33] K. M. de Winter-de Groot *et al.,* "Stratifying infants with cystic fibrosis for disease severity using intestinal organoid swelling as a biomarker of CFTR function," *Eur. Respir. J.,* vol. 52, no. 3, 2018.

[34] G. Berkers *et al.,* "Rectal organoids enable personalized treatment of cystic fibrosis," *Cell Rep.,* vol. 26, no. 7, pp. 1701–1708, 2019.

[35] K. He and W.-J. Gan, "Wnt/ -Catenin Signaling Pathway in the Development and Progression of Colorectal Cancer," *Cancer Manag. Res.,* pp. 435–448, 2023.

[36] "Novel Approach Allows Expansion of Indication for Cystic Fibrosis Drug," 18/05/2017. https://www.fda.gov/drugs/news-events-human-drugs/novel-approach-allows-expansion-indication-cystic-fibrosis-drug

[37] J. F. Dekkers *et al.,* "Characterizing responses to CFTR-modulating drugs using rectal organoids derived from subjects with cystic fibrosis," *Sci. Transl. Med.,* vol. 8, no. 344, pp. 344ra84-344ra84, 2016.

[38] D. Muilwijk *et al.,* "Prediction of real-world long-term outcomes of people with CF homozygous for the F508del mutation treated with CFTR modulators," *J. Pers. Med.,* vol. 11, no. 12, p. 1376, 2021.

[39] G. Berkers *et al.,* "Lumacaftor/ivacaftor in people with cystic fibrosis with an A455E–CFTR mutation," *J. Cyst. Fibros.,* vol. 20, no. 5, pp. 761–767, 2021.

[40] S. Y. Graeber *et al.,* "Comparison of Organoid Swelling and In Vivo Biomarkers of CFTR Function to Determine Effects of Lumacaftor–Ivacaftor in Patients with Cystic Fibrosis Homozygous for the F508del Mutation," *Am. J. Respir. Crit. Care Med.,* vol. 202, no. 11, pp. 1589–1592, 2020.

[41] D. Muilwijk *et al.,* "Forskolin-induced Organoid Swelling is Associated with Long-term CF Disease Progression," *Eur. Respir. J.,* 2022.

[42] J. W. Lefferts *et al.,* "CFTR Function Restoration upon Elexacaftor/Tezacaftor/Ivacaftor Treatment in Patient-Derived Intestinal Organoids with Rare CFTR Genotypes," *Int. J. Mol. Sci.,* vol. 24, no. 19, p. 14539, 2023.

[43] P. van Mourik, S. Michel, A. M. Vonk, J. M. Beekman, and C. K. van der Ent, "Rationale and design of the HIT-CF organoid study: stratifying cystic fibrosis patients based on intestinal organoid response to different CFTR-modulators," *Transl. Med. Commun.,* vol. 5, pp. 1–8, 2020.

[44] Y. Du *et al.,* "Development of a miniaturized 3D organoid culture platform for ultra-high-throughput screening," *J. Mol. Cell Biol.,* vol. 12, no. 8, pp. 630–643, 2020.

[45] J. X. Jiang *et al.,* "A new platform for high-throughput therapy testing on iPSC-derived lung progenitor cells from cystic fibrosis patients," *Stem cell reports,* vol. 16, no. 11, pp. 2825–2837, 2021.

[46] A. Berg *et al.,* "High-throughput surface liquid absorption and secretion assays to identify F508del CFTR correctors using patient primary airway epithelial cultures," *SLAS Discov. Adv. Life Sci. R&D,* vol. 24, no. 7, pp. 724–737, 2019.

[47] E. Driehuis *et al.,* "Oral mucosal organoids as a potential platform for personalized cancer therapy," *Cancer Discov.,* 2019.

[48] H. E. Francies, A. Barthorpe, A. McLaren-Douglas, W. J. Barendt, and M. J. Garnett, "Drug sensitivity assays of human cancer organoid cultures," *Organoids Stem Cells, Struct. Funct.,* pp. 339–351, 2019.

[49] W. Zhao and S.-P. Zhao, "Different effects of statins on induction of diabetes mellitus: an experimental study," *Drug Des. Devel.* Ther., vol. 9, p. 6211, 2015.

[50] A. Bonifacio, G. M. Sanvee, J. Bouitbir, and S. Krähenbühl, "The AKT/mTOR signaling pathway plays a key role in statin-induced myotoxicity," *Biochim. Biophys. Acta (BBA)-Molecular Cell Res.,* vol. 1853, no. 8, pp. 1841–1849, 2015.

[51] N. E. Kreiselmeier, N. C. Kraynack, D. A. Corey, and T. J. Kelley, "Statin-mediated correction of STAT1 signaling and inducible nitric oxide synthase expression in cystic fibrosis epithelial cells," *Am. J. Physiol. Cell. Mol. Physiol.,* vol. 285, no. 6, pp. L1286–L1295, 2003.

[52] S. Chin *et al.,* "Cholesterol interaction directly enhances intrinsic activity of the cystic fibrosis transmembrane conductance regulator (CFTR)," *Cells,* vol. 8, no. 8, p. 804, 2019.

[53] K. P. Garnock-Jones, "Roflumilast: A Review in COPD," *Drugs,* vol. 75, no. 14, pp. 1645–1656, 2015, doi: 10.1007/s40265-015-0463-1.

[54] M. J. Turner, K. Abbott-Banner, D. Y. Thomas, and J. W. Hanrahan, "Cyclic nucleotide phosphodiesterase inhibitors as therapeutic interventions for cystic fibrosis," *Pharmacol. Ther.,* vol. 224, p. 107826, 2021, doi: 10.1016/j.pharmthera.2021.107826.

[55] K. F. Rabe, "Update on roflumilast, a phosphodiesterase 4 inhibitor for the treatment of chronic obstructive pulmonary disease," *Br. J. Pharmacol.,* vol. 163, no. 1, pp. 53–67, 2011.

[56] J. Guo, J. Wang, J. Zhang, J. Fortunak, and A. Hill, "Current prices versus minimum costs of production for CFTR modulators," *J. Cyst. Fibros.,* vol. 21, no. 5, pp. 866–872, 2022.

[57] H. Jick, A. Wilson, P. Wiggins, and D. P. Chamberlin, "Comparison of Prescription Drug Costs in the U nited S tates and the U nited K ingdom, Part 1: Statins," *Pharmacother. J. Hum. Pharmacol. Drug Ther.,* vol. 32, no. 1, pp. 1–6, 2012.

[58] P. G. Middleton *et al.,* "Elexacaftor–tezacaftor–ivacaftor for cystic fibrosis with a single Phe508del allele," *N. Engl. J. Med.,* vol. 381, no. 19, pp. 1809–1819, 2019.
[59] J. L. Taylor-Cousar, P. D. Robinson, M. Shteinberg, and D. G. Downey, "CFTR modulator therapy: transforming the landscape of clinical care in cystic fibrosis," Lancet, 2023.
[60] SKGZ, "Uitspraak Trikafta Vergoeding, L927P/W1282X patiënt Erasmus Ziekenhuis," 2024. https://www.skgz.nl/document/?d=e99a3d59-d774-452f-9310-71ee9b2ee441
[61] S. van Koningsbruggen-Rietschel *et al.,* "GLPG2737 in lumacaftor/ivacaftor-treated CF subjects homozygous for the F508del mutation: A randomized phase 2A trial (PELICAN)," *J. Cyst. Fibros.,* vol. 19, no. 2, pp. 292–298, 2020.
[62] S. C. Bell *et al.,* "CFTR activity is enhanced by the novel corrector GLPG2222, given with and without ivacaftor in two randomized trials," *J. Cyst. Fibros.,* vol. 18, no. 5, pp. 700–707, 2019.
[63] G. A. R. Gonçalves and R. de M. A. Paiva, "Gene therapy: advances, challenges and perspectives," *Einstein (Sao Paulo),* vol. 15, pp. 369–375, 2017.
[64] S. M. Rowe *et al.,* "Inhaled mRNA therapy for treatment of cystic fibrosis: Interim results of a randomized, double-blind, placebo-controlled phase 1/2 clinical study," *J. Cyst. Fibros.,* 2023.
[65] M. H. Geurts *et al.,* "CRISPR-Based Adenine Editors Correct Nonsense Mutations in a Cystic Fibrosis Organoid Biobank," *Cell Stem Cell,* vol. 26, no. 4, pp. 503-510.e7, 2020, doi: 10.1016/j.stem.2020.01.019.
[66] A. Lopez, C. Daly, G. Vega-Hernandez, G. MacGregor, and J. L. Rubin, "Elexacaftor/tezacaftor/ivacaftor projected survival and long-term health outcomes in people with cystic fibrosis homozygous for F508del," *J. Cyst. Fibros.,* 2023.
[67] G. Liu *et al.,* "Therapeutic targets in lung tissue remodelling and fibrosis," *Pharmacol. Ther.,* vol. 225, p. 107839, 2021.
[68] C. Fitzmaurice *et al.,* "Global, regional, and national cancer incidence, mortality, years of life lost, years lived with disability, and disability-adjusted life-years for 32 cancer groups, 1990 to 2015: a systematic analysis for the global burden of disease study," *JAMA Oncol.,* vol. 3, no. 4, pp. 524–548, 2017.
[69] P. Maisonneuve, B. C. Marshall, and A. B. Lowenfels, "Risk of pancreatic cancer in patients with cystic fibrosis," *Gut,* vol. 56, no. 9, pp. 1327–1328, 2007.
[70] M. C. Southey *et al.,* "CFTR ΔF508 carrier status, risk of breast cancer before the age of 40 and histological grading in a population-based case-control study," *Int. J. cancer,* vol. 79, no. 5, pp. 487–489, 1998.
[71] J. Xu *et al.,* "High level of CFTR expression is associated with tumor aggression and knockdown of CFTR suppresses proliferation of ovarian cancer in vitro and in vivo," *Oncol. Rep.,* vol. 33, no. 5, pp. 2227–2234, 2015.
[72] R. J. Birch *et al.,* "The risk of colorectal cancer in individuals with mutations of the cystic fibrosis transmembrane conductance regulator (CFTR) gene: An English population-based study," *J. Cyst. Fibros.,* vol. 22, no. 3, pp. 499–504, 2023.
[73] A. K. Fink *et al.,* "Cancer risk among lung transplant recipients with cystic fibrosis," *J. Cyst. Fibros.,* vol. 16, no. 1, pp. 91–97, 2017.

[74] I. Gory, G. Brown, J. Wilson, W. Kemp, E. Paul, and S. K. Roberts, "Increased risk of colorectal neoplasia in adult patients with cystic fibrosis: A matched case–control study," *Scand. J. Gastroenterol.,* vol. 49, no. 10, pp. 1230–1236, 2014.
[75] P. Maisonneuve, B. C. Marshall, E. A. Knapp, and A. B. Lowenfels, "Cancer risk in cystic fibrosis: a 20-year nationwide study from the United States," *J. Natl. Cancer Inst.,* vol. 105, no. 2, pp. 122–129, 2013.
[76] D. E. Niccum, J. L. Billings, J. M. Dunitz, and A. Khoruts, "Colonoscopic screening shows increased early incidence and progression of adenomas in cystic fibrosis," *J. Cyst. Fibros.,* vol. 15, no. 4, pp. 548–553, 2016.
[77] M. M. J. Fallatah, F. V Law, W. A. Chow, and P. Kaiser, "Small-molecule correctors and stabilizers to target p53," *Trends Pharmacol. Sci.,* 2023.
[78] D. M. Talsness, J. J. Belanto, and J. M. Ervasti, "Disease-proportional proteasomal degradation of missense dystrophins," *Proc. Natl. Acad. Sci.,* vol. 112, no. 40, pp. 12414–12419, 2015.
[79] J. Lefferts *et al.*, "OrgaSegment: deep-learning based organoid segmentation to quantify CFTR dependent fluid secretion", *Commun Bio*l vol. 7, no. 319, 2024

Chapter | 10

Addenda

Introductie

Taaislijmziekte: de meest voorkomende, zeldzame ziekte

Het begrijpen van zeldzame, genetische ziektes en het ontwikkelen van effectieve behandelingen voor deze ziektes zijn grote uitdagingen in medisch onderzoek. Traditioneel zijn de meeste behandelingen voor genetische ziektes gericht op het verlichten van symptomen, maar niet op het corrigeren van de onderliggende genetische oorzaken. In de afgelopen decennia zijn er echter grote stappen gezet in de zogenaamde precisiegeneeskunde voor verschillende ziekten. Precisiegeneeskunde houdt in dat de onderliggende oorzaak van een ziekte wordt aangepakt, rekening houdend met de genetische achtergrond van de individuele patiënt.

In dit proefschrift, bestuderen we de erfelijke ziekte taaislijmziekte (cystic fibrosis, ofwel CF), een ziekte waarvoor precisiegeneeskunde cruciaal is gebleken met betrekking tot de ontwikkeling van nieuwe, zeer effectieve behandelingen. CF is een zeldzame ziekte veroorzaakt door een defect in het *CFTR*-gen, dat in de gezonde situatie zorgt voor de productie van CFTR-eiwit **(Figuur 1)**. CF wordt vaak beschreven als de meest voorkomende zeldzame ziekte, met ongeveer 1 geval per 3000 geboorten in Europa en de Verenigde Staten. In gezonde cellen is CFTR betrokken bij transport van chloride en bicarbonaationen, wat vervolgens leidt tot watertransport de cel uit. Wanneer CFTR niet goed werkt, is het watertransport verstoord, wat leidt tot productie van erg taai slijm dat niet goed de longen wordt uitgetransporteerd. Dit heeft tot gevolg dat alle organen waar CFTR zijn rol uit zou moeten oefenen niet goed functioneren, met name de luchtwegen en de darmen. Traditioneel werd vooral gepoogd symptomen van mensen met CF te verlichten, bijvoorbeeld door slijmverdunners en fysiotherapie om de ademhaling te bevorderen.

Nieuwe behandelmethodes – maar niet voor iedereen

De afgelopen decennia aan CF-onderzoek hebben geleid tot de ontwikkeling van zogenaamde CFTR-modulatoren, die doeltreffend de functie van gemuteerd CFTR kunnen herstellen in een groot deel van de mensen met CF. Er zijn twee types CFTR-modulatoren: CFTR-correctoren corrigeren CFTR-eiwitvouwing, en CFTR-potentiatoren verbeteren de chloortransport functie van CFTR op het celmembraan. De meest recent ontwikkelde combinatie van modulatoren bestaat uit twee correctoren: elexacaftor en tezacaftor, en potentiator ivacaftor (ETI, verkocht als Trikafta). De klinische effecten van ETI zijn indrukwekkend, met name bij mensen met CF met een F508del mutatie, de meest voorkomende CFTR-mutatie die bij ongeveer 80% van de mensen met CF voorkomt. Wat betreft wetgeving is het belangrijk te benoemen dat er een verschil zit tussen Europa en de Verenigde Staten met betrekking tot welke mensen met CF in aanmerking komen voor ETI. De FDA (de autoriteit achter de goedkeuring van medicijnen in Amerika) en de EMA (de autoriteit achter de goedkeuring van medicijnen in Europa) hebben vandaag de dag ETI goedgekeurd voor alle mensen met CF met ten minsten één F508del CFTR-mutatie, waarnaast de FDA ETI ook heeft goedgekeurd voor een aantal zeldzame CFTR-mutaties. Deze goedkeuring staat aan de basis voor wetgeving voor wanneer een verzekeraar behandeling met ETI

Figuur 1

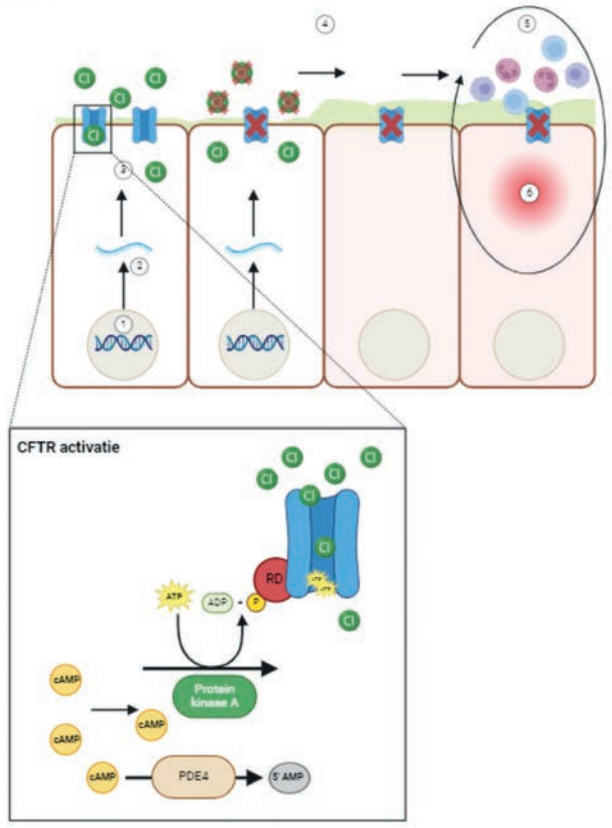

Figuur 1. CFTR (dys)functie

CFTR is een transportkanaal dat zorgt voor chloride en watertransport de cel uit. In de gezonde situatie, wordt het *CFTR*-gen afschreven tot CFTR-mRNA, waar vervolgens tijdens translatie een CFTR-eiwit van gemaakt wordt **(1-3).** Van ieder gen hebben we 2 exemplaren in onze cellen, wanneer op beide CFTR-genen een mutatie ligt, zorgt dit voor het disfunctioneren van CFTR en ontwikkelt de persoon CF. CF wordt gekarakteriseerd door een verlaagde waterconcentratie in het geproduceerde mucus, met als gevolg obstructies door het te taaie mucus **(4).** Bacteriën kunnen hier in groeien **(5),** wat zorgt tot een vicieuze cirkel van ontstekingen en een pro-inflammatoire staat van het weefsel **(6).** Uiteindelijk leidt dit tot progressief verlies van weefselfunctie. Zoom-in: wanneer CFTR aanwezig is op het celmembraan, moet het nog geactiveerd worden. Dit wordt gedaan door cAMP. cAMP zorgt ervoor dat het enzym PKA, met behulp van energie-molecuul ATP, het R-domein van CFTR fosforyleert, waarna CFTR van conformatie verandert en kan zorgen voor chloride-secretie. Een ander belangrijk enzym dat een rol speelt bij dit proces, is PDE4. PDE4 is het enzym dat cAMP kan omzetten tot 5′ AMP, en op die manier kan zorgen voor verlaagde activatie van CFTR.

vergoed: de dure CFTR-modulatoren alleen vergoeden voor de CFTR-mutaties die door de FDA en EMA zijn aangeven als responsief.

Naar schatting hebben 10-15% van de mensen met CF CFTR-mutaties die niet reageren op CFTR-modulatoren. Daarnaast zijn modulatoren niet voor alle mensen met CF beschikbaar, met name door de extreem hoge kosten van deze modulatoren ($250.000 per persoon per jaar) en daarmee samenhangende maatschappelijke uitdagingen als wetgevings- en goedkeuringsproblemen. Ondanks de vele vooruitgang, blijft meer onderzoek dus hard nodig.

CFTR-functie bestuderen in darm-organoïden van mensen met CF

Om CFTR-functie in het lab, ofwel preklinisch, te bestuderen, kunnen verschillende modellen gebruikt worden. De laatste jaren hebben vele onderzoeken aangetoond dat het vooral waardevol is om onderzoek te doen op cellen afgenomen direct van mensen met CF, die gegroeid kunnen worden in het lab. Een doorbraak in het onderzoek naar CF is met name de opkomst van organoïden als modelsysteem. Organoïden zijn driedimensionale celculturen gekweekt vanuit patiënten-weefsel, die de structuur en functie van het oorspronkelijke weefsel nauwgezet nabootsen. Met betrekking tot CF, zijn met name darm-organoïden erg nuttig gebleken voor preklinisch onderzoek naar CFTR-functie en de ontwikkeling van behandelingsmethodes. Door middel van een rectaal biopt kunnen cellen verkregen worden vanuit de darmen van mensen met CF, die opgekweekt kunnen worden in het lab tot organoïden. Deze organoïden bevatten dezelfde CFTR-mutaties als de persoon waarvan de cellen afkomstig zijn en zijn dus representatief voor de patiënt. Om CFTR-functie in de darm-organoïden te beoordelen, maken we gebruik van een zogenaamd zwellingsassay. Wanneer CFTR goed functioneert, zorgt de toevoeging van forskoline voor activatie van CFTR. In darm-organoïden leidt dit tot chloride- en watertransport de organoid in, wat leidt tot organoid-zwelling. Echter, bij organoïden van mensen met CF vindt dit chloride- en watertransport niet plaats, wat resulteert in een groot verschil in morfologie. De mate van forskoline-geïnduceerde zwelling (FIS) weerspiegelt dus CFTR-functie en kan dan ook gebruikt worden om te bepalen of een bepaalde behandeling effectief is voor het herstellen van CFTR-functie.

Vorig onderzoek heeft hiernaast aangetoond dat er een duidelijke link is tussen de mate van CFTR-functie gemeten in het FIS-assay, en longfunctieachteruitgang. Studies hebben hiernaast aangetoond dat wanneer medicijnen zorgen voor herstel van CFTR-functie in het FIS-assay, dezelfde medicijnen waarschijnlijk succesvol zullen zijn in klinische studies. Het goed kunnen voorspellen van uitkomsten van klinische studies of persoonlijke vooruitgang na behandeling, is ontzettend interessant voor mensen met CF en maakt dit model erg waardevol. Tot slot is een opmerkelijke eigenschap van organoïden dat ze zich eindeloos kunnen blijven vermenigvuldigen, wat betekent dat ze kunnen worden bewaard in zogenaamde biobanken en continu opnieuw gebruikt kunnen worden voor onderzoek. Al deze voordelen onderstrepen de waarde van de combinatie van darm-organoïden en het zwellingsassay voor CF-onderzoek en in dit proefschrift maken we dan ook met name gebruik van darm-organoïden van mensen met CF **(Figuur 2).**

Figuur 2

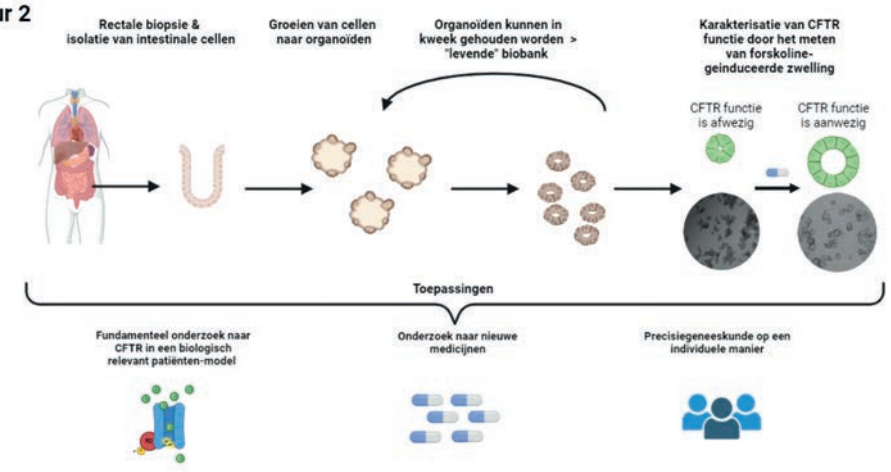

Figuur 2. CFTR-functie bestuderen in darm-organoïden van mensen met CF
Darmcellen kunnen worden geïsoleerd uit rectale biopsies en opgekweekt tot 3D darm-organoïden. Deze organoïden kunnen in kweek gehouden worden en onder specifieke omstandigheden worden bewaard, waardoor de creatie van een levende biobank mogelijk is. Ze dienen daarnaast als een uitstekend model voor de karakterisering van CFTR-functie, met behulp van het zogenaamde forskoline-geïnduceerde zwelling-assay (FIS-assay). Hierbij zorgt forskoline voor CFTR-activatie en watertransport de organoïd in, resulterend in daaropvolgende zwelling van de organoïden. Het FIS-assay is uitermate geschikt voor verschillende toepassingen, variërend van fundamenteel onderzoek tot de identificatie van efficiënte therapeutische regimes en selectie van mensen met CF die baat zouden kunnen hebben bij deze therapeutische regimes.

Het onderzoek in dit proefschrift kan in twee delen verdeeld worden. In **hoofdstuk 2-5** onderzoeken we strategieën om CFTR met een specifiek mutatietype, zogenaamde stopmutaties, te herstellen, en in **hoofdstuk 6-9** onderzoeken we of medicijnen die al gebruikt worden voor andere ziektes dan CF, hergebruikt kunnen worden voor CF.

Een oplossing voor stopmutaties

Een deel van de 10-15% van de mensen met CF die niet profiteren van modulatoren, hebben een stopmutatie (ofwel nonsense mutatie). In plaats van een stopcodon aan het einde van een eiwit-coderend CFTR mRNA, zorgt zo'n stopmutatie voor de aanwezigheid een prematuur stopsignaal (PTC) eerder in het mRNA dan het normale stopsignaal. mRNAs met een PTC worden herkend door zogenaamde nonsense-mediated decay (NMD) machinerie en vervolgens afgebroken voordat de productie van het eiwit begint, om te voorkomen dat onvolledige eiwit-varianten ontstaan. In het kleine deel mRNAs dat aan deze NMD-herkenning ontsnapt, wordt tijdens de eiwitproductie de PTC herkent als stopsignaal, wat leidt tot een voortijdige stop en dus een onvolledig CFTR-eiwit.

Het meeste onderzoek naar behandeling van stopmutaties, is naar zogenaamde readthrough (RT) medicijnen. RT-medicijnen stimuleren het doorlezen op de PTC-plek in het CFTR-mRNA tijdens de productie van CFTR-eiwit. Zogenaamde tRNAs spelen hier een grote rol bij, door het koppelen van het juiste aminozuur aan de groeiende aminozuur-keten (het eiwit in wording). Echter, terwijl preklinische resultaten met RT-medicijnen veelbelovend zijn, hebben klinische studies geen positieve uitkomsten opgeleverd.

In **hoofdstuk 2** geven we een overzicht van preklinisch en klinisch onderzoek over RT-medicijnen en identificeerden we factoren die bijdragen aan het feit dat er een dergelijk verschil in succes zit tussen preklinische en klinische studies. We zagen ten eerste dat veel preklinische studies met RT-medicijnen gedaan zijn in gesimplificeerde cel-modellen, waarbij vaak gekeken wordt naar de aanwezigheid van een bepaald eiwit in plaats van daadwerkelijk de functie. Dergelijke experimenten zijn nuttig voor het ontdekken van medicijnen, maar minder geschikt voor het valideren van hun toepasbaarheid en klinische effectiviteit. In vervolgexperimenten moet dus sneller prioriteit gegeven worden aan experimenten in biologisch relevantere, complexere cel-modellen waarin gekeken wordt naar herstel van functie van eiwitten met een stopmutatie. Idealiter worden preklinische experimenten gebruikt waarbij de uitkomsten correleren met klinische parameters, zodat er daadwerkelijk iets geconcludeerd kan worden over potentiële klinische effecten. Ten tweede zagen we dat het lastig was om klinische studies over RT-medicijnen met elkaar te vergelijken, omdat deze erg verschilden in hoe de studies in elkaar zaten. Al helemaal wanneer patiënt-aantallen laag zijn, zoals voor mensen met CF met PTC-mutaties, en er wellicht maar weinig effect is van de geteste therapie, is het goed opzetten en standaardiseren van klinische studies essentieel. Daarnaast kan het bij dergelijke studies met lage patiënt-aantallen helpen om meerdere metingen over tijd te doen, meerdere cycli van behandeling en placebo af te wisselen en kleine trials te doen waarbij effecten in 1 patiënt worden bekeken. Tot slot, hoewel verbeteringen in de opzet van preklinische en klinische studies kunnen leiden tot een betere beoordeling van RT-medicijnen, vroegen wij ons af of de huidige RT-medicijnen wel kunnen werken als monotherapie. Zoals hierboven genoemd, worden PTC-mutatie dragende CFTR-mRNAs snel herkend en afgebroken door NMD-machinerie. Dit gebeurt voordat de RT-medicijnen kunnen zorgen voor de productie van een volledig CFTR-eiwit, en zorgt er dus voor dat RT-medicijnen nauwelijks hun werk kunnen doen. Een strategie kan zijn om NMD te remmen, waardoor er meer CFTR-mRNA kopieën zijn en de RT-medicijnen wél hun werk kunnen doen.

Deze tactiek van het combineren van verschillende medicijnen met verschillende werkingsmechanismes, beschrijven we in **hoofdstuk 3.** Zoals hierboven al deels benoemd, is herstel van PTC-mutaties met1 RT-medicijn uitdagend door a) NMD afbraak van CFTR-mRNA en b) het feit dat RT-medicijnen vaak resulteren in de inbouw van een ander eiwit-stukje (aminozuur) dan het geval was in de originele situatie. Hoewel er wellicht een volledig eiwit gevormd wordt, kan de inbouw van het random aminozuur alsnog zorgen voor CFTR-varianten met minder functie. In **hoofdstuk 3** laten we zien dat we inderdaad de functie kunnen herstellen van PTC-CFTR door een combinatie van drie type medicijnen: RT-medicijn ELX-02, NMD-remmer SMG1i en CFTR-modulatoren ETI. We bekeken dit in darm-organoïden met verschillende varianten PTC-mutaties, en zagen dat de combinatie ELX-02/SMG1i/ETI voor vrijwel alle type PTC-mutaties effectief was, terwijl alle medicijnen individueel niet effectief waren. Hoewel dit een erg positief resultaat was, is het onwaarschijnlijk dat mensen met CF snel zullen profiteren van deze combinatietherapie aangezien zowel ELX-02 als SMG1i nog niet beschikbaar is voor klinisch gebruik. ELX-02 is onderzocht in klinische trials als enkele behandeling en in deze setting ineffectief gebleken, wat correspondeert met onze resultaten. Ondanks dat ELX-02 nuttig kan zijn in combinatie met andere medicijnen, is het onduidelijk of ELX-02 verder ontwikkeld wordt door de fabrikant. Er zijn daarnaast geen klinische studies opgestart met SMG1i. Om mensen met CF te laten profiteren van de veelbelovende resultaten behaald met de combinatie therapie in onze studie is er verder onderzoek nodig naar de ontwikkeling van klinisch toepasbare SMG1i-achtige medicijnen.

Hoewel we in **hoofdstuk 3** beschrijven dat RT-medicijnen uitdagend zijn als monotherapie, heeft recent onderzoek geleid tot een nieuwe generatie RT-medicijnen met nieuwe werkingsmechanismen die wellicht wél kunnen werken als monotherapie. In **hoofdstuk 4**, beschrijven we dat RT-medicijn DAP effectief blijkt als monotherapie. Als we de resultaten van **hoofdstuk 3,** vergelijken met de resultaten van **hoofdstuk 4**, blijkt dat DAP net zo krachtig is als de combinatie van ELX-02/SMG1i/ETI. Dit kan waarschijnlijk worden toegeschreven aan het onderliggende moleculaire mechanisme van DAP, dat ervoor zorgt dat tRNAs die het aminozuur tryptofaan ($tRNAs^{Tryptofaan)}$ met zich meedragen, worden verandert. Als gevolg hiervan herkennen $tRNAs^{Tryptofaan}$ bepaalde PTC-mutaties en bouwen tryptophaan in. Deze afname in de nauwkeurigheid van $tRNAs^{Tryptofaan}$ resulteert in het inbouwen van tryptofaan op de PTC-plek, en daaropvolgend de productie van volledig eiwit. In het geval van een *CFTR*-mutatie waarbij het originele aminozuur een tryptofaan was, zorgt DAP dus voor herstel van het originele CFTR-eiwit waardoor de noodzaak van aanvullende CFTR-modulatoren wordt omzeild. Toekomstig onderzoek naar RT-medicijnen die een vergelijkbaar werkingsmechanisme hebben als DAP, maar dan resulteren in specifieke inbouw van andere aminozuren heeft veel potentie.

In **hoofdstuk 5** onderzoeken we tot slot een andere strategie die tot readthrough kan leiden, namelijk het toedienen van aangepaste tRNAs (ACE-tRNAs) die aan een stopcodon binden en daardoor voor incorporatie van een aminozuur kunnen zorgen. Hoewel we bewijs leveren van het principe dat ACE-tRNAs werken en kunnen leiden tot het herstel van PTC-CFTR functie, zijn meer studies naar ACE-tRNA's nodig, met name met betrekking tot hoe we de ACE-tRNAs het beste in cellen kunnen krijgen.

Samenvattend, de resultaten in **hoofdstuk 2-5** laten vooruitgang zien met betrekking tot de ontwikkeling van nieuwe RT-tactieken. Echter, deze resultaten zijn nog niet snel te vertalen naar de kliniek. Veel van de besproken medicijnen worden nog niet bestudeerd in klinische trials, zoals NMD inhibitors, of hebben in klinische trials tot teleurstellende resul

taten geleid, zoals ELX-02. In deel 2 van dit proefschrift **(hoofdstuk 6-8),** beschrijven we een tweede strategie die zich beter leent voor snelle translatie van preklinische studies naar een klinische setting.

Hergebruiken van bestaande medicatie voor CF

Een veelgebruikte strategie om nieuwe behandelingsmethoden te ontdekken, is te onderzoeken of bepaalde medicijnen die al zijn goedgekeurd voor klinisch gebruik mogelijk ook effectief zijn bij de behandeling van andere ziekten. Bij dergelijk hergebruik van een medicijn is bijvoorbeeld de veiligheid van het medicijn al aangetoond in eerder klinische studies, waardoor de kans op veiligheidsproblemen in latere klinische studies afneemt alswel de totale kosten van het medicijn naar de markt brengen een stuk lager uitvallen. In dit opzicht kan het hergebruik van medicijnen een aantrekkelijke benadering zijn in de context van CF. Voor het zoeken naar medicijnen die hergebruikt kunnen worden voor CF, heeft het FIS-assay een hoge potentie door de eerder beschreven voordelen van dit assay. Echter, om de kans te vergroten om zogenaamde hits te vinden is het van belangrijk een groot aantal medicijnen te testen. Normaal gesproken werd het FIS-assay in zogenaamd 96-wells format uitgevoerd, wat betekent dat er 96 condities in 1 experiment vergeleken kunnen worden. Om de verwerkingssnelheid te verhogen, beschrijven we in **hoofdstuk 6** een 384-wells versie van het FIS-assay, waarmee in **hoofdstuk 6 en 7** overkoepelend 1443 FDA-goedgekeurde medicijnen in 80 verschillende organoïden zijn getest, resulterend in meer dan 60.000 datapunten.

In **hoofdstuk 6** hebben we gezocht naar medicijnen die CFTR-functie verbeterden specifiek voor PTC-CFTR. We ontdekten dat statines zorgden voor enig functie-herstel van PTC-CFTR, wanneer gecombineerd met CFTR-modulatoren. Hoewel statines bekend staan om hun cholesterol-verlagende effecten, leek dit niet te maken te hebben met het werkingsmechanisme met betrekking tot herstel van CFTR-functie. Vervolgonderzoek is nodig om beter te begrijpen hoe statines bijdragen aan CFTR-functie herstel.

In **hoofdstuk 7** hebben we 76 organoïden met verschillende CFTR-mutaties gescreend die nu niet in aanmerking komen voor CFTR-modulator therapie. We vonden ten eerste dat in een aantal organoïden, CFTR-modulatoren wel degelijk zorgden voor een toename van CFTR-functie en dat er dus meer CFTR-mutaties baat hebben bij CFTR-modulatoren dan tot nu toe gedacht. Daarnaast tonen we aan dat zogenaamde PDE4-inhibitors als roflumilast zorgen voor een toename van CFTR-functie. Voor sommige CFTR-mutaties waarbij er nog enige CFTR-functie aanwezig is, kunnen PDE4-remmers als monotherapie gebruikt worden. Daarnaast vertoont de combinatie van roflumilast met andere medicijnen synergetische effecten bij het herstellen van PTC-CFTR-functie, en kan dit de noodzaak voor bijvoorbeeld een NMD-remmer voor dit type mutatie weghalen. In een klinische setting worden PDE4-remmers daarnaast gebruikt voor andere luchtwegziektes als COPD en astma, waar ze zorgen voor gladde spierontspanning en ontstekingsremming. Klinische toepassing van PDE4-remmers in een luchtwegziekte als CF, is dan ook relatief gemakkelijk. Daarnaast is het opmerkelijk dat een dagelijkse dosis van de PDE4-remmer roflumilast

wordt geschat op $1.428 op jaarbasis, een erg laag bedrag in vergelijking met $250.000 voor CFTR-modulatoren. Dit benadrukt de noodzaak van verdere karakterisering van roflumilast in klinische onderzoeken als monotherapie en als onderdeel van combinatietherapie.

Over het algemeen tonen deze studies de vele voordelen aan van het bestuderen van hergebruikpotentiaal van klinisch gebruikte medicijnen, en kunnen ze het traditionele geneesmiddelenontwikkelingsproces enorm versnellen.

Van lab naar kliniek

Gebaseerd op de resultaten van hoofdstuk 6 en 7, hypothetiseerden wij dat een combinatie van ETI, roflumilast en een statine samen beter CFTR-functie zouden kunnen herstellen dan de individuele medicijnen. Aangezien al deze medicijnen al zijn goedgekeurd voor klinisch gebruik zou een eventueel klinische studie relatief eenvoudig zijn, mits preklinische data positieve resultaten zou laten zien. In **hoofdstuk 8** hebben we de volledige combinatie getest in organoïden van twee personen met CF met *CFTR*-mutaties die momenteel niet in aanmerking komen voor CFTR-modulatoren en eerder zijn gekarakteriseerd als niet-responsief op ETI-monotherapie. We zagen inderdaad dat de volledige combinatie aan medicijnen zorgde voor significante verbetering van CFTR functie, terwijl de medicijnen alleen of in duo's grotendeels ineffectief waren. Vergelijking van de resultaten met data van organoïden met F508del/F508del CFTR behandeld met modulatoren (waarover bekend is dat modulatoren effectief zijn voor dit genotype), gaf aan dat de effecten van de volledige combinatie in een klinisch relevante range zaten. Op basis van deze resultaten en het feit dat de gezondheid van 1 van de patiënten waarvan de organoïden getest waren snel achteruitging, initieerden we een klinische interventie met de complete combinatie aan medicijnen in deze patiënt. We zagen bijzonder grote klinische verbeteringen op meerdere vlakken, van longfunctie tot door de patiënt zelf aangegeven scores met betrekking tot fysieke en emotionele gesteldheid.

In dit proefschrift beschrijven we verschillende strategieën waarin CFTR-modulatoren een grote rol spelen. In deze studies gaan we echter niet in op de grote maatschappelijke uitdagingen die naar voren komen bij deze CFTR-modulatoren; met name de prijsstelling, wetgeving en goedkeuring voor vergoeding. Recente studies schatten de productiekosten voor ETI in op $5.676 per jaar, een stuk lager dan de Amerikaanse prijs van $250.000. De preklinische resultaten in **hoofdstuk 3, hoofdstuk 6, hoofdstuk 7 en hoofdstuk 8** van dit proefschrift, laten duidelijk zien dat meer personen met CF baat kunnen hebben bij CFTR-modulatoren als monotherapie of als onderdeel van een combinatietherapie, maar het huidige prijsmodel beperkt de toegang tot de beste beschikbare therapie.

Dit wordt benadrukt door onze studie in **hoofdstuk 8.** Ondanks de overtuigende preklinische en klinische resultaten van de combinatietherapie roflumilast/simvastatine/ETI, was de zorgverzekeraar niet bereid de kosten van ETI te vergoeden voor de patiënt, aangezien zijn mutaties niet op de officiële FDA/EMA lijsten staan waar de medicijnen voor zijn goedgekeurd. De Nederlandse CF patiëntenorganisatie (NCFS) en het team van behandelend

artsen, vochten deze beslissing aan met als gevolg dat de Geschillencommissie Zorgverzekeringen in januari 2024 het bindende besluit nam dat de zorgverzekeraar de kosten van ETI moet vergoeden, op basis van de positieve, overtuigende preklinische en klinische gegevens. Hierdoor kan de patiënt de volledige behandelingskuur voortzetten. Het is de eerste keer in Nederland dat zo'n verzoek voor vergoeding van ETI-behandeling voor *CFTR*-mutaties die níet officieel op de goedgekeurde mutatie-lijst staan is goedgekeurd en wij hopen dat deze specifieke zaak als opmaat dienen voor vergelijkbare situaties.

Tot slot, een andere manier om de toegang tot CFTR-modulatoren te verbeteren is door onderzoek te blijven doen naar andere CFTR-modulatoren. Momenteel zijn de CFTR-modulatoren geproduceerd door Vertex de enige klinisch goedgekeurde CFTR-modulatoren, maar verschillende andere CFTR-modulatoren worden nu onderzocht in preklinische en klinische studies. In **hoofdstuk 9,** beschrijven we ABBV/GLPG modulator-therapie, bestaande uit 2 CFTR-correctoren en 1 CFTR-potentiator. ABBV/GLPG-Triple therapie was effectiever dan lumacaftor/ivacaftor in homozygote F508del/F508del organoïden, wat wijst op potentieel klinisch effect. Vervolgonderzoek naar dergelijke alternatieven voor de al klinisch goedgekeurde CFTR-modulatoren zal moeten uitwijzen hoe goed deze alternatieven zijn.

Conclusie

Voor de laatste 10-15% van mensen met CF die niet reageren op CFTR-modulatoren, zijn nieuwe oplossingen nodig. In dit proefschrift hebben we verschillende strategieën verkend om aan de onvervulde klinische behoeften van deze groep mensen te voldoen, met name in de context van stopmutaties. We hebben preklinische experimenten uitgevoerd in de waardevolle setting van functionele FIS-assays in darm-organoïden van mensen met CF, waardoor onze preklinisch resultaten tot op zekere hoogte vertaald kunnen worden naar een klinische setting én de resultaten een basis leggen voor gepersonaliseerde behandelstrategieën.

Fundamentele studies zijn cruciaal om de onderliggende moleculaire defecten van ziektes volledig te begrijpen en dus potentiële doelen voor precisiebehandelingen te ontdekken. Echter, zoals dit proefschrift aantoont, is het essentieel om vervolgexperimenten te doen die zo klinisch relevant mogelijk zijn. Dit kan leiden tot een ultieme persoonlijke aanpak in precisiegeneeskunde, zoals we aantoonden in de klinische studie in dit proefschrift.

Hoewel er nog vele uitdagingen moeten worden aangegaan, hopen en verwachten we dat het werk gepresenteerd in dit proefschrift bijdraagt aan het verder brengen van precisiegeneeskunde voor CF en dat de concepten die we hier verkennen, kunnen worden overgedragen naar andere ziekten. We hopen en verwachten dat aanvullende lopende en toekomstige studies, gebaseerd op het hier gepresenteerde werk, uiteindelijk zullen leiden tot therapieontwikkeling én beschikbaarheid van deze therapieën, voor alle mensen met CF.

List of publications

This thesis

* = shared first author

*De Poel, E., ***Spelier, S.,** Korporaal, R., Lai, K. W., Boj, S. F., Conrath, K., van der Ent, C.K., & Beekman, J. M. *"CFTR rescue in intestinal organoids with GLPG/ABBV-2737, ABBV/GLPG-2222 and ABBV/GLPG-2451 triple therapy"* (September 2021). Frontiers in Molecular Biosciences, Volume 8, Article Number 698358

*De Poel, E., ***Spelier, S.,** Suen, S. W. F., Kruisselbrink, E., Graeber, S. Y., Mall, M. A., Weersink, E., van der Eerden, M., Koppelman, G.H., van der Ent, C.K., & Beekman, J. M. *"Functional restoration of CFTR nonsense mutations in intestinal organoids"* (March 2022). Journal of Cystic Fibrosis, Volume 21, Issue 2, P246-253

***Spelier, S.,** *de Poel, E., Ithakisiou, G. N., Suen, S. W., Hagemeijer, M. C., Muilwijk, D., Vonk, A.M., Brunsveld, J.E., Kruisselbrink, E., van der Ent, C.K., & Beekman, J. M. *"High-throughput functional assay in cystic fibrosis patient-derived organoids allows drug repurposing"* (October 2022). ERJ Open Research, Volume 9, Issue 1

*Leroy, C., ***Spelier, S.,** Essonghe, N. C., Poix, V., Kong, R., Gizzi, P., Bourban, C., Amand, S., Bailly, C., Guilbert, R., Hannebique, D., Persoons, P., Arhan, G., Prévotat, A., Reix, P., Hubert, D., Gérardin, M., Chamaillard, M., Prevarskaya, N., Rebuffat, S., Shapovalov, G., Beekman, J. & Lejeune, F. *"Use of 2, 6-diaminopurine as a potent suppressor of UGA premature stop codons in cystic fibrosis"* (January 2023). Molecular Therapy, Volume 31, Issue 4, P970-985

*De Poel, E., ***Spelier, S.,** Hagemeijer, M. C., van Mourik, P., Suen, S. W. F., Vonk, A. M., Brunsveld, J.E., Ithakisiou, G.N., Kruisselbrink, E., Oppelaar, H., Berkers, G., de Winter-de Groot, K., Heida-Michel, S., Jans, S.R., van Panhuis, H., Bakker, H., van der Meer, R., Roukema, J., Dompeling, E., Weersink, E., Koppelman, G.H., Blaazer, A.R., Muijlwijk-Koezen, J.E., van der Ent, C.K., & Beekman, J. M. *"FDA-approved drug screening in patient-derived organoids demonstrates potential of drug repurposing for rare cystic fibrosis genotypes"* (May 2023). Journal of Cystic Fibrosis, Volume 22, Issue 3, P548-559

Spelier, S., van Doorn, E. P., van der Ent, C. K., Beekman, J. M., & Koppens, M. A. *"Read-through compounds for nonsense mutations: bridging the translational gap"* (April 2023). Trends in Molecular Medicine, Volume 29, Issue 4, P297-314

Spelier, S., de Winter-de Groot, K., Keijzer-Nieuwenhuijze, N., Liem, Y., van der Ent, C.K., Beekman, J. & Kamphuis, L. *"Organoid-guided Synergistic Treatment of Minimal Function CFTR Mutations with CFTR modulators, Roflumilast and Simvastatin: A Personalized Approach"* (January 2024), European Respiratory Journal, Volume 63, Issue 1,

Other publications

Schene, I. F., Joore, I. P., Baijens, J. H. L., Stevelink, R., Kok, G., Shehata, S., Ilcken E.F., Nieuwenhuis E.C.M., Bolhuis D.P., van Rees R.C.M., **Spelier S.,** van der Doef H.P.J., Beekman J.M., Houwen R.H.J., Nieuwenhuis E.S. & Fuchs, S. A. *"Mutation-specific reporter for optimization and enrichment of prime editing"* (March 2022). Nature Communications, Volume 13, Issue 1.

Amatngalim, G. D., Rodenburg, L. W., Aalbers, B. L., Raeven, H. H., Aarts, E. M., Sarhane, D., **Spelier S.,** Lefferts J.W., Al Silva I., Nijenhuis W., Vrendenbarg S., Kruisselbrink E., Brunsveld J.E., van Drunen C.M., Michel S., de Winter-de Groot K.M., Heijerman H.G., Kapitein L.C., Amaral M.D., van der Ent C.K., & Beekman, J. M. *"Measuring cystic fibrosis drug responses in organoids derived from 2D differentiated nasal epithelia"* (August 2022). Life Science Alliance, Volume 5, Issue 12.

Dankwoord

Samen is alles beter. Ten eerste in de wetenschappelijke wereld waar (inter)nationale samenwerkingen zorgen voor de beste resultaten, zowel in preklinische labstudies als uiteindelijk voor mensen met CF in de kliniek. Meer dan de helft van dit proefschrift bestaat uit samenwerkingen en ik denk dat dit erg heeft bijgedragen aan de waarde van deze studies. Ook buiten de wetenschappelijke wereld is 1+1 meer dan 2, van alle vrienden die alles altijd leuker maken tot de Skate4Air groep waarmee ons WKZ-team samen al schaatsend nog meer onderzoek naar CF mogelijk heeft kunnen maken. Ik wil graag iedereen bedanken die de afgelopen 4 jaar hebben bijgedragen aan de studies in dit proefschrift, als daarbuiten aan mijn PhD-traject, en in het bijzonder een aantal van jullie specifiek.

Jeff, wat hebben wij onze draai in samenwerken gevonden. Toen ik 4 jaar geleden begon wist ik niet altijd wat ik moest als je het whiteboard begon vol te schrijven met ideeën die alle kanten opgingen, maar het antwoord bleek te liggen in mijn welbekende lijstjes in OneNote; leren dat ik je prima kan onderbreken om je terug te brengen naar mijn lijstje; en soms het lijstje juist lekker links te laten liggen om vol mee te gaan in alle gedachtes en ideeën. Juist al die ideeën hebben ervoor gezorgd dat je de groep zo hebt weten te vormen tot hoe die nu is en ik heb daar veel respect voor. Ik kijk ernaar uit samen te blijven werken, te blijven te onderhandelen over hoeveel te vroeg je op een vliegveld mag zijn wanneer we op congres gaan, figuren te maken met extra veel kleurtjes en symbolen die je afschiet en wilt versimpelen en vooral lekker direct naar elkaar te blijven en veel samen te lachen (zodat de hele kantine het kan horen, zoals je altijd zegt).

Kors, eigenlijk geldt hetzelfde als voor Jeff: wat hebben jullie samen iets waardevols neer weten te zetten. Toen ik begon met mijn PhD was de klinische invalshoek en hoe belangrijk het is oog hiervoor te hebben nieuw voor mij, maar juist het belang van vertalen wat we in het lab doen naar de mensen met CF om wie het daadwerkelijk gaat is voor mij ontzettend waardevol geworden. Bedankt voor het helpen bij het verkrijgen van dit inzicht.

Members of my reading committee, *John, Louis, Margarida, Marvin and Roos,* thank you for your efforts of reading this thesis. *John and Margarida,* I look forward to seeing your international toga's to complement the UU ones and *John:* thanks for having me over for the super nice mini-expat-experience in Rochester. From your warm welcome, including Adirondacks hikes and familiarizing myself with Rochesters culture like Wegmans and Kozy Shack, to letting me learn many new things in the lab, was the best!

Dear *co-authors and collaborators,* thank you very much for all the collaborations and the valuable input and contributions to this thesis. I dare say that all chapters in this thesis are the result of collaborations, yet especially valuable were three team efforts that I want to point out. First, the massive team efforts in the drug screening chapters would not have been possible without Beekman lab-members such as *Sylvia, Eyleen and Annelotte* as well as clinicians from other hospitals helping to obtain biopsies from people with CF. Also, I highly appreciated our collaborative projects on DAP and ACE-tRNAs with *dr. John Lueck and dr. Fabrice Lejeune,* I have high hopes for ACE-tRNAs and DAP! Lastly, *dr. Lieke Kamphuis*, together we succeeded in successfully treating a person with CF with compounds characterized based on organoid experiments. The personal approach of this study made a big impression on me, and I sincerely hope this case can serve as basis for future organoid-based theratyping and modulator reimbursement.

Mara and Nefeli, my paranymphs. *Mara,* ondertussen gaat onze vriendschap een jaar of 10 terug, van Spelcie tot samen PhD'en in het Hubrecht. Ik ben ontzettend blij met a) het samen kunnen bijkomen van PhD-leven door bij te kletsen met koffietjes, b) dat je in het Hubrecht blijft na je PhD, c) al je gezelligheid buiten werk om (van macaron-clinics tot de meest geweldige vakantie ooit afgelopen jaar in Zweden) and d) je feedback op mijn introductie en discussie, dankjewel voor de observatie dat ik iets te veel a/b/c/d opsommingen deed, ik heb er veel van geleerd! *Nefeli,* dreamteam-lab-partner. I am super grateful for having you around, from student to technician to PhD colleague. There's a reason I still cannot delete our weekly "dreamteam"-RSV meeting in Teams, working with you is simply a privilege - and when I see that meeting, I still think back about how nice Lisbon was!. Your kind attitude towards everyone is the best and I'm super happy to have you by my side.

Iedereen van het *Beekman lab,* bedankt. Never leave a winning team gaat goed op bij jullie, ik ben blij in "onze flex-office" te blijven hangen.

Mede-PhD'ers, bedankt voor alles op het lab én daarbuiten de afgelopen jaren. *Suzanne,* je bent een superfijne, gezellige collega: van samen pipetteren tot een kamer delen op Malta, hopelijk komt er komende jaren meer van beiden! *Bram en Pim,* eindelijk een wat betere man-vrouw balans! Het is ontzettend gezellig met jullie en waardevol dat jullie erbij zijn gekomen, van extra praten over sport tot waardevolle AI-insights (alles met computers heet AI toch?).

Isabelle, Heleen, Roos-Anne, Shannon en Loes: zonder jullie geen werkend lab, zo simpel is het gewoon. Bedankt voor alle hulp bij alles om het lab draaiend te houden, van WNT duty tot vials halen, van ELab organisatie en mij pushen om toch wat meer structuur in dingen aan te brengen, tot jullie specifieke lab-kennis over van alles en nog wat. Ik vond het ontzettend leuk dat jullie mee gingen naar Malta afgelopen jaar! *Isabelle*, wat vond ik het fijn en gezellig om intensief met je te gaan samenwerken afgelopen jaar. Ik ben trots op hoe erg je gegroeid bent en ben stiekem een beetje blij dat je er in juni nog bent om nog even samen af te sluiten; je toekomstige collega's mogen zich in de handjes knijpen.

Bahar, Gimano, Sam, Martijn, bedankt voor al jullie input in de afgelopen jaren. *Martijn,* we hebben een mooi review geschreven samen, dankjewel voor de hulp hierbij. In dit dankwoord heb ik lekker geen woorden-limiet, maar door jou is dat manuscript toch uiteindelijk kort genoeg geworden (MAND).

Een lab verandert snel, er zijn veel oud-collega's die hebben bijgedragen aan resultaten in dit proefschrift als mede een ontzettend leuke 4 jaar. *Eyleen en Sylvia,* jullie staan aan de basis voor meer dan de helft van dit proefschrift. Bedankt voor het opzetten van projecten die ik af heb mogen maken en voor jullie gezelligheid op en buiten werk. *Juliet, Lisa en Hetty,* ik mis jullie nog steeds op de Beekman-office. Praten over sport, sporten, (hetzelfde ritme hebben op) congressen, yoga-sessies op het strand op Albufeira en veel gezellig kletsen. Gelukkig zitten onze vaste etentjes er nog in! *Else,* ook jij bent eigenlijk een oud-collega. Als master-supervisor heb je meer invloed op me gehad dan je misschien door had, door jou kreeg ik het zelfvertrouwen dat een PhD misschien wel wat voor mij was. Ik heb van je geleerd dat als je denkt dat je snel werkt, het nóg wat sneller kan met bepaalde trucjes en dat je naast hard werken; vooral ook veel leuke dingen moet blijven doen!

Om tot de resultaten beschreven in dit proefschrift te komen, was de samenwerking met de kliniek ontzettend waardevol. *Karin, Sabine M. en Marlou* bedankt voor al jullie werk in de kliniek om samen uiteindelijk voor impact voor mensen met CF te kunnen zorgen. *Marlou, Danya, Marit en Sabine L* superleuk jullie wat beter te leren kennen in NY en Phoenix! *Wilma en Myriam,* bedankt voor al jullie hulp met meer dan op te noemen en het zijn van 2 van de fijnste mensen die ik ken. *Regina,* ik kijk uit naar onze samenwerking in de komende tijd!

Naast onderzoek doen heb ik ook veel tijd besteed aan lesgeven. *Simone:* bedankt voor alle levenslessen, ik denk er oprecht vaak aan terug. *Susanna, Wilke, Lobke, Suzanne, Eline, Joris en Lars,* bedankt voor alle intervisie-momenten. *Marlies* en *Linda*, ik ben blij jullie tegen te zijn gekomen bij Genoom, ik kijk ernaar uit samen te blijven werken!

Onderzoek doen was niet de enige manier waarop ik betrokken was bij CF-onderzoek. Ik ben ontzettend blij *Skate4Air* te zijn tegen gekomen tijdens mijn PhD; *Gittan, Daniëlle en Jochem,* wat een indrukwekkende organisatie hebben jullie neergezet. Samen met mijn WKZ-teamgenoten *(Lisa, Juliet, Roos-Anne, Thomas en Jeff)* deelnemen aan Skate4Air was 1 van mijn PhD-hoogtepunten. Ik ben blij dat ik heb kunnen bijdragen aan jullie mooie doel en dankbaar voor wat Skate4Air mij persoonlijk gebracht heeft.

Anne-Sophie en Saskia, bedankt voor al een jaar of 16 klaar staan voor mij; PhD-gerelateerd of niet en dichtbij of heel ver weg. Wat er ook is, jullie zijn er - en dat waardeer ik ontzettend.

Mara, Wytze, Simon, Ronja, Alicia, Vince, Joanne en Mike. Wat een avonturen hebben we samen beleefd in de afgelopen jaren (van WC-slee tot noorderlicht, en van uitgebreide lunches ondertussen met Lewis, Mae en Aean tot weekendjes op avontuur). Als ik jullie in de agenda zie staan weet ik dat er veel gelachen gaat worden, het is heerlijk.

Jit, Ella, Veerle en Klaske, bedankt voor jullie vriendschap. Ook als ik moe was bracht rustig eten met jullie me rust en gezelligheid. Ik ben blij met onze Jitsi-gezelligheid, maar kijk nog even uit naar dat we over korte tijd allemaal weer in Nederland zijn!

Jeffrey, Wieteke, Bas, Lian, Anne, Robert, Tijmen, Rosan, Linde, Roy en Lyke, bedankt voor jullie gezelligheid, leuke weekendjes, fietstochten, taartplek-inspiratie, boekenclubs en liefste Nora en Roan foto's.

Sterre, ook wij gaan alweer 10 jaar terug! Ik vind het altijd leuk je op te zoeken op Texel en vind het waardevol zo tegelijk ons leven door te lopen met o.a. tegelijk aan een PhD te beginnen.

Eline, Eline en Johanna, jullie verdienen absoluut een plek in dit meest gelezen stukje proefschrift. Zonder survival was ik niet geweest hoe de meeste mensen me kennen, alle trainingen (hoe afmattend ook), survivalruns, taartjes en gezelligheid met jullie waren de perfecte uitlaatklep wanneer ik dat nodig had, ik genoot daar ontzettend van. Het schaatsen (of een kleine blessure hier en daar) zorgden voor wat lagere frequenties laatste tijd, maar ik ben er weer helemaal klaar voor! *Johanna,* op naar die LSR (nu staat het in een boek, dus het moet)!

Papa en Martha. Papa, wat deed je je best afgelopen tijd om toch maar alles bij te houden wat Thomas en ik nu weer op onze vork namen. Ik vind het ontzettend lief hoe trots je op Pim en mij bent, en ben ontzettend blij voor je met hoe alles er zo voor staat (in Gouda, met Martha, en je twee kinder-dr's!). *Martha,* ik bent ontzettend blij je naam hier neer te kunnen zetten. Ik ben je dankbaar voor wat je voor papa betekent, en geniet van jullie samen zien. Dankjewel voor al je interesse in alles wat we doen. *Pim,* dr. Spelier numero 2, ik ben trots op je en accepteer volledig dat ik als oudere zus net wat later promoveer dan jij. Ik vind het ontzettend leuk te zien hoe je hebt gevonden wat je het leukste vind om te doen (van wiskunde tot boulderen), en kijk ernaar uit dat we binnenkort allebei in Utrecht wonen!

Jan en Linda, ik kreeg niet alleen een Thomas 9 jaar geleden, maar kreeg jullie erbij. Er zijn oprecht geen woorden voor hoe dankbaar en blij ik daarmee ben. Wat deden jullie je best op mijn congres-posters die ik naar Haarlem mee nam, wat een expertise in eiwitten en organoïden hebben jullie vergaard. Ik kijk ernaar uit jullie te blijven updaten – en om dat dan te combineren met alle uitjes die we maar kunnen verzinnen met zijn allen. Er zijn nog ontzettend veel vakanties en avonturen die ik graag met jullie op ga zoeken. *Jan* nog in het speciaal, dankjewel voor dit proefschrift zo prachtig maken. Ik vond het ontzettend leuk en extra bijzonder om dit zo samen te doen. *Myrthe; Wout en Jojan,* bedankt voor al jullie gezelligheid en het kunnen kletsen over FACS'en, cellen, klinische studies, spelletjes spelen en alle trips!

Lieve Thomas, dit proefschrift was er niet zonder jou (of het was 2x zo dik omdat ik zonder jou nog meer uren in een dag zou proberen te stoppen). Als nodige rem zorg jij ervoor dat het allemaal net niet te veel wordt als ik te enthousiast het gaspedaal maar in blijf drukken. Dankjewel voor accepteren hoe druk het soms was, me tegenhouden wanneer ik de wekker nóg eerder wilde zetten, accepteren dat ik altijd te vroeg wil zijn overal, me uit de wind houden bij onze >5000 schaatsrondjes en vele fiets- en skate-kilometers en voor het opzoeken samen van alles wat ons opvrolijkt in het dagelijks leven. Jij bent mijn alles en ik kan nu al niet wachten op alles wat we komende altijd gaan meemaken samen, klein (croissantjes-streak!) tot groot.

About the author

Sacha Spelier was born on the 2nd of July 1995 in Utrecht. She grew up in The Hague, where she attended the Sorghvliet Gymnasium. She moved to Utrecht after and obtained a bachelor's degree in Biology at Utrecht University (UU). Hereafter she continued at the UU in 2018, graduating cum laude for her master's 'Cancer, stem cells & developmental biology' in 2020. During this master's, she developed a great interest in translational sciences and performing laboratory research in such a way, that it holds potential to significantly impact patients in a clinical setting. Consequently, the lab of prof. dr. Jeffrey Beekman was the right place to start her PhD in 2020. Here, she focused on using intestinal organoids for studies on personalized treatment of people with CF. One of her main focus points throughout her PhD specifically was studying potential treatment regimens for people with CF with non-sense mutations. The results of these studies are presented in this thesis.

After her PhD Sacha will stay in the lab of Jeffrey as postdoc to try to further contribute to CF research by working on several projects, including a novel study on the association between CF and colorectal cancer.

Sacha lives in Utrecht together with her partner Thomas. In her spare time, she likes doing sports and loves bringing whoever shows the slightest enthusiasm to the survivalrun track. Similarly, her ice-skating adventures in the context of gathering money for Skate4Air together with Lisa, Juliet, Roos-Anne, Jeffrey and Thomas were among her highlights of her PhD-time.

Addenda